ASSESSMENT OF VARIOUS GROUNDWATER RECHARGE METHODS IN THE LOWER KELANTAN RIVER BASIN, MALAYSIA

NUR HAYATI BINTI HUSSIN

FACULTY OF SCIENCE
UNIVERSITI MALAYA
KUALA LUMPUR

2020

ASSESSMENT OF VARIOUS GROUNDWATER RECHARGE METHODS IN THE LOWER KELANTAN RIVER BASIN, MALAYSIA

NUR HAYATI BINTI HUSSIN

THESIS SUBMITTED IN FULFILMENT OF THE REQUIREMENTS FOR THE DEGREE OF DOCTOR PHILOSOPHY

DEPARTMENT OF GEOLOGY
FACULTY OF SCIENCE
UNIVERSITI MALAYA
KUALA LUMPUR

2020

UNIVERSITI MALAYA

ORIGINAL LITERARY WORK DECLARATION

Name of Candidate: **NUR HAYATI BINTI HUSSIN**

Matric No: **SHC120117**

Name of Degree: **DOCTOR OF PHILOSOPHY**

Title of Thesis (“this Work”):

ASSESSMENT OF VARIOUS GROUNDWATER RECHARGE METHODS IN THE LOWER KELANTAN RIVER BASIN, MALAYSIA

Field of Study:

HYDROGEOLOGY

I do solemnly and sincerely declare that:

(1) I am the sole author/writer of this Work;
(2) This Work is original;
(3) Any use of any work in which copyright exists was done by way of fair dealing and for permitted purposes and any excerpt or extract from, or reference to or reproduction of any copyright work has been disclosed expressly and sufficiently and the title of the Work and its authorship have been acknowledged in this Work;
(4) I do not have any actual knowledge nor do I ought reasonably to know that the making of this work constitutes an infringement of any copyright work;
(5) I hereby assign all and every rights in the copyright to this Work to the University of Malaya (“UM”), who henceforth shall be owner of the copyright in this Work and that any reproduction or use in any form or by any means whatsoever is prohibited without the written consent of UM having been first had and obtained;
(6) I am fully aware that if in the course of making this Work I have infringed any copyright whether intentionally or otherwise, I may be subject to legal action or any other action as may be determined by UM.

Candidate’s Signature Date:

Subscribed and solemnly declared before,

Witness’s Signature Date:

Name:

Designation:

ASSESSMENT OF VARIOUS GROUNDWATER RECHARGE METHODS IN THE LOWER KELANTAN RIVER BASIN, MALAYSIA

ABSTRACT

Groundwater recharge is a natural process to replenish the aquifer system. Since 1930s the groundwater demand has risen as it has supported 70% of water supply in Lower Kelantan River Basin. However, a comprehensive study on groundwater recharge mechanism has never been reported. This study evaluated various methods to identify recharge flow processes using stable isotopes of deuterium (^{2}H) and oxygen-18 (^{18}O), tritium (^{3}H), radon (^{222}Rn) and hydrogeochemical (HC) and quantify recharge rate using chloride mass balance (CMB), water table fluctuation (WTF), temperature-depth profile (TDP) and groundwater modelling coupled with water balance GM(WB) followed by the construction of a conceptual model of recharge mechanism. Stable isotope indicates local rainfall origin from monsoon meteoric air masses that have experienced primary and secondary evaporation while tritium indicates rainfall of modern water age of <5 year to 10 years. Rainfall is the main source of surface water and diffuse recharge into the groundwater system. The fast transmit time of rainfall runoff, that percolates and infiltrates through unsaturated zone into aquifer has recharged Layer 1 with modern water age while deep aquifer (Layer 2 and Layer 3) contains a mix of recharge water of modern to sub-modern water caused by long transmit time and mixing with available water in the aquifer. Isotopes and hydrogeochemical methods reveal that the interactions of river-groundwater and aquifer-aquifer within the basin were triggered by infiltration, leaking and mixing besides controlled by the major processes of silicate weathering, dissolution and ion exchange. Through this process, groundwater in shallow aquifer (Layer 1) evolved from $CaHCO_3$ to $NaHCO_3$ towards the coastal area. As the depth increases, groundwater shows a trend of depletion in stable isotopes, decreasing in tritium and increasing in radon concentration. Recharge estimation using CMB, WTF, TDP and

GM(WB) showed high variability within 8% to 68% of annual rainfall. CMB ranges from 16% to 68%, WTF 11% to 19%, TDP 8% to 11%, and GM(WB) 11% of annual rainfall, respectively. At 11%, recharge from GM(WB) was the best method for estimation because the model was constructed and calibrated using locally derived input parameters. GM(WB) is the only method involved with calibration and validation process to reduce the uncertainty. The WTF method based on long-term hydrological records gives a reasonable recharge value, in good agreement with GM(WB) and these methods can be paired to ensure the reliability of recharge value approximation in the same ranges. Applying various methods has given insight into methods selection to quantify recharge at LKRB and it is recommended that a lysimeter is installed as a direct method to estimate recharge. The integrated outcomes of groundwater recharge mechanism is useful as a baseline study for effective and sustainable groundwater resources management at LKRB and Malaysia.

Keywords: Lower Kelantan River Basin, recharge flow, recharge rate, stable isotope, tritium, radon, hydrogeochemical, chloride mass balance, water table fluctuation, temperature-depth profiles, groundwater modelling

PENILAIAN PELBAGAI KAEDAH IMBUHAN AIR TANAH DI LEMBANGAN BAWAH SUNGAI KELANTAN, MALAYSIA

ABSTRAK

Imbuhan air tanah adalah proses semulajadi pengisian semula ke dalam sistem akuifer. Semenjak 1930an, permintaan air bawah tanah telah meningkat dan telah menyumbang 70% bekalan air di Lembangan Bawah Sungai Kelantan. Walau bagaimanapun, kajian komprehensif terhadap mekanisme imbuhan air bawah tanah tidak pernah dilaporkan. Kajian ini menilai pelbagai kaedah untuk mengenal pasti proses aliran imbuhan menggunakan isotop stabil iaitu deuterium (^{2}H) dan oksigen-18 (^{18}O), tritium(^{3}H), radon (^{222}Rn) dan hidrogeokimia (HC) dan penentuan kadar imbuhan menggunakan keseimbangan klorida massa, (CMB), turun naik paras air (WTF), profil suhu-kedalaman (TDP) dan permodelan air bawah tanah bersama keseimbangan air GM(WB) diikuti dengan pembinaan model konseptual mekanisme imbuhan. Isotop stabil menunjukkan asalan air hujan dari jisim monsun udara meteorik yang telah mengalami penyejatan primer dan sekunder manakala tritium menunjukkan hujan berumur air moden kurang lima ke sepuluh tahun. Hujan adalah sumber utama air permukaan dan mengimbuh ke dalam sistem air bawah tanah. Pergerakan cepat air larian hujan secara perkolasi dan menyusup melalui zon tak tepu terus ke akuifer telah mengimbuh Lapisan 1 dengan umur air moden manakala akuifer dalam (Lapisan 2 dan Lapisan 3) mengandungi campuran imbuhan air iaitu air moden dan air separa moden yang disebabkan oleh masa pergerakan yang lebih panjang dan percampuran dengan air sedia ada di dalam akuifer. Komposisi isotop dan hidrogeokimia membuktikan interaksi sungai-air bawah tanah dan akuifer-akuifer di lembangan adalah melalui penyusupan, kebocoran dan percampuran yang dipengaruhi oleh luluhawa silika, pencairan dan pertukaran ion sebagai proses utama. Melalui proses ini, air bawah tanah (Lapisan 1) berevolusi dari $CaHCO_3$ ke $NaHCO_3$ ke

arah kawasan pantai. Dengan pertambahan kedalaman akuifer, air bawah tanah menunjukkan corak pengurangan isotop stabil, pengurangan tritium dan peningkatan kepekatan radon. Penentuan kadar imbuhan mengunakan CMB, WTF, TDP dan GM(WB) menunjukkan variasi yang tinggi di antara 8% ke 68% dari hujan tahunan. CMB adalah dari 16% hingga 68%, WTF 11% hingga 19%, TDP 8% hingga 11% dan GM (WB) 11% daripada hujan tahunan. 11% imbuhan dari GM(WB) adalah kaedah terbaik penentuan imbuhan kerana model yang dibina dan dikalibrasi adalah menggunakan data tempatan. GM(WB) adalah satu-satunya kaedah yang melibatkan proses kalibrasi dan validasi untuk mengurangkan ketidakpastian. Kaedah WTF berdasarkan rekod hidrologi jangka panjang menunjukkan nilai imbuhan yang munasabah, bersesuaian dengan GM(WB) dan kaedah ini boleh digunakan bersama untuk memastikan kebolehpercayaan nilai imbuhan dalam julat yang sama. Penggunaan pelbagai kaedah telah memberikan pemahaman terhadap pemilihan kaedah pengukuran imbuhan di KLRB dan adalah disarankan pemasangan lysimeter sebagai kaedah secara terus penentuan imbuhan. Hasil bersepadu meknisme imbuhan air bawah tanah adalah sangat berguna sebagai kajian asas pengurusan sumber air bawah tanah yang berkesan dan mampan di LKRB dan Malaysia.

Kata kunci: Lembangan Bawah Sungai Kelantan, aliran imbuhan, kadar imbuhan, isotop stabil, tritium, radon, hidrogeokimia, jisim keseimbangan klorida, turun naik paras air, profil suhu-kedalaman, permodelan air tanah

ACKNOWLEDGEMENTS

All praises to Allah S.W.T. for giving me an opportunity, strength and guidance to weather the vagaries of Ph.D. life. Also, peace and blessings be upon the Prophet Muhammad S.A.W. as a great last messenger.

My sincere appreciation and deeply gratitude to my supervisors Professor. Dr. Ismail Yusoff (also his wife, Professor. Dr. Yatimah Alias), Dr. Wan Zakaria Wan Muhamad Tahir (Malaysian Nuclear Agency) and Dr. May Raksmey (UNIMAS) for their constructive advice and criticisms, patience, motivation, and invaluable knowledge given throughout the research period. To Dr. Ratan Kumar Majumder for giving me the example TDP spreadsheet.

I also extend the gratitude to the Universiti Malaya (PV112-2012A, PG132-2014A), Ministry of Higher Education (MyBrain15-MyPhD), Malaysian Nuclear Agency (IAEA/RAC-RAS/7/022), Air Kelantan Sdn. Bhd. (AKSB), Department of Mineral and Geoscience Malaysia (Kelantan), Department of Irrigation & Drainage (DID) Malaysia and Kelantan, Department of Agriculture (DOA) and Malaysian Meteorological Department (MMD) for the research funding, financial support, and providing valuable data for this research studies.

Special thanks to the lecturers and staffs at Geology Department, Institute of Mathematics, Civil Engineering Department, Mechanical Engineering Department of Universiti Malaya, Malaysian Nuclear Agency, Air Kelantan Sdn. Bhd., Department of Mineral and Geoscience Malaysia (Kelantan) and Department of Irrigation and Drainage Malaysia (Kelantan) for giving a helping hand in fieldwork, laboratory analysis, data analysis, computer problems and others.

My dearest friends in Geology, Biology, Chemistry and for those who know me directly or indirectly a million thanks for the support and bittersweet memory we have together.

Lastly, to my beloved family Mak, Ayah, Kak Long, Abang Ngah, Andak and Adik. I am grateful to have all of you in my life. Thank you for your continuous love, understanding and support throughout this journey.

TABLE OF CONTENTS

LIST OF FIGURES

LIST OF TABLES

LIST OF SYMBOLS AND ABBREVIATIONS

%	:	Percentage
$^{0}/_{00}$	:	Per mil
°C	:	Celcius
^{13}C /^{14}C	:	Carbon-13/ Carbon-14
^{36}Cl	:	Chlorine-36
^{2}H	:	Deutrium/Hydrogen-2
^{3}H	:	Tritium-3
^{3}He	:	Helium-3
^{129}I	:	Iodine-129
^{6}Li	:	Lithium-6
^{14}N	:	Nitrogen-14
^{18}O	:	Oxygen-18
^{222}Rn	:	Radon-222
Br	:	Bromide
Ca	:	Calcium
Cl	:	Chloride
HCO_3	:	Bicarbonate
Fe	:	Iron
K	:	Potassium
Mg	:	Magnesium
Mn	:	Manganese
Na	:	Sodium
NH_4	:	Ammonia
NO_3	:	Nitrate

SF_6	:	Sulphur Hexaflouride
SiO_2	:	Silica
Bq/L	:	Becquerel per litre
cm	:	Centimeter
km^3/yr	:	Kilometre Cubic per Year
m	:	Metre
ml	:	Milimetre
mm	:	Millimetre
m/yr	:	Metre per Year
mm/yr	:	Millimetre per Year
m^3/d	:	Metre Cubic per Day
mg/kg	:	Milligram per Kilogram
mg/L	:	Milligram per Litre
MLD/Ml/d	:	Million Litre per Day
MCM/month	:	Million Cubic Metre per Month
µSv/hr	:	Microsievert/hour
µm	:	Micrometer
rpm	:	Revolutions per Minute
AKSB	:	Air Kelantan Sdn. Bhd.
CAl	:	Chloro-alkaline Indices
CFC	:	Chloroflourocarbon
CMB	:	Chloride mass balance
DID	:	Department of Irrigation and Drainage
DOA	:	Department of Agriculture
EC	:	Electrical Conductivity
GIS	:	Geographical Information System

GM	:	Groundwater Modelling
GNIP	:	Global Network of Isotopes in Precipitation
HCA	:	Hierarchical Cluster Analysis
IAEA	:	International Atomic Energy Agency
IC	:	Ion Chromatography
ICP-OES	:	Inductively Coupled Plasma Optic Emission Spectrometry
LKRB	:	Lower Kelantan River Basin
LRA-WTP	:	Loji Rawatan Air/Water Treatment Plant
MGD	:	Department of Mineral and Geoscience Malaysia
MODFLOW	:	Modular Finite-Different Flow
TDP	:	Temperature Depth Profile
TDS	:	Total dissolved solid
TU	:	Tritium Unit
WHO	:	World Health Organization
WTF	:	Water Table Fluctuation

LIST OF APPENDICES

CHAPTER 1: INTRODUCTION

1.1 Introduction

This chapter will introduce the thesis topic and briefly address the research studies related to the topic. The research area took place in the state of Kelantan, the one and only state that has been utilising the natural resources of groundwater for water supply in Malaysia. This research is titled "Assessment of Various Groundwater Recharge Methods in the Lower Kelantan River Basin, Malaysia". The title itself has significantly represented the main purpose of the research and has highlighted several methods that will be used later in this study. The main components of this study such as statement of the research problems, research objectives and scope of works, significance of the research study, limitations faced during research study and thesis outlines are briefly highlighted.

1.2 Groundwater Resources

Worldwide groundwater reserved stored underneath the earth is estimated to be about 8 million km^3 to 10 million km^3 stored on earth (van der Gun, 2012). 35% of fresh groundwater is in large sedimentary basin, 18% is stored in complex geological region and the remaining 47% occurs in local and shallow aquifers which is limited to the alteration zone of the bedrock that locally may contain productive aquifer (Richts *et al.*, 2011). Groundwater has been abstracted ~986 km^3/year (60%) worldwide and most of this for agricultural, domestic and industrial uses (NGWA, 2016). Groundwater resources are used by approximately 2.5 billion people of the world to support their daily needs (UNESCO, 2015).

Extensive exploitation of groundwater abstraction started during the twentieth century, also called the 'silent revolution' was driven by agricultural needs worldwide without proper planning by farmers (Llamas & Martínez-Santos, 2005; Llamas & Martínez-Cortina, 2009). The 'silent revolution' wave started in Italy, Mexico, USA and Spain, whereas the second wave began in South Asia, North China, part of Middle East and Northern Africa and the third wave in African regions, Sri Lanka and Vietnam (Shah *et al.*, 2007). Over exploitation of groundwater has introduced unprecedented groundwater stress problem in some regions. The greatest stress on groundwater occurred mostly in arid and semi-arid areas of the world (Famiglietti, 2014).

In the tropical region, groundwater stress has triggered or exacerbated land subsidence, aquifer compaction, groundwater depletion, salt water intrusion, arsenic contamination and groundwater quality deterioration, as reported at Chao Phraya River Basin, Mekong River Basin, the Greater Jakarta Basin, Irrawaddy Delta, Bengal Mega Delta and others (Babel *et al.*, 2006; Delinom, 2008; Taylor *et al.*, 2014; Ha *et al.*, 2016). The stress become worse especially during periods of drought.

The projection of global groundwater depletion during the twenty first century according to the influence of groundwater extraction costs and resources, range from 180 km^3/year to 480 km^3/year (restricted renewable water) and 110 km^3/year to 210 km^3/year (expanded renewable water), which is lower than the 2050 prediction and also less than model predicted by Wada and Bierkens (2014) and Kim *et al.* (2016) [detailed in (Turner *et al.*, 2019)]. The stresses on groundwater are still increasing and present unconsiderable risk and uncertainty. Whether there will be a sufficient groundwater in the future with good quality is still undetermined. Thus, sustainable groundwater resources management is important to avoid the key issues related with groundwater stress as mentioned previously. Nonetheless, sustaining the groundwater usage has become a global issue especially in economic and food supplies.

One of the key elements for sustainable groundwater resources management is groundwater recharge. Groundwater recharge is the process where water infiltrates into subsurface until it reaches the water tables forming an addition to the groundwater reservoir (de Vries & Simmers, 2002; Nimmo *et al.*, 2005; Healy, 2010). Understanding the hydrogeological system of groundwater recharge mechanism of the recharge sources, the groundwater flow paths, groundwater quality and quantifying the recharge rate are crucial to the stakeholders because it varies in space and time and it is challenging to measure the recharge directly (Moeck *et al.*, 2020). Climate change and urbanization are the main factors that can reduce the groundwater recharge (Jayakumar & Lee, 2017; Minnig *et al.*, 2018; Hepburn *et al.*, 2019). Information related to groundwater recharge will help to manage an over extraction of groundwater and prevent groundwater stress in order to sustain the resources as well. In some regions, managed aquifer recharge (MAR) has successfully overcome and improved the quantity and quality of groundwater (Dillon *et al.*, 2019; Sallwey *et al.*, 2019). Reviews on recharge mechanism are explained in Chapter 2, especially on methods that will be applied in this study.

1.3 Problem Statement

Malaysia is a country that is blessed with huge amount of groundwater storage of approximately 5000 billion m^3 (Abdullah & Mohamed, 1998). 65% of ground water is being utilised for public water supply, 30% in industry and 5% for irrigation purposes (KeTTHA, 2010). The utilisation of groundwater is relatively low at only 3% (DID, 2000) because surface water is the main source of water supply. Therefore, there are no comprehensive studies related to groundwater recharge mechanism conducted on recharge source and flow process as well as methods to quantify the recharge rate in Malaysia even though recharge is a major component and needs to be considered in term of effective water resources management in this country. The portion of groundwater recharge is usually estimated from water balance study.

In Kelantan, groundwater has been used since 1935, and the groundwater demand has risen in the last 30 years (DID, 2000). This state is exalted with a lot of groundwater storage underneath especially at LKRB. This natural resource is managed by Air Kelantan Sdn. Bhd. (AKSB) as the main operator responsible for the development, operation and maintenance of the groundwater supply for public water supply in Kelantan. Groundwater has been exploited from shallow and deep aquifers. The total groundwater consumption is about 165 million litre per day (MLD), which constitutes more than 45% of the total water production at AKSB's water treatment plants and demand for groundwater increases 2.5% annually (Suratman, 2010). In order to meet the increase in water demand usage, AKSB has constructed river bank filtrtaion (RBF) system in a few places and is planning to construct river barrage and sub storage dam within the basin in the future (Wan Ismail, 2019). Groundwater was used for households, agricultures and industry (Islami *et al.*, 2012; Hussin *et al.*, 2014). Fast developing urban area inevitably has affected the recharge process by changing the land use pattern.

LKRB is situated in humid tropical rainforest climate and has been sanctified to receive high rainfall intensity with more than 2000 mm annually which reflects the abundance of groundwater resources. Precaution should be made to protect over exploitation of these groundwater resources as mentioned in section 1.2. Proper groundwater resources management and planning are needed for future needs. Studies related to groundwater recharge mechanism have not been done so far in the basin to gain insight on recharge flow processes and the best methods to be applied for humid tropical area to estimate the recharge are still questioned. It is hoped that this study will provide a base for future groundwater resources assessments at LKRB. All available data will be gathered to help in understanding the recharge mechanism systematically.

1.4 Objective and Scope of Works

The research objective is to determine the recharge source, recharge flow processes, recharge rate and overall concept of recharge mechanism at Lower Kelantan River Basin (LKRB).

1. Identify the groundwater recharge sources, recharge flow processes (origin, process and residence time (age))of groundwater
2. Apply and compare various methods for groundwater recharge rate and evaluate the best methods to be applied to estimate recharge rate
3. Construct a conceptual model of groundwater recharge mechanism

The scope of works to achieve the objective are:

1. Using stable isotopes (^{2}H and ^{18}O), tritium (^{3}H), radon (^{222}Rn) and hydrogeochemical (HC) to achieve Objective 1
2. Using Chloride Mass Balance (CMB), Water Table Fluctuation (WTF), Temperature Depth Profile (TDP) and Groundwater Modelling coupled with water balance (GM(WB)) methods to achieve Objective 2
3. Develop a conceptual model of groundwater recharge mechanism based on outputs from scope 1 and scope 2

1.5 Significance of Research Study

As an important water supply in LKRB, groundwater resources management and planning are important to maintain the sustainability of the groundwater resources. Therefore, enlightenment on the groundwater recharge flow processes and recharge rate is beneficial for groundwater resources management and planning in LKRB. It is expected that this research could be a stepping stone or baseline study for groundwater recharge mechanism in Kelantan particularly and Malaysia as a whole.

1.6 Limitations

The limitations faced during the research studies are:

a) Direct measurement of recharge using lysimeter was unable to be installed because of difficulty in obtaining approval and permission from the land-owner

b) Groundwater modelling attempt to be constructed within limited data available of the LKRB

c) Available wells are not well distributed throughtout the LKRB

d) Some of the methods lacked long-term data and certain parameters related are not available

1.7 Thesis Outline

This thesis consists of seven chapters. Chapter 1 will describe an overview of the research study and a brief of problem statements. Objectives and scope of works, significance of the study and limitations as well as the thesis organisation will be described at the end of the chapter. Chapter 2 will review the relevant literatures related to the study. The literatures on groundwater recharge mechanism are focused on detailed methods on recharge flow processes and methods to quantify recharge rate used in this study. Meanwhile, the research methodologies related to sampling locations, sampling procedures, samples analysis, quality assurance and quality control and recharge estimation methods applied in this study will be explained in Chapter 3. In chapter 4, geomorphology, geology, hydrology, hydrogeology and previous study of the study area will be discussed in detail. Chapter 5 will present the result findings whilst chapter 6 will discuss the findings for each method. Groundwater recharge flow processes and groundwater recharge estimation rate will be evaluated towards the end of the chapter. The research findings will be concluded in chapter 7 with some advocations to improve the research study in the future.

CHAPTER 2: LITERATURE REVIEW

2.1 Introduction

This chapter will review and explain the core topic of the thesis concisely. Groundwater recharge will be introduce in the context of hydrologic cycle, history of recharge study, the important of recharge mechanism and recharge methods in terms of recharge flow processes and recharge rate estimation.

Global hydrologic cycle is a system consists of three sub systems: the atmospheric water system, the surface water system and subsurface water system and this cycle is a continuous processes (Todd and Mays, 2005) is shown in Figure 2.1. Recharge is one of the important component in the subsurface water system as indicated in Figure 2.1. Recharge will replenish the aquifer system through rainfall, spring, river, wetland, canals, lakes and man induced through irrigation and urbanization (Lerner *et al.*, 1990).

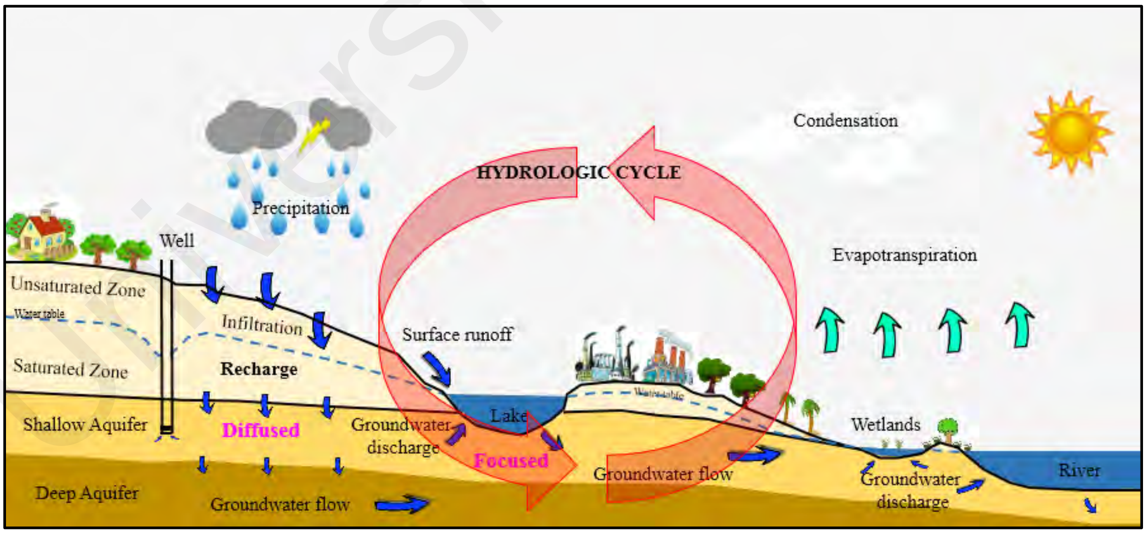

Figure 2.1: Groundwater recharge in hydrologic cycle [figure edited from Winstanley (2007)]

For the past four decades, there is a number of text books, academic dissertations, review papers and reports dedicated to the groundwater recharge studies (Simmers, 1988; Lerner *et al.*, 1990; Simmers, 1997; Scanlon *et al.*, 2002; Adams *et al.*, 2004; Scanlon *et al.*, 2006; Seiler & Gat, 2007; Healy, 2010; Henry, 2011; Beyer *et al.*, 2014; Chung *et al.*, 2016; Koeniger *et al.*, 2016; Ali & Mubarak, 2017; Cartwright *et al.*, 2017; Doble & Crosbie, 2017; Xu & Beekman, 2019; Moeck *et al.*, 2020). Groundwater recharge is a downward movement of water infiltrate through the subsurface before it enters the water table (Lerner *et al.*, 1990; Healy, 2010). It is typically expressed as a volume [L^3], in units being m^3 or acre-ft. Recharge rate is expressed either as a flux [L^3T^{-1}] into a specified portion of aquifer, a flux density [LT^{-1}] (volume per unit surface area) into an aquifer at a point (Nimmo *et al.*, 2005) or as a percentage of the annual rainfall or as an average rate of water [mm/year] (Obuobie, 2008).

Assessment of effective and sustainable groundwater resources management requires an estimation of the groundwater recharge (Foster, 1988; Scanlon et al., 2002b; Chand et al., 2005; Gleeson et al., 2016; Gleeson et al., 2020; Thomann et al., 2020). Determination of recharge sources, recharge flow processes and quantification recharge rate are the most difficult challenges in hydrological sciences especially in evaluation of groundwater resources (Bredenkamp *et al.*, 1995; Simmers, 1997; Henry, 2011). Knowledge on recharge rates is important to predict the sustainable safe yield for now and future sustainable exploitation of the groundwater resources because the future growth is depend on this resources at the most parts of the world (Gonfiantini *et al.*, 1998; Sophocleous & Schloss, 2000; Sanford, 2002; Scanlon *et al.*, 2002; Obuobie, 2008; Healy, 2010; Hartmann *et al.*, 2017).

Recharge amount goes into an aquifer can be said equivalent to the *safe yield* or quantity of water that could be removed from aquifer for sustainable basis. Sustainable yield of an aquifer is almost always appreciably less than recharge (Sophocleous & Schloss, 2000) because sustainable yield must allow for adequate provision of water to sustain stream, spring, wetlands, and groundwater dependent ecosystem (Sophocleous, 1997, 1998, 2000) but recharge rates itself are not sufficient for determining the sustainability (Bredehoeft *et al.*, 1982; Healy, 2010). More challenges are faced especially in arid and semi-arid region as surface water resources are difficult to find that makes groundwater crucial compared to humid area (Scanlon *et al.*, 2006). As population growth increased, water sarcity will become a major concern in the future.

2.2 Groundwater Recharge Flow

The principle of recharge flow to the groundwater system from various sources can be found in (Lerner *et al.*, 1990; Scanlon *et al.*, 2002; Healy, 2010). Two types of recharge flows can be distinguished as *diffused* recharge and *focused* recharge (Healy, 2010) as shown in Figure 2.1. *Diffused* recharge is referred as the response to precipitation that infiltrates the soil and percolates through the unsaturated zone before reaching the water table, distributes over large area in water added to the groundwater reservoir in excess of soil-moisture deficits and evapo-transpiration by direct vertical percolation through the vadose zone. This process also known as *direct* recharge (Simmers, 1997).

Focused recharge is the movement of water from surface water bodies such as streams, canals, or lakes to the aquifer system (Healy, 2010). Lerner *et al.* (1990) has defined *focused* recharge into; 1) *localized* recharge (concentrated recharge from small depressions, joints or cracks) and 2) *indirect* recharge (from mappable features such as rivers, canals and lakes). Both *diffused* and *focused* recharge will enter groundwater system, which varies in recharge flow processes from region to region and even site to site within a region (Healy, 2010).

Scanlon *et al.* (2002), state that *diffuse* recharge is dominant in humid regions while arid regions are dominated by *focused* recharge. Humid regions are characterised by shallow water table and gaining streams where aquifers are often full and usually discharged through evapotranspiration and baseflow to streams. The recharge rates are limits by the ability of aquifers to store and transmit water, a process that strongly affected by the subsurface geology. Arid regions are well-known with their deep water tables and losing streams commonly in alluvial valleys. Recharge rates are minimal depending on the available water on the land surface due to climate factors of rainfall, evapotranspiration and geomorphological features.

To understand the groundwater recharge sources and flow processes at LKRB, four methods will be applied and will be briefly reviewed in details in section 2.2.1 to 2.2.4. These methods are stable isotopes (SI) of deuterium (^{2}H) and oxygen-18 (^{18}O), tritium (^{3}H), radon (^{222}Rn) and hydrogeochemical (HC), respectively.

2.2.1 Stable Isotopes of Deuterium (^{2}H) and Oxygen-18 (^{18}O)

Stable isotope of deuterium (^{2}H) and oxygen-18 (^{18}O) occur naturally and is abundant in various environments (Mook, 2000). The signature of ^{2}H and ^{18}O also known as '*conservative tracers*'. The composition of ^{2}H and ^{18}O is measured according to the SMOW (Standard Mean Ocean Water) standard (Domenico & Schwartz, 1990) and reported as permil ($^{0}/_{00}$). The changes in composition of isotopic precipitation have been documented by Craig (1961), Dansgaard (1964), Craig and Gordon (1965), Rozanski *et al.* (1993) and Araguás-Araguás *et al.* (1998). Clark and Fritz (1997b), Kendall and

McDonnell (1998) and Hoefs (2009) have compiled a summarise of the processes and applications related to ^{2}H and ^{18}O stable isotope in hydrology.

Since ^{2}H and ^{18}O are part of the water molecule, variation of ^{2}H and ^{18}O in natural water is largely controlled by the isotopic fractionation as shown in Figure 2.2. This isotopic fractionation occurs due to physical and chemical processes of ion exchange, evaporation, hydration and condensation (Domenico & Schwartz, 1990). The isotopic fractionation results in water bodies with isotopically distinct signatures and produces a defined relationship between ^{2}H and ^{18}O for global meteoric precipitation known as the Global Meteoric Water Line (GMWL) (Craig, 1961). The extent deviation of natural water isotopic signature from the GMWL along the evaporation lines will reflect the magnitude of kinetic effect in which the greater the deviation from the line indicates the more extensive evaporation (Craig & Gordon, 1965; Gat, 1971; Domenico & Schwartz, 1990).

^{2}H and ^{18}O isotopic compositions differ geographically by temperature, latitude, amount of rainfall, continental effects and elevation (Dansgaard, 1964; Clark & Fritz, 1997a; Cook & Herczeg, 2000). In Southeast Asia, temporal variations are significant in some part of tropical area whereas rainfall amount associated well with the depletion of isotopic signatures (Araguás-Araguás *et al.*, 1998, 2000). These processes determine the isotopic signature of precipitation as well as the evolution of the isotopic signature of surface waters, both of which may contribute to groundwater recharge. Directly infiltrated groundwater from precipitation have the isotopic signature of precipitation, while the groundwater that was recharged by other sources, such as river and lake, will show the mean isotopic content of the contributing river or lake and they are expected to have different signature from that of local precipitation (IAEA, 2011b).

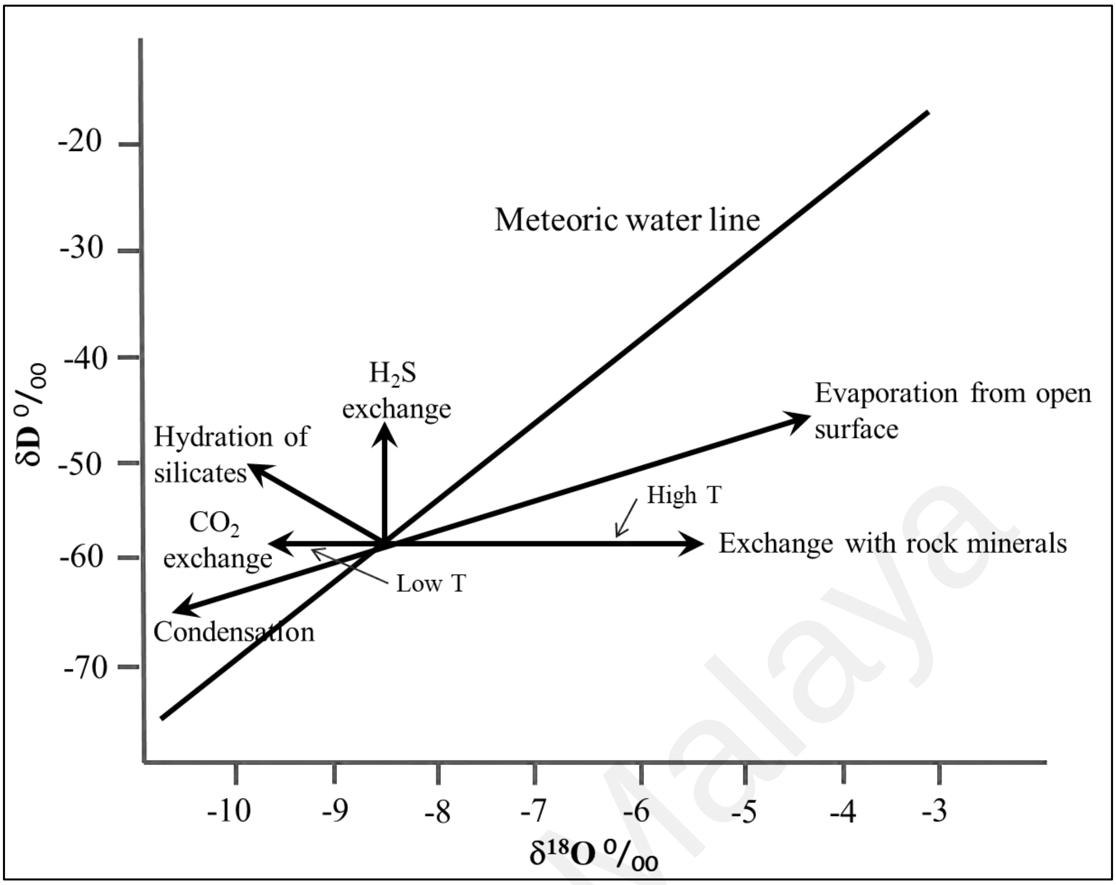

Figure 2.2: Isotopic fractionation from meteoric water line cause by various processes [Figure from (Domenico & Schwartz, 1990) used with permission from publisher John Wiley & Sons Limited]

The signatures of ^{2}H and ^{18}O isotopic has been widely used to enlightenment the hydrological system and regional groundwater processes in different climate condition of arid, tropical and temperate. ^{2}H and ^{18}O are successfully applied to identify the origin and mechanism of groundwater recharge (Das *et al.*, 1988; Leontiadias *et al.*, 1988; Krishnamurthy & Bhattacharya, 1991; Mizota & Kusakabe, 1994; Ahmed & Burgess, 1995; Girard *et al.*, 1997; Aggarwal *et al.*, 2000; Salem *et al.*, 2004; Blasch & Bryson, 2007; Li *et al.*, 2008; Heilweil *et al.*, 2009b; Rapti-Caputo & Martinelli, 2009; Al-Gamal, 2011; Majumder *et al.*, 2011; Yin *et al.*, 2011a; Yuan *et al.*, 2011b; Peng *et al.*, 2012; Singh *et al.*, 2013; Fynn *et al.*, 2016; Liu *et al.*, 2016; Wirmvem *et al.*, 2017; Hao *et al.*, 2019; Wang *et al.*, 2020), groundwater evolution (Gat & Tzur, 1967; Gibson *et al.*, 2002; Robertson & Gazis, 2006; Fynn *et al.*, 2016; Barzegara *et al.*, 2020; Xiong *et al.*, 2020), surface water-groundwater interaction (Jacobson *et al.*, 1991; Acheampong & Hess, 2000; Andreo *et al.*, 2004; Meredith *et al.*, 2009; Li *et al.*, 2014; Wang *et al.*, 2014; Laonamsai & Putthividhya, 2016; Kambuku *et al.*, 2018; Du *et al.*, 2019), intrusion effects of sea water on groundwater quality (Kim *et al.*, 2003; Mukherjee *et al.*, 2007; Eissa *et al.*, 2016; Eissa *et al.*, 2018), water sources constrains in surface water basins (Flusch *et al.*, 2005), identify the interaction between surface water bodies (Yao *et al.*, 2009) and other applications.

Wirmvem *et al.* (2017) studied the recharge mechanism of shallow aquifer at Ndop Plain, northwest Cameron. The results suggest that a single homogeneous shallow unconfined aquifer is being recharged by local precipitation through a direct/diffuse heterogeneous recharge mechanism. 80% of the rainwater infiltrates directly into the shallow aquifer through minor openings in the unconsolidated sediments. 20% of the groundwater originates from localised recharge from mountainous chain or mixed with the inflowing river. The timing of recharge is based on the similarities of ^{2}H and ^{18}O in the rain and groundwater between May and June is characterized by abundant monsoon rain and insignificant recharge during July-September.

Fynn *et al.* (2016) evaluated the source and evolution of groundwater in parts of the Nabogo catchment of White Volta Basin, Ghana using the signature of ^{2}H and ^{18}O in pore water (vadose zone), rainwater, surface water and groundwater. Their finding shows that the local precipitation, presents a relatively isotopically heavier signature compared to the average signature of global meteoric water. The local groundwater in the area presents relatively enriched isotopic signatures. Stable isotope profiles suggest piston flow as the main mechanism of vertical water movement in the vadose zone, indicates that direct groundwater recharge from local precipitation is principally based on this mechanism of transport. A progressive declining in the deuterium excess data of pore water vertically down the soil profile is consistent with an evolutionary pattern caused by fractionation processes attending evaporation of infiltrating water. Mineral-weathering processes have not been noted to influence the isotopic signature of groundwater in the area. However, it appears to be a significant impact of evaporation on the total dissolved solid content of surface water in the area.

Liu *et al.* (2016) traced the recent groundwater recharge processes at Hohhot basin, China and compared their finding with Shao (1989). The recharge mechanism for shallow groundwater unconfined aquifer is due to precipitation in eastern and northern hilly areas and changed from the vertical infiltration from precipitation and lateral flow of surface water in piedmont plain to the infiltration of surface water in the piedmont area and lateral flow recharge during the past 30 years. The deep groundwater in confined aquifer has the same recharge mechanism as the shallow groundwater in unconfined aquifer in northern area of lateral flow.

Girard *et al.* (1997) studied the recharge processes of the fractured aquifer. In the Kobio basin, the fractured aquifer appears to be recharged by evaporated kori waters at the Gouroubi–Lomona confluence (which corresponds to a lineament node and probably to a fractured zone). The recharging water is traced by their ^{18}O signature indicative of evaporated water. As this recharging plume of evaporated water flows northward away from the recharge zone, along the Lomona lineament axis, it mixes progressively with older (no tritium) and isotopically lighter aquifer water. This strongly suggests aquifer continuity along this flow direction. A pump test in one of the three wells studied would confirm these hypotheses. In Niamey, the aquifer seems to be recharged by a similar mechanism. An 'injection' of evaporated river water into the aquifer is observed and may it contribute considerably to the overall recharge of the Niamey aquifer. The plume of evaporated water, traced by its isotopic composition, migrates from the river towards the sampled wells and appears to be progressively diluted by isotopically lighter aquifer water along its course. In light of the remarkable geomorphologic homogeneity of cratonic West African Sahel regions, aquifer recharge by the surface water network may be generalized to the entire subregion. Furthermore, aquifers in other semi-arid areas may also be recharged in this fashion, for example as reported in Sudan by Edmunds *et al.* (1992).

2.2.2 Cosmogenic Isotopes of Tritium (^3H)

Tritium (^3H) is a cosmogenic isotope with half-life of 12.32 years (Lucas & Unterweger, 2000). The tritium content was reported as 'Tritium Unit' (TU), defined as equal to 1 tritium atom per 10^{18} atoms (Kendall & McDonnell, 1998). It is produced naturally in the atmosphere by the interaction of cosmic ray radiation of ^{14}N in the stratosphere (Ingraham, 1998; Loveland *et al.*, 2017) and in subsurface by spontaneous fission of ^6Li from neutrons produced during uranium and thorium series decay in sedimentary to volcanic rock types (Cook & Herczeg, 2000).

The human made anthropogenic sources of tritium in the atmosphere are induced by the thermonuclear bomb testing, nuclear power reactor plant and weapons manufacture (Houston, 2007). A great spike (tritium pulse or tritium bomb pulse) of tritium into the atmosphere via thermonuclear bomb testing during 1950s and 1960s was measured in precipitation as high as 10 000 TU (Ingraham, 1998) compared to the pre-bomb of 3 to 6 TU for Europe and North America and 1 TU to 3 TU for southern Australia (Healy, 2010). In 1963, tritium precipitation in the northern hemisphere was higher than the one that has been recorded at the southern hemisphere in 1964 where 3278 TU was reported at Ottawa,Canada while 38 TU at Kaitoke,New Zealand, respectively. This happened because most of the nuclear tests were conducted at the northern part (Cook & Herczeg, 2000). Ocean is believed to act like a sink for tritium while the ocean/land portion is vital in affecting the amount of tritium precipitation (Seiler & Gat, 2007).

Figure 2.3 shows the long-term tritium observed at Ottawa and Kaitoke generated from GNIP database (IAEA/WMO, 2017). The steady declines of tritium content in atmosphere after the nuclear weapon testing during the 1950s and 1960s was caused by the combined effect of tritium removal by rainwater, radioactive decay of tritium and cessation of atmospheric testing (Morgenstern *et al.*, 2010; Stewart *et al.*, 2012; Wirmvem *et al.*, 2017) The decreasing of world tritium content is said to be back to the normal level of world tritium before nuclear testing.

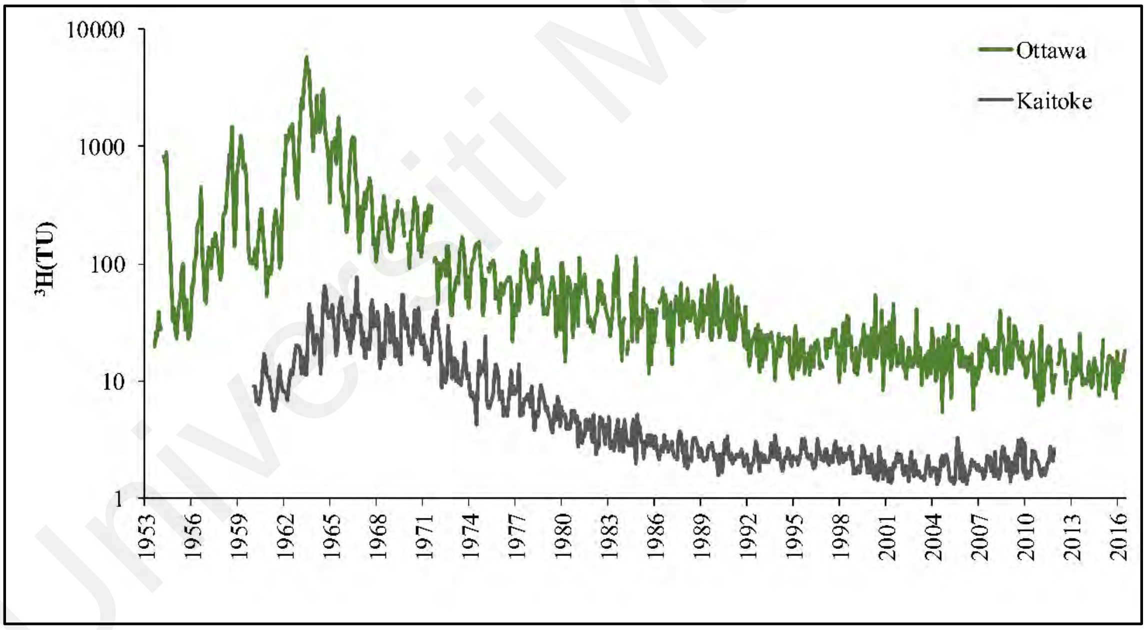

Figure 2.3: Tritium in precipitation at Ottawa and Kaitoke stations [data were downloaded from GNIP database (IAEA/WMO, 2017)]

Since the Atmospheric Test Ban Treaty was signed in 1963, the amount of tritium content entering the atmospheric was reduced. In total there were 2056 nuclear test explosions at the USA, USSR/Russia, UK, France, China, India, Pakistan and North Korea test sites recorded since July 1965 till September 2017 (Kimball, 2017). In 1996, a Comprehensive Test Ban Treaty (CTBT) was opened for signing but no enforcement to stop nuclear weapon test explosion or nuclear explosion and to establish an international test monitoring and verification system. Only USA, USSR/Russia, UK, France, China have signed this CTBT. Even though the nuclear test is still ongoing, the tritium content in precipitation has declined to the low natural level because of decaying process and end of cessation nuclear test (Harms *et al.*, 2016; Wirmvem *et al.*, 2017). The release of tritium emission from nuclear power reactor (modern development) is negligible into the environment since the radioactive waste was managed properly (Ferronsky & Polyyakov, 2012).

Tritium is a part of water molecule with the heaviest hydrogen isotope that behave conservatively and enters the hydrologic cycle either by snow or rainwater (Loveland *et al.*, 2017). Therefore, it was an excellent tracer for identifying young water (modern water) up to 100 years because of the short half-life of 12.32 years, not influenced by any chemical/microbial processes during the travel time and has no effect towards the interactions with aquifer materials as tritium is controlled by the radioactive decay process (Geyh, 2000; Morgenstern *et al.*, 2010; Ravikumar & Somashekar, 2011b, 2011a; Cartwright & Morgenstern, 2012; Stewart *et al.*, 2012; Ako *et al.*, 2013; Hasegawa *et al.*, 2015; Gusyev *et al.*, 2016; Harms *et al.*, 2016; Thomson, 2016; Santos *et al.*, 2017). Tritium is widely used for dating and estimating the residence time or transmit time to enhance understanding the recharge mechanism in the river basin (Bauer *et al.*, 2001; Bajjali, 2006; Gooddy *et al.*, 2006; Koh *et al.*, 2006; Ahmed *et al.*, 2011; Zuber *et al.*, 2011; Haque *et al.*, 2012; Smerdon *et al.*, 2012; Ako *et al.*, 2013; Kralik *et al.*, 2014; Joshi *et al.*, 2018; Li *et al.*, 2019b; Xiong *et al.*, 2020).

Tritium was the only tracer that able to date groundwater directly. Therefore, it can be used to identify the recharge processes either pre or post bomb of tritium in the basin (Kelly, 1997; Hancox *et al.*, 2010; Al-Charideh & Hasan, 2013). This qualitatively assessment of recharge processes are based on Clark and Fritz (1997a) classification for alluvial and hard rock area. The interpretation of tritium is usually in paired with isotopes ^{2}H and ^{18}O to enchance our knowledge related to groundwater water flow process by allowing young or old water to be distinguished (Chen *et al.*, 2006; Majumder *et al.*, 2011; Qian *et al.*, 2013; Madioune *et al.*, 2014; Ammar *et al.*, 2016; Ayadi *et al.*, 2016; Verbovsek & Kanduc, 2016; Wirmvem *et al.*, 2017).

The tritium decay has enabled researchers to quantify the recharge rates based on the calculated residence time and transmit time time in the basin (Clark & Fritz, 1997a; Stewart & Morgenstren, 2001; Zuber *et al.*, 2011; Cartwright & Morgenstern, 2012; Samborska *et al.*, 2013; Caschetto *et al.*, 2016; Jerbi *et al.*, 2019). Clark and Fritz (1997a) stated that the quantification of recharge rates using groundwater ages was less as the interpretation of tritium has been tough by the nuclear testing in the 1950s and 1960s where the tritium content increased in the atmospheric. As a consequence of the peak in atmospheric tritium levels from the bomb-pulse, modelled groundwater ages have commonly produced non-unique ages, because atmospheric tritium concentrations decreased at a similar rate to radioactive decay (King *et al.*, 2017). However, in the Southern Hemisphere, the remnant bomb pulse tritium activity has now decayed below the natural background (Figure 2.2) and residence times can be calculated by applying an assumed flow model to a single tritium measurement (Cartwright and Morgenstern 2012). The simple lump parameter models were used to determine the residence time. This model has six different models which is piston-flow model (PFM), exponential mixing model (EMM), exponential piston-flow model (EPM), partial-exponential model (PEM), dispersion model (DM) and binary mixing model (BMM) (Jurgens *et al.*, 2012). Model selection is depended on the condition of flow in the basin (input and output), long time series data (precipitation as background data and samples) and the knowledge of the modeller itself (Zuber *et al.*, 2011; Jurgens *et al.*, 2012) to avoid misinterpretation and to have reliable age interpretation.

The low tritium level at Central Tunisia has made Jerbi *et al.* (2019) to apply radioactivity decay model using historical tritium to compare with current tritium measurment. The groundwater renewal rate ranges from 0.06% to 6.46% of annual mean rainfall for three aquifers. Their study shows that the estimated recharge was comparable with previous study and reliable for homogenous lithology with localised area and method was less consistent for detrial aquifer (composed lenticular sediments). Since the recent tritium content mostly less than 3 TU, tritium was not significant to be used in some region which made the interpretation very difficult. Therefore, the used of recently measured tritium content alone was clearly unreliable without considering older data (over the period 1950–1970). Their finding does not reduce the importance of tritium as a tracer for use in other fields of hydrology. Indeed, the use of tritium with other approaches is appropriate.

The application of tritium was not limited with tritium itself but researchers nowadays are likely to use tritium in combination (multi-tracer study) with it stable daughter isotope of helium (^{3}He), stable isotopes (^{18}O and ^{2}H), carbon (^{13}C and ^{14}C), chlorofluorocarbon (CFC), sulphur hexafluoride (SF_6), krypton (^{85}Kr) and other isotopes to enhance the knowledge that infers the water flow processes, resolved the extent of mixing occurred in groundwater and to be able to compare the recharge rates (Bauer *et al.*, 2001; Bajjali, 2006; Gooddy *et al.*, 2006; Koh *et al.*, 2006; Visser *et al.*, 2009; Ahmed *et al.*, 2011;

Zuber *et al.*, 2011; Haque *et al.*, 2012; Smerdon *et al.*, 2012; Ako *et al.*, 2013; Kralik *et al.*, 2014; Gil-Márquez, 2019; Wirmvem *et al.*, 2020).

2.2.3 Radiogenic Isotope of Radon (^{222}Rn)

The radiogenic isotope of radon exists as three isotopes of ^{219}Rn, ^{220}Rn and ^{222}Rn. Radon is a product from natural radioactive decay of actinon-uranium series, while thorium series and uranium series are the daughters through alpha disintegration from ^{223}Ra, ^{224}Ra and ^{226}Ra isotopes (Giap, 2003; Ferronsky & Polyyakov, 2012) as shown in Figure 2.4. ^{222}Rn is the most stable isotope and it has longer half-life of 3.83 days compared to ^{219}Rn and ^{220}Rn which have short half-life (4 and 55 seconds) and the present in natural air and water are less (Cecil & Gesell, 1992; Kendall & McDonnell, 1998; Wu *et al.*, 2004; Grolander & Kärnbränslehantering, 2009). Uranium-238 is abundant in Earth crust about 99.3% of total uranium (Ravikumar *et al.*, 2014). It presents ubiquity in almost all types such as sedimentary, metamorphic and granitic rocks and soils (Rajashekaraa *et al.*, 2007; Lefebvre *et al.*, 2013; Stellato *et al.*, 2013).

For the last 25 decades, ^{222}Rn (referred as radon) has been used as an excellent tracer in air, soils and water studied. This is because the features of radon itself which are naturally occurring, a type of inert gas, possessing short half-life, chemically stable and does not react or affected by the complex geochemical processes with the surrounding environment, colourless, tasteless and odourless (Grolander & Kärnbränslehantering, 2009; Ravikumar *et al.*, 2014). The health risks due to the exposure of radon were associated with an increase of lung and stomach cancer through inhalation or ingestion (UNSCEAR, 2000) where the exposure to radon by inhalation is four times higher than by ingestion from water consumption. Radon entered the hydrological cycle due to ingrowth from radium-226 (^{226}Ra) existing in geological materials and waters. The

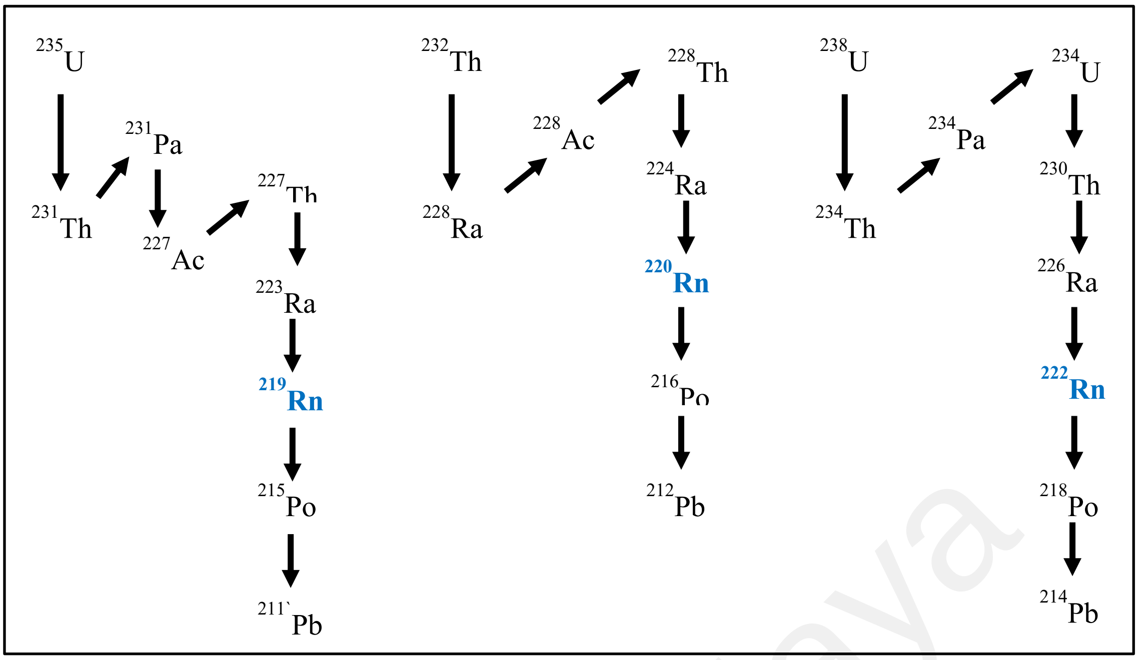

Figure 2.4: Radioactive decay chain of action-uranium-235 series, thorium-232 series and uranium-238 series to produce radon daughters of ^{219}Rn, ^{220}Rn and ^{222}Rn (Ferronsky & Polyyakov, 2012), modified with permission from publisher Springer

process by which radon escapes from the solid material is known as emanation and this emanation processes consists of both chemical and a physical process [detailed in Grolander and Kärnbränslehantering (2009)].

Radon as a tracer was extensively applied in the hydrological studies to identify the interaction between surface water and groundwater from different geological aspects (fractured rock to alluvial system) and landscape conditions (alpine/mountain to coastal) especially in water resources perspective. The different radon concentration in were applied to study the exchange/connectivity of river and groundwater (Green & Stewart, 2008; Baskaran *et al.*, 2009; Oyarzún *et al.*, 2014). Groundwater will have radon concentration two or three times higher than surface water because radon in surface water tend to lose to the atmosphere caused by turbulent condition in river (Bertin & Bourg, 1994).

Radon was effectively used to trace the river infiltrated (river discharge) into an aquifer and/or groundwater discharge or seepage into lakes, river and ocean by estimating and quantifying the flow in and flow out by considering the loss gas exchange and radioactive decay of radon during the process (Hoehn & von Gunten, 1989; Ellins *et al.*, 1990; Yoneda *et al.*, 1991; Bertin & Bourg, 1994; Wu *et al.*, 2004; Hoehn & Cirpka, 2006; Kluge *et al.*, 2007; Burnett *et al.*, 2008; Santos *et al.*, 2008; Stellato *et al.*, 2008; Schmidt *et al.*, 2009; Dugan *et al.*, 2012; Su *et al.*, 2012; Guida *et al.*, 2013; Stellato *et al.*, 2013; Unland *et al.*, 2013; Yu *et al.*, 2013; Cartwright *et al.*, 2014; Cartwright & Gilfedder, 2015; Martindale, 2015; Unland *et al.*, 2015; Quinodoz *et al.*, 2017; Du *et al.*, 2019; Gilfedder *et al.*, 2019; Yang *et al.*, 2020). By analysing the variation and trend of radon in surface water and groundwater along three stream dicth, Du *et al.* (2019) has identified section along the stream, the section in which the river water and groundwater discharged. They used radon tracer principle, to quantify the transformation between goundwater and surface water with average seepage rate was 2708 m^3/d/m in the upstream section and the average groundwater recharge was 17.6 m^3/d/m.

Short half-life is good for understanding the rapid mixing processes between surface water and groundwater (Stellato *et al.*, 2008; Stellato *et al.*, 2013; Kim *et al.*, 2020). Stellato *et al.* (2013) using a model describing radon concentrations in groundwater as the result of both parents/daughter nuclide equilibrium. Mixing process (radon mixing/saturation model) was used to describe observed radon concentrations and mixing index trends with the aim of evaluating water mean infiltration velocities along the transect. The stream bank infiltration velocities obtained by the model ranged from 1 m/day during groundwater recharge periods, when river water infiltration is lower, to 39 m/day during recession phases, when river water infiltration is larger. Their studies highlighted that the advantage of radon method was that, the infiltration velocities were calculated without information on hydraulic conductivity, effective porosity and hydraulic gradient between river and groundwater that difficult to measure accurately. Kim *et al.* (2020) reported to investigate the mixing processes between groundwater and surface water where the groundwater heat pump (GWHP) system was located at the riverside of Han River. Radon mixing ratios showed patio–temporal variations, influenced by the dam discharge rate, seasonal effects, and GWHP. The average mixing ratio values using strontium were in accordance with the results of radon. The microbial heat map also supported the mixing processes as they found unique bacterial taxa (anomalies in bacterial community structure) that caused by exchange between two water bodies. The interactive and dynamic mixing occurred in the riverside area in relation to external factors causing hydraulic disturbances.

Another useful application of radon as a portioning tracer is to detect the sources, quantify and estimate the migration of light or dense NAPLs (non-aqueous phase liquid) contaminant in soil and groundwater for remediation purposes (Semprini *et al.*, 2000; Davis *et al.*, 2003; Schubert *et al.*, 2007; Semprini & Istok, 2008; Yoon *et al.*, 2013; Chen *et al.*, 2014; Yang *et al.*, 2014; Ponsin *et al.*, 2015; Simone *et al.*, 2017; Briganti *et al.*, 2020). The distribution of radon concentration in contact with NAPLs was reduced radon has a strong affinity to NAPLs. The reduction in radon was referred to as radon deficiency (Semprini *et al.*, 2000). This deficiency is correlated with the NAPLs content. Therefore, comparing the radon in site-contaminant and nearby monitoring wells enables evaluation of the remediation process. MTBE contaminated groundwater were studied by Briganti *et al.* (2020) after 15 years to identify the occurance of residual area. Blobs of NAPLs are probably located where former underground gasoline were placed, but only the most soluble substances (MTBE and to a lesser extent benzene and total hydrocarbons expressed as n-hexane) are occasionally detected in groundwater. The results of radon deficit were constant during the study preriod due to total residual NAPL mixture and not only to the most soluble MTBE which is irregularly mobilized by the rising water table after rainfall events.

2.2.4 Hydrogeochemical (HC)

Hydrogeochemical shows a variation in concentration of groundwater. A long way back, classical graphical method (CGM) of Piper trilinear diagram (Piper, 1944), Stiff pattern (Stiff, 1951), Schoeller diagram (Schoeller, 1955 1965) and Durov plot (Durov, 1948) was always an option to depict those data. Data represented using CGM usually considered major ions in the water merely. Nowadays, with the cutting-edge technology, a wide range of chemical parameters of minor and trace elements can be analysed and provided comprehensively in the hydrogeochemical characteristic of groundwater. Therefore, multivariate statistical method (MSM) such as hierarchical cluster analysis (HCA), principal components analysis (PCA) and factor analysis (FA) have given insight to researchers as a tool to improve hydrogeochemical data interpretation (Steinhorst & Williams, 1985; Farnham *et al.*, 2000; Alberto *et al.*, 2001; Lopez-Chicano *et al.*, 2001; Stetzenbach *et al.*, 2001; Locsey & Cox, 2003; Pereira *et al.*, 2003; Belkhiri *et al.*, 2010). Unlike CGM, MSM can be used to handle large data sets and any combination of physical and chemical parameters of the hydrogeochemical data.

A combination of CGM and MSM in related publication of hydrogeochemical studies has succesfully proven to identify the geochemical processes that affect the groundwater flow path, groundwater evolution and groundwater quality (Ceron *et al.*, 2000; Farnham *et al.*, 2000; Stetzenbach *et al.*, 2001; Gu¨ler *et al.*, 2002; Gu¨ler & Thyne, 2004; Helsrup *et al.*, 2007; Papatheodorou *et al.*, 2007; Andrade *et al.*, 2008; Cloutier *et al.*, 2008; Li & Zhang, 2008; El Yaouti *et al.*, 2009; Dassi, 2011; Monjerezi *et al.*, 2011; Singaraja *et al.*, 2014; Ghesquiere *et al.*, 2015; Yang *et al.*, 2016; Zhu *et al.*, 2017; Wang *et al.*, 2018; Alain *et al.*, 2020). Enhancing knowledge of geochemical processes through integrated CGM and MSM as well as with the hydrogeological and geological context can improve understanding on the regional groundwater hydrogeochemical system in the basin for sustainable development and effective groundwater management.

Wang *et al.* (2018) have integrated the traditional and multivariate methods to understand the interaction of groundwater flow patterns and geochemical evolution within Manas River Basin by analysing the surface water and groundwater. HCA and PCA have indicated three zones of recharge, transition and discharge with different groundwater types of Ca-HCO_3-SO_4 (primarily impacted by the dissolution of calcite and silicate weathering), Ca-HCO_3-SO_4-Cl (impacted by rock dissolution and reverse ion exchange) and Na-Cl (impacted by evaporation and reverse ion exchange). The groundwater type generally changes from Ca-HCO_3-SO_4 in the recharge area to Na-Cl in the discharge area along the regional-scale groundwater flow paths. Anthropogenic activities also have impacted the groundwater chemistry in the basin.

Ghesquiere *et al.* (2015) studied the hydrogeochemistry of the Charlevoix/Haute-Côte-Nord (CHCN) aquifer system using CGM and MSM together with stable isotopes δ^2H and $\delta^{18}O$. Stable isotopes analysis suggested that the origin of groundwater was from recharge water in a temperate to cold climate. The MSM was analysed using HCA and R-mode factor analysis (RFA). Four clusters were identified. Cluster 1 composed of low-salinity Ca-HCO_3 groundwater corresponding to recently infiltrated water in surface granular aquifers in recharge areas. Cluster4 Na-(HCO_3-Cl) groundwater was more saline and corresponds to more evolved groundwater probably from confined bedrock aquifers. Cluster 2 and Cluster 3 (Ca-Na)-HCO_3 and Ca-HCO_3 groundwater, respectively, correspond to mix or intermediate water between Cluster 1 and Cluster 4 from possibly inter-connected granular and bedrock aquifers. The main processes affected the hydrogeochemical evolution of groundwater in the CHCN was groundwater recharge, water–rock interactions, ion exchange, solute diffusion from marine clay aquitards, saltwater intrusion and hydraulic connections between the Canadian Shield and the granular deposits.

Cloutier *et al.* (2008) have identified 7 clusters from 144 samples and 14 parameters of the Paleozoic Basses-Laurentides sedimentary rock aquifer system in Que´bec. Clusters C3, C4, C6 and C7 have samples located in preferential recharge areas with most of the samples having Ca–Mg–HCO_3 recharge groundwater (C3, C6, C7) and Na–HCO_3 evolved groundwater (C4). C1, C2 and C5 were under confined conditions with majority of samples have Na–HCO_3 evolved groundwater (C1, C5) and Na–Cl ancient groundwater that exhibits elevated concentrations in Br^- (C2). The distribution of clusters was influenced by minor and trace elements from geological formation such as Fe^{2+}, Mn^{2+}, Sr^{2+}, F^- and Ba^{2+}. The first five components of the PCA account for 78.3% of the total variance in the dataset. Component 1 was defined by highly positive loadings in Na+, Cl^- and Br^- and was related to groundwater mixing with Champlain Sea water and solute diffusion from the marine clay aquitard. The high positive loadings in Ca^{2+} and Mg^{2+} of component 2 suggested the importance of dissolution of carbonate rocks in this aquifer system. The first two components were defined as the ‘‘salinity’’ and ‘‘hardness’’ components, respectively. Components 3–5 were related to more local and geological effects. CGM and MSM with hydrogeological and geological information have divided the region into four geochemical areas. The three factors that have influenced the evolution of groundwater in every geochemical area, 1) geological characteristics including sedimentary rock type and mineralogy; (2) hydrogeological characteristics represented by the level of confinement and the hydraulic gradient; and (3) geological history by the latest glaciation as well as Champlain Sea invasion.

2.3 Groundwater Recharge Rate

A wide variety of groundwater recharge methods has been studied (Lerner *et al.*, 1990; Taylor & Howard, 1996; Hendrickx & Walker, 1997; Kinzelbach *et al.*, 2002; Scanlon *et al.*, 2002; Jones & Banner, 2003; Delin & Risser, 2007; Dripps & Bradbury, 2007; Takounjou *et al.*, 2011; Barron *et al.*, 2012). The difficulty arise in which methods will provided a reliable recharge estimation as various factors will affected such as spatial and temporal variability, climate, soil and geology, surface topography, hydrology, vegetation and land use. These factors need to be considered when choosing a method for quantifying groundwater recharge rate (Simmers, 1997; Scanlon *et al.*, 2002; Dripps & Bradbury, 2007; Barron *et al.*, 2012).

Lerner *et al.* (1990) have simplified the methods according to the sources of recharge and Scanlon *et al.* (2002) classified groundwater recharge based on hydrological zones of surface water, unsaturated zone, and saturated zone. These zones are further classified into physical, tracer and numerical modelling methods. Healy (2010), in his book compiled the methods that provides critical evaluation or understanding of the theory and assumption that underlies each method for estimating groundwater recharge in various hydrologic zones and climates. A good practice is to match the recharge estimation methods with the conceptual models of recharge processes at individual site to ensure that the assumptions underlying the methods are consistent with the conceptual models. Thus, this practice will guided hydrogeologists in decision-making on the methods selection and application of the methods based on the conceptual models.

Table 2.1 simplified and updated the methods for estimating groundwater recharge according to climates and hydrologic zone from Gebremeskel (2015) as guideline information. The most reliable method to estimate groundwater recharge is lysimeter. Lysimeter is known as a direct method as it provides direct point measurement of recharge compared to other indirect methods. Here, the review as described in section 2.3.1 to 2.3.4 will emphasise on the methods that will be applied in this study by using chloride mass balance (CMB), water table fluctuation (WTF), temperature-depth profiles (TDP) and groundwater modelling (GM). The methodology of all methods are briefly discussed in detail in Chapter 3.

2.3.1 Chloride Mass Balance (CMB)

Estimation of groundwater recharge using the chloride mass balance (CMB) method has been studied because of its simplicity and inexpensiveness. Chloride ion is known as a conservative natural tracer because its property, which neither leaches from, nor is absorbed by the sediment particles, is highly soluble (high solubility) in water, and is rarely found in solid phase. It does not react with geochemical or biochemical reaction process during its movements through an unsaturated zone to at saturated zone and is not taken up by plants (root zones) during evapotranspiration process that will contibutes to an accumulation chloride in soil moisture (Ting *et al.*, 1998; Carrier *et al.*, 2008; Scanlon *et al.*, 2009; Healy, 2010). Thus, chloride ion is suitable to be applied for understanding the hydrological system and capable to provide more precise results (Gaye & Edmunds, 1996).

The atmospheric deposition of chloride were varied temporally and spatially (Crosbie *et al.*, 2010; Guan *et al.*, 2010; Alcala & Custodio, 2015). The primary source of atmospheric chloride was through evaporation process of ocean water (Healy, 2010). Sea

Table 2.1: Recharge estimation method according to climate and hydrological zone [modified after Gebremeskel (2015)]

Hydrologic zone	Groundwater recharge estimation method	
	Arid and semiarid climate	**Humid climate**
Surface water	Channel water budget Seepage meters Dracy's law Heat tracers Chemical and Isotopic tracers (Cl, ^{3}H, ^{226}Rn) Watershed modelling Streamflow duration curves Streamflow hydrograph analysis	Channel water budget Seepage meters Heat tracers Chemical and Isotopic tracers (Cl, ^{3}H, ^{222}Rn) Watershed modelling Streamflow duration curves Streamflow hydrograph analysis
Unsaturated zone	Lysimeters *(direct measurement)* Zero-flux plane Dracy's law Soil-water content Pressure head Water budget Tracers [environmental (Br, Cl, ^{36}Cl, ^{3}H) historical (^{36}Cl, $^{3}H/^{3}He$, ^{129}I, CFCs, SF_6)] Heat tracers Numerical modelling	Lysimeters *(direct measurement)* Zero-flux plane Dracy's law Soil-water content Pressure head Water budget Tracers [environmental (Br, Cl, ^{36}Cl, ^{3}H) historical (^{36}Cl, $^{3}H/^{3}He$, ^{129}I, CFCs, SF_6)] Heat tracers Numerical modelling
Saturated zone	Tracers [historical (CFCs, $^{3}H/^{3}He$) environmental (Cl, ^{14}C)] Heat tracers Numerical modelling Water budget	Water table fluctuations Darcy's Law Tracers [historical (CFCs, ^{3}H, $^{3}H/^{3}He$)] Heat tracers Numerical modelling Water budget

salt aerosols bring about 10% of the total chloride to the continent and able to deposit it within 100 km from the coastal area (Eriksson, 1959, 1960) cited in (Guan *et al.*, 2010). The chloride deposition onto land surface are carried out by two mechanisms of dry and wet deposition (Healy, 2010). The dry deposition is where the chloride ions are attached to the dust particles while the wet deposition is where the chloride ions are entrained in rainwater or snow. The concentration of atmospheric chloride is greater near the ocean land margin and decreasing towards inland ranging from 200 mg/L to 0.02 mg/L (Feth, 1981). Chloride concentration deposited on land surface is contributed by the rainfall amount, distance from coast and wind (Hutton, 1976; Keywood *et al.*, 1997).

Bresciani *et al.* (2014) identified that open field atmospheric chloride deposition at Uley South was decreased less 10 km from the coastal. This reduction is caused by dry chloride deposition and not the decrease in rainfall amount or rainfall concentration. Deng *et al.* (2013) enhanced the quantification of chloride input to the land surface at coastal forest South Australia to increase the accuracy of CMB method. Chloride input was quantified traditionally in open field using bulk precipitation but there is question in it applications in forest catchment. Studies by Lovett *et al.* (1996); Moreno *et al.* (2001); Staelens (2006) have indicated that chloride deposition was enhanced by tree canopies around 50% to 75% in the coastal area. The results indicated that chloride deposition was significantly higher than open field by 28% enhancement at the eucalyptus site and 89% at the pine site. The enhancement value of 95% for shrubs, 145% for mallees and 1125% for she-oaks as measured by Bresciani *et al.* (2014) where vegetation cover almost 80% of Uley South. Underestimation of groundwater recharge if effect of enhancement were neglected in the CMB application.

The chloride concentration in the subsurface (unsaturated or saturated zone) is either by infiltrating rainfall, anthropogenic sources, dissolution of chloride minerals from soils or dissolution of entrapped sea water during the sea level changes. Water containing chloride infiltrates into the soil zone will be lost through transpiration by plants and evaporation leaving the residual chloride in the soil water. Thus, the concentration of chloride is proportional to the amount of water removed. Below the root zone, chloride signature transported into the water table. In humid regions, with high downward water fluxes, the chloride concentration is relatively constant below the root zone. In contrast to arid zones with low water fluxes, the chloride concentration below the root zone will be balanced by the downward moving chloride in the soil water against any diffusive flux across the unsaturated/saturated boundary (Herczeg & Love, 2007).

Early studies using chloride to estimate groundwater recharge were by Eriksson and Khunakasem (1969) at the Coastal Plain aquifer of Israel, Eriksson (1976) in the Delhi region of India followed by Allison and Hughes (1978) at Gambier Plain of Australia. Since then, application of CMB method in groundwater recharge studies has spread globally because this method enable to apply either in unsaturated zone or saturated zone (Scanlon *et al.*, 1997; Herczeg & Edmunds, 2000). This method is the simplest as it utilises mass balance and less expensive (Allison *et al.*, 1994; Edmunds *et al.*, 2002) therefore suitable for hydrological processes study. The CMB was based on the ratio between chloride concentration at atmospheric and subsurface with the rainfall in that area.

CMB method was successfully applied in, e.g. Asia (Bazuhair & Wood, 1996; Ting *et al.*, 1998; Sukhija *et al.*, 2003; Subyani, 2004; Liu *et al.*, 2009; Marei *et al.*, 2010; Huang & Pang, 2011; Yin *et al.*, 2011b; Yuan *et al.*, 2011a; Huang *et al.*, 2013; Atiaa *et al.*, 2014; Huang *et al.*, 2016; Huang *et al.*, 2017; Li *et al.*, 2017; Tesfaldet *et al.*, 2019), America (Scanlon, 1991; Wood & Sanford, 1995; Murphy *et al.*, 1996; Nolan *et al.*, 2007; Manna *et al.*, 2016; Niazi *et al.*, 2017; Pavlovskii *et al.*, 2019), Africa (Edmunds *et al.*, 1988; Bromley *et al.*, 1997; Dassi, 2010; Takounjou *et al.*, 2011; Diouf *et al.*, 2012; Stone & Edmunds, 2012; Mensah *et al.*, 2014; Afrifa *et al.*, 2017; El Mekki *et al.*, 2017; Lwimbo *et al.*, 2019; Ifediegwu, 2020), Europe (Lo Russo *et al.*, 2003; Alcala & Custodio, 2014; Marrero-Diaz *et al.*, 2015; Hornero *et al.*, 2016) and Australia (Allison & Hughes, 1978; Guan *et al.*, 2010; Ordens *et al.*, 2012; Deng *et al.*, 2013; Bresciani *et al.*, 2014; Somaratne & Smettem, 2014; Suckow *et al.*, 2020) in various hydrological setting such as hard rock aquifer, karst, volcanic, mountain, wadi, arroyos, loess and quaternary aquifer. Most of the studies mentioned above were applied in the arid and semi-arid regions as reviewed by Scanlon *et al.* (2006) while less in the humid and sub-humid regions.

Scanlon *et al.* (2006) reviewed the global synthesis of groundwater recharge in arid and semi-arid regions and have indicated that the CMB was widely used to estimate groundwater recharge compared to other methods (e.g. water balance; unsaturated model; water level fluctuation; tracers). For example, in Australia more than half of the recharge estimation cases were conducted using CMB method (Deng *et al.*, 2013). These regions received less rainfall, high evapotranspiration and deep water tables, thus groundwater was more vital and application of other methods acquired field parameters is challenging especially during the dry season (Mutoti, 2015) compared to CMB. Precaution in measurements was important where recharge rates were low ranges from 0.2 mm/yr to 35 mm/yr (Scanlon *et al.*, 2006) and relatively accurate (Allison *et al.*, 1994; Subyani & Sen, 2006) in arid and semi-arid.

In contrast, less studies on CMB method were found at tropical humid and sub-humid regions with high rainfall and shallow water tables where groundwater is usually discharged through evapotranspiration and baseflow to the rivers. The groundwater recharge estimated in these regions ranges from 108 mm/yr to 1172 mm/yr accounting 7% to 47% of the annual rainfall (Ting *et al.*, 1998; Lo Russo *et al.*, 2003; Takounjou *et al.*, 2011; Mensah *et al.*, 2014; Lwimbo *et al.*, 2019; Tesfaldet *et al.*, 2019; Lu *et al.*, 2020).

Rapid economic growth at Pingtung Plain, Taiwan has caused over pumping and reduced the hydraulic heads in aquifer which affected the coastal and agriculture area (Ting *et al.*, 1998). CMB was estimated at four sites with bare or sparsely vegetated land with and without irrigation. The estimated recharge was 15% of the annual precipitation excluding recharge from additional irrigation water. The recharge was unevenly distributed within the Pingtung Plain. They suggested a careful determination of chloride inputs at different agricultural fields from irrigation water, pesticides, and fertilizers. The sites should be chosen on soils with different texture in sections that are parallel to the prevailing flowlines, preferably in uniform, non-polluted areas unaffected by brackish-water influences. Lo Russo *et al.* (2003) evaluated annual groundwater recharge in the alluvial Po Plain, Italy. The maize cropped area has high input anthropogenic chloride compared to natural sources. The annual recharge estimated using steady-state chloride concentration profiles was 205 mm/yr compared to 216 mm/yr using approximate diffusive movement equation. They successfully indicated that chloride method can be applied onto not only natural environments but also to cultivated area by considering the anthropogenic input and output (fertilizer and irrigation) as well as yield removal by crops and knowing the fertilizer addition as well atmospheric deposition rates as assumed to be steady.

The first hydroclimate record of 1007 years with two year sampling resolution was successfully reconstructed by Lu *et al.* (2020) using 95 mm unsaturated zone (USZ) chloride profile for sub humid area. The minimal recharge uncertainty is 16% over a 10 years time scale.The reconstructed hydroclimate record from the semi-humid region has a higher resolution than that of the arid zones, likely because the semi-humid, fine-grained thick USZ, possesses higher velocity piston flow, relatively to diffusion and dispersion of Cl signals. The record compared well with other related records, suggesting that the Cl proxy can be used in sub-humid areas, and is sensitive to wet/dry alternations that are largely driven by the Asian monsoon intensity. This study can play a role in deepening the cognition of the hydrological processes in the USZ and regional hydroclimate history, along with promoting the development of hydropedology and global change science.

In tropical humid area, Takounjou *et al.* (2011) has estimated the groundwater recharge from shallow aquifer at Anga'a river watershed, Cameroon. The estimated recharge from CMB ranges from 16.24 mm/yr to 236.95 mm/yr with mean of 108.45 mm/yr which represents 7% of mean annual rainfall. This value is high compared to hybrid WTF of 87.14 mm/yr which represents 5.7% of annual rainfall. They concluded that high discrepancy obtained between CMB and WTF imply the ineffectiveness of the CMB on their forested and humid environment. CMB was applied in shallow aquifer at Thepkasattri, Phuket, Thailand by Tesfaldet *et al.* (2019). The recharge varied from 443 mm/yr to 1439 mm/yer with mean of 1172 mm/yr, represent 47% of annual rainfall. The spatial prediction of recharge estimation shows that the eastern and western catchments have higher recharge, while the central and southwest parts of the study area were represented by average and low recharge. They also found out that the spatial distribution of recharge was related to land use and land cover.

Wood and Sanford (1995) have applied the CMB technique by Eriksson and Khunakasem (1969) in their studies at Southern High Plains aquifer by putting some assumptions in the analysis as recharge in arid and semi-arid was very heterogenous in time and space. The regional groundwater recharge to the aquifer has yielded an approximately 11 mm/yr (2% of annual rainfall) and this result was comparable with the physical approach from previous researchers. Their studies also combined with stable isotopes and tritium in both groundwater and unsaturated zone where spatial and temporal distribution of recharge has indicated that nearly half of the recharge to the Southern High Plains has occurred as piston flow through playa basin floor and macropore recharge might be important in the remaining recharge.

Manna *et al.* (2016) expanded the CMB equation by considering the chloride from surface runoff to calculate the groundwater recharge as studied by Aishlin and McNamara (2011) because neglecting any effect of runoff may lead to overestimation of recharge values. The evaluated groundwater samples (in total 1490) either have anthropogenic input sources by using Cl/Br ratio as it is widely used by Alcalá and Custodio (2008) and TCE before calculating the CMB. The estimated mean annual recharge is 19 mm (4.2% of mean precipitation 450 mm) which is similar with other studies in sandstone aquifer of semi-arid regions: Edmunds *et al.* (1988) estimated a recharge variable between 2.5 and 4% of the total precipitation in Sudan; Sami and Hughes (1996) estimate 4.5 mm of annual recharge on a mean annual rainfall of 460 mm in South-Africa and Heilweil *et al.* (2009a) estimate a recharge for a sandstone aquifer in the Sand Hollow Basin (Utah, US) to be equal to the 4% of precipitation. Scanlon *et al.* (2006) have compiled the results of numerous recharge studies in semi-arid regions and have concluded that recharge varies from 0.1% to 5% of the annual precipitation.

2.3.2 Water Table Fluctuation (WTF)

Water table fluctuation (WTF) method as reviewed by Healy and Cook (2002) has been used since 1920s (Meinzer, 1923; Meinzer & Stearns, 1929). Since then, WTF has been applied by many researchers (Rasmussen & Andreasen, 1959; Gerhart, 1986; Rai *et al.*, 1994; Moon *et al.*, 2004; Crosbie *et al.*, 2005; Delin *et al.*, 2007; Obuobie *et al.*, 2012; Jassas & Merkel, 2014; Crosbie *et al.*, 2015; Yang *et al.*, 2018; Hall *et al.*, 2020; Şimşek *et al.*, 2020) within different climate conditions.

The application of WTF method requires the knowledge of specific yield and changes in groundwater levels caused by recharging aquifer (Healy & Cook, 2002; Healy, 2010). Because of the abundance of available groundwater level data and the simplicity of estimating recharge rates from temporal or spatial patterns of water level (Healy & Cook, 2002) had attributed a wide used of this method. The WTF method is best applied in estimating recharge over a short time period in area with shallow unconfined aquifer that shows sharp rise and fall of groundwater levels (Healy & Cook, 2002; Scanlon *et al.*, 2002; Moon *et al.*, 2004) due to rainfall event.

This method is simple, easy to use and there is no assumption made on the mechanism of water movement through the unsaturated zone. The occurrence of preferential flow path does not limit the application and the estimated recharge rates are able to represent an area of several to thousand square meters. The recharge estimate using WTF method gives the actual value and it is more reliable compared to potential recharge estimation by other methods (Obuobie *et al.*, 2012). Many approaches for WTF have been studied and modified in time series analysis for estimating groundwater recharge because of its simplicity (Moon *et al.*, 2004; Crosbie *et al.*, 2005; Lee *et al.*, 2005; Park & Parker, 2008; Cuthbert, 2010; Ghanbari & Bravo, 2011; Jie *et al.*, 2011; Park, 2012; Varni, 2013; Cai

& Ofterdinger, 2016; Chae *et al.*, 2016; Izady *et al.*, 2017; Hung Vu & Merkel, 2019; Labrecque *et al.*, 2020) and to improve the accuracy of the estimation of results from underestimated or overestimated of recharge estimation.

In unconfined aquifer, the water table fluctuation is not necessarily resulted from recharge process but also can be induced by the evapotranspiration, atmospheric pressure, entrapped air (*Lisse* effect), pumping wells, tides and surface loads as described in Healy (2010). Shallow water tables may exhibit diurnal fluctuations in which there is declining during daylight hours in response to evapotranspiration and rising through the night when evapotranspiration of groundwater is zero. The changes in atmospheric pressure can cause the fluctuation of water tables to be around 10 mm because pressure is transmitted rapidly through open water well than through the sediments overlying the aquifer.

Infiltrating rainwater can trap air in the unconfined aquifer that can gives false impression of recharge (Nachabe *et al.*, 2004; Fan *et al.*, 2014). This condition is more prevalent in fine soil texture when surface soils become saturated and impermeable to air. The trapped air will potentially reduced the water storage capacity, causing less water to rise at the same water table relatively without the entrapped air effects. This phenomenon is known as the *Lisse* effect (Krul & Liefrinck, 1946). This effect usually affects an area where the difference between water table and ground surface is less than 1.0-1.3 m (Weeks, 2002; Crosbie *et al.*, 2005). In coastal sandy environment, the *Lisse* effect can be considered minimal (Healy & Cook, 2002; Crosbie *et al.*, 2005). Pumping of wells induced changes in surface water elevation in which can greatly affect groundwater levels. Ocean tides and changes in groundwater flow in or out also can affect the water table fluctuation.

In the fractured rock aquifer, the use of WTF method are more challenging compared to unconfined aquifer (Healy & Cook, 2002). Fracture aquifer usually serve as primary conduits for water movement both in laterally and vertically which account for small percentage of total storage available in the aquifer. Recharge to low porosity is often characterized by large variation in groundwater levels. The low permeability will require more time to fill and drain the aquifer. Some fracture aquifers will have deep water table that only display seasonal fluctuation. This could provide a poor record of water level variations within the aquifer itself. The measurement of groundwater level in the observation well can represent an area for at least several ten square meters. Therefore, WTF method can be viewed as an integrated approach and to the lesser extent as a point measurement compared to a method based on strictly local data in the unsaturated zone (Izady *et al.*, 2017).

Specific yield (*Sy*) is an important parameter in WTF approach-based method in recharge estimations. It is a ratio of the volume of water in which after saturated it will be yielded by gravity to its own volume (Meinzer, 1923) and treated as a storage term. In fact, *Sy* is not just a function of porous media but also depth to water table, drainage duration, and antecedent moisture conditions among other variables (Shah & Ross, 2009). The selection of appropriate values of *Sy* in WTF method remains puzzling and difficult even with carefully planning in both laboratory or field (Healy, 2010). Crosbie *et al.* (2020) has implemented a depth dependent specific yield (*Sy*) within WTF method with the *Sy* estimated jointly constrained by chloride mass balance (CMB) and water balance using evapotranspiration (ET). *Sy* was treated as a conceptual parameter that cannot be measured and has been constrained by using a rejection sampling approach using probabilistic estimates of net recharge from the CMB method and excess water derived from the difference between precipitation and remotely sensed actual evapotranspiration.

The method developed has provided probabilistic estimates of the ultimate specific yield and a probabilistic time series of gross recharge, both important in shallow water table environments. This jointly constraining the three different recharge types were assured of being internally consistent The method was demonstrated using four catchments in Northern Australia (58 bores) and has shown that *Sy* of the Cretaceous sediments is comparable to the consolidated rock and the alluvium has a higher *Sy*. The uncertainties in the *Sy* and the long term average recharge as expressed as the difference between the 5th and 95th percentiles is closed to the magnitude of the median estimates of the *Sy* and recharge.

Some of the limitations (Healy, 2010) when using WTF are: i) recharge rates may vary substantially within a watershed because of differences in elevation, geology, land-surface slope, vegetation, and other factors (Lee et al., 2005), ii) data from multiple wells should be used to ensure that recharge estimates are representative of the catchment as a whole, iii) in the WTF method, recharge is assumed to occur as discrete events in time, in direct contrast to methods, such as the unit hydraulic gradient method, in which a steady recharge rate is assumed. If the recharge rate to an aquifer was constant and equal to the drainage rate away from the aquifer, the groundwater levels would not change, and the WTF method would estimate a recharge rate of zero, iv) difficulties in estimating specific yield also contribute to the overall uncertainties of the method, v) the frequency with which water levels are measured can affect recharge estimates.

2.3.3 Temperature-Depth Profiles (TDP)

Review on temperature (heat) as a signature in environmental tracer have been written wisely (Anderson, 2005; Constantz, 2008; Saar, 2011; Rau *et al.*, 2014; Ren *et al.*, 2018; Kurylyk *et al.*, 2019). Research on the usage of temperature started a way back in the

1960s (Suzuki, 1960; Bredehoeft & Papadopulos, 1965; Stallman, 1965). Since then, number of studies has increased in the application of temperature to study groundwater-surface interaction within the streambed (Constantz, 1998; Constantz *et al.*, 2003; Bense & Kooi, 2004; Hatch *et al.*, 2006; Calvache *et al.*, 2011; Saar, 2011; Kumar *et al.*, 2012; Luce *et al.*, 2013; Rau *et al.*, 2014; Glose *et al.*, 2019), climate (past and future) and land use (deforestation/urbanization) changes (Gosnold *et al.*, 1997; Harris & Gosnold, 1999; Taniguchi *et al.*, 1999a; Taniguchi *et al.*, 1999b; Uchida *et al.*, 2003; Ferguson & Woodbury, 2004, 2005; Miyakoshi *et al.*, 2005; Taniguchi & Uemura, 2005; Uchida & Hayashi, 2005; Gunawardhana & Kazama, 2012; Colombani *et al.*, 2016; Irvine *et al.*, 2017; Dong *et al.*, 2018) and groundwater flow (recharge and discharge) (Cartwright, 1970; Sakura, 1993; Taniguchi, 1993; Dapaah-Siakwan & Kayane, 1995; Taniguchi *et al.*, 1999b; Taniguchi, 2002; Taniguchi *et al.*, 2003b; Ferguson & Woodbury, 2005; Majumder *et al.*, 2013; Kurylyk *et al.*, 2017; Li *et al.*, 2019a).

The heat flow in subsurface is closely related with the movement of water (Ingebritsen *et al.*, 2006) because groundwater transports the thermal energy and disturbs subsurface thermal regime not only by conduction but also by advection caused by the groundwater movement (Taniguchi, 1993). By lowering the temperature probe down into a borehole, groundwater temperature can easily be measured although precaution must be taken to assure that the recorded temperature is representative the water in the aquifer and not influenced by the movement of water in the borehole (Anderson, 2005). Various analytical solutions such as 1-dimensional (1D), 2-dimensional (2D) and 3-dimensional (3D) and groundwater modelling are applied and improved to examine the behaviour of this subsurface temperature profiles (Bredehoeft & Papadopulos, 1965; Taniguchi, 1993; Shan & Bodvarsson, 2004; Colombani *et al.*, 2016; Irvine *et al.*, 2017; Kurylyk *et al.*, 2017).

Bredehoeft and Papadopulos (1965) asserted that analytical solution has often been used to estimate vertical fluxes in aquifers e.g. (Stallman, 1965; Cartwright, 1970; Lu & Ge, 1996; Ferguson *et al.*, 2003). The type curves estimate 1-dimensional (1D) groundwater fluxes based on a steady state heat conduction-advection equation. Another 1D analytical solution of transient heat and steady water flow is proposed by Carslaw and Jaeger (1959). This analytical solution was applied by (Taniguchi *et al.*, 1999a; Taniguchi *et al.*, 1999b; Taniguchi, 2002; Taniguchi *et al.*, 2003a; Majumder *et al.*, 2011; Majumder *et al.*, 2013) to analyse the vertical fluxes based on the temperature-depth (*T-z*) profiles. 2D subsurface thermal regime with groundwater flow was studied by Domenico and Palciauskus (1973). Their type curves show that temperature-depth profiles with downward water fluxes are concave (recharge area) while with upward fluxes are convex (discharge area) and the undisturbed thermal gradient would be constant without vertical fluxes as shown in Figure 2.5. Taniguchi *et al.* (1999a) illustrated that the thermal regime in vertical 2D cross section under both effects of surface warming and regional groundwater flow (e and f).

Lu and Ge (1996) extended the Bredehoeft and Papadopulos (1965) theory by including the horizontal heat and fluid flow in the horizontal direction in the semi-confining layer of aquifer. Results showed that the horizontal heat and fluid flow have a negligible effect on the vertical temperature distribution (less than 10% of vertical) but became apparent near recharge and discharge area (>30% of vertical). The effect is largest if vertical leakage rate is high.

Taniguchi *et al.* (1999a) studied on vertical groundwater fluxes under the condition of a linear in surface temperature of 2.5 C during the past 100 years at Tokyo metropolitan area. The subsurface thermal regime is represented by different vertical groundwater

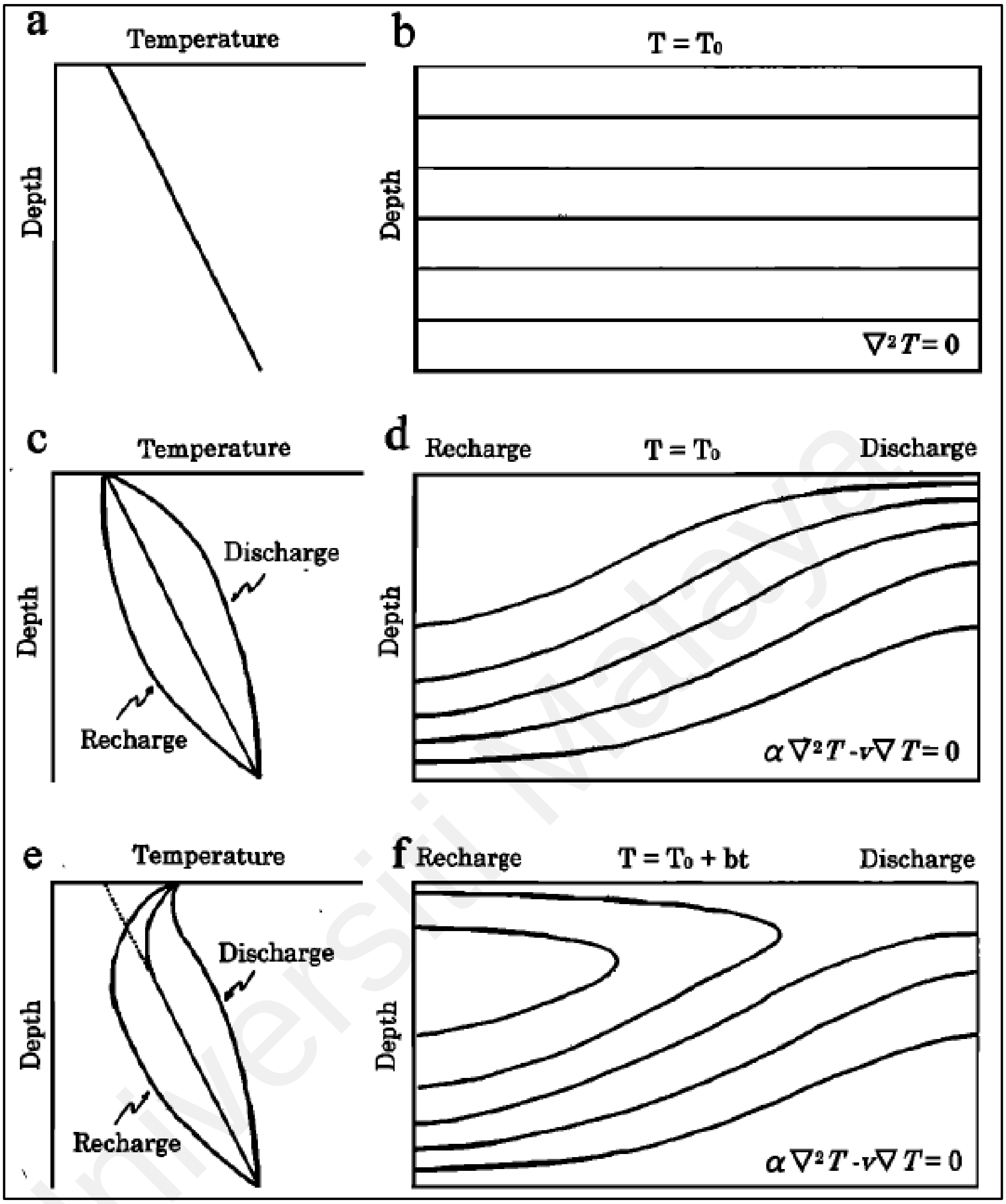

Figure 2.5: Schematic diagrams of the groundwater flow system and subsurface thermal regime under the condition of (a) and (b) no groundwater flow, (c) and (d) regional groundwater flow and (e) and (f) regional groundwater flow with surface warming. [from Taniguchi *et al.* (1999a)] use with journal permission

fluxes (0.37 to 0.67 m/yr and -0.4 to -0.6 m/yr) which indicates that thermal regime under the surface warming is mostly reflected by the regional groundwater flow system. Taniguchi *et al.* (2003a) had evaluated the groundwater flow system at Kumamoto Plain in combined with surface warming effect using the *T-z* profiles. Subsurface temperature increased during the last 15 years due to surface warming in the recharge area (mountain area with downward groundwater fluxes) and decreased in the discharge area (flat plain in western part with upward groundwater fluxes) because of decreasing in groundwater flow and recharge rates.

Majumder *et al.* (2013) revealed the existence of shallow and deep groundwater flow system at Bengal Delta aquifers using the observed-calculated *T-z* profile. The wells in the northern area are recharge type while southern area are discharge type wells. 2D cross section shows that shallow groundwater temperature in discharge area is higher than the northern recharge area. Shallow wells have recharged ranging from 0.04 to 1.35 m/yr and discharge ranging from -0.2 to -0.79 m/yr while deep wells give recharge from 0.05 to 0.16 m/yr and discharge of -0.15 m/yr, respectively.

2.3.4 Groundwater Modelling (GM)

The groundwater flow model has been widely used as a useful tool for professional hydrogeologists to solve the governing partial differential equations of groundwater flow, salute transport and heat transport processes for the past three decades (Sudhakar *et al.*, 2016; Hariharan & Uma Shankar, 2017; Pathak *et al.*, 2018; Panda & Narasimham, 2020). The groundwater flow system is numerically solved by applying the finite different method or finite element method. The modular finite-different flow model (MODFLOW) established by the United States Geological Survey (USGS) (McDonald & Harbaugh, 1988). The modular packages (boundary conditions and solution methods) are frequently updated and newly added to improve numerical simulation results unsaturated-saturated flow processes of aquifer system. Moreover, MODFLOW components are widely recognized by academicians and consulting firms around the world and it is easy to set up the pre- and post-process files. Like, Visual MODFLOW, the license is affordable for academic purposes.

However, Visual MODFLOW has a limitation to simulate complex geological features, inclined faults, and significant hydraulic gradients during rewetting or drying conditions. On the other hand, the finite element flow model, e.g. Finite Element subsurface FLOW System (FEFLOW) from the Institute of Water and Environment (DHI), numerically integrates complex geological structures and is able to handle the rewetting or drying cells. Much budget is required to afford the FEFLOW license, and it takes a long time to comprehend the application features and set up the conceptual model.

The available groundwater model softwares are Visual MODFLOW (Waterloo Hydrogeologic Inc.), (FEFLOW) by DHI, Groundwater Modelling Software (GMS) by Aquaveo, MIKE-SHE by DHI, SEAWAT by USGS, Groundwater Vistas by Environmental Simulations Inc. and others. The application of groundwater flow models have been used: (1) as interpretative tools for investigating groundwater system dynamics and understanding the flow patterns; (2) as simulation tools for analyzing responses of the groundwater system to stresses; (3) as assessment tools for evaluating recharge, discharge and aquifer storage processes, and for quantifying sustainable yield; (4) as predictive tools for predicting future conditions or impacts of human activities; (5) as supporting tools for planning field data collection and designing practical solutions; (6) as screening tools for evaluating groundwater development scenarios; (7) as management tools for assessing alternative polices; and (8) as visualization tools for communicating key messages to public and decision-makers (Zhou & Li, 2011).

Vishal *et al.* (2014) had successfully predicted the groundwater recharge using visual MODFLOW for National Capital Territory (NCT), Delhi. They divided the NCT into 9 zones for estimation of groundwater recharge. The variation of recharge zones is reflected to the diversity in geology and urbanization that influenced the overall recharge in the study area. Chen *et al.* (2013) applied MODFLOW and MODPATH to qualify the effects after a recharge area was polluted at the Choshuihsi Alluvial Fan. Contamination was distributed on the surface of shallow aquifer inside the recharge area. Results indicate that parts of particles flow into deep aquifer and parts of them flow into the distal-fan for 200 years simulation. Second aquifer was polluted the most because recharge to this aquifer is reliant on the lateral recharge from recharge area. The same goes for the third aquifer.

MODFLOW was used to evaluate the effect of the upland field on the groundwater recharge at Izena Island, Japan (Yuge *et al.*, 2005). The simulation results indicated that groundwater storage, when all forests are converted into the upland field, is larger than the groundwater storage under the present condition of land use. This result showed that the irrigation water in the upland field contributes to the ground water recharge and the water loss by the rainfall runoff and the evapotranspiration at the upland field is less than amount of the forest.

WetSpass and MODFLOW was successfully achieved to quantify the groundwater recharge in multilayer aquifer at northeastern Tunisia. Simulated spatial distribution of the groundwater recharge indicated that areas with low slope and with vegetation cover are characterized by high groundwater recharge (Ghouili *et al.*, 2017). Groundwater recharge and groundwater potential zones were successfully estimated using an integrated MIKE 11 and MIKE SHE models in the Mhinga, South Africa (Shamuyarira, 2017). The estimated recharge was very low around 0.42% of mean annual precipitation. The groundwater potential maps produced indicated that Mhinga is predominantly covered by regions with very low and low groundwater potentials which associated with type of geology.

To understand the importance of recharge areas, the development of recharge function as well as impact assessment of climate change on groundwater recharge were applied using the groundwater model (MODFLOW) and Global Climate model (GCM) in Ho Chi Minh City area (Ha & Koontanakulvong, 2015). The GCM was used to study the impact of climate change to groundwater recharge while MODFLOW was applied to estimate historical recharge as well as to simulate the groundwater flow under the impacts of climate change. The projected recharge shows that recharge will decrease in 2030s and increase again in the far future.

Yidana (2011) used MODFLOW incorporated in the GMS (Groundwater Modelling System) to build and calibrate a steady-state groundwater flow model for the Voltanian aquifer which consists of 5 different hydrostratigraphic units. The hydraulic conductivity and recharge were successfully calibrated even though the paucity of the data of these two parameters are critical.

Inverse modelling using numerical groundwater flow models is an alternative method of recharge estimation. This involves the inference of recharge through calibration or "history matching" (i.e., minimizing the discrepancy between field observations and corresponding model-generated outputs). The application of groundwater models in this context is appealing because of their ability to account for important nonlinear interactions between recharge, discharge, evapotranspiration and changes in groundwater storage (Sanford, 2002). Very few studies have been conducted on quantifying the contribution of different sources of recharge, including both natural and artificial recharge systems (Vazquez-Sune *et al.*, 2010)

Fu *et al.* (2018) created a forecast model on Visual MODFLOW and coupled with the established hydrogeological model using the groundwater management (GWM) process to evaluate the maximum exploitation potential of karst groundwater Yangzhuang Basin, China. The recharge enchancement measures were greening area and retaining dam construction. Their models show that the exploitation volume calculated by the non-stationary future precipitation series outperforms that by the historical precipitation series in prediction accuracy; the allowable exploitation volume should be determined as 258,000 m^3/d. By the most conservative estimate, the groundwater exploitation volume of the groundwater source fields can be maximized at 243,500 m^3/d.

2.4 Summary

In-depth literature review findings are summarised below:

a) Groundwater recharge is a main compenant of subsurface water system in the hydrologic cycle
b) Knowledge on groundwater recharge mechanism is crucial to understand the recharge sources, recharge flow path and and recharge rate to implement sustainable groundwater resources management in the basin for now and future needs
c) Literature focus on stable isotope of deutrium and oxygen-18, tritium, radon and hydrogeochemical as a method to understand the recharge flow by identifying the recharge source and process, grondwater age, water residence time, surface water-groundwater interaction and aquifer-aquifer interaction within the basin

d) Literature focus on CMB, WTF, TDP and GM(WB) methods as a suitability method used to quantify the recharge rate in the humid tropical area

e) Through the literature reviews related to (c) and (d), very few research studies on groundwater recharge mechanism in the country located at humid tropical area compared to the arid area.

CHAPTER 3: RESEARCH METHODOLOGY

3.1 Introduction

This chapter will describe the research materials and methodology used to answer the research objectives. This research begins with a desk study which includes searching and summarizing the related research literature reviews on groundwater recharge source, flow and rate, study area, data compilation related to meteorology, geology, hydrology and hydrogeology and converting data into ArcGIS database. All data were received with the permission from Air Kelantan Sdn. Bhd. (AKSB), Department of Mineral and Geoscience Malaysia (MGD), Department of Irrigation and Drainage Malaysia (DID), Malaysian Meteorological Department (MMD), Department of Agriculture (DOA) and registered with Global Network of Isotopes in Precipitation (GNIP) database as listed in Table 3.1

This was followed by a series of fieldworks to collect the water samples of rainwater, river water, groundwater and soil samples including field test measurement on selected parameters. Then, samples would be analysed accordingly depending on the research objectives. After completing the samples analysis, all results will be further analysed, visualised and interpreted using simple statistics and equations related to the methods used and related softwares. The expected output at the end of the research studies are able to help understanding the groundwater flow process, assess the groundwater recharge rate and construct a conceptual model of groundwater recharge for LKRB. The simplified research outline is shown in Figure 3.1.

Table 3.1: List of agency and type of data provided

Agency	Type of Data
AKSB	Information production wells design and groundwater abstraction rates
DID	Rainfall, river discharge, river stage
MMD	Rainfall, relative humidity, mean temperature and evaporation
MGD	Hydrogeology, monitoring wells information of wells design, water level, hydrochemistry, hydraulic properties and related reports
DOA	Land use
GNIP	Tritium

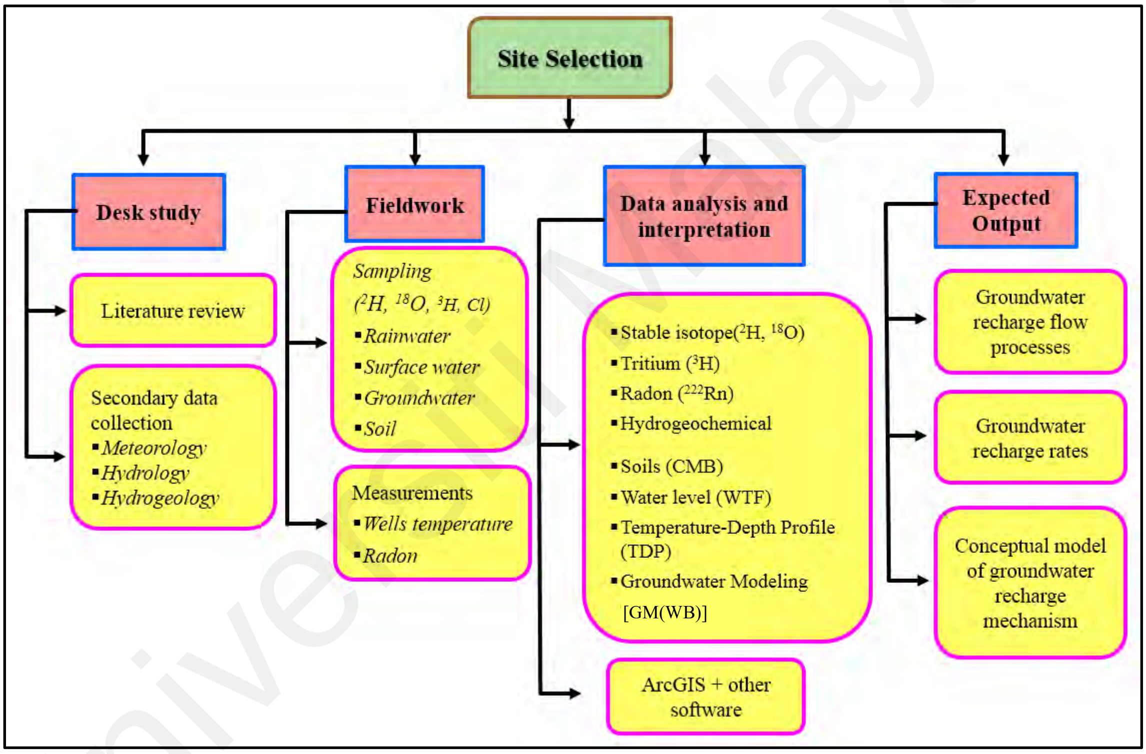

Figure 3.1: Research outline of groundwater recharge study

3.2 Sampling Locations

The sampling involved the collection of rainwater, surface water, groundwater and soil samples. Temporary rain gauge was installed at Kg. Puteh wellfield. The surface water sampling was taken from Kelantan River, Pengkalan Datu River, Kemasin River and Tok' Uban Lake. Groundwater samples were sampling from Department of Mineral and Geoscience Malaysia (MGD) wells, Air Kelantan Sdn. Bhd. (AKSB) wells and dug wells belong to local people. Soil samples were collected around Kota Bharu areas. The sampling campaign was carried out between 2012 to 2015 which included dry and wet seasons. Figure 3.2 shows the sampling location while Table 3.2 summarised the sampling locations and type of samples collected during the sampling campaign.

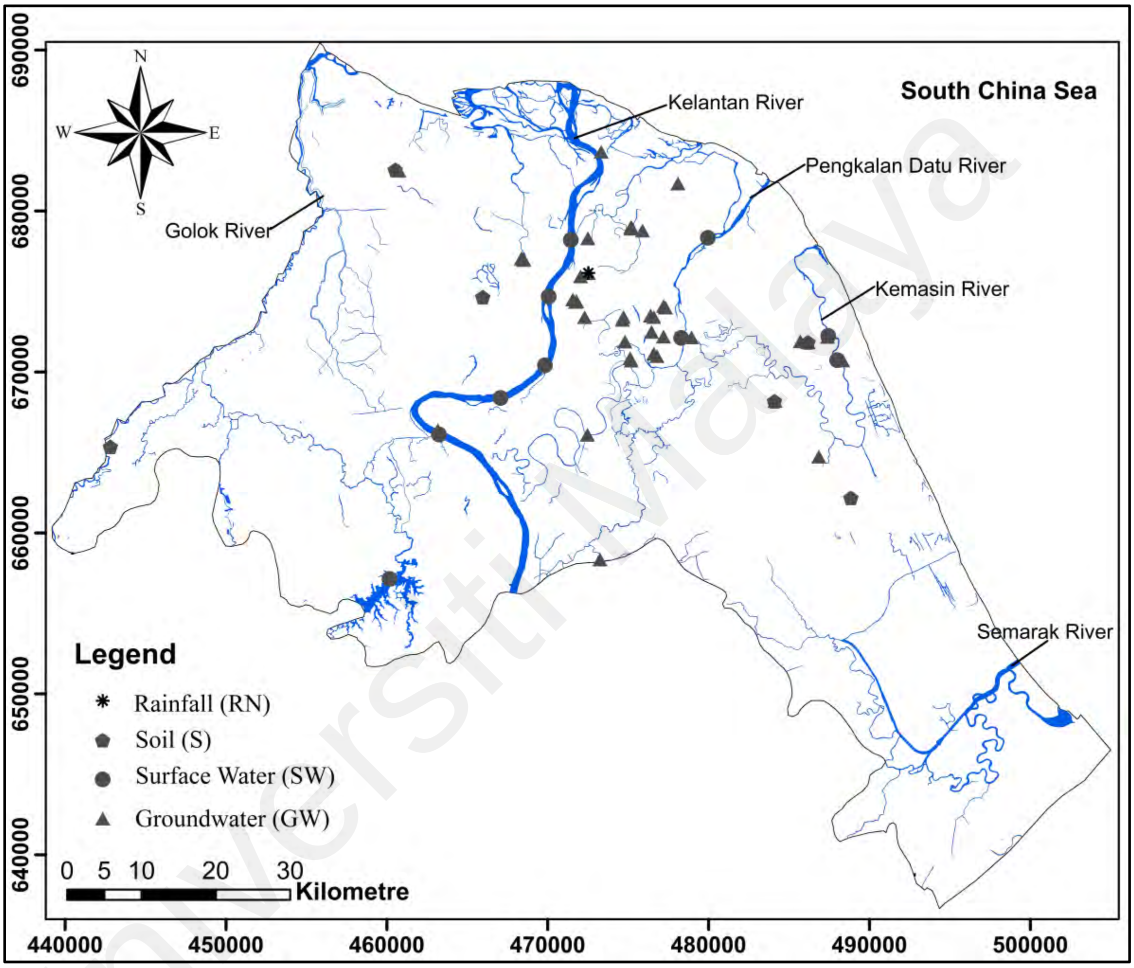

Figure 3.2: Sampling location of rain, river, groundwater and soil samples

Table 3.2: Detail samples collected during sampling campaign

Code	Location	X	Y	Depth (m)	Aquifer Layer	SI	TH	RN	WC	CMB	WTF	TDP
	Rainfall	472532	676139			√		√				
SW1	Kelantan-Tmbtn Diraja	471441	678198			√	√	√				
SW2	Kelantan-Kelar	463244	666114			√	√	√				
SW3	Tok Uban	460175	657145			√						
SW4	Kemasin-Pnkln Baru(M2)	487447	672236			√	√	√				
SW5	Kemasin-Telok(M3)	488000	670733			√	√	√				
SW6	Pnkln Datu-Panchor(D2)	479964	678333			√		√				
SW7	Pnkln Datu-Binjai(D3)	478303	672111			√		√				
SW8	Kelantan - Pintu Geng(PTG)	470064	674682			√		√				
SW9	Kelantan - Tendong(TDG)	469835	670407			√		√				
SW10	Kelantan - Markasar(MKR)	467074	668385			√		√				
GW1	Kg. Puteh Wf (Well # 9)	472532	676139	14.88	L1	√	√	√				
GW2	Pintu Geng Wf (Well# 7)	471724	674352	13.7	L1	√		√				
GW3	Pintu Geng Wf (Well# 3)	471723	674352	13.72	L1	√						
GW4	Pintu Geng (KB49)	471550	674500	13.7	L1	√	√					
GW5	Ketereh	473254	658352	11.4	L1	√		√				

Table 3.2, continued.

Code	Location	X	Y	Depth (m)	Aquifer Layer	SI	TH	RN	WC	CMB	WTF	TDP
GW6	Wakaf Bharu (Pw#2)	468526	676957	11.28	L1	√						
GW7	Wakaf Bharu (Pw#6)	468370	677064	16.46	L1	√						
GW8	Wakaf Bharu Pw8	468472	677006	15.06	L1	√	√	√				
GW9	Wakaf Bharu (Pw#9)	468357	677044	14.02	L1	√		√				
GW10	Kubang Kerian (Well#1)	476597	673406	15.5	L1	√		√				
GW11	Pasir Hor Pw5	474653	673232	22.56	L1	√	√	√				
GW12	Penyadap Pw5	474803	671889	20.78	L1	√	√	√				
GW13	Kubang Panjang (Dw)	460758	682495	5.0	L1	√	√					
GW14	Kg Teluk Dw1	488338	670711	2.49	L1	√	√	√				
GW15	Kedai Buloh Dw	473328	683670	5	L1	√						
GW16	Kg Pengkalan Baru Dw	487403	672177	1.55	L1	√		√				
GW17	Tanjung Mas Wf (KB10)	475174	678991	35	L2	√	√	√				
GW18	Kg. Chap, Bachok (Rw)	484132	668195	31.32	L2	√	√	√				
GW19	Pengekalan Chepa Wf (KB5)	478100	681700	30	L2	√	√					
GW20	Kenali (Well#2)	477322	673999	33.69	L2	√	√	√				
GW21	Seribong Pw4	475189	670706	36.27	L2	√	√	√				

Table 3.2, continued.

Code	Location	X	Y	Depth (m)	Aquifer Layer	SI	TH	RN	WC	CMB	WTF	TDP
GW22	Pasir Tumboh Pw2	476793	670982	42.27	L2	√	√	√				
GW23	Beris Kubor KB 35	485700	671900	29.2	L2	√	√					√
GW24	Kelar Pw1	463171	666389	44	L2	√	√	√				
GW25	Kg. Puteh Wf (Well # 3)	472524	676136	91.44	L3	√						
GW26	Tanjung Mas Wf (KB6)	475200	678900	42.68	L3	√	√					
GW27	Tanjung Mas Wf (PW#1)	475227	678959	79.27	L3	√	√					
GW28	Chicha Tm (PW#3)	477200	672191	91.44	L3	√	√	√				
GW29	Perol Wf (Well#3)	472469	666099	65.5	L3	√	√	√				
GW30	Pengekalan Chepa Wf (KB1)	478100	681700	114	L3	√	√					
GW31	Pengekalan Chepa Wf (KB4)	478100	681700	64	L3	√	√					
GW32	Kubang Kerian (KB25)	476400	673500	59.4	L3	√	√					
GW33	Beris Kubor (KB 31)	486188	671836	131.4	L3	√	√	√				√
GW34	Jln Merbau (KB15)	472500	678300	66	L3	√	√					
GW35	Jln Merbau (KB18)	472500	678300	150	L3	√	√					
GW36	Kg Puteh -W1	472524	676137	91.44	L3			√				
GW37	KB24	486855	664739	9.4	L1				√		√	

Table 3.2, continued.

Code	Location	X	Y	Depth (m)	Aquifer Layer	SI	TH	RN	WC	CMB	WTF	TDP
GW38	KB27	476400	673500	14.4	L1				√		√	
GW39	KB30	471743	674360	14.2	L1				√		√	
GW40	KB37	477203	674100	13	L1				√		√	
GW41	KB39	478943	672145	17	L1				√		√	√
GW42	KB42	474711	673407	12	L1				√		√	
GW43	KB43	475126	670852	16.1	L1				√		√	√
GW44	KB44	476599	671137	15.5	L1				√		√	
GW45	KB45	476453	672484	15	L1				√		√	
GW46	KB47	472300	673400	15	L1				√		√	
GW47	KB49	471792	674386	15	L1				√		√	√
GW48	KB51	475894	678784	14.6	L1				√		√	
GW49	KB53	472048	675934	14.5	L1				√		√	
GW50	KB57	475211	678947	12	L1				√		√	
GW51	KB32	486188	671836	101.2	L3							√
GW52	KB33	486188	671836	83.4	L3							√
GW53	KB34	486188	671836	44.4	L2							√

Table 3.2, continued.

Code	Location	X	Y	Depth (m)	Aquifer Layer	SI	TH	RN	WC	CMB	WTF	TDP
GW54	KB2	478100	681700	91	L3							√
GW55	KB3	478100	681700	73	L3							√
GW56	KB17	472500	678300	88	L3							√
GW57	KB38	477300	675800	17	L1				√			
GW58	KB40	480000	675900	21.3	L1				√			
GW59	KB41	474300	671500	18.2	L1				√			
GW60	KB46	473700	674100	15	L1				√			
GW61	KB48	471900	671100	18	L1				√			
GW62	KB52	477100	677500	23	L1				√			
GW63	KB54	471700	676600	15	L1				√			
GW64	KB55	470200	676900	13.5	L1				√			
GW65	KB59	471900	676200	12	L1				√			
GW66	KB60	471900	676200	14	L1				√			
GW67	KB61	478150	681700	8	L1				√			
GW68	KB68	478700	678300	15.5	L1				√			
GW69	KB69	474900	677400	10.5	L1				√			

Table 3.2, continued.

Code	Location	X	Y	Depth (m)	Aquifer Layer	SI	TH	RN	WC	CMB	WTF	TDP
S1	Alor Pulai	488855	662175							√		
S2	Kg Chap	484105	668179							√		
S3	Beris Kubor	486182	671836							√		
S4	Pengkalan Chepa	478121	681483							√		
S5	Kubang Panjang	460527	682550							√		
S6	Bunut susu	465966	674647							√		
S7	Lati	458904	677573							√		
S8	Gelang Mas	458939	676969							√		
S9	Kedai Tanjung	454384	671459							√		
S10	Rantau Panjang	442823	665349							√		

SI: stables isotopes; TH: tritium; RN: radon; CMB:chloride mass balance; WTF:water level fluctuation; TDP:temperature depth profile

3.3 Sampling Methods

Rainwater, surface water and groundwater were collected accordingly to the need of analysis at each sampling locations. Rainwater was collected using simple and temporary rain gauge of 25 L. Parffin oil used to prevent evaporation of rainwater. Surface water was taken using the bucket/von Dorn sampler at depth 6 to 10 cm below the water surface as in Figure 3.3. Groundwater from wells were purged with submersible pump by removing three volumes of water or until the electrical conductivity (EC) reading gives a constant value (Figure 3.4) to assure only representative samples were collected for further analysis in laboratory. The sampling techniques were performed according to the Victoria EPA (2009) and IAEA (2014) guidelines and also procedures in Hashemi *et al.* (2013).

Stable isotopes sample was filled into a 30 mL dark glass bottle without air bubble and closed with an air tight cap as shown in Figure 3.2 (red cap dark glass bottle). Tritium sample was filled into a 1L polyethylene botte also without air bubble and closed with an air tight cap as shown in Figure 3.3 (white square bottle). Radon as in Figure 3.5 was measured on site and water sampling for radon was usually done with utmost care as there was possiblity of radon gas getting released from water under agitated condition (Najeeb *et al.*, 2014).

Soil samples were taken using hand auger (25 cm depth) and core boring (50 cm depth) samples as shown in Figure 3.6. All samples were taken up to water table of unsaturated zone. The samples from hand auger were sealed in polyethylene bags while the core samples were sealed using wax at the top and bottom of the cores to maintain the moisture. The collected water samples and soil samples were preserved, and stored accordingly to the requirement for further analysis of stable isotopes (^{18}O and ^{2}H), tritium (^{3}H), and radon (^{222}Rn) and chloride (Cl).

The subsurface wells temperatures of shallow and deep aquifer were measured by deploying the water level - temperature meter (RST, Germany) into the wells as shown in Figure 3.7. This meter has an accuracy of 0.01 ºC and 0.01 m. The subsurface temperatures were measured and recorded at 1 m depth interval.

Figure 3.3: Surface water sampling using von Dorn sampler and bucket

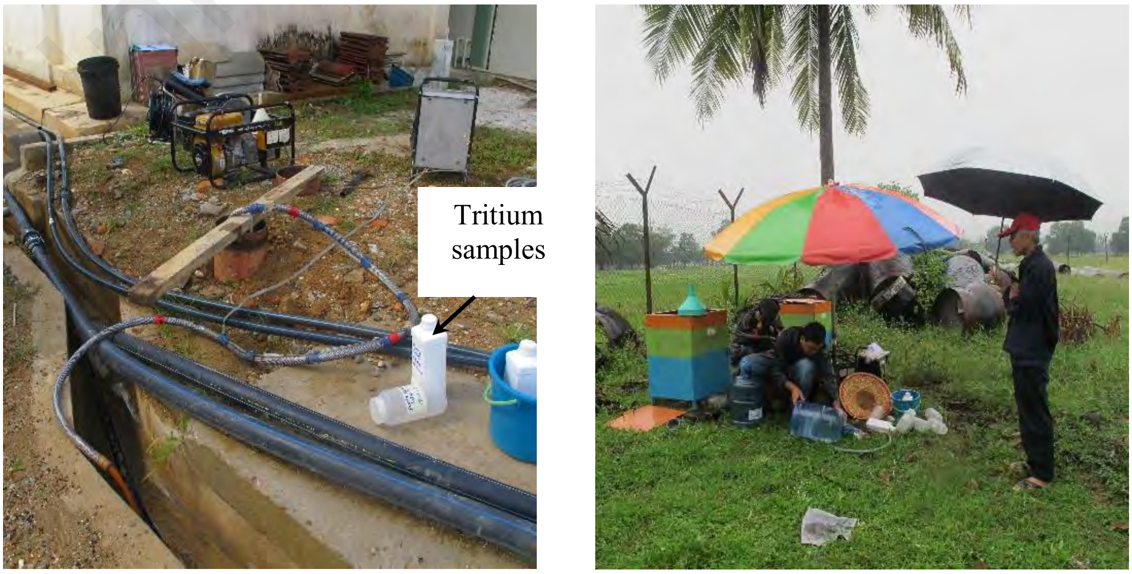

Figure 3.4: Groundwater sampling (well purging followed by collecting water samples)

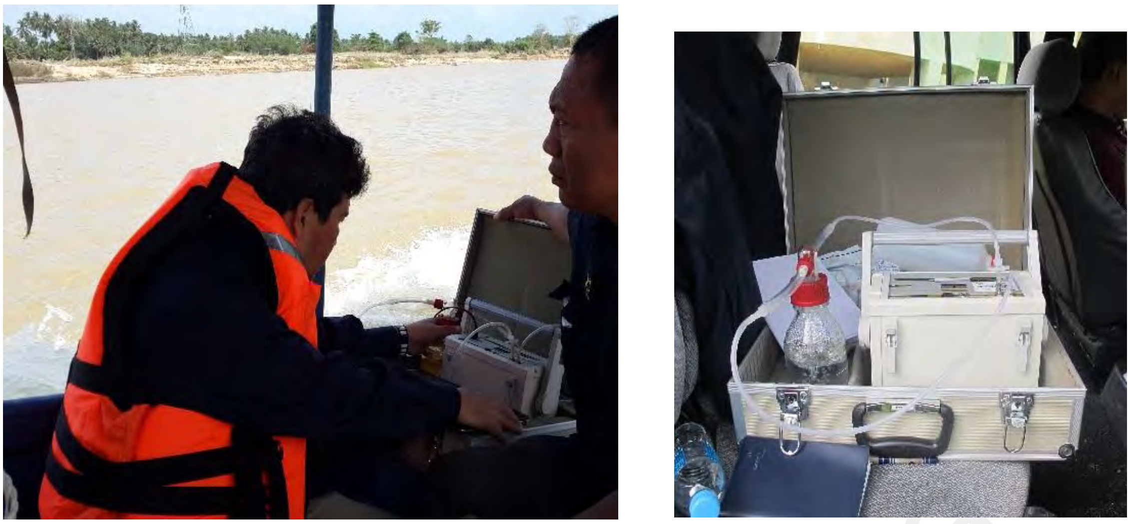

Figure 3.5: Radon measurement during sampling campaign

Figure 3.6: Soil sampling using hand auger and core boring

Figure 3.7: Temperature-depth measurement during sampling campaign

3.4 Samples Analysis

Chloride concentration in rainwater measured at LRA Kg. Puteh laboratory and at the Department of Geology, University of Malaya using Ion Chromatography (Metrohm, Switzerland).

Stable isotopes (SI) were determined using SERCON GEO 20-20 Continous Flow Isotope Ratio Mass Spectrometer (CF-IRMS) at IRMS Laboratory, Malaysian Nuclear Agency, Bangi, Selangor. All isotopic results were reported as the δ-notation ($^{0}/_{00}$) relative to SMOW (Standard Mean Ocean Water) standard. The precisions for oxygen-18 ($\delta^{18}O$) and deuterium ($\delta^{2}H$) data were ± 0.2 $^{0}/_{00}$ and ± 1 $^{0}/_{00}$, respectively.

For tritium analysis, water samples were courier to Hydrosys Labor Kft., Budapest, Hungary (IAEA laboratory) for analysis. The tritium (^{3}H) analysis procedure is based on the principal of selective isotopic enrichment using electrolysis. The volume of the water samples was reduced from 250 ml / 800 ml to 14 - 15 ml by using electrolytic enrichment system, factor of tritium enrichment was about 15-16 or 30-35. The tritium activity of enriched water samples was counted by liquid scintillation analyser with lower detection limit of > 0.2 TU. Standard reference material of SRM 4361C H-3 radioactivity standard was used for the quality control test.

Radon concentration was analysed onsite within 2 hours of samples collection without any air bubble during sampling processes. Radon was analysed using a radon in air monitor RTM1688-2 (SARAD GmbH, Germany) connected with 500 mL bubbling flask to create a close-loop aeration. The concentration of radon was not measured directly, but rather the radioactivity it produced. Radon concentration in water is usually expressed in Becquerel per cubic meter (Bq/m^3) or Becquerel per litre (Bq/L). Radon air monitor was calibrated before used and was set up into ‘Fast’ mode with analysis confidence interval sigma 2 (95.45%).

The soil samples in steel core were removed at the Department of Civil Engineering, then were slices at 10 cm each. Gravimetric-moisture content was determined by drying the soil at 105°C for 48 hours. Dry soil samples were separated for; 1) grain size analysis and 2) chloride concentration analysis. Grain size analysis was performed according to the BS1377 (1990) method using a mechanical sieve apparatus to determine the distribution of the coarser particles. The fine particle (< 63 micron) content was analysed using MALVERN MasterSizer (Malvern Instruments Ltd, UK). For chloride analysis, the dry soils needed to be grained to produced homogenised samples using pastel and mortar and automatic grinder (Retsch, Germany). Ultra-pure water (UPW) was added to the grained soil samples in a 1:1 or 2:1 ratio. Samples then were agitated on a reciprocal shaker table for 8 hours. This was followed by samples into a centrifugatione at 5,000 rpm for 10 minutes at the Department of Mechanical Engineering. This procedure was done accordingly (Scanlon, 1991). The supernatant was filtered through 0.45 µm filters chloride concentration was analysed using ion chromatography (Metrohm, Switzerland).

3.5 Quality Assurance and Quality Control (QA/QC)

Quality assurance (QA) is all of the actions, procedures, checks and decisions undertaken to ensure the accuracy and reliability of analytical results while quality control’ (QC), integral to laboratory analysis activities (Victoria EPA, 2009). Samples were handled with care to avoid any cross contamination. Ultrapure water (UPW) was used to rinse the meter probe and laboratory apparatus, to dilute samples and prepared standard solutions for analysis. During sampling campaign, duplicate samples were collected for laboratory analysis. Orion Star A329 portable multimeter (Thermo Fisher

Scientific, USA) and Radon monitor RTM1688-2 (SARAD GmbH, Germany) was used to measure radon on-site. The equipment was calibrated following the calibration manual before sampling. Water level-temperature meter (RST, Germany) was calibrated by factory. Laboratory analysis of chloride ion and soil particle sizes using ion chromatography (Metrohm, Switzerland) and MALVERN MasterSizer (Malvern Instruments Ltd, UK) were also calibrated following the calibration manual of the equipments. Isotope analyis of ^{2}H, ^{18}O and ^{3}H was sent to the accredited laboratory registered under IAEA at Malaysian Nuclear Agency, Bangi, Selangor and Hydrosys Labor Kft., Budapest, Hungary. In order to guarantee the quality of data presented in this research study, all techniques and procedures applied during the sampling campaign and samples preparation and analysis in laboratory strictly followed the standard. This standard included the standard operating procedures (SOP), instrumentation calibration with standards, reagent blanks analysis and analysis of replicates.

Secondary data were reviewed for adequacy relative to stated acceptance criteria. This assessment utilized various methods including statistical analysis for completeness, comparison against field verified data and through metadata review. Data sources were selected based on relevance, completeness, accuracy, quality and the age of the data.

3.6 Groundwater Recharge Estimation Methods

3.6.1 Chloride Mass Balance (CMB)

The chloride mass balance (CMB) technique assumes that the chloride ion behaves conservatively and is not easily affected by reactions through an unsaturated zone to the saturated zone. If this assumption is valid, it follows that the chloride ion can adequately trace groundwater recharge processes and can thus provide reasonable estimates of groundwater recharge. Its reliability therefore hinges on the compatibility of the precipitation event that recharged the system under the study and recent precipitation (Mensah *et al.*, 2014). The only source of chloride in soil and groundwater is assumed from precipitation and not from weathering or anthropogenic sources (Gaye & Edmunds, 1996). The CMB methodology has been widely tested and regarded as one of the most reliable method for estimating groundwater recharge in regional hydrogeological studies and basin wide groundwater resources assessments (Wood & Sanford, 1995; Bazuhair & Wood, 1996; Subyani, 2004; Dassi, 2010). Estimation of aquifer recharge rate (R) by the CMB method is determined as follow :

$$R = P * (Cl_P/Cl_{uz}) \tag{3.1}$$

Where, R is recharge (mm/year); P is annual average rainfall (mm/year); Cl_P is the weighted average of chloride concentration (mg/L) in rainfall and Cl_{uz} is the average chloride concentration in pore water of the unsaturated zone profile (mg/L) and or in groundwater. The weighted average (Cl_P) was calculated according to the following equation:

$$Cl_P = P_1 \text{ x } C_1 + \ldots\ldots. + P_n \text{ x } C_n / (P_1 + \ldots\ldots\ldots + P_n) \tag{3.2}$$

Where, P_1 is the first rainfall event (mm) and C_1 is the corresponding chloride concentration in the rainfall (mg/L) in the area for 1 to n events. To determine the weighted chloride average for each hydrological year, the chloride concentration of each rainfall event is first multiplied by the amount of rainfall. The summation of these individual components is then divided by the total annual rainfall.

3.6.2 Water Table Fluctuation (WTF)

The water table fluctuation method is used to estimate groundwater recharge in saturated zone from groundwater level time series data. This WTF is based on the premise that rises in groundwater levels in unconfined aquifers are due to recharge water arriving at the water tables (Healy, 2010). The recharge is calculated from:

$$\Delta S_{gw} = R = S_y \frac{\Delta h}{\Delta t} \tag{3.3}$$

ΔS_{gw}: changes in storage;

R: recharge;

S_y: specific yield;

Δh: changes in water table;

Δt: period of time interval

The graphical approach was used to determine the groundwater level rise (Δh) as shown in Figure 3.8. The equation assumes that the water arriving at the water table goes immediately into storage and all other water-budget components are zero during the period of recharge. For each individual water level rise, an estimation of total or gross recharge will be generated. To determine the total recharge, Δh is set equal to the difference between the peak of the rise and low point of the extrapolated antecedent recession curve at the time of peak. The difference between recharge and net recharge in subsurface storage is equal to the sum of evapotranspiration from groundwater, baseflow and net subsurface flow from the site. The antecedent recession curves are extrapolated manually based on visual inspection of the entire data set. This approach involves more subjectivity and different users with no doubt, would produce slightly different recession curves (Delin *et al.*, 2007).

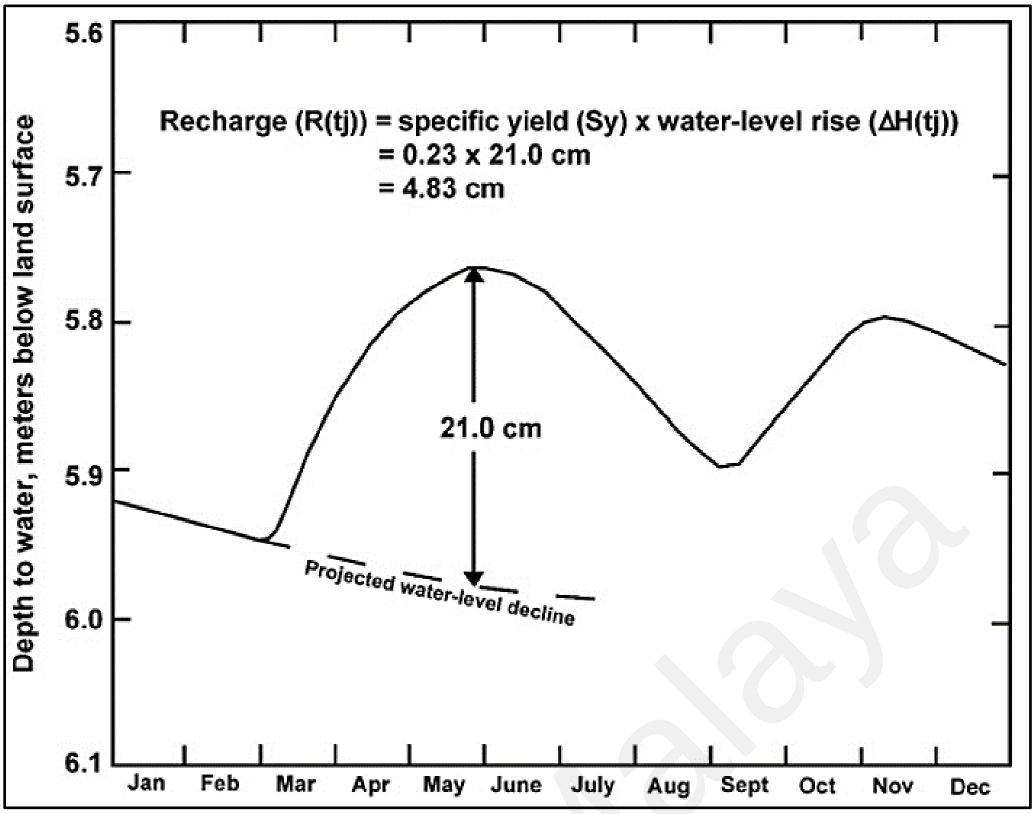

Figure 3.8: Graphical approach of WTF for estimating groundwater recharge (Delin *et al.*, 2007) use with journal permission

3.6.3 Temperature-Depth Profile (TDP)

Heat in subsurface layers is principally distributed by conduction and advection caused by recharging or discharging water flow. The upward heat from the interior is influenced by the high aquifer temperature compared to the ground surface temperature. Under the condition of a linear increase in subsurface temperature, the analytical solution for one-dimensional heat conduction-convection (Carslaw and Jaeger, 1959) is applied as in the Equation 3.4.

$$T(z,t) = T_o + T_G(z+Ut) + \{(b+T_G)/2U\}\left[(z+Ut)e^{\frac{Uz}{\alpha}} \times \right.$$

$$\left. erfc\left\{(z+Ut)/2(\alpha t)^{\frac{1}{2}}\right\} + (Ut-z)erfc\left\{(z-Ut)/2(\alpha t)^{\frac{1}{2}}\right\}\right] \quad (3.4)$$

Where T denotes the temperature, z represents the depth from the surface (positive downward), t is the time after semi-equilibrium condition (Taniguchi *et al.*, 1999a, b) and considered as 100 years, T_o is the surface temperature at $t = 0$, T_G is geothermal gradient, b is the increase in surface temperature, $U = vc_o\rho_o/c\rho$ where v is the vertical groundwater flux, $c_o\rho_o$ is the heat capacity of water, and $c\rho$ is the heat capacity of the aquifer), *erfc* is the complementary error function and α is thermal diffusivity. The modelling is limited to semi-infinite layers with only vertical conduction and convection, and vertical groundwater flux is assumed to be constant with depth.

3.6.4 Groundwater Modelling

The groundwater model of Visual MODFLOW Classic Interface 4.6.0.168 from Waterloo Hydrogeologic will be used to analyse the recharge rate. This numerical model is based on (Harbaugh, 2005) groundwater flow equation as written below:

$$\frac{\partial}{\partial x}\left(K_{xx}\frac{\partial h}{\partial x}\right) + \frac{\partial}{\partial y}\left(K_{yy}\frac{\partial h}{\partial y}\right) + \frac{\partial}{\partial z}\left(K_{zz}\frac{\partial h}{\partial z}\right) + Q' + R = S_s\frac{\partial h}{\partial t} \tag{3.5}$$

where, K_{xx}, K_{yy} and K_{zz} are values of hydraulic conductivity along the x, y and z coordinate axes which are assumed to be parallel to the major axes of hydraulic conductivity (L/T); h is the piezometric head (L); Q' is a volumetric flux per unit volume representing sources and/sinks of water, with $Q' < 0.0$ for flow out of the groundwater system and $Q' > 0.0$ for flow into the system (T^{-1}); Ss is the specific storage of the porous materials (L^{-1}) and t is time (T).

Figure 3.9 shows the regional LKRB boundary that will be used as a model area in the simulation. The model boundary extends to the coastline from the north to southeast, Sg. Golok along the border with Thailand from west to north and quaternary formation boundary from west to south.

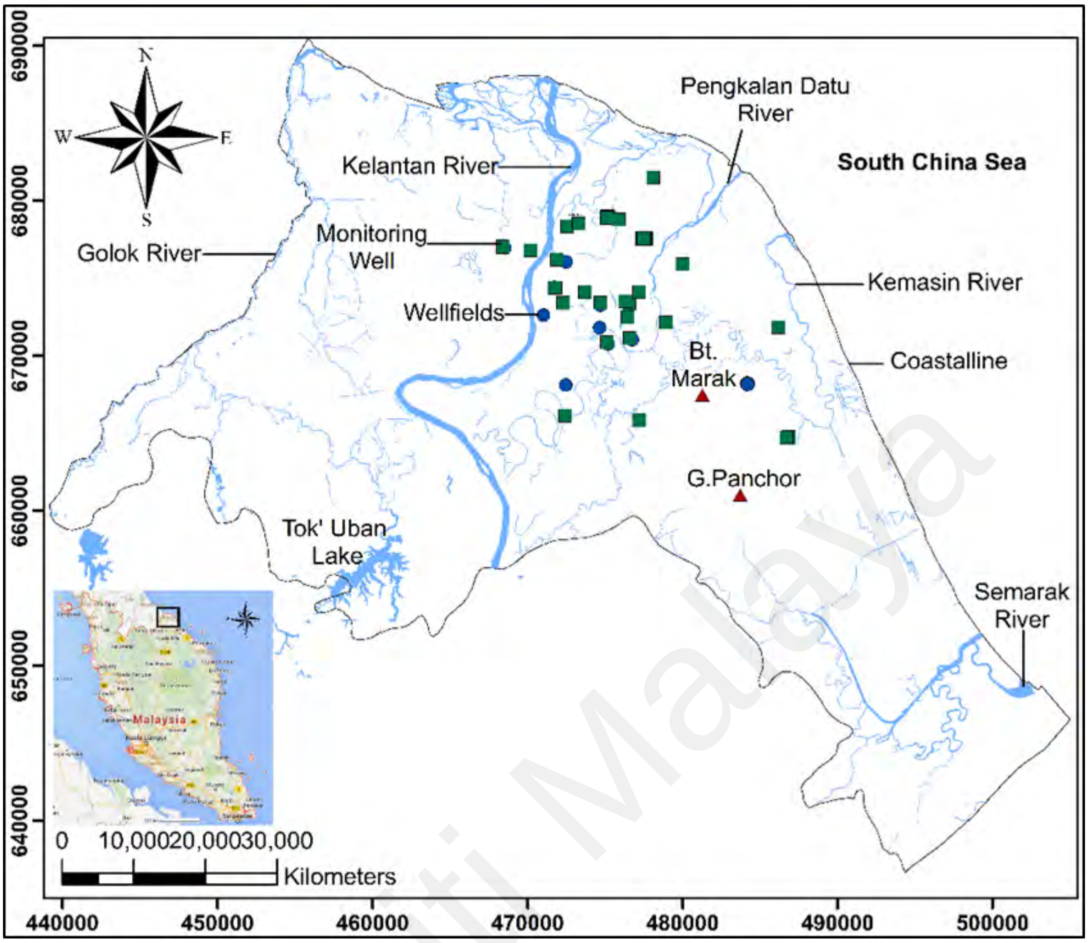

Figure 3.9: Regional model area of LKRB

3.6.4.1 Conceptual Model

A conceptual model is a pictorial representation of the groundwater flow system in the form of a block diagram or a cross section (Anderson & Woessner, 1992). It is design to simplify the actual system by including hydrological, hydrogeological and hydrochemical within generalized boundary conditions (Zhou & Herath, 2017). Understanding the conceptual model will help over or under simplification of the model since the hydrogeological system is complex. The stratigraphy conceptual model by Sofner (1992) as shown in Figure 4.12 will be applied as a base for groundwater modelling. Details on hydrogeology is described briefly in Section 4.6.

3.6.4.2 Model Discretization

Model grid

The model area discretization consist of 155 columns and 144 rows is presented in Figure 3.10 with four layers as shown in Figure 3.11. The general grid sizes are 1000 m x 1000 m. The grid was refined into 250 m uniform spacing between nodes around the active pumping wellfields and 10.5 m uniform spacing between nodes in the area around Kg. Chap and Pintu Geng wellfields. The grid spacing was refined into smaller grid size especially near the area of interest. The 3D distribution of aquifer stratigraphic units representing the natural heterogeneous condition of the aquifer system in the numerical simulation is presented in Figure 3.11. The whole aquifer system consists of four main aquifer units proposed in the current numerical simulation. Unit 1 is represented the shallow unconfined aquifer with the fine to coarse sand materials and thickness ranging from 5 to 20 m. Unit 2 is the protective layer consisted of the silty clay materials and thickness ranging from 5 to 25 m. The deep aquifers composed of the mixed materials are divided into two, Unit 3a consisted of the gravely sand extending from the centre to southwest and thickness ranging from 5 to 35 m and Unit 3b is the medium to coarse sand with silty clay extending from the centre to the northeast i.e. coastal zone and thickness ranging from 5 to 35 m. Unit 4 is the confined aquifer with coarse sand and thickness ranging from 5 to 90 m.

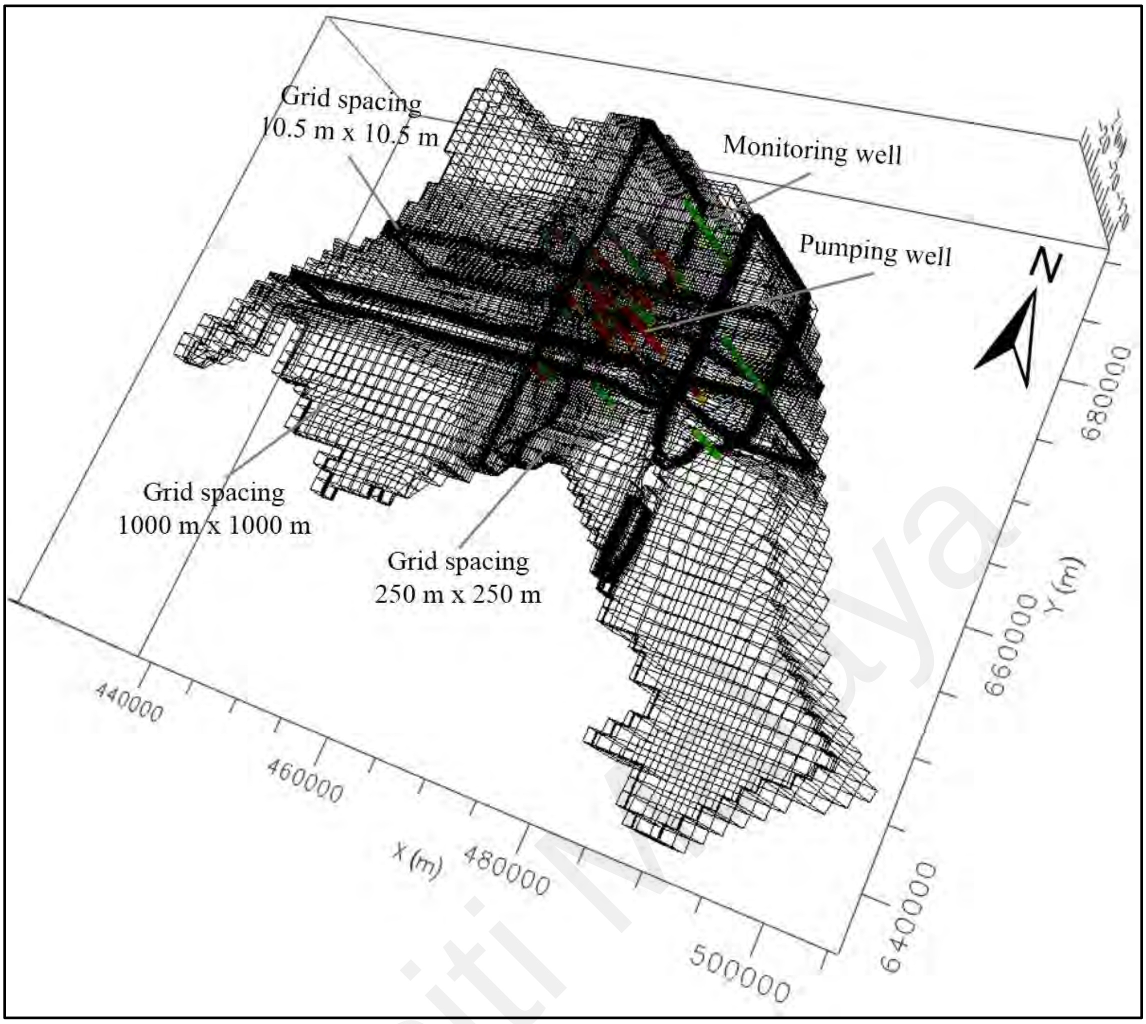

Figure 3.10: Variable spacing grid of model area

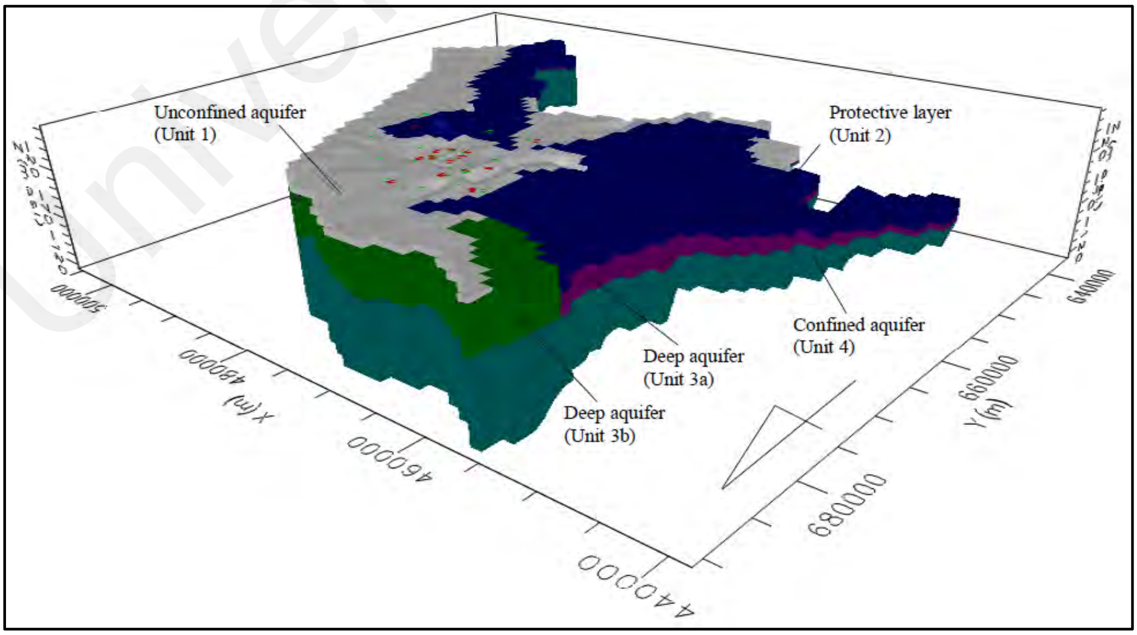

Figure 3.11: 3D distribution of the aquifer units represents the natural heterogeneous condition of the aquifer system in the numerical simulation. The vertical unit is in meter above sea level (m. ASL)

Boundary Conditions

In the numerical simulation, two types of boundary condition (BC) were assigned such as Dirichlet-type BC (Constant head BC) and Neumann-type BC (Recharge BC, river BC, and no-flow BC). As in Figure 3.9, the South China Sea in the northeastern boundary of the modeled area was assigned as constant head BC as well as Lemal River connected to Tok' Uban Lake. River BCs were assigned at the western side of the study area (Golok River) and rivers in the area, e.g. Kelantan River, Pengkalan Chepa River, Pengkalan Datu River, Kemasin River, Mulong River, Ketereh River, Semarak River, Lemal River, and Meranti River. All riverbed materials were suggested to have the hydraulic conductivity (Kr = 10^{-4} m/s). Tok' Uban Lake has been assigned as River BC with different value of riverbed conductivity ($Kr = 10^{-6}$ m/s) because it is an artificial reservoir where the bed materials are made of the protective unit (Unit 2). The southern part of the modeled area and both mountains were assigned as no-flow BC. For the recharge BC, it is recommended that the value between 5 to 20% of the annual rainfall as a reasonable percentage for the groundwater recharge (Waterloo Hydrogeologic, 2005).

Recharge BC was assigned accordingly to the available aquifer units that exposed on the ground surface which were zone 1 of Unit 1, zone 2 of Unit 2, and zone 3 of Unit 3b, respectively as shown in Figure 3.12. The recharge used in this groundwater modelling is estimated from water balance study by considering 11% of annual rainfall (MGD, 2014b). For this groundwater modelling works, recharge was estimated form the mean annual rainfall of 22 rainfall stations within LKRB as listed in Table 3.3. 11% of recharge was assigned for zone 1 while for zone 2 and zone 3 the percentage of recharge was lower than zone 1 depending on the hydraulic conductivity of the zones as tabulated in Table 3.4.

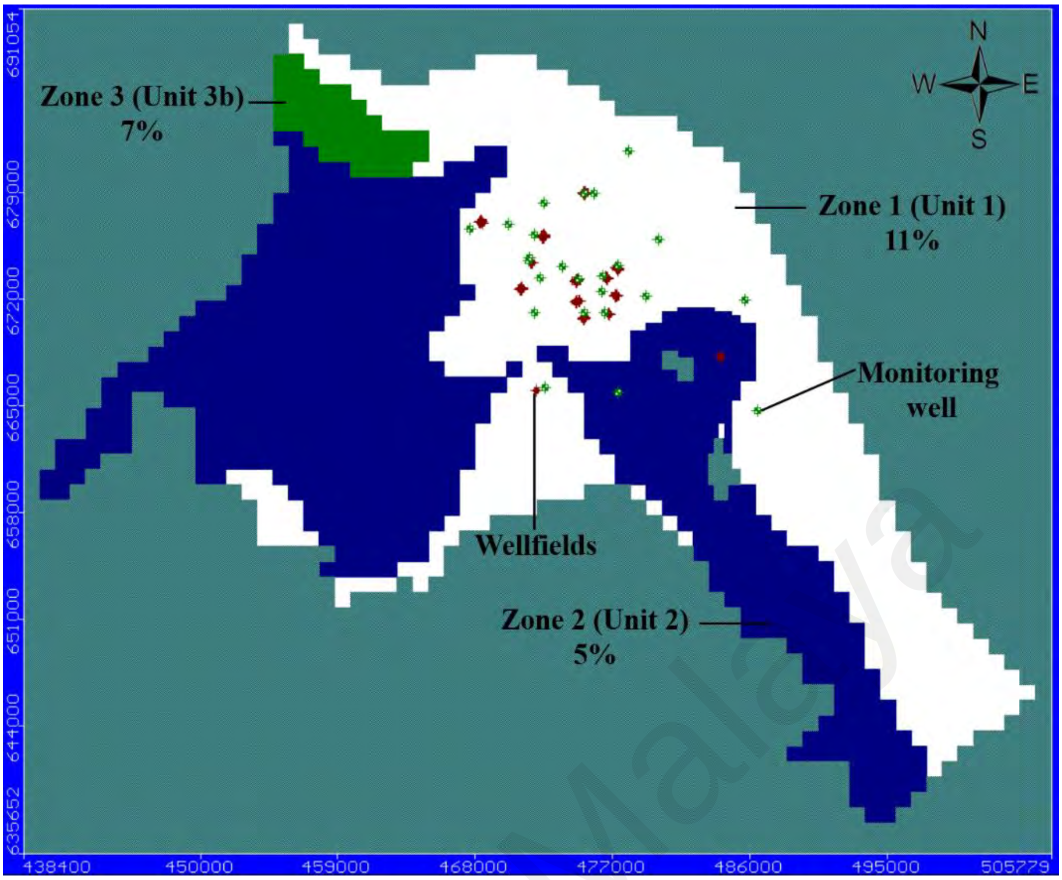

Figure 3.12: Distribution of recharge zones in the model

Hydraulic Parameters

The hydraulic conductivities are assigned accordingly to the units as in Figure 3.11. The range of hydraulic conductivity for each unit proposed by Sofner (1992) is listed in Table 3.5. The hydraulic conductivity will be adjusted during the calibration process.

Piezometer Heads and Groundwater Abstraction

The location of monitoring wells and wellfields is shown in Figure 3.9. In total forty-nine (49) piezometer head of MGD monitoring wells will be used with long-term record of 1989 to 2000. The total withdrawal of groundwater from 14 wellfields is approximately 256,777 m^3/d as tabulated in Table 3.6. The accumulated pumping rates are used in the model calibration processes.

Table 3.3: Annual rainfall received from rainfall stations at LKRB

Station Name	Agency	Period	Annual (mm/yr)
Kota Bharu	MMD	1989-2000	2619.52
Mardi Kubang Keranji	MMD	1989-2000	2826.74
Pusat Pertanian Bachok	MMD	1989-2000	2782.84
Pusat Pert. Lundang	MMD	1989-2000	2877.68
Pusat Pertanian Melor	MMD	1989-2000	2931.47
Pusat Pert. Pasir Mas	MMD	1989-2000	2858.32
Sg.Petai Pasir Puteh	DID	1998-2000	2858.83
Ibu Bekalan Tok' Uban	DID	1989-2000	2736.08
Stn. Pertanian Melor	DID	1989-2000	2944.07
Serdang, Gunong Barat Bachok	DID	1989-2000	2836.18
Tok Ajam	DID	1989-2000	3046.70
Rumah Kastam, Rantau Panjang	DID	1989-2000	2769.40
Rumah Pam Repek	DID	1989-2000	2434.06
Rumah Kerajaan JPS, Meranti	DID	1989-2000	2482.50
Chabang Tiga Pendek	DID	1989-2000	2647.02
Kg. Binjai	DID	1989-2000	2785.60
Teratak Pulai	DID	1989-2000	2550.79
Jab. Pertanian Bachok	DID	1989-2000	2655.53
Kuala Jambu	DID	1989-2000	2535.39
Kg. Kebakat	DID	1989-2000	2621.30
Stsn. Keretapi Tumpat	DID	1989-2000	2399.00
Stor JPS Kota Bharu	DID	1989-2000	2397.91
		Mean	**2708.95**

Table 3.4: Recharge zones assigned at LKRB

Annual rainfall	Unit 1	Unit 2	Unit 3b
2708.95 (mm/yr)	297.98	135.45	189.63
Recharge (% of annual rainfall)	11	5	7

Table 3.5: Hydraulic parameters of subsurface units

Unit	*Hydraulic Conductivity*(m/s)		*Effective Porosity (n)*	*Storage (S)*
	K_h	K_v/K_h		
1	$10^{-2} – 10^{-3}$	1/10	0.2 – 0.3	0.25 – 0.05
2	$10^{-6} – 10^{-8}$	1/10	0.02 – 0.05	-
3a*	$10^{-4} – 10^{-6}$	1/10	0.1 – 0.2	10^{-3}
3b	$10^{-5} – 10^{-7}$	1/10	0.05 – 0.15	10^{-3}
4	10^{-4}	1/10	0.2 – 0.3	10^{-3}

*K_{3a} possibly ranges from 30 to 123 m/d (Bachik, 1989)

Table 3.6: Wellfields properties and pumping rates included in the simulation

Location	Wellfield (number of wells)	X	Y	Cumulative Pumping rate (m^3/d)	Screen location
Wakaf Bharu	Wakaf Bharu (9)	468368	677011	23,188	Unit 1
Tanjung Mas	Tanjung Mas (8)	475202	678881	18,143	Unit 4
Chicha	Pasir Hor (7)	477186	672236	107,362	Unit 3a
	Penyadap (5)	474658	673127		Unit 3a
	Seribong (5)	474595	671817		Unit 3a
	P. Tumboh (2)	475145	670755		Unit 3a and 4
	Kubag Kerian (6)	476792	670979		Unit 1
	Kenali (5)	476587	673422		Unit 3a
	Chicha (4)	477361	674001		Unit 4
Kg. Puteh	Kg. Puteh (20)	472465	676057	73,670	Unit 1 and 4
	Kota (8)	470966	672597		Unit 3a
Pintu Geng	Pintu Geng (4)	471625	674357	19,334	Unit 1 and 4
Kg. Chap	Kg. Chap (4)	484131	668193	8,971	Unit 3a
Perol	Perol (1)	472000	666000	6,109	Unit 3a
			Total	**256 777**	

3.6.4.3 Model Calibration, Validation and Sensitivity Analysis

Model calibration was carried out under steady-state condition resulting in changes or refinement in the conceptual model. Model input parameters are changed to achieve a better representation of the physical system (ASTM, 2006) or other words to match the field conditions at a site so it is properly characterized. Calibration is run repeatedly following the standard trial-and-error method (Anderson & Woessner, 1992). After the model was calibrated, model was validated using a new data set to test the calibrated model.

A sensitivity analysis is performed during model calibration and during predictive analysis. It is a process to determine the effect of parameter variation on the model results by quantifying the uncertainties in the calibrated model caused by uncertainty in the estimates of aquifer parameters, stresses and boundary conditions. It is a method to identify the most influenced parameters on the model simulation and it helps to achieve a better calibration results that gives satisfaction to the modeller itself. This analysis will provide modeller with an understanding of the level of confidence in model results and it is used to identify data deficiencies (ASTM, 2006).

The performance of model calibration and sensitivity analysis were considered through the graphical fit between calculated heads and observed heads or statistical comparison of root mean squared (RMS), correlation coefficient (R^2), residual mean (RM) and absolute residual mean (ARM) (Anderson & Woessner, 1992). Explanation of the formula was described in Visual MODFLOW 2011.1 user's manual by Schlumberger Water Services.

CHAPTER 4: THE STUDY AREA

4.1 Introduction

This study was conducted within the Lower Kelantan River Basin (LKRB). The LKRB is one of the important basins in Kelantan state which is laying in Quaternary deposit. This chapter will briefly describe the location of the study area, topography, climate condition, land use, hydrology, geology, hydrogeology and previous studies that have been conducted in the basin.

4.2 Location and Topography

The Lower Kelantan River Basin (LKRB) is situated in the northeast coast of the Malaysia Peninsula as shown in Figure. 4.1. The study area lies between latitudes 5.75°N to 6.25°N and longitudes 101.94°E to 102.54°E, is bounded by the Thailand at the northwest, South China Sea in the north and east and Southern Kelantan area in the south.

4.3 Topography

Generally, the LKRB area is approximately 1450 km^2 and has flat topography with a mean ground elevation of 7 m above sea level (ASL). The maximum elevation in the basin of hilly area is located at the southwestern with elevation about 40 m ASL while at the southeast the elevation is approximately 100 and 192 m ASL, respectively (Figure 4.2).

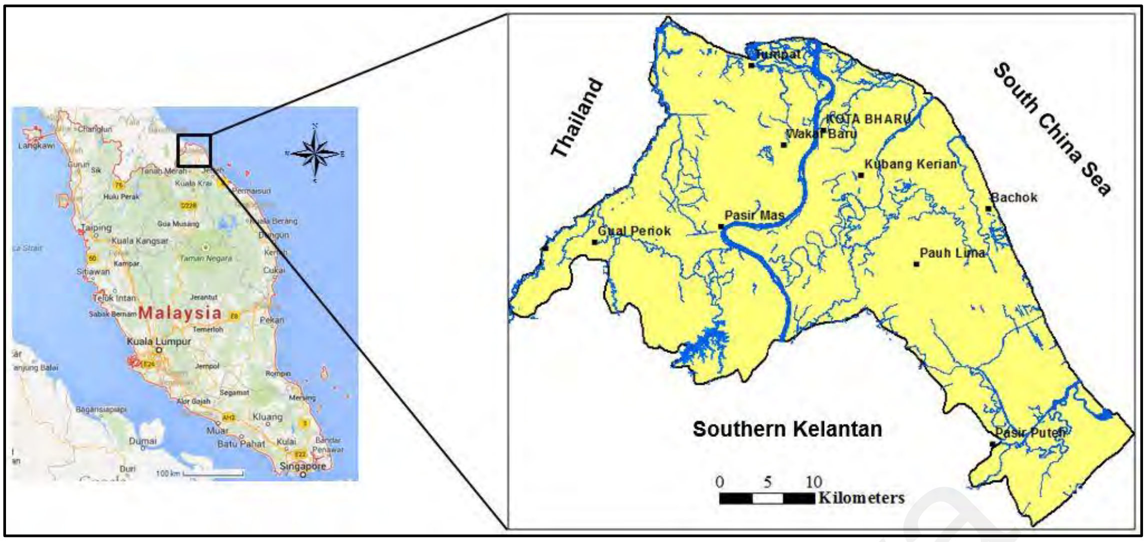

Figure 4.1: Location of the study area in LKRB

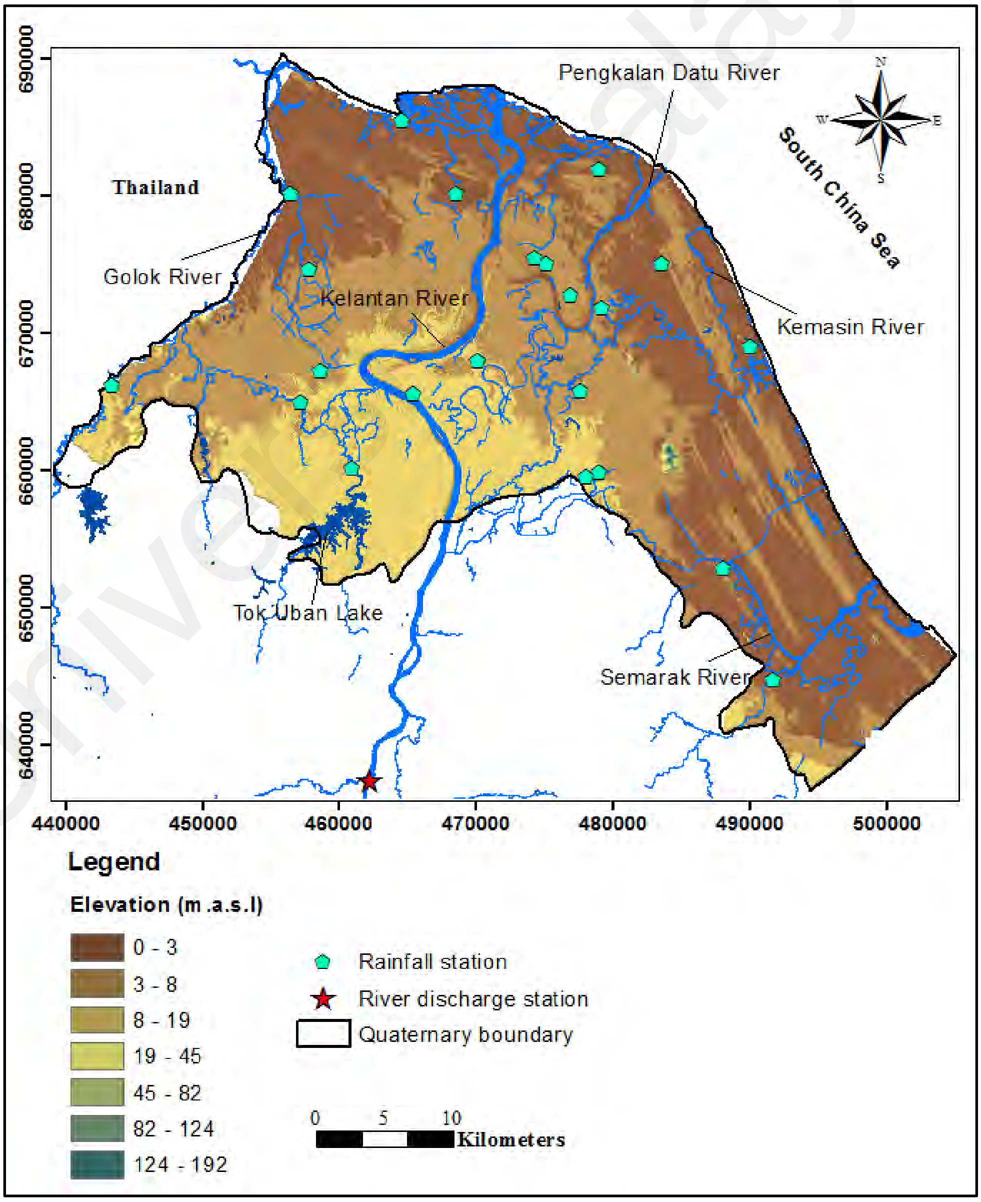

Figure 4.2: Topographical conditions of LKRB with rainfall and river discharge stations

4.4 Climate Conditions

The LKRB experiences a humid tropical climate, controlled by two monsoon seasons. The southwest Monsoon is occured between April to October often bringing less rainfall whereas the northeast Monsoon from November to March frequently generates high rainfall intensity over the study area. The annual rainfall recorded from 22 rainfall stations (see Figure 4.2) varies between 2400 – 3110 mm with mean annual of 2774 mm as presented in Figure 4.3. The mean annual temperature (1968-2013) is 27 ºC ranges from 26.2 ºC to 27.9 ºC while mean relative humidity (1968-2013) is 82% ranges from 79 % to 85%, respectively. The mean surface wind speed (1979-2013) is 2.2 m/s ranges from 1.3 m/s to 2.7 m/s. The climates data are gathered from drainage and Irrigation Department (DID) and Malaysian Meteorological Department (MMD). Mean annual potential evapotranspiration (PE) is 1037 mm/year (17 years) is estimated based on six types of surfaces; crops, Open water, Oil palm, Grass, Tropical and Towns (Hussin, 2011).

4.5 Land Use

The total land use area at LKRB is 185 860 hectare (Ha) according to the data from Department of Agriculture (DOA). This land use occupied the district of Kota Bharu, Tumpat, Bachok, Pasir Puteh and Pasir Mas (a part of it) with an area of 40 145 Ha, 18 343 Ha, 27 665 Ha, 57 215 Ha and 42 492 Ha, respectively. The land used is separated into 10 categories as shown in Figure 4.4. The highest percentage of land use is short term crops (29.80%) for the whole LKRB. This is followed by tree, palm and other permanent crops (23.80%), plantation areas (17.79%), swamps (7.63%), abundant grassland areas (7.42%), settlement and associated non-agriculture areas (4.07%), water bodies (3.94%), forest (3.76%), others (1.15%) and livestock area (0.64%). Agricultural land covers only 78.42% of the whole district with an area of 145 752 Ha. The land use area is changed accordingly to the necessity of human activity such as municipal, housing, agricultural and others.

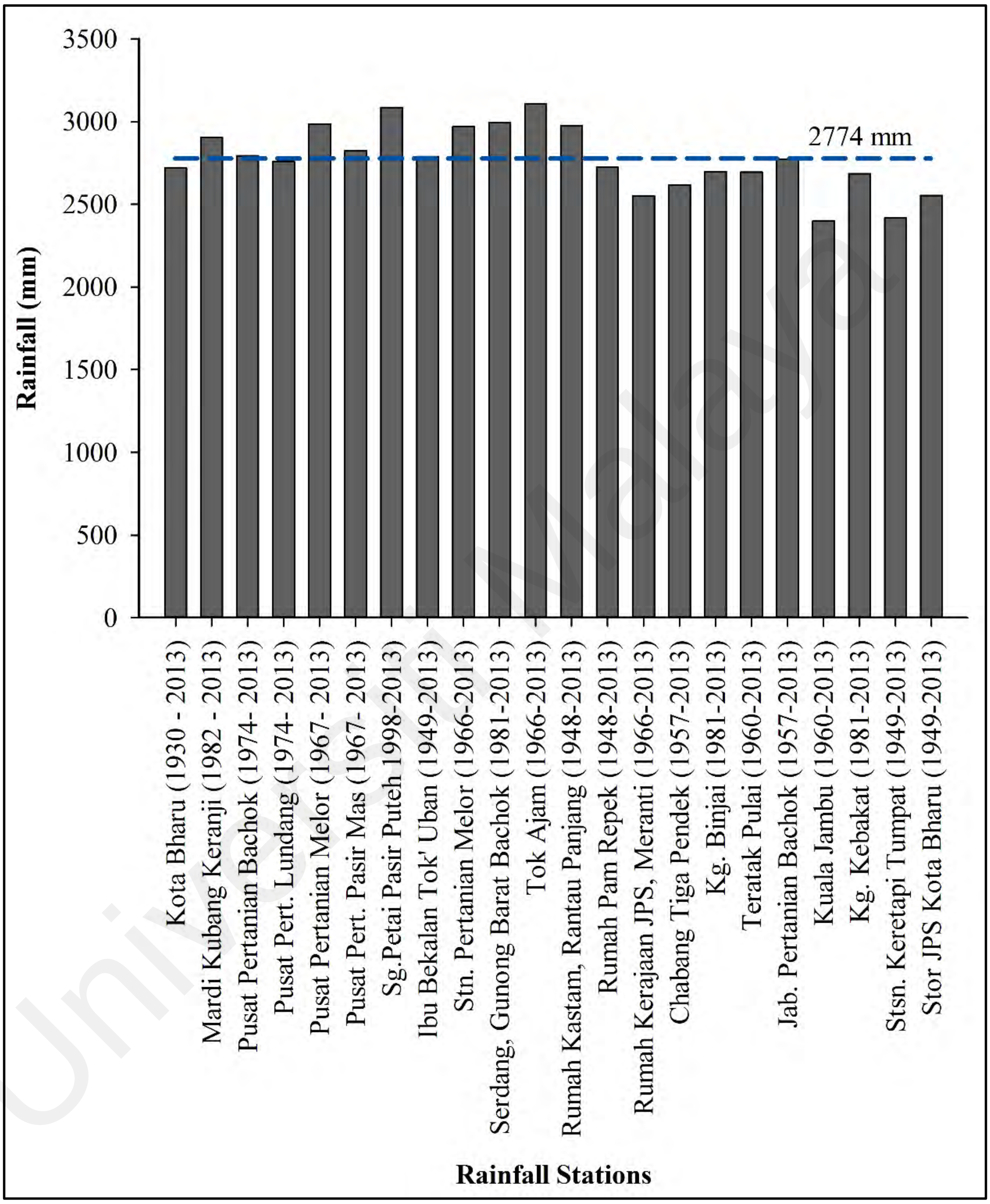

Figure 4.3: Annual rainfall distribution (mean annual rainfall 2774 mm)

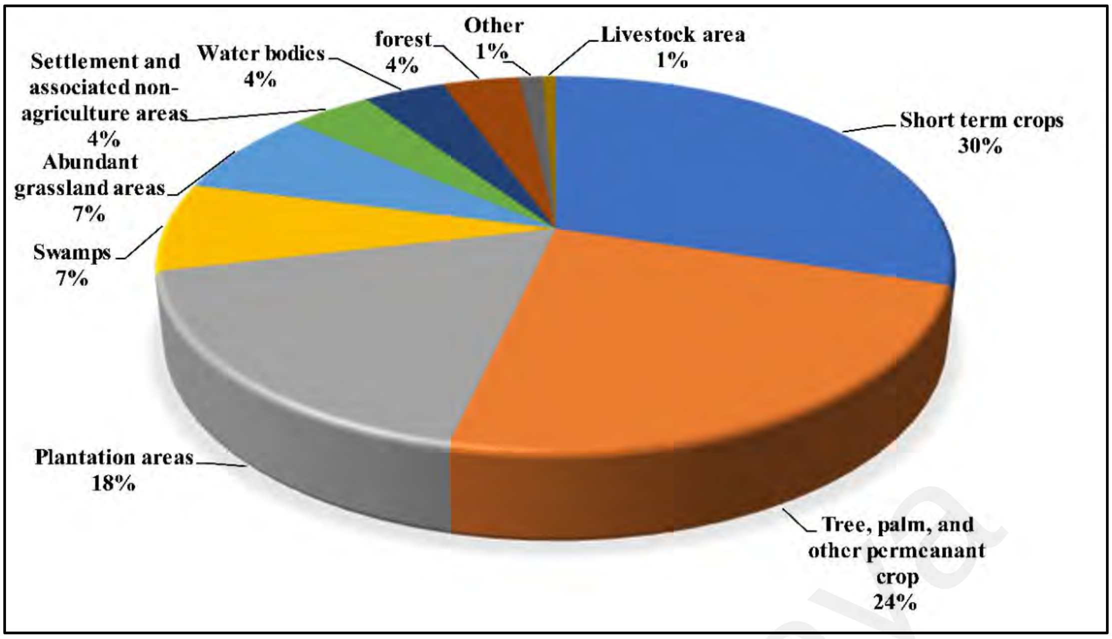

Figure 4.4: Total land use percentage for Kota Bharu, Bachok, Tumpat, Pasir Puteh and Pasir Mas

4.6 Hydrology

The drainage system in LKRB is controlled by five rivers, which are Golok River, Kelantan River, Pengkalan Datu River, Kemasin River and Semarak River that shows a dendritic drainage pattern (see Figure 4.2). The Golok River lies on the border between Malaysia (Kelantan) and Thailand. Kelantan River is the main river for Kelantan state with 248 km length (Ibbitt *et al.*, 2002) while Pengkalan Datu River, Kemasin River and Semarak River are with 13 km, 53 km and 24 km length, respectively. Figure 4.5 represents temporal changes of river stage (Jeti Kastam station 204441) and rainfall (Kota Bharu station) from 2001-2012. River discharge of Kelantan River is estimated from Gulliemard Bridge station about 22 km along the reaches outside the study area boundary (see Figure 4.2). This is the only station close to the LKRB. The mean annual river discharge from 1979 to 2013 is 478 m^3/s as shown in Figure 4.6. The highest discharge rate is recorded in 1994 with 679 m^3/s while the lowest discharge rate is recorded in 2012 with 308 m^3/s.

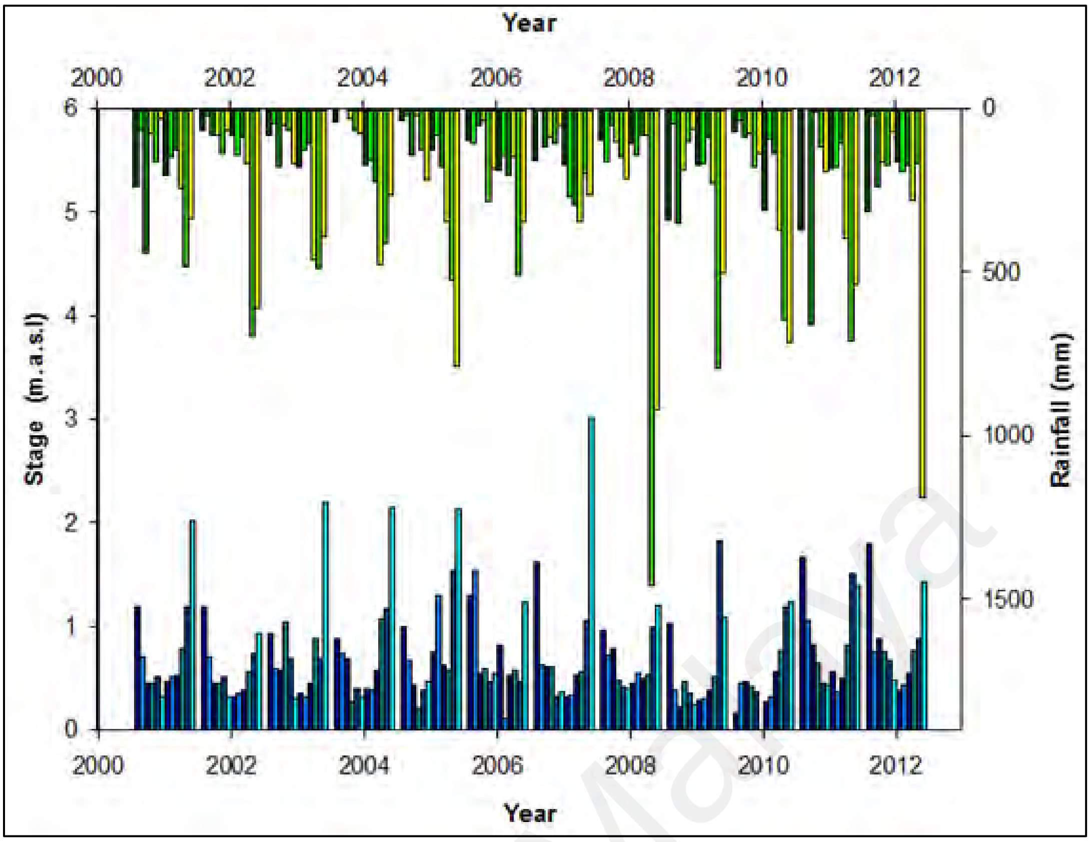

Figure 4.5: Monthly river stage (Jeti Kastam station) and rainfall (Kota Bharu station)

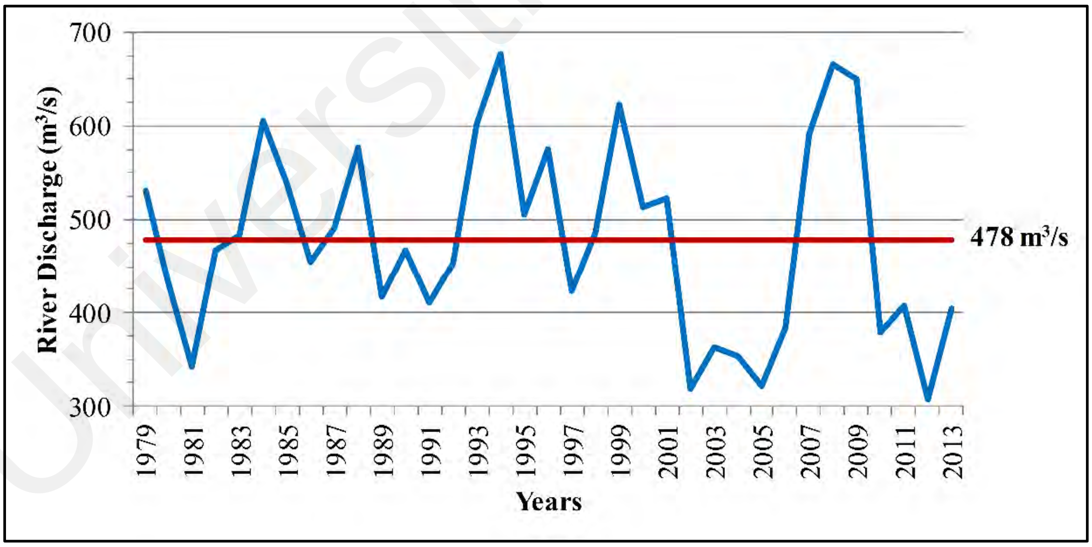

Figure 4.6: Annual river discharge at Gulliemard Bridge station (mean of 478 m^3/s)

4.7 Geology

4.7.1 Quaternary Deposit

The study area is covered by alluvium deposits of Quaternary age as shown in Figure 4.7 and underlained by granite and metamorphic as bedrock. These Quaternary deposits can be divided into Pleistocene and Holocene deposit as mapped by (Bosch, 1986). The Pleistocene consists of Simpang Formation while Holocene consists of the Gula Formation and Beruas Formation that were underlain by granite bedrock. The Quaternary deposits mainly consist of unconsolidated to semi consolidated gravel, sand, clay and silts that occupies the north of Kelantan state and along the river valley (Md Hashim, 2002). The first 13 to 15 m deposit is recent of age (Soh, 1972; Noor, 1980) and composed of silty to clay. Towards the coast, the thickness of alluvium may reach up to more than 200 m (Suratman, 1997) and form a shape like thick wedge towards the sea. This sediment is complicated and made up of interstratified and intercalated deposit with marine and non-marine strata (Udie Lmasudin, 2000). The mixtures of marine and non-marine sediment caused by sea level changes during the Quaternary age (Tjia, 1973).

4.7.2 Gula Formation

Gula Formation is mainly made up of clay and silt while sand and gravel are also present in a small amount. The boundary is often underlained by the Simpang Formation or bedrock with thickness of more than 40 metres. Organic matters and shells present are such as foraminifera (*Ammonia beccarii*, *Asterorotalia pulchella*), gastropod (*Coralliophila sp.*, *Natica sp.*), ostracod (*Cytherella semitalis, Cyprideis sp.*), pelecypod (*Anadara sp., Corbula sp.*) and others. The environment of deposition is shallow marine to estuarine (Suntharalingam & Teoh, 1985; Loh, 1992) The upper part is differentiated into Matang Gelugor Member and Port Weld Member (Suntharalingam & Teoh, 1985).

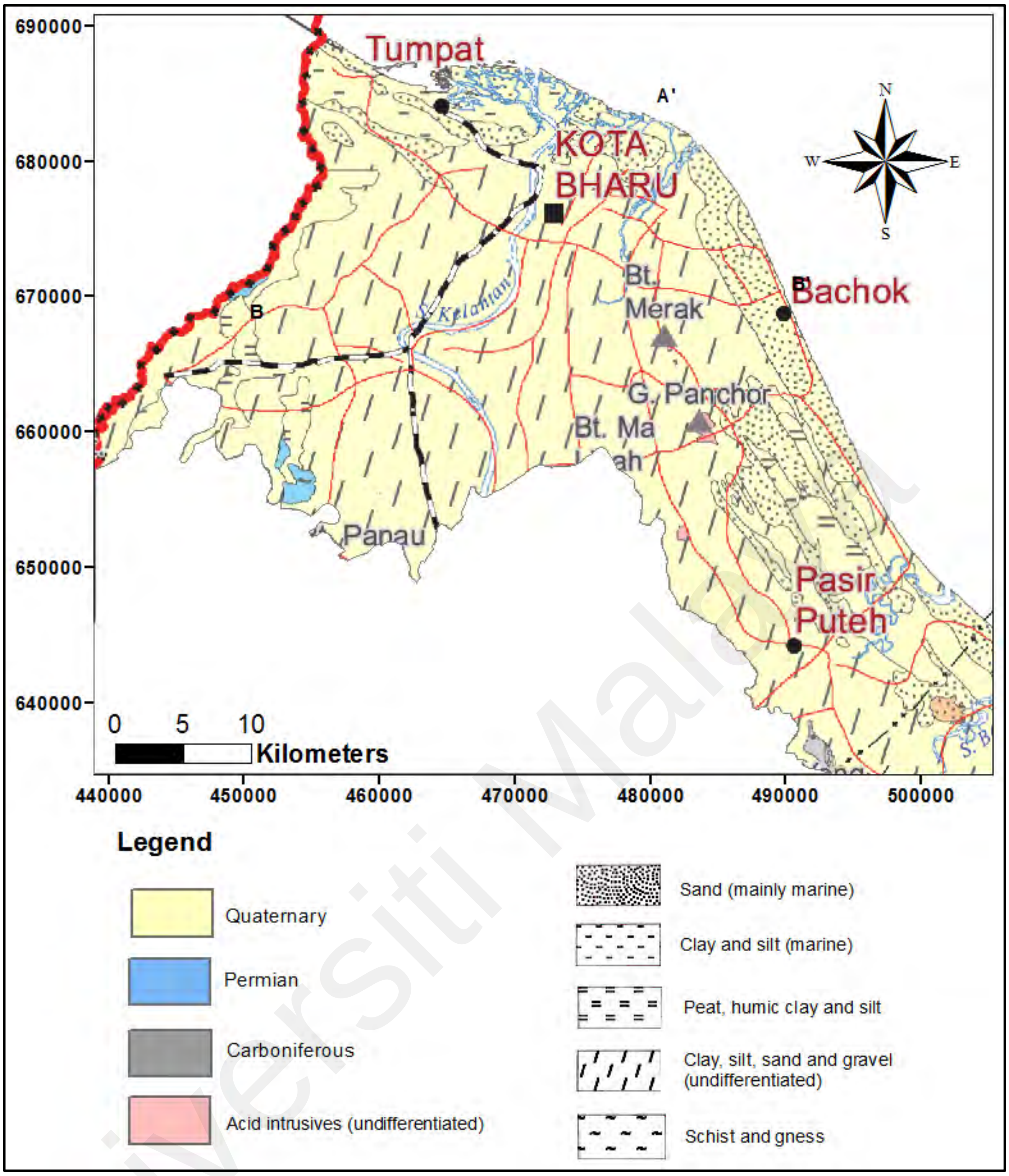

Figure 4.7: Geological Map of Lower Kelantan River Basin [modified from MGD (2014a)]

Matang Gelugor Member

The lithology of Matang Gelogor Member composes of sediments varying from clayey sand to sand with rare layers of lenses of clay. Sand is mainly in the upper part while clayey sand is common in the lower part of succession. The thickness is approximately 4 m with shallow marine (coastal) environment of deposition.

Port Weld Member

The lithology of Port Weld Member is predominantly clay with occasional lenses or layers of fine to medium sand and silt. The clay varies from brown-black or brownish grey to greenish grey. The clay generally consists of moderate to abundant humic materials layered or arranged in haphazard manner. The thickness is approximately 2 m with marine origin as environment of depositional.

4.7.3 Simpang Formation

Simpang Formation which is Pleistocene in age, is found mainly in the center part of the study area. This formation is made predominantly of clay, silt and sand with subordinate amounts of gravel towards the lower part of the succession. The sediments are usually mixtures of gravel, sand, silt and clay. The sand and clay are intercalated with one another. Peat and peaty clay are also present. The boundaries are unconformable basal boundary with bedrock and conformable upper boundary with Gula Formation. The thickness is usually more than 30 m with the presence of plants fossils. The environment of deposition is fluvial (Suntharalingam & Teoh, 1985; Loh, 1992). As stated by Suntharalingam and Teoh (1985), the formation is equivalent to the 'Old Alluvium'(Walker, 1956) Pleistocene sediments of Kinta Valley area which are now referred as Simpang Formation.

4.7.4 Granite and Meta-sediment

A little patch of granite hills occurs in the southeast of the study area (see Figure 4.7). These granite hills are known as Bukit Marak and Bukit Kechik with 373 m and 307 m heights, respectively. This granite belongs to the Boundary Range Granite according to their similarities of location and mineral composition. While meta-sediment is more pronounced in the western area.

4.8 Hydrogeology

LKRB is characterized by thick sequence of Quaternary alluvium deposit ranging from 25 m inland up to 200 m at the coastal area (Suratman, 1997). Figure 4.8 shows a hydrogeological map of LKRB. This area is indicated as a fresh water area and classified with very high aquifer potential area (MGD, 2008). Five hydrogeological cross sections lines were drawn during technical cooperation with German (Sofner, 1992) to enhance the understanding of the LKRB subsurface geology as shown in Figure 4.9. Detail subsurface profiles of each cross-section line are presented in Figure 4.10. In general, the aquifer system shows a complex groundwater system where the impermeable clay layer is not continuous and formed lenses at certain areas making it difficult to differentiate the aquifer layers. The aquifer thickness varies by location.

A fence diagram in Figure 4.11 shows a general aquifer system at LKRB which is separated into two aquifer system of shallow and deep aquifers as shown. Based on hydrogeological cross sections and fence diagram, Sofner (1992) proposed that the former concept of a three-fold aquifer systems which might be true for limited sections and has to be considered under regional aspects. Figure 4.12 shows the conceptual stratigraphy of the Lower Kelantan River Basin aquifer, according to Sofner (1992). The whole aquifer system consists of four aquifer units. Unit 1 is shallow unconfined aquifer, followed by Unit 2 which is the protective clay layer, Unit 3a and 3b which are of the gravely sand and sandy silty clay respectively, and then Unit 4 which is the coarse sand confined aquifer.

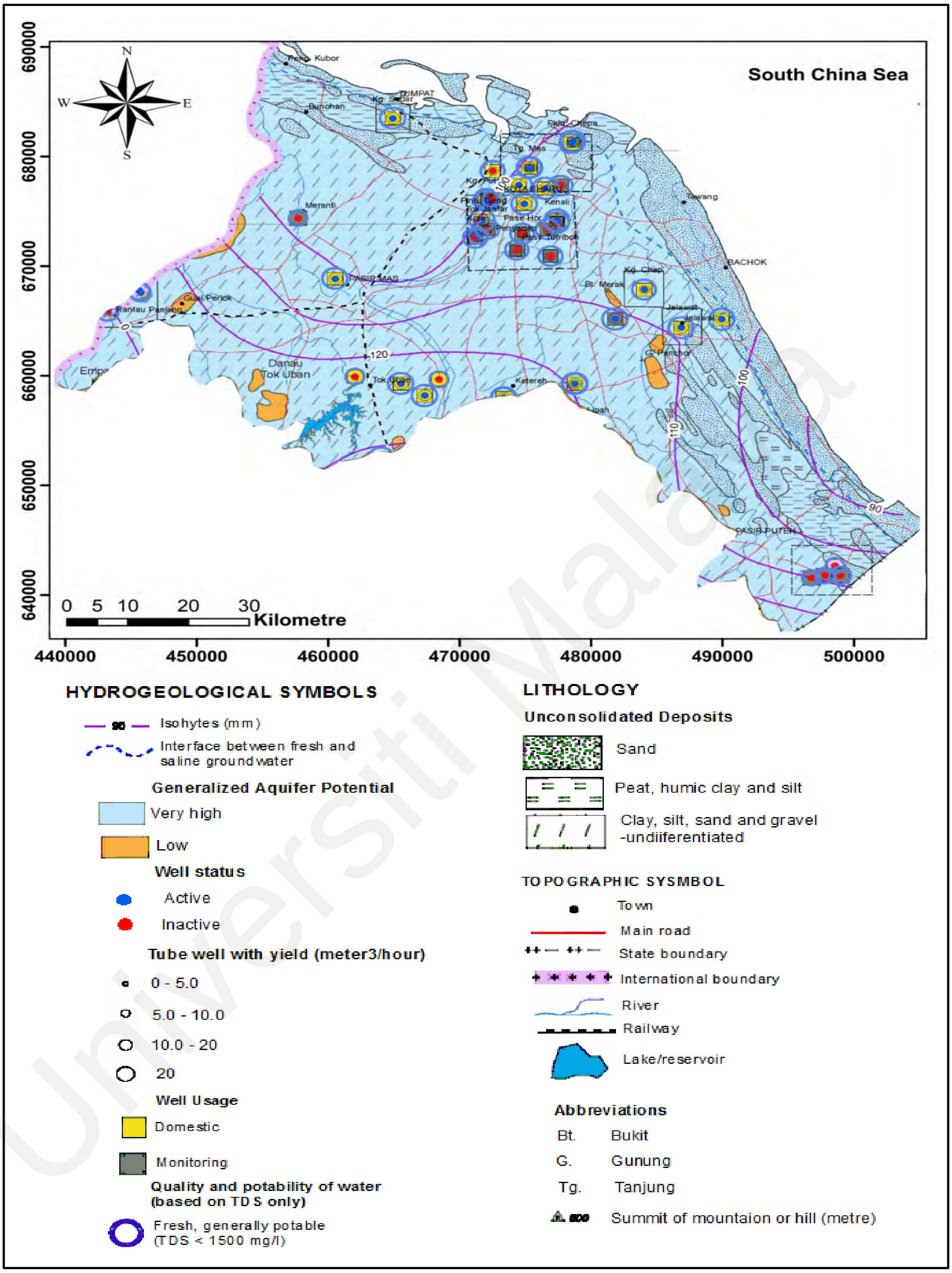

Figure 4.8: Hydrogeological map of LKRB [modified from MGD (2008)]

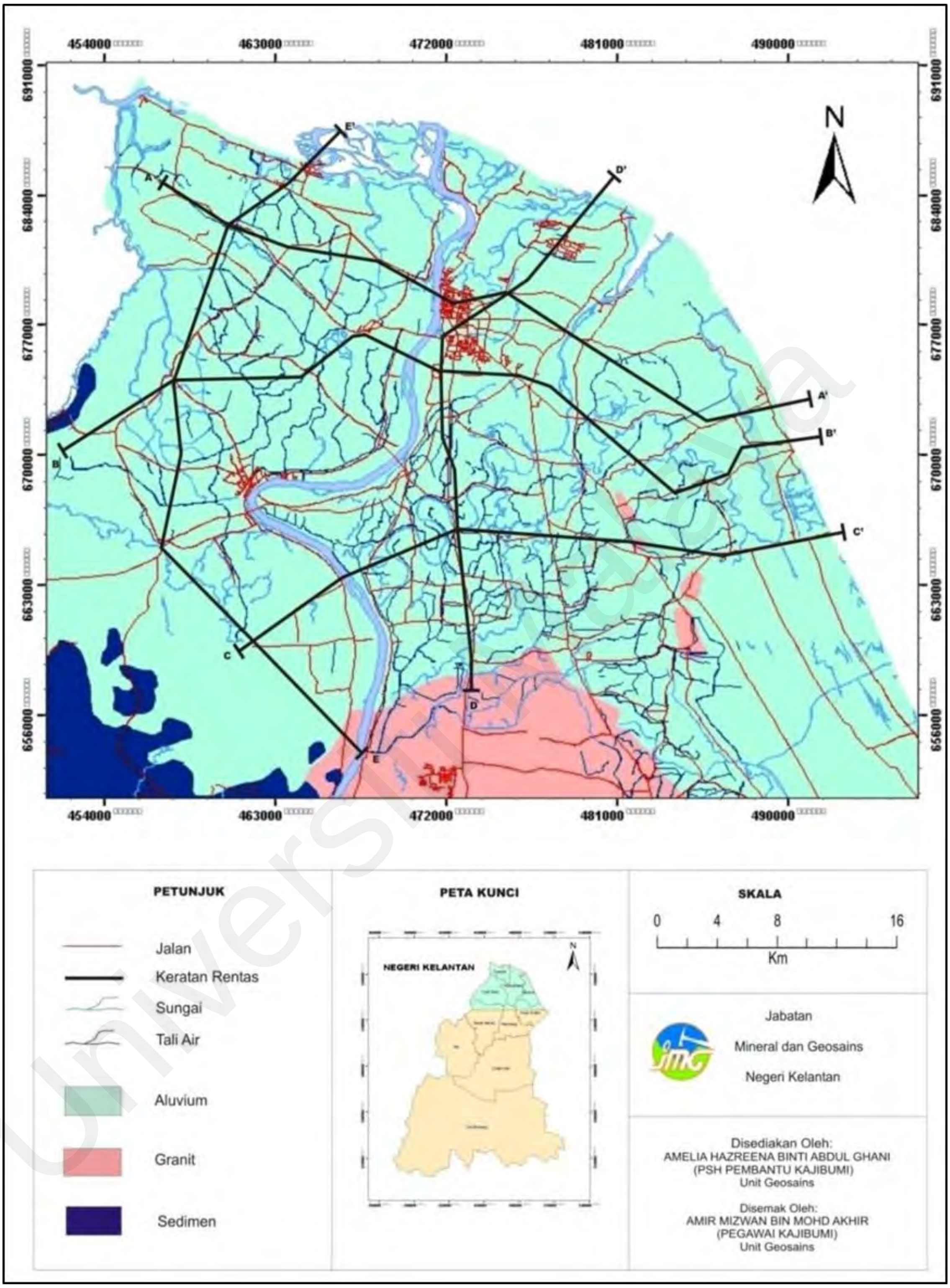

Figure 4.9: Hydrogeological cross section lines in LKRB

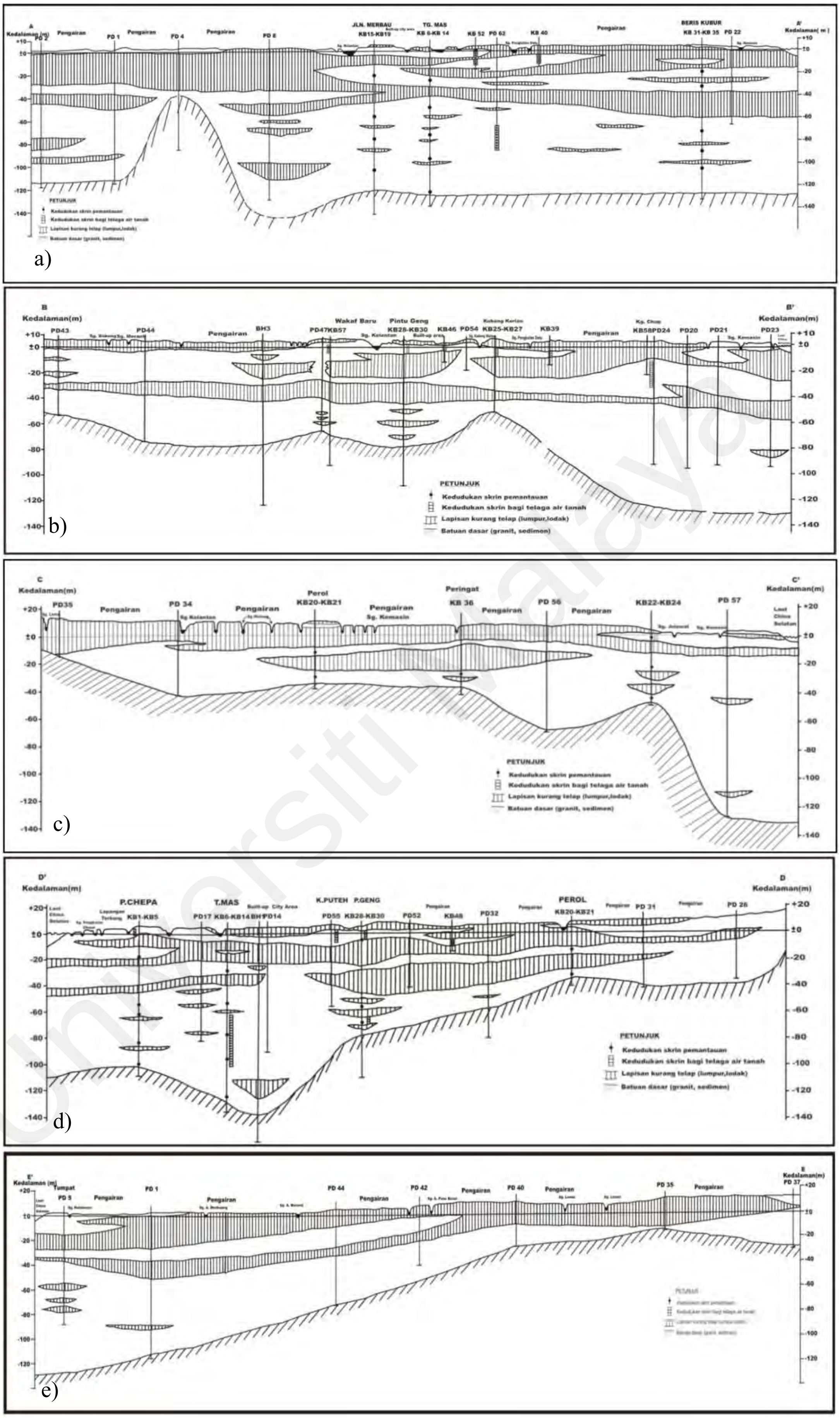

Figure 4.10: Hydrostatigraphic of LKRB (a) Cross section A-A', (b) B-B', (c) C-C', (d) D-D', and (e) E-E'of LKRB

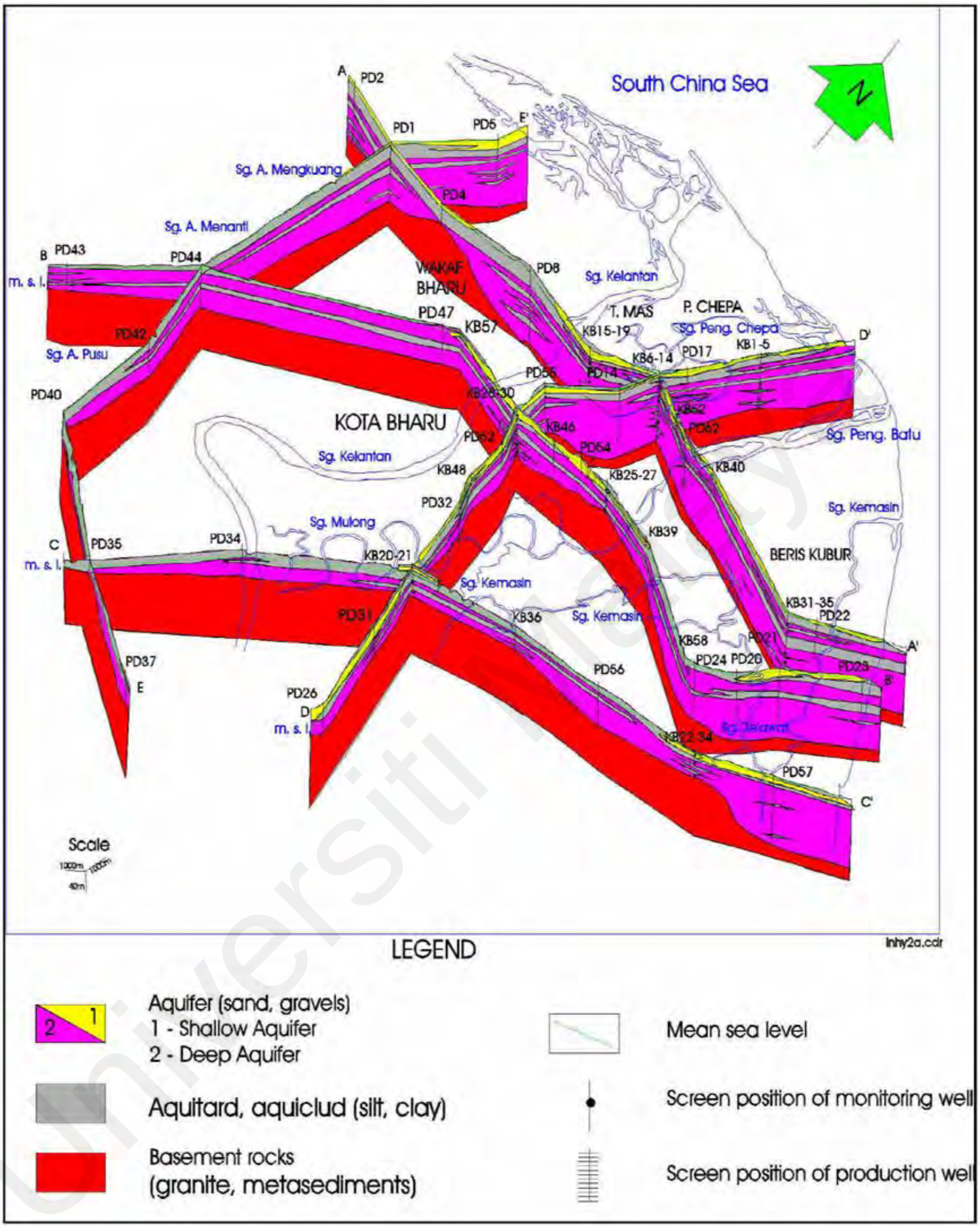

Figure 4.11: Hydrogeological fence diagram [source from MGD (2014b)]

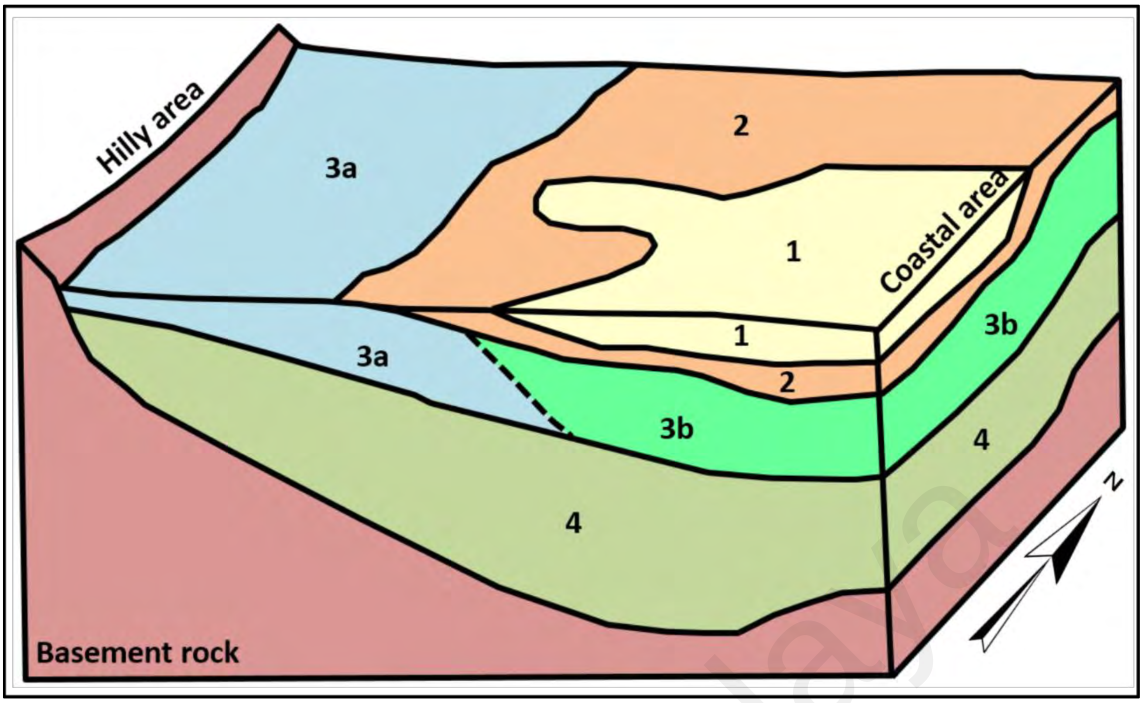

Figure 4.12: 3D Conceptual stratigraphy of LKRB Layer. (1) is the shallow unconfined aquifer, (2) is the protective clay layer, (3a) and (3b) are the deep aquifers consisting of the gravely sand and sandy silty clay respectively, and (4) is the coarse sand confined aquifer [modified from Sofner (1992)].

4.8.1 Groundwater Resources at LKRB

Groundwater resources investigation in Kelantan especially Lower Kelantan River Basin (LKRB) has started since Second Malaysian Plan (1971 to 1975) with the assistance from Federal Republic of Germany and it was continued in the Third Malaysian Plan (1976 - 1980). In the beginning, the investigation covered the eastern part of the LKRB and was followed by the western area. The investigation included the construction of the monitoring wells, pumping test for determination of aquifer properties, identifying the aquifers presence in the basin, groundwater quality monitoring, optimum yield of groundwater system to be extracted, identifying potential threat and other related studies. Detail reviews on this can be read through in KeTTHA (2010). The report also included an update on identifying the extended aquifer resources using skyTEM and ground geophysical to complement the past data, proposed new wells for production and monitoring, and implementation of the SCADA system as a practice for sustainable groundwater resource management.

W Ismail (2011) studied the groundwater management system using hydrogeological model in Sg. Kelantan River Basin. He suggested a few activity plans such as i) groundwater survey, groundwater model, test drilling and pumping, and water sample analysing in order to establish “Groundwater Resource Management (GWRM)” system with support of GIS and database system to handle and store all water resource relevant informations, ii) evaluate all existing use of water and redefine sustainable use and regulate rate of abstraction, and iii) establish a monitoring system with observation wells for level and quality of water.

Prologue to the extensive extraction of groundwater, under Tenth Malaysian Plan of National Groundwater Resources Study, MGD (2012) has modelled the shallow aquifer of Lower Kelantan River Basin (LKRB) using Groundwater Vistas based on the conceptual model in Sofner (1992). The model has indicated a clear interaction between surface water and groundwater. The estimated safe yield through the model analysis is approximately 509 MLD which is 4.28 times higher during that time of extraction rate. MGD (2014b) has also known to model both the shallow and deep aquifer using Visual MODFLOW software. The model analysis has estimated safe yield from the aquifer system was around 366 MLD which was 1.43 times higher. The estimated safe yield from shallow aquifer was nearly 406 MLD while from deep aquifer was about 116 MLD.

River bank infiltration – horizontal well collector (RBF-HCW) system has been constructed by Air Kelantan Sdn. Bhd. (AKSB) to optimize the water supply in Kelantan (Wan Ismail, 2012). Currently, at LKRB, five locations under the RBF-HCW system has been completed and has operated at Pasir Tumboh, Pintu Geng, Wakaf Bharu, Kelar and

Kg. Chap while Kg. Telok is still under construction with a capacity of 20 MLD to 50 MLD. In total, seven RBF-HCW system were constructed in Jeli, Tanah Merah and Gua Musang area with a capacity of 3 MLD to 20 MLD. This system is renowned as green technology and beneficial in terms of reduction of costs in operation, energy and maintenance, reduction of risks in quality of water, failure on operation and environmental damages and reduction on threats in climate change impact, pollution of river and 'war' on use of water.

4.8.2 Groundwater Chemistry

Groundwater quality of LKRB was studied by Hussin (2011) using long-term data from monitoring wells monitored by MGD. Hydrochemical facies reveal two main facies; Na-HCO_3 facies in the inland area while Na-Cl facies towards the coastal area. She has divided the aquifer into three layers. Layer 1 lies at a depth of approximately 20 m below the ground surface. Layer 2 lies approximately between a depth of 20 to 50 m while Layer 3 lies at a depth of 50 m. All layers contained natural iron concentration exceeding the WHO guideline standard of 0.30 mg/L. Groundwater in Layer 1 and Layer 3 are classified as fresh water while the groundwater in Layer 2 is a mixture of fresh and brackish water (TDS more than 1000 mg/L). High concentration of nitrate and ammonia was found at depth interval below 20 m (Layer 1). While high sodium, chloride and iron concentration was discovered at depth interval of 20 – 50 m (Layer 2). Iron remained high at depth interval of more than 50 m. Water quality indicated that groundwater in Layers 1 and 3 were more suitable to be used for drinking purposes compared to Layer 2 but water needs to be treated to meet the requirement guidelines of drinking water quality. MGD (2012, 2014b) modelling had indicated that no landfill leachates and tobacco will reach the AKSB water treatment plants or abstraction well fields. Assessment of radon concentration in groundwater in Kelantan was done by Sulaiman *et al.* (2019). The radon concentration ranges from 0.05 Bq/L to 22.63 Bq/L with mean of 5.1 Bq/L. The mean value was lower than UNSCEAR (2000) average of 10 Bq/L and far less than WHO (2011) reference level of 100 Bq/L. The variation of radon vary between wells location and depth. The calculated effective dose (according to mean radon concentration) from drinking water containing radon was 9 μSv/y. This dose level was very low and will not have a harmful effect on the human.

The use of radon as a tracer tool to study the interaction between surface water and groundwater has not been studied in LKRB or other part of Malaysia. So far, the application of radon was used to study the water quality and health risk of exposure to radon radiation. For water quality, radon activity concentration was measured from hot spring, surface water, drinking water (reverse osmosis), mineral water, tap water and groundwater wells at selected states of Malaysia (Hamzah *et al.*, 2011; Saat *et al.*, 2014; Abdul Malik *et al.*, 2015). In general, the measured radon level was below the maximum contamination limit (MCL) recommended by United State Environmental Protection Agency (USEPA) of 11.1 Bq/L. Only a few of wells have radon level above the MCL and these wells were in granitic rock. The exposure to surface radiation dose ranges from 0.096 to 0.232 μSv/hr. This range is higher than the ranges of global surface radiation dose (0.079 to 0.13 μSv/hr) at selected area.

CHAPTER 5: RESULTS

5.1 Introduction

This chapter presented the results of groundwater recharge mechanism according to the methods applied for recharge flow processes and recharge estimation rate.

5.2 LKRB Groundwater Recharge Flow Processes

5.2.1 Stable Isotopes (SI)

Stable isotopes of Deuterium (^{2}H) and oxygen-18 (^{18}O) as briefly explained in Chapter 2 had been proven as a unique tracer tool to gain insights into the groundwater recharge processes and groundwater flow system over various hydrogeological and climate conditions. The ^{2}H and ^{18}O sampling location and analysis have been described in Chapter 3. The ^{2}H and ^{18}O isotopic data of precipitation, surface water and groundwater are tabulated in Appendix A for ease of comparison and interpretation.

5.2.1.1 Signatures of D and ^{18}O in Rainwater

The isotopic composition of rainwater provides an important information on atmospheric circulation and climate change (Yurtesever & Gat, 1981). In general, the distribution of ^{2}H and ^{18}O isotopic composition in rainwater is governed by several factors which include altitude, temperature and amount effects (Ingraham, 1998; Gat *et al.*, 2001; Yin *et al.*, 2011a). The statistic isotopic signatures of ^{2}H and ^{18}O in rainwater during May 2013 to January 2015 is summarized in Table 5.1 and the monthly data collected during sampling campaign is listed in Appendix A. The range of $\delta^{18}O$ is from $-9.72^{0}/_{00}$ to $-2.78^{0}/_{00}$ and $\delta^{2}H$ ranges from $-63.34^{0}/_{00}$ to $-11.12^{0}/_{00}$, respectively. The weighted mean isotopic composition in rainwater is $-6.11^{0}/_{00}$ and $-39.84^{0}/_{00}$ for $\delta^{18}O$ and $\delta^{2}H$, respectively.

Table 5.1: Statistics summary isotopes signatures of δ^2H and $\delta^{18}O$ in rainfall

	δ^2H (‰)	**$\delta^{18}O$ (‰)**	**δ*D-excess* (‰)**
Minimum	-63.34	-9.72	1.08
Mean	-33.76	-5.32	8.82
Maximum	-11.12	-2.78	14.42
Standard deviation	13.97	1.84	3.70
Mean weighted	-39.84	-6.11	9.03

The variation of monthly ^2H and ^{18}O isotopic composition is shown in Figure 5.1. The most depletion of ^2H and ^{18}O occurred in June (^2H = -52.12$^0/_{00}$, ^{18}O = -8.00$^0/_{00}$, temperature = 28.40°C) while the most enrichment occured during Mar (^2H = -11.12$^0/_{00}$,^{18}O = -2.8$^0/_{00}$, temperature = 27.05°C). The surface air temperature, relative humidity and wind speed does not fluctuate significantly in seasonal variation as shown in Figure 5.1. This is because the isotopic composition at LKRB is influenced by amount effect during the monsoon seasons which is a pronounced feature of tropical regions like Southeast Asia (Rozanski *et al.*, 1993; Araguás-Araguás *et al.*, 1998, 2000; Majumder *et al.*, 2011).

This similar effect occurred at tropical karst island aquifer of Barbados, Puerto Rico and Guam (Jones *et al.*, 2000; Jones & Banner, 2003). Identifying the final mechanism that governs the isotopic composition of rainfall is important when discussing the rainfall data. The temperature effect is generally pronounced at high latitude continental regions where the isotopic composition decreases with temperature drops and increases with the amount of rainfall (amount effect). This amount effect is more pronounced in the tropical regions.

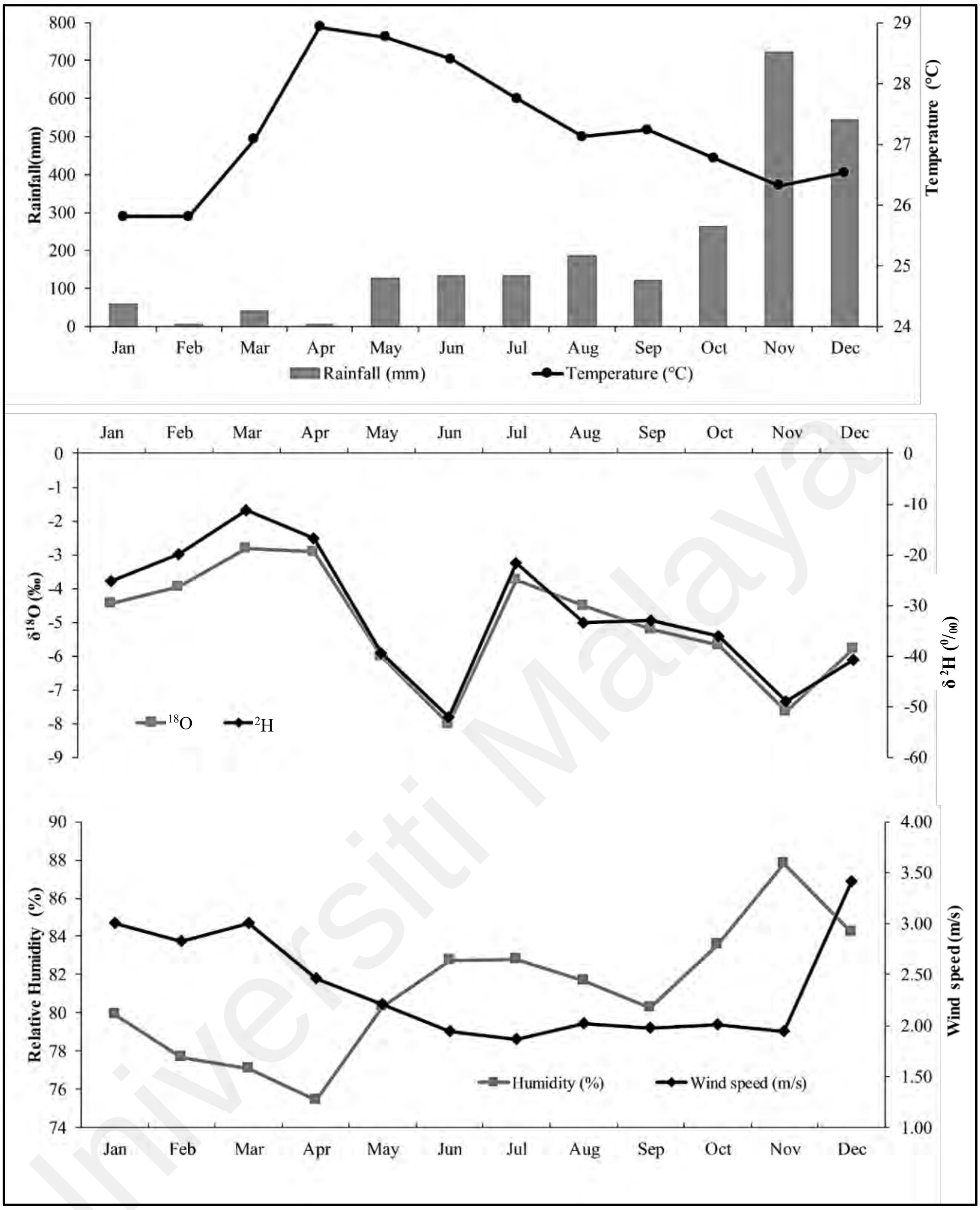

Figure 5.1: Variation of monthly ^{2}H and ^{18}O isotopic compostion, rainfall, temperature, relative humidity and wind speed from May 2013 to Jan 2015 at the LKRB

5.2.1.2 Signatures of ^2H and ^{18}O in Rainwater with Meteoric Water Lines

The global meteoric water line (GMWL) is established by (Craig, 1961) with linear regression of $\delta^2H = 8\delta^{18}O + 10$. This GMWL is a global average of world local meteoric water lines, where each line is controlled by local climate factors including the origin of water vapour mass, secondary evaporation during rainfall and the seasonality of precipitation (Kabeya *et al.*, 2007). The slope ~8 of GWML by Craig (1961) indicated that condensation of atmospheric moisture is under equilibrium condition. The slope that is less than or greater than 8 can indicate that the system is dominated by evaporation and recharged/recycled moisture, respectively (Craig, 1961). The intercept of GWML (~10) is exemplified by Dansgaard (1964) as deuterium excess (*d-excess*), $d = \delta^2H - 8\delta^{18}O$ to characterize the kinetic fraction of moisture vapour origin of water (Gat & Carmi, 1970). The *d-excess* value greater than $10^0/_{00}$ may indicate sources of recycled water, snow formation and cooler/dry air masses; known as 'primary evaporation'. Value less than $10^0/_{00}$ may indicate secondary evaporation (e.g. from cloud formation or terrestrial waters) and more humid air masses (Dansgaard, 1964; Clark & Fritz, 1997b; Gupta & Deshpande, 2005).

According to Clark and Fritz (1997a) the low *d-excess* of rainfall reflects slow evaporation at its source region due to high humidity, while the high *d-excess* reflects fast evaporation at its source region due to low humidity. Cappa *et al.* (2003) asserted that the *d-excess* value of water vapour is a function of the temperature, humidity, and isotopic characteristics of the ambient water vapour and the evaporating water. The local meteoric water line (LMWL) is established from Malaysian rainfall stations with linear regression of $\delta^2H = 8\ \delta^{18}O + 13.7$ (Wan Muhd Tahir *et al.*, 2014). GMWL and LMWL are used as a basic information to describe the water cycle processes in a particular area and for regional or locals investigatio., It is important to compare surface water and groundwater data with LMWL (Clark & Fritz, 1997b). Therefore, these lines will enhance the understanding on the variation of ^{2}H and ^{18}O isotopes composition of surface water and groundwater as comparison with the rainfall.

The GMWL, LMWL and the distribution of ^{2}H and ^{18}O of rainwater is shown in Figure 5.2. The rainwater isotopes scatter along and disperse below LMWL and GMWL. The mean weighted of rainwater ($^{2}H = -39.84^{0}/_{00}$ and $^{18}O = -6.11^{0}/_{00}$) is also shown in the figure. The deviation of rainwater from GMWL and LMWL suggests that rainwater has undergone evaporation process during rain clouds and before it reached the ground surface. The calculated mean value of *d-excess* $9.03^{0}/_{00}$ (see Table 5.1) is semblanced to the signature of global water (Craig, 1961) and indicates that the current rainfall at LKRB is slightly evaporated in relation to global meteoric water. The lower values of *d-excess* from GMWL and LMWL indicated that the current rainfall is evaporated in relation to local and global meteoric water lines whereas rainfall occurs at the relative high humidity less than 100% and high temperatures. The range of *d-excess* (37% of samples) show *d-excess* values higher than 10 which indicates that the probable inputs of recycled water vapor (Koster *et al.*, 1993; Gat *et al.*, 1994; Machavaram & Krishnamurthy, 1995) of local monsoon air masses and the contribution continental surface flow to the rain clouds due to low humidity (Clark & Fritz, 1997b). Later, the discussion of surface water and groundwater will be based on the GMWL and LMWL as reference lines to understand the fractionation processes in the basin.

5.2.1.3 Seasonal Variations in Isotopic Signatures of ^{2}H and ^{18}O

The seasonal variation of ^{2}H and ^{18}O in rainwater, surface water and groundwater is summarized in box and whiskers plot as shown in Figure 5.3 and Figure 5.4 for dry and wet season. The details of the datasets for surface water and groundwater are listed in

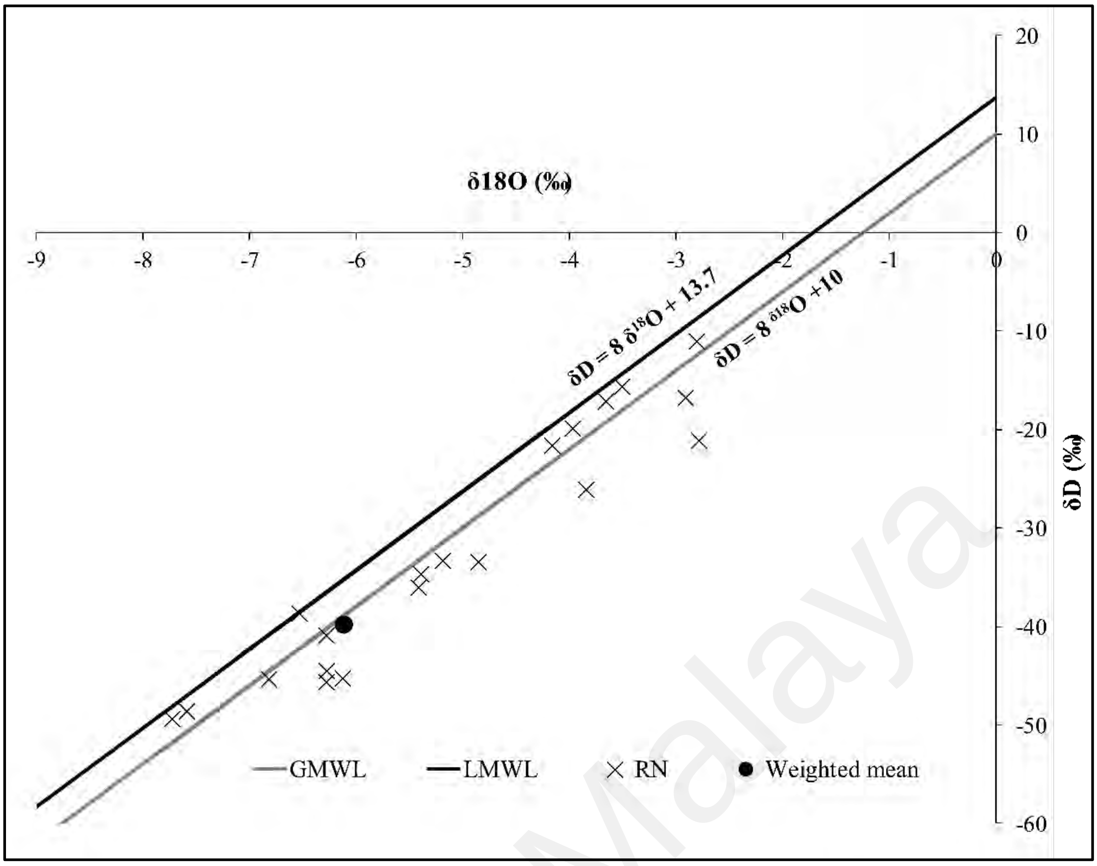

Figure 5.2: Distribution of $\delta^{18}O$ and $\delta^{2}H$ isotopic composition of rainwater (RN)

Appendix A. Although all data emerged to be dispersed, rainwater shows high dispersion for ^{2}H and ^{18}O isotopes in both seasons. The variability of rainwater as mentioned in section 5.2.1.2 is influenced by the rainfall amount as well as humidity and temperature during evaporation. The rainwater data for ^{2}H and ^{18}O ranges from-63.34$^{0}/_{00}$ to -17.17$^{0}/_{00}$ and -9.72$^{0}/_{00}$ to -2.78$^{0}/_{00}$ with mean of -35.91±14.56$^{0}/_{00}$ and -5.50±2.02$^{0}/_{00}$, respectively during dry season. Meanwhile, during the wet season, the ^{2}H and ^{18}O ranges from -49.40$^{0}/_{00}$ to -11.12$^{0}/_{00}$ and -7.72$^{0}/_{00}$ to -2.80$^{0}/_{00}$ with means of -34.42±15.51$^{0}/_{00}$, -5.51±1.87$^{0}/_{00}$, respectively.

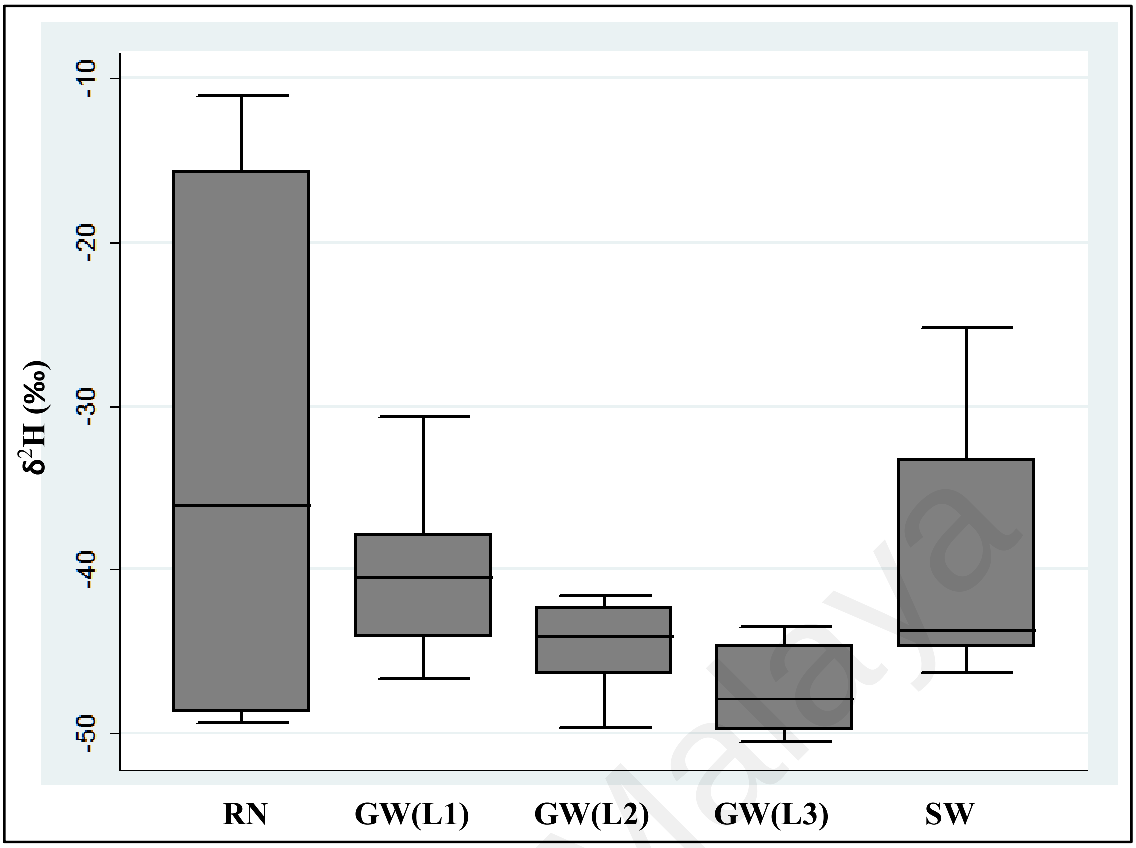

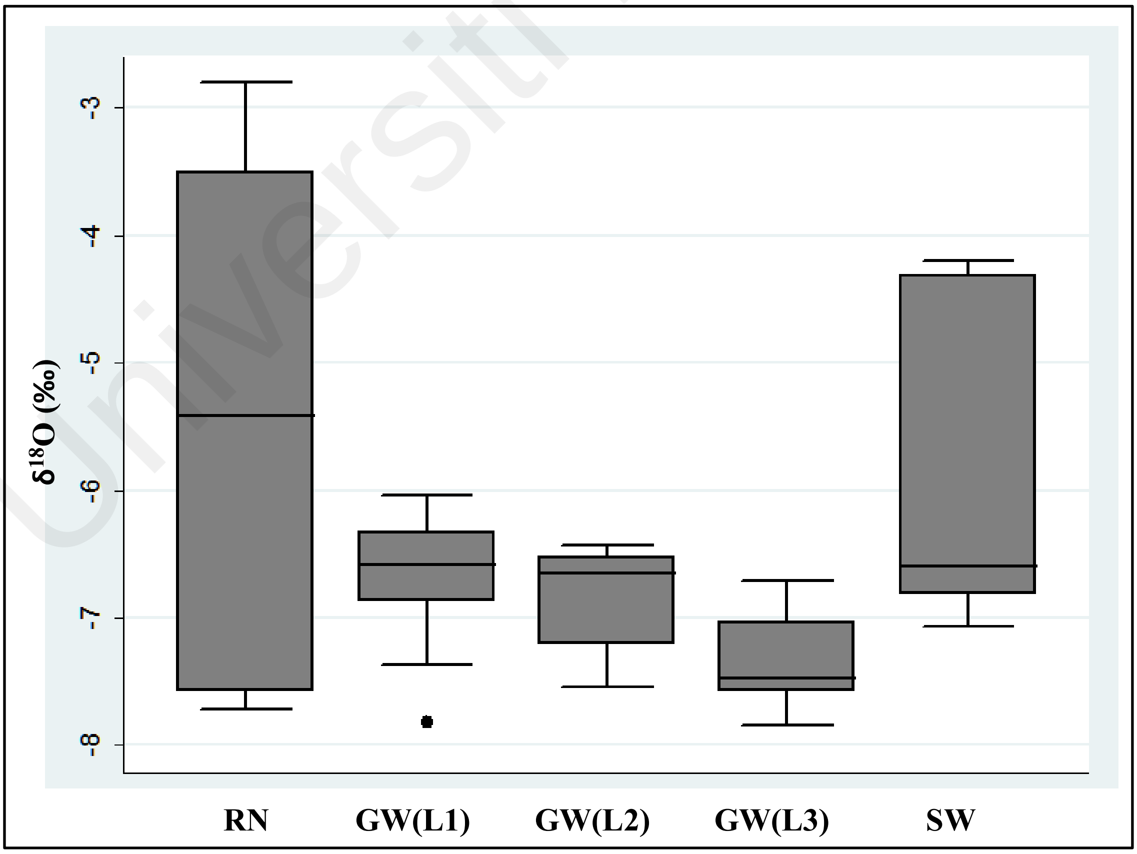

Figure 5.3: Box and whisker plots variations of ^{2}H and ^{18}O signatures of rainwater (RN), surface water (SW) and groundwater (GW) during wet season

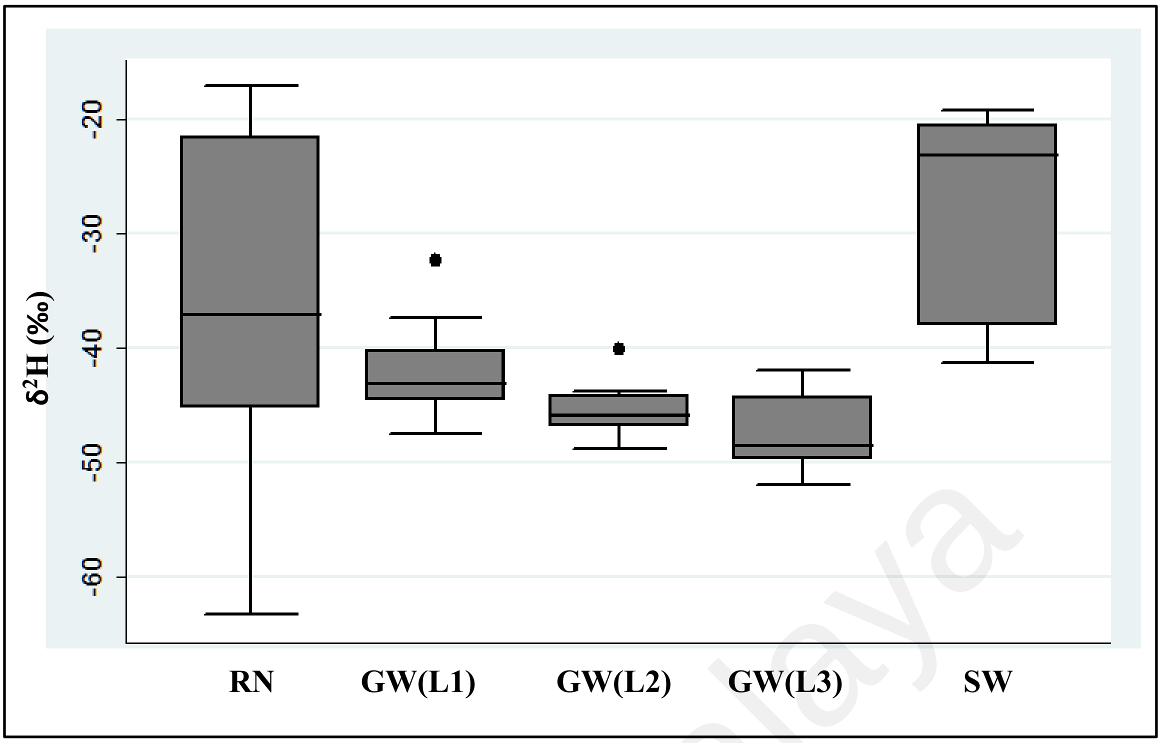

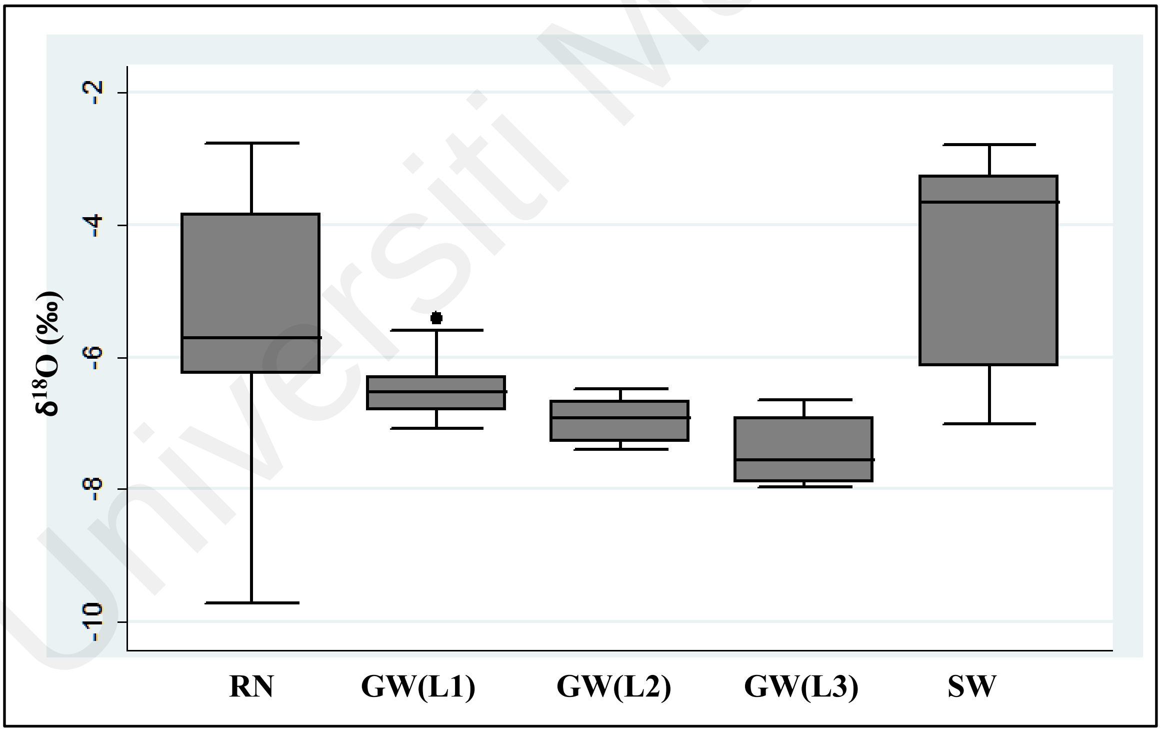

Figure 5.4: Box and whisker plots variations of ^{2}H and ^{18}O signatures of rainwater (RN), surface water (SW) and groundwater (GW) during dry season

The apparent high dispersion for surface water for ^{2}H and ^{18}O isotopes in both seasons are attributed by the fact that rainwater is the main source of the surface water in humid tropical climate where the annual rainfall received is 2774 mm (see section 4.2). This high dispersion also resembles a study by Fynn *et al.* (2016). The study stated where the ^{2}H and ^{18}O isotopes in surface water are attributed to the diverse kinds of surface impoundments in which some are ephemeral and others are perennial. However, the surface water in LKRB are taken from perennial rivers that flows throughout the year and artificial lake which sometimes will turn into a '*lake*' as the interconnected river may sometimes be dry especially during the dry season. The most enriched surface water samples were taken from Kemasin river (SW4 and SW5) and Pengkalan Datu river (SW6 and SW7) that shows negatively signatures of both isotopes observed suggest the effect of high evaporative enrichment as the river is closed to the sea.

The surface water data for ^{2}H and ^{18}O ranges from $-41.35^{0}/_{00}$ to $-19.23^{0}/_{00}$ and $-7.02^{0}/_{00}$ to $-2.79^{0}/_{00}$ with mean of $-28.06\pm9.08^{0}/_{00}$ and $-4.56\pm1.65^{0}/_{00}$, respectively during dry season. Meanwhile, during the wet season, the ^{2}H and ^{18}O ranges from $-46.28^{0}/_{00}$ to $-25.25^{0}/_{00}$ and $-7.07^{0}/_{00}$ to $-4.20^{0}/_{00}$ with mean of $-39.38\pm7.72^{0}/_{00}$, $-6.00\pm1.21^{0}/_{00}$, respectively. The mean isotopic composition of surface water is more depleted compared to rainwater, indicating that rainfall is the primary source of surface water at LKRB. Surface water is enriched with heavy isotope during dry season compared to wet season. A trend of depletion in isotopic composition of Kelantan, Kemasin and Pengkalan Datu river can be seen towards the downstream (see Appendix A). Surface water depleted with light isotopes as compared with groundwater as the surface water is exposed to the full force of the weather throughout the year and thus very subject to evaporation (Fynn *et al.*, 2016).

The groundwater samples suggest intermediate conditions between rainwater and surface water bodies for ^{2}H and ^{18}O isotopes in both seasons in the study area. This possibly reflects the mixtures of recent rainfall and surface water (Fynn *et al.*, 2016). The isotopic composition of groundwater ^{2}H ranges from $-47.59^{0}/_{00}$ to $-32.41^{0}/_{00}$, $-48.90^{0}/_{00}$ to $-40.19^{0}/_{00}$ and $-52.03^{0}/_{00}$ to $-42.05^{0}/_{00}$ with mean of $-42.22\pm3.69^{0}/_{00}$, $-45.42\pm2.61^{0}/_{00}$ and $-47.61\pm3.14^{0}/_{00}$ and ^{18}O ranges from $-7.08^{0}/_{00}$ to $-5.41^{0}/_{00}$, $-7.39^{0}/_{00}$ to $-6.50^{0}/_{00}$ and $-7.98^{0}/_{00}$ to $-6.65^{0}/_{00}$ with mean value of $-6.48\pm0.47^{0}/_{00}$, $-6.95\pm0.33^{0}/_{00}$ and $-7.41\pm0.47^{0}/_{00}$, respectively for GW(L1), GW(L2) and GW(L3) during dry season. During wet season, the ^{2}H ranges from $-46.70^{0}/_{00}$ to $-30.71^{0}/_{00}$, $-49.62^{0}/_{00}$ to $-41.61^{0}/_{00}$ and $-50.58^{0}/_{00}$ to $-43.48^{0}/_{00}$ with mean of $-40.75\pm4.44^{0}/_{00}$, $-44.63\pm2.73^{0}/_{00}$, and $-47.57\pm2.47^{0}/_{00}$ and ^{18}O ranges from $-7.82^{0}/_{00}$ to $-6.04^{0}/_{00}$, $-7.54^{0}/_{00}$ to $-6.44^{0}/_{00}$ and $-7.84^{0}/_{00}$ to -6.71^{0}/00 with mean value of $-6.69\pm0.56^{0}/_{00}$, $-6.84\pm0.42^{0}/_{00}$ and $-7.33\pm0.39^{0}/_{00}$, respectively for GW(L1), GW(L2) and GW(L3).

Groundwater data suggest more depletion in heavy isotopes compared to surface water. Groundwater shows a small range variation of isotopic signatures within the aquifer layers, and a trend of depleting in heavy isotopes of ^{2}H and ^{18}O composition (see Figure 5.3 and Figure 5.4). During dry season, groundwater in Layer 1 is slightly enriched in heavy isotope as compared to wet season. Groundwater in Layer 2 and Layer 3 are slightly enriched in light isotope during dry season but depleted in wet season. As the depth increased as shown in Figure 5.5, the small variation of ^{18}O illustrates a mixing pattern between the aquifer layers and groundwater flow may come from similar sources even though the aquifer system is heterogeneous (details in section 5.2.1.4).

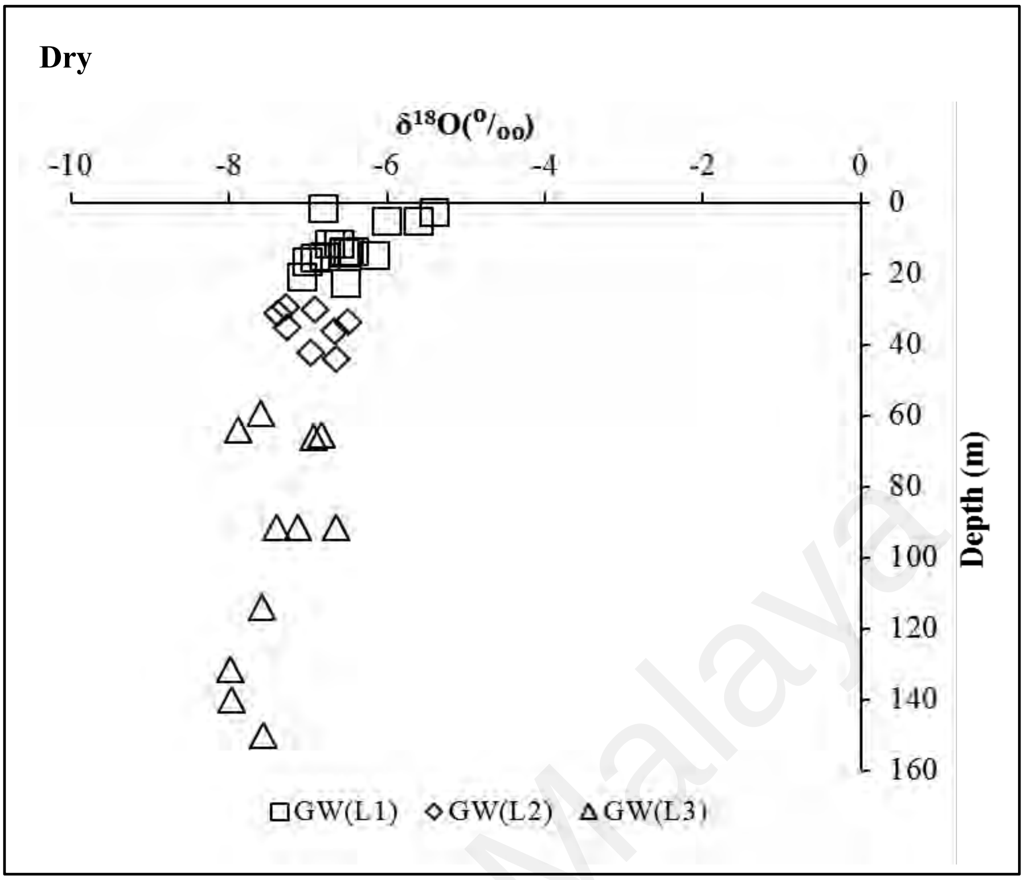

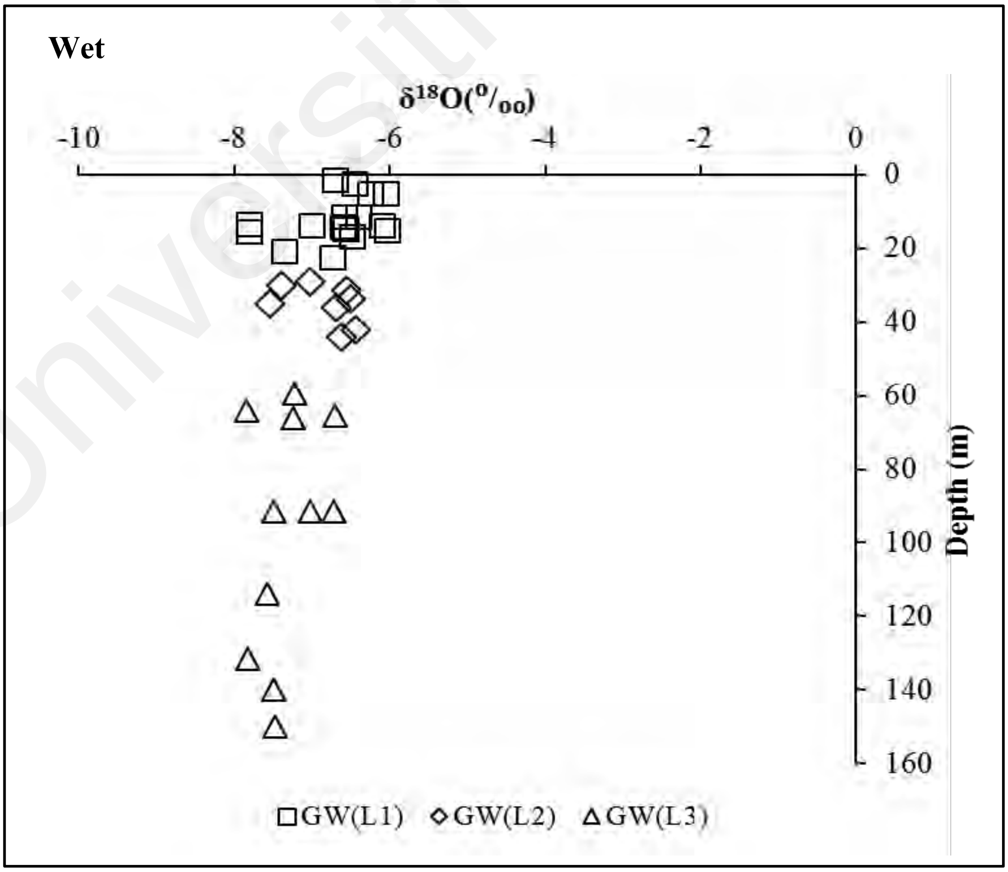

Figure 5.5: Variation of $\delta^{18}O$ and with depth in groundwater (dry and wet season)

5.2.1.4 Isotopic Signatures of ^{2}H and ^{18}O in Surface Water and Groundwater with GMWL, LMWL and Evaporation Line

The relationship between ^{2}H and ^{18}O isotopic signatures of surface water and groundwater are represented in Figure 5.6 for dry and wet seasons. The average weather condition of surface air temperature, relative humidity, rainfall and wind speed during dry and wet seasons are 27.9℃, 81%, 137 mm, 2.07 m/s and 26.3℃, 81%, 2.73 mm, 2.84 m/s, respectively. The linear regression line of GMWL and LMWL are also drawn in the Figure 5.6 as reference lines. The dash line is referred as 'Evaporation Line'. This line is drawn according to the regression of surface water or groundwater samples data. All these lines are applied for understanding the processes involved on the variation of D and ^{18}O isotopes composition of surface water and groundwater at LKRB.

Most of the isotopic compositions are scattered to the left side of the plots for both seasons. Literally, samples that are plotted at or near the LMWL arelikely undergone direct recharge from local rainfall (meteoric origin) with minimal evaporation through infiltration while other samples that are relatively deviated from the LMWL will have undergone evaporation processes during rainfall and/or during infiltration before recharging to the groundwater (Clark & Fritz, 1997a; Mook, 2000). The samples are closely plotted near the weighted mean rainfall implying that the recharge sources of this water are mainly from recent rainfall. Selected surface water samples are dispersed far to the right side of the plot especially in dry season.

All groundwater shows enrichment in lighter isotopic composition (more negative) whereas the position is to the left of the plot. The small ranges of ^{2}H and ^{18}O isotopes signature indicate that the source water comes from the same origin. The overlapping of the isotopic composition of surface water with groundwater and shallow (Layer 1) with

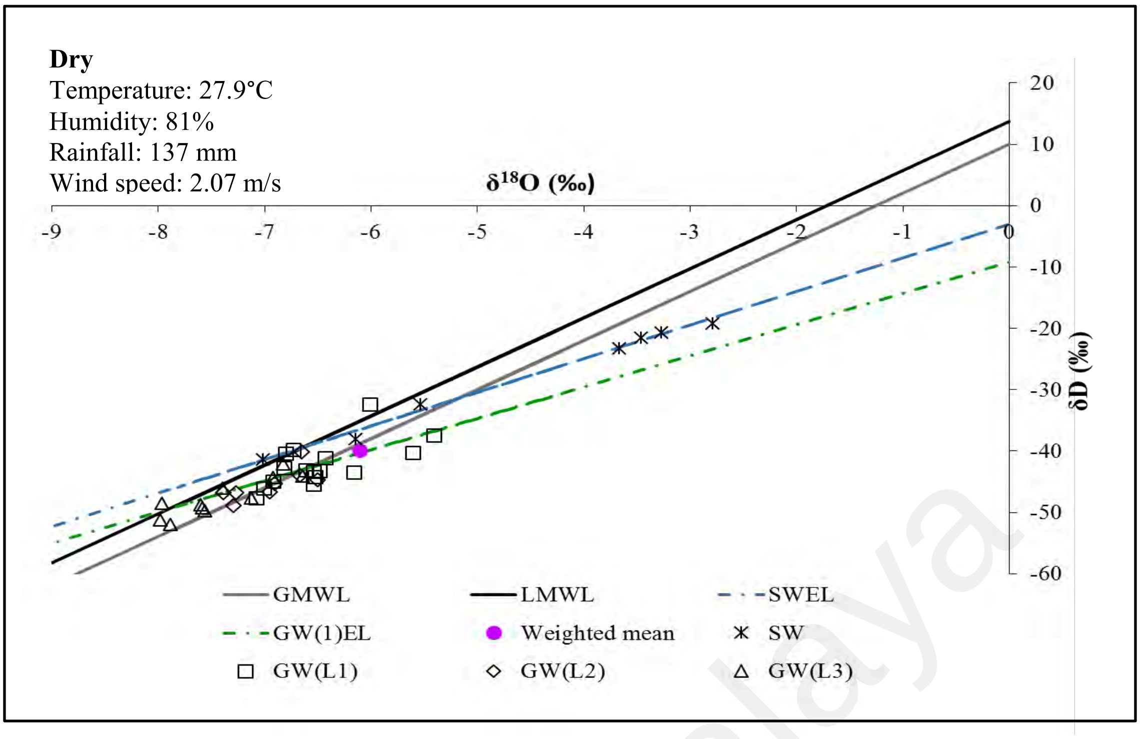

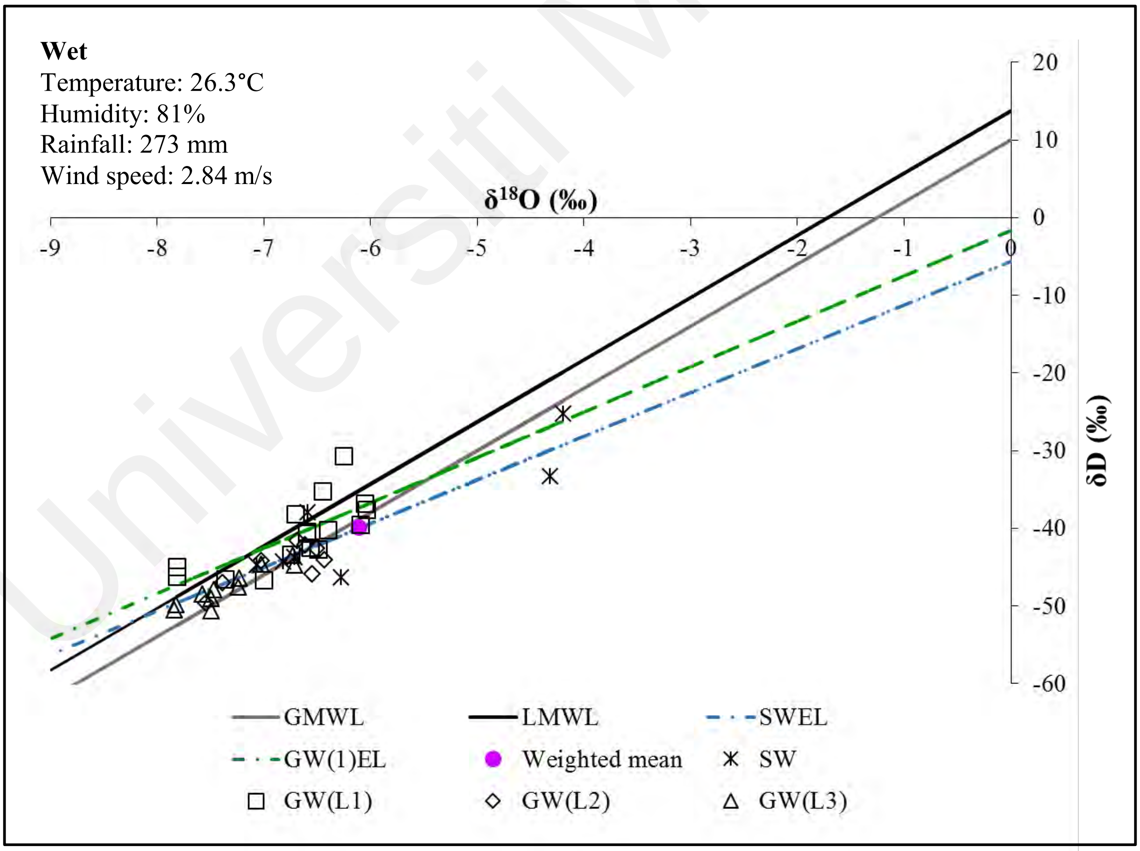

Figure 5.6: Variation of D and ^{18}O; (a) dry season, (b) wet season

deep (Layer 2 and Layer 3) aquifer indicates a similar isotopic composition and possibility of leaking and/or mixing processes occurrs at the basin. According to Adomako *et al.* (2011) this variation is probably caused by local processes; a) rainfall infiltration and b) groundwater mixing with water from anthropogenic activities or agriculture return flows.

In the tropical regions, the isotopic composition of ^2H and ^{18}O can be considerably modified from local rainfall due to strong isotopic enrichment in water during evaporation. The evaporation line of surface water (SWEL) is in blue colour (see Figure 5.6). The linear regressions are D=5.48^{18}O - 3.06 with R^2=0.99 and D=5.62^{18}O - 5.61 with R^2=0.78 respectively for dry and wet seasons as listed in Table 5.2. The intercept point between evaporation line and LMWL resulted in the $\delta^2H = -40.0^0/_{00}$, $\delta^{18}O = -6.70^0/_{00}$ and $\delta^2H = -51.5^0/_{00}$, $\delta^{18}O = -8.15^0/_{00}$, respectively for dry and wet season. This intersection indicates the origin of isotopic composition that recharged the surface water at LKRB before evaporation.

Table 5.2: Regression lines equation for surface water and groundwater

Samples	Regression line equations	
	Wet	**Dry**
Surface water (SW)	$\delta^2H = 5.62\ \delta^{18}O - 5.61$	$\delta^2H = 5.48\ \delta^{18}O - 3.06$
Groundwater, GW(L1)	$\delta^2H = 5.84\ \delta^{18}O - 1.65$	$\delta^2H = 5.08\ \delta^{18}O - 9.26$
Groundwater, GW(L2)	$\delta^2H = 4.97\ \delta^{18}O - 10.60$	$\delta^2H = 5.84\ \delta^{18}O - 4.79$
Groundwater, GW(L2)	$\delta^2H = 5.95\ \delta^{18}O - 3.89$	$\delta^2H = 5.94\ \delta^{18}O - 3.58$

As previously mentioned in section 5.2.1.3, rainfall is the main source of surface water. The isotopic composition of surface water near or at the LMWL indicates surface water is of meteoric origin. The slope of 5.48 and 5.62 (dry and wet) which is lower than GWML and LMWL (~8) as mentioned in Section 5.2.1.2, indicates that the isotopic composition of surface water has undergone evaporation before it reaches the ground surface as runoff or percolates water into the surface water bodies. This was supported by the variation of calculated *d-excess* as shown in Figure 5.8 with means of $8.61^{0}/_{00}$ and $8.39^{0}/_{00}$ respectively for dry and wet season which is below GWML ($10^{0}/_{00}$). The range of *d-excess* in Figure 5.8 indicates surface water at LKRB has undergone both primary and secondary evaporation.

The evaporation processes have enriched the isotopic composition especially during dry season and depleted during the wet season of the samples that deviated from GMWL and LMWL (see Figure 5.6). River water is enriched with heavy isotopes at Kemasin River during wet season and Kemasin and Pengkalan Datu during dry seasons. The rivers show significant increased in heavy isotopes from inland towards the coastal area in the series of Kelantan River, Pengkalan Datu River and followed by Kemasin River. From the upstream to downstream of these rivers, the trend of increasing heavy isotopes for both seasons was shown. It can be said that evaporation process are high towards the sea.

Apparently, surface water shows indication of leaking and/or mixing with shallow groundwater (Layer 1) (see Figure 5.6) whereas this condition is typical for baseflow river**.** The lower mean of *d-excess* compared to groundwater of $11.24^{0}/_{00}$ (average all layer) suggests that there could be some level of hydraulic connection or mixing of surface water with groundwater especially between shallow groundwater in the basin to favour the surface flow throughout the year. It can be said that, during dry season subsurface flow through baseflow will discharge to surface water. Alternatively, in wet season, leakage from surface water will recharge the shallow groundwater. Thus, groundwater that has similar compositions to those of surface water indicated that the source of the groundwater is related to surface water. Therefore, the isotopic composition of surface water is considered being composed of rainwater and groundwater of shallow aquifer.

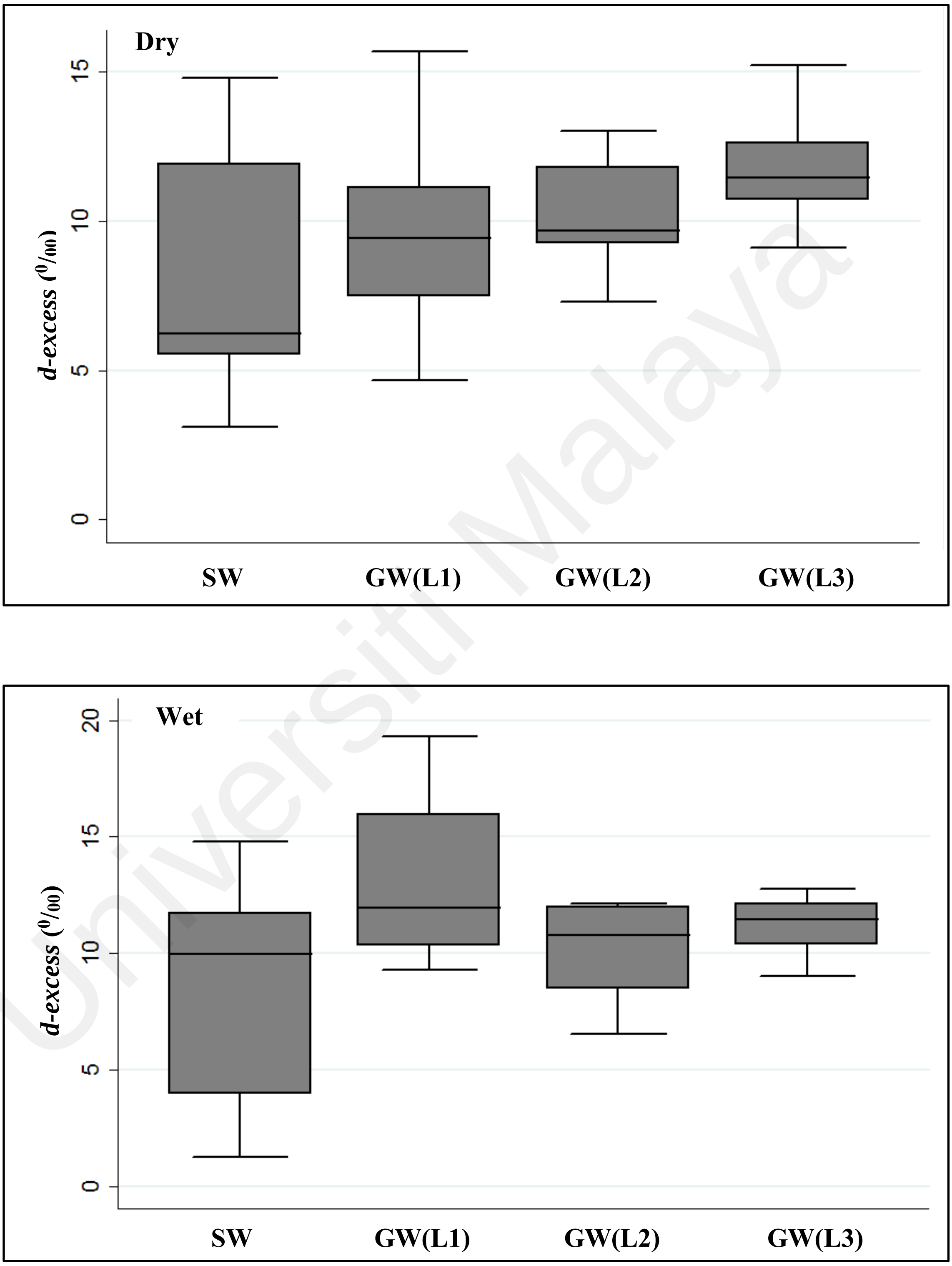

Figure 5.7: Box and whisker plot of *d-excess* for surface water and groundwater a) dry, b) wet season

The green evaporation line is referred as GW(1)EL (see Figure 5.6). This line indicates relationship between the ^{2}H and ^{18}O isotopes of groundwater in Layer 1 aquifer. The evaporation lines of groundwater in Layer 2 and Layer 3 aquifer are not illustrated in the plot, but the linear regression is shown in Table 5.2. The linear regression in groundwater Layer 1 are $^{2}H = 5.08^{18}O - 9.26$ with $R^2=0.43$ and $^{2}H = 5.84^{18}O - 1.65$ with $R^2=0.54$, Layer 2 are $^{2}H = 5.84^{18}O - 4.79$ with $R^2=0.56$ and $^{2}H = 4.97^{18}O - 10.60$ with $R^2=0.59$ and Layer 3 are $^{2}H = 5.94^{18}O - 3.58$ with $R^2=0.78$ and $^{2}H = 5.95^{18}O - 3.89$ with $R^2=0.86$, respectively for dry and wet seasons. The intersection point between GW(1)EL with the LMWL ($^{2}H = -50^{0}/_{00}$ $^{18}O = -7.9^{0}/_{00}$ and $^{2}H = -43.5^{0}/_{00}$ $^{18}O = -7.15^{0}/_{00}$), GW(2)EL with the LMWL ($^{2}H = -55^{0}/_{00}$ $^{18}O = -8.5^{0}/_{00}$ and $^{2}H = -50^{0}/_{00}$ $^{18}O = -8.1^{0}/_{00}$) and GW(3)EL with the LMWL ($^{2}H = -55^{0}/_{00}$ $^{18}O = -8.5^{0}/_{00}$ and $^{2}H = -58^{0}/_{00}$ $^{18}O = -8.7^{0}/_{00}$) for dry and wet season.

Same goes for surface water whereby, this intersection point characterized the isotopic composition of recharging rainfall to the groundwater before evaporation (Yin *et al.*, 2011a; Ayadi *et al.*, 2016; Fynn *et al.*, 2016). Relatively, smaller slopes of 5.08, 5.84, 5.84, 4.97, 5.94 and 5.95 (see Table 5.2), being less than 8 indicate that the isotopic composition of groundwater is subjected to evaporation during the recharge processes as the values are within 4 to 6 (Gibson *et al.*, 1993). The variation of d-excess in Figure 5.8 shows that groundwater in all layers have primary and secondary evaporation processes.

The negative relationship between ^{18}O and *d-excess* in Figure 5.8 clearly supported that groundwater has mixed recharge water and experienced a variable degree of evaporation before recharge to groundwater (Tsujimura *et al.*, 2007; Shah, 2013; Abreha, 2014) that is if water evaporates, the *d-excess* decreases. Evaporation of rainfall and considerable enrichment of the precipitation water prior to recharge may take place either in the free surface or on the raindrops before reaching the soil zone (Peling-Ba, 2009). It

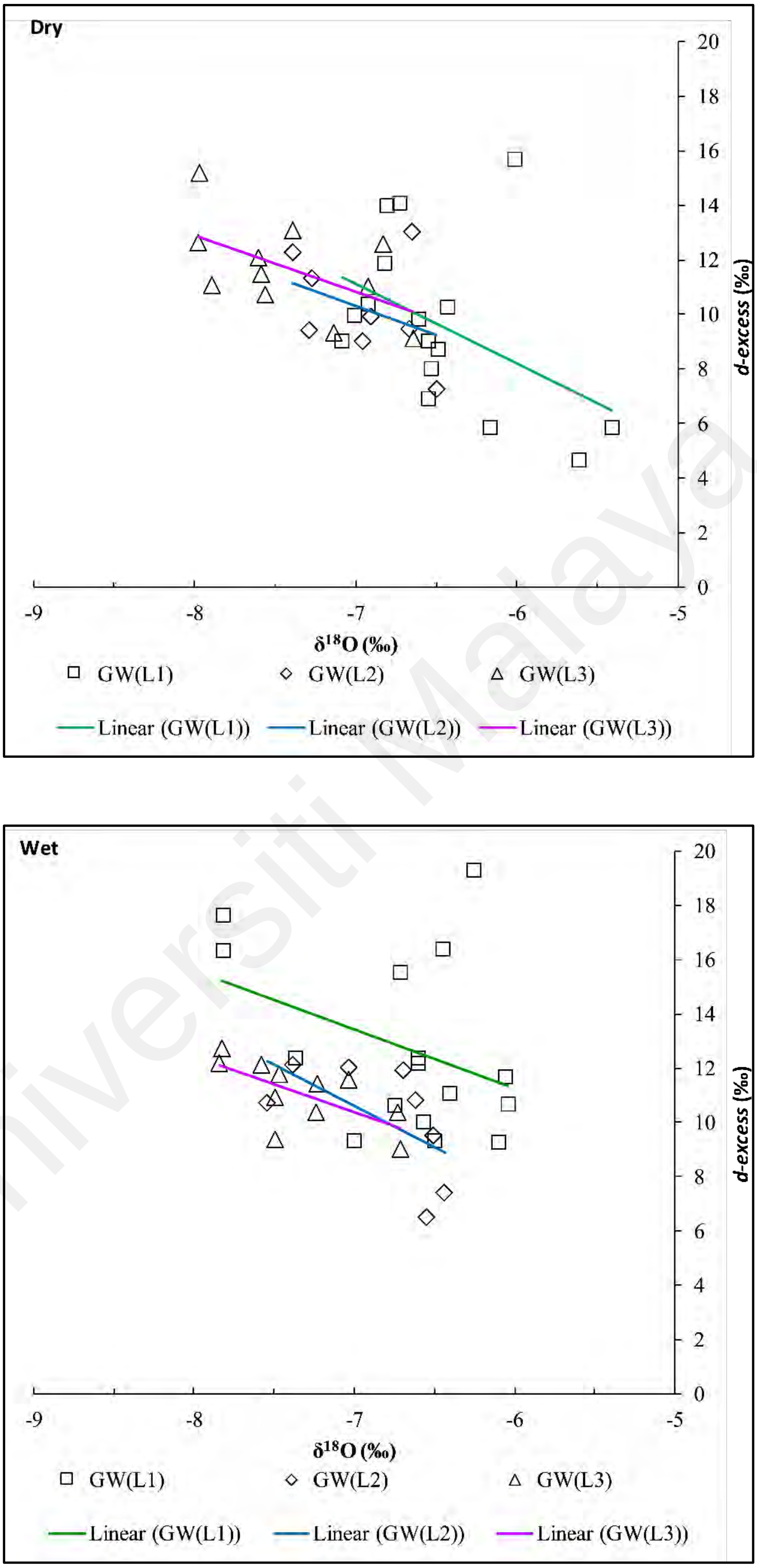

Figure 5.8: Relationship $\delta^{18}O$ with *d-excess* in groundwater (dry and wet season)

is believed that groundwater has undergone a combination of both evaporation and leaking and/or mixing processes rather than evaporation processes only (Gat & Dansgaard, 1972; Kattan, 2001; Ammar *et al.*, 2016). The high median values (Figure 5.7) could be a result from longer residence time it takes to reach the aquifer, mixing with rainwater, surface water, irrigation or anthropogenic or old water in the aquifer which leads to small variation and depletion in isotopic composition from shallow to deep aquifer (Figure 5.5).

During recharge to Layer 1, the isotopic composition position is relatively close to LMWL or above LMWL indicating negligible evaporation prior to recharge and that it has experienced rapid infiltration process of rainwater which does not allow time for evapotranspiration. This condition occurred especially during wet season where rainwater is highly evaporative during rapid diffuse recharge to the groundwater. Recharge is facilitated by rapid diffuse infiltration of rainwater through or past the soil zone. This condition occurs when soils are highly permeable with hydraulic conductivity of 10^{-3} m/s (see section 5.3.4) and have high soil infiltration rates especially during wet season when moist soils have the greatest capacity to transmit (Jones *et al.*, 2000).

According to Banoeng-Yakubo *et al.* (2010) the role of clay minerals in the unsaturated zone is to mediate and limit groundwater recharge. The spatial variation in the fraction of the clay in the material of unsaturated zone will determine the rate of direct infiltration of rainwater and consequent recharge to the saturated zone. When the clay fraction is high, infiltration rates may be considerably reduced, rendering the infiltrating water much more susceptible to the effects of evapotranspiration rates within the unsaturated zone.

The isotopic compositions that lays relatively near to the evaporation line indicates that groundwater experienced secondary evaporation before recharge to the aquifer. This condition occur when rainwater at near surface water bodies or in unsaturated zone during diffuse recharge re-evaporated which enriched the isotopic composition especially during dry season. The *d-excess* of groundwater which is higher than surface water indicates that there is inter-connection/interaction between groundwater and surface water. This connection is revealed by the similarity of the isotopic composition of Kelantan and Pengkalan Datu rivers with the neighbouring wells of Kedai Buluh (GW15), Kg. Puteh (GW1), Pintu Geng (GW4), Pasir Hor (GW11), Penyadap (GW12), Kenali (GW20), Seribong (GW21) and Pasir Tumboh (GW22) as in Appendix A. The river – groundwater interaction vice versa is up to Layer 2 as indicated by the isotopic composition of Kelantan River at Kelar (SW2) ($-6.72^{0}/_{00}$ and $-6.15^{0}/_{00}$) and Kelar well (GW24) ($-6.62^{0}/_{00}$ and $-6.65^{0}/_{00}$) for both seasons (Appendix A). Groundwater is recharges by river during wet season and groundwater is discharges to the river during dry season where interaction between river - groundwater shows that leaking and/or mixing processes are occurred in the LKRB.

The source of recharge to the aquifer in Layer 2 is leaking and or mixing from shallow aquifer of Layer 1 while recharge to the aquifer Layer 3 is leaking and/or mixing from aquifer Layer 2. As the water infiltrates, it brings the isotopic signature of evaporation water as indicated by the slope and regression line of Layer 2 and Layer 3 as mentioned previously. However, the isotopic composition is depleted as the depth increased that could posibbly water takes longer residence time to arrive to the respective aquifer layers and later on it will be mixed with old water in the aquifer which reduced the isotopic composition of ^{18}O and ^{2}H.

The inter-aquifer relationship between Layer 2 and Layer 3 are revealed at Tanjung Mas, Pengkalan Chepa and Beris Kubor area. The isotopic composition at Tanjung Mas are 7.54$^{0}/_{00}$ and -7.27$^{0}/_{00}$ (GW17, Layer 2) with -7.49$^{0}/_{00}$ and -7.97$^{0}/_{00}$ (GW 26, Layer 3) and -7.50$^{0}/_{00}$ and -7.39$^{0}/_{00}$ (GW27, Layer 3), Pengkalan Chepa are -7.39$^{0}/_{00}$ and -6.91$^{0}/_{00}$ (GW19, Layer 2) with -7.58$^{0}/_{00}$ and -7.58$^{0}/_{00}$ (GW30, Layer 3) and -7.84$^{0}/_{00}$ and -7.89$^{0}/_{00}$ (GW31, Layer 3) and Beris Kubor are-7.03$^{0}/_{00}$ and -7.29$^{0}/_{00}$ (GW23, Layer 2) with -7.83$^{0}/_{00}$ and -7.98$^{0}/_{00}$ (GW33, Layer 3) for both season. The position of wells are scattered at Tanjung Mas and inline at Pengkalan Chepa and Beris Kubor. It was also found that Layer 1 and Layer 3 are hydraulically connected as indicated by the isotopic composition wells at Kubang Kerian of 7.82$^{0}/_{00}$ and -6.92$^{0}/_{00}$ (GW10, Layer 1) with –7.23$^{0}/_{00}$ and -7.60$^{0}/_{00}$ (GW32, Layer 3). It is possible that mixing by upward vertical leakage from Layer 3 to Layer 2 and from Layer 2 to Layer 1 to occur because groundwater at LKRB is exploited for water resources from shallow and deep aquifer. The inter-aquifer relationship as mentioned above indicates that the leaking/mixing pattern of aquifer is close to the coastal area due to the basin sedimentation processes in LKRB. Therefore, based on the isotopic signatures at LKRB, it is confirmed that groundwater – river interaction and inter-aquifer connection between aquifer occurred at LKRB which indicates that aquifer is heterogeneous with or without continuous aquifer layers.

5.2.2 Tritium (^{3}H)

The cosmogenic isotope of tritium (^{3}H) has been reviewed in Chapter 2 and it is an excellent tool for determining the ages of water in the river basin. Sampling location and analysis are briefly described in Chapter 3. The tritium content of precipitation, surface water and groundwater are tabulated in Appendix B for ease of comparison and interpretation of the groundwater recharge processes.

5.2.2.1 Tritium (^3H) in Rainwater

The long term tritium content in rainfall of Kota Bharu station was downloaded from Global Network of Isotopes in Precipitation (GNIP) database, IAEA/WMO (2017). This database is a cooperation between the World Meteorological Organization (WMO) and the International Atomic Energy Agency (IAEA). Kota Bharu station is selected as the nearest station within the study area. The available monthly rainfall data were from April 1980 to December 1994 with a total of 43 samples. The downloaded tritium content of rainfall is listed in Appendix B and the statistical summary is presented in Table 5.3. The long-term tritium data range from 0.9 TU to 9.9 TU with a mean of 5.0 ±2.1 TU. Data are plotted as a time series as shown in Figure 5.9. For comparison with recent tritium content, analysis results of rainwater collected at LRA Kg. Puteh is plotted in Figure 5.10 (blue line) and tabulated in Appendix B.

Table 5.3: Statistical summary of tritium content in rainfall

Rainfall	**GNIP (Apr 1980 – Dec 1994)**	**LKRB (Apr 2014- Jan 2015)**
n	***43***	***10***
Minimum	0.9	2.6
Mean	5.0	3.8
Maximum	9.9	5.8
Standard deviation	2.1	0.9

The recent tritium content at LKRB ranges from 2.6 to 5.8 TU with a mean of 3.8 ±0.9 TU as presented in Table 5.3. This 3.8 TU value is similar with the tritium in Melbourne precipitation ~ 3.5 TU (IAEA, 2011a) which indicated modern rainfall. The recent rainfall data are plotted continuously from the long-term rainfall of Kota Bharu station as in Figure 5.10. It is clearly shown that the tritium content at LKRB shows a decreasing trend which is a similar trend with Ottawa and Kaitoke of Northern and Southern Hemisphere (see Figure 2.3). Even though the LKRB is located at the

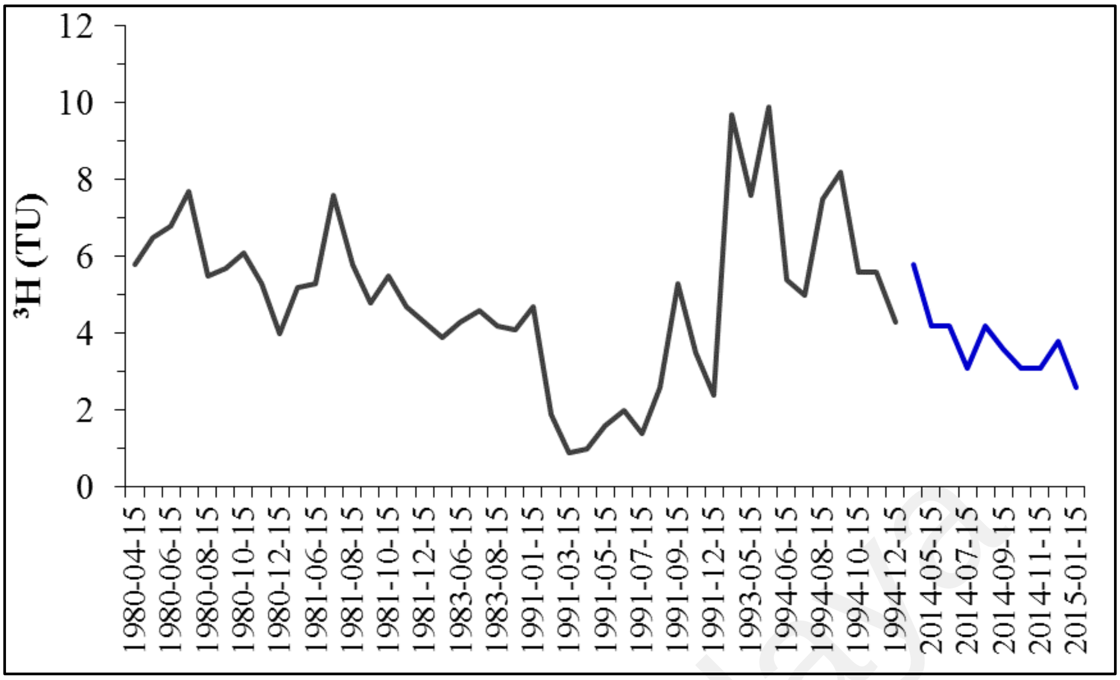

Figure 5.9: Long-term tritium content in rainfall generated from GNIP database (black line) and tritium content in rainfall from LRA Kg. Puteh, Kota Bharu (blue line).

Equatorial, far from the Northern and close to Southern Hemisphere, the declines in trend followed the decrease of world tritium content. The measurement of tritium in rainwater is essential for local tritium studies and will provides site–specific information for scaling of the establishment input function to nearby location (Gusyev *et al.*, 2016).

5.2.2.2 Tritium (^{3}H) in Surface Water and Groundwater

Box and whisker plot in Figure 5.10 shows the variation of tritium content in surface water and groundwater while Table 5.4 summarized the statistical values as listed in Appendix B. The range of tritium content in surface water is 2.1 TU to 3.0 TU with a mean of 2.6±0.4 TU. Tritium content in groundwater ranges from 1.7 TU to 2.8 TU with a mean of 2.5±0.4 TU, 1.4 TU to 2.4 TU with a mean of 1.8±0.3 TU and 1.4 TU to 2.5 TU with a mean of 1.7±0.4 TU for Layer1, Layer 2 and Layer 3 respectively. The means of surface water and groundwater are lower than the mean of rainfall tritium of 3.8 TU as shown in Table 5.4. The variation of tritium content in surface water is similar/close with groundwater Layer 1 while tritium content of groundwater Layer 2 is similar/close with groundwater Layer 3. It can be said that hydraulic connectivity occurred between them. Tritium in LKRB groundwater shows a decreasing content compared to previous study by Mohamad and Mohd Ali (1981) which ranged from 0 TU to 7 TU.

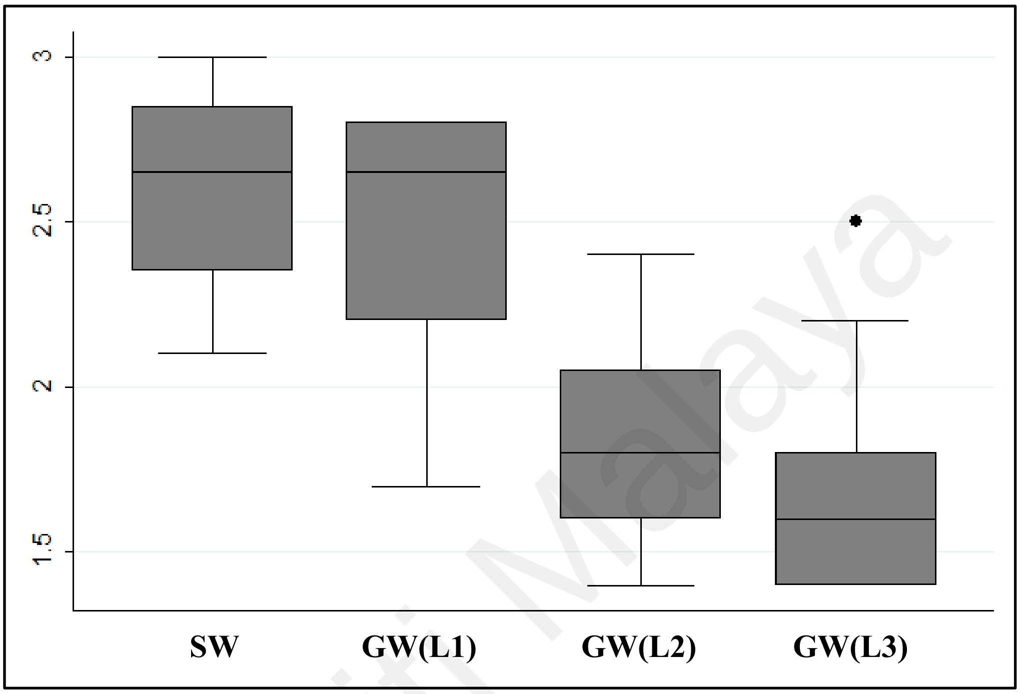

Figure 5.10: Box plot of tritium in surface water (SW) and groundwater (GW)

Table 5.4: Statistical summary of tritium content in surface water and groundwater

Tritium	Surface water	Groundwater		
		Layer 1	Layer 2	Layer 3
n	***4***	***8***	***8***	***10***
Minimum	2.1	1.7	1.4	1.4
Mean	2.6	2.5	1.8	1.7
Maximum	3.0	2.8	2.4	2.5
Standard deviation	0.4	0.4	0.3	0.4

The spatial distribution of tritium in surface water is shown in Figure 5.11 while spatial distributions in groundwater are shown in Figure 5.12. Surface water samples show an increase of tritium content as the water flows towards the downstream. Kelantan River samples at Kelar (SW2) and Tambatan Diraja (SW1) have tritium content of 2.7 TU and 3.0 TU while Kemasin river samples at Telok (SW5) and Pengkalan Baru (GW4) have tritium content of 2.1 TU and 2.6 TU respectively. The spatial distribution of groundwater in Layer 1 indicated that only sample at Pasir Hor (GW4) has tritium content of 1.7 TU while other samples are above 2.0 TU (Appendix B). In Layer 2, only samples at Kenali (GW20) and Seribong (GW21) have tritium contents of 2.4 TU and 2.2 TU while other samples are below 2.0 TU (Appendix B). In Layer 3, only samples at Chicha (GW28) and Perol (GW29) have tritium contents of 2.2 TU and 2.5 TU while other samples are below 2.0 TU (Appendix B). A decreasing trend of tritium content with depth in groundwater is observed from the mean values of 2.5 TU (Layer 1) to 1.7 TU (Layer 3) as in Table 5.4 and Figure 5.13. This trend shows that tritium experienced a decaying process during the travel time (Cartwright & Morgenstern, 2012)

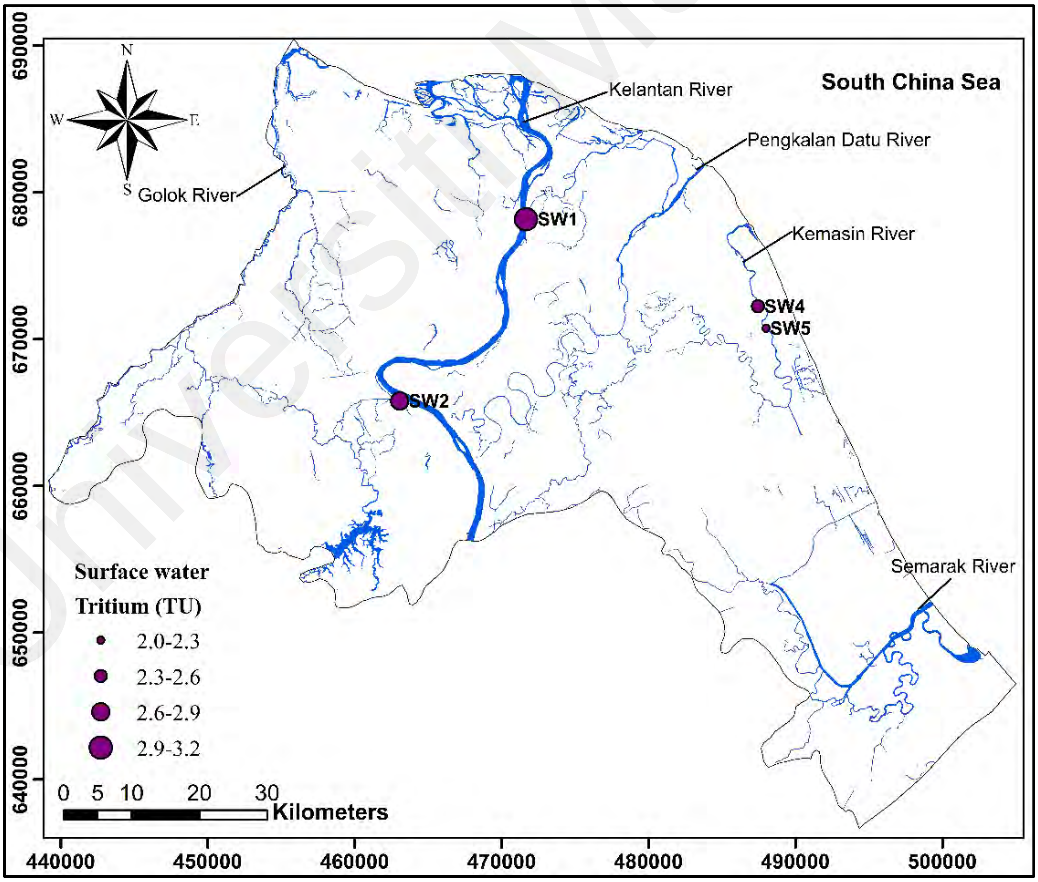

Figure 5.11: Spatial distribution of tritium at surface water

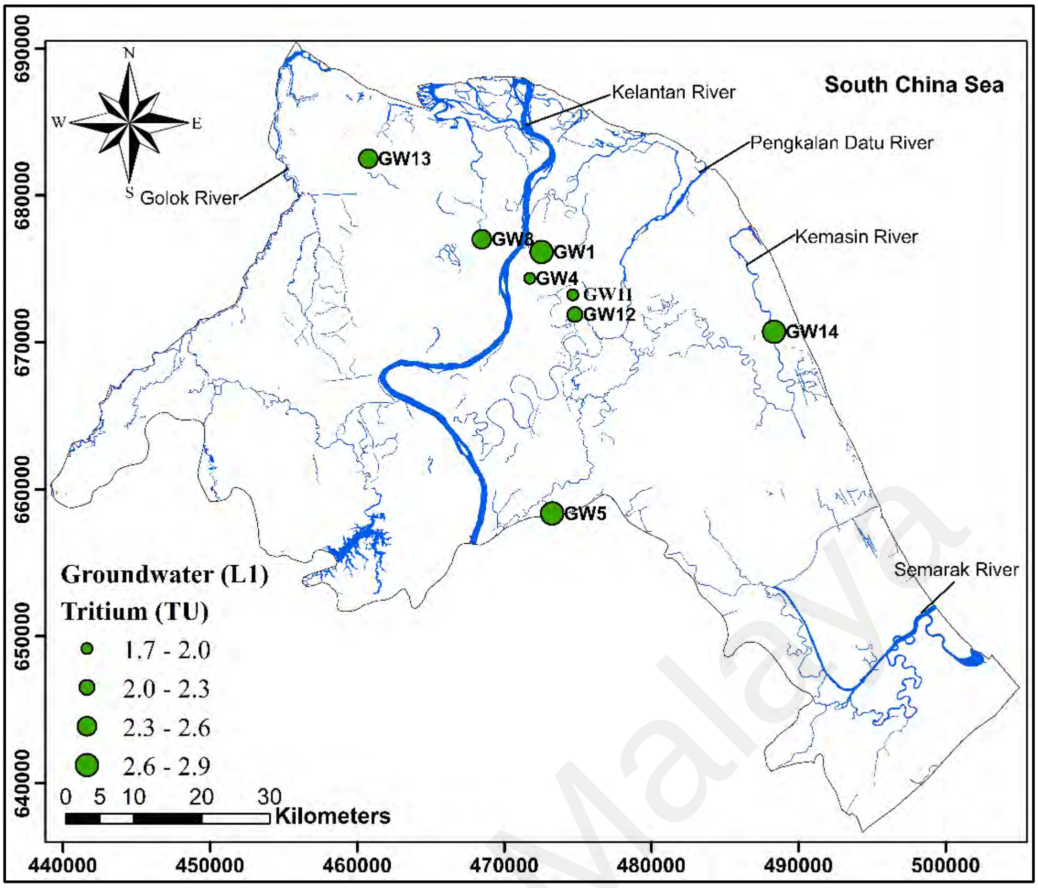

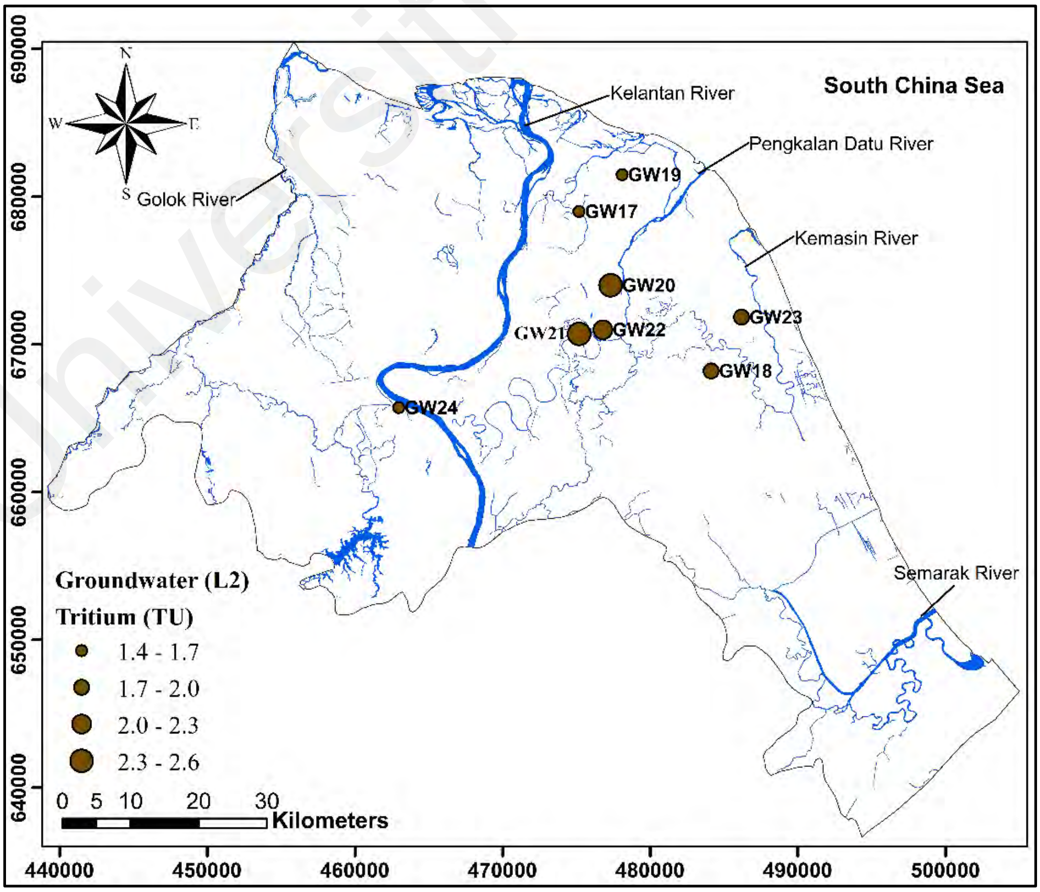

Figure 5.12: Spatial distribution of tritium in groundwater (Layer 1, Layer 2 and Layer 3)

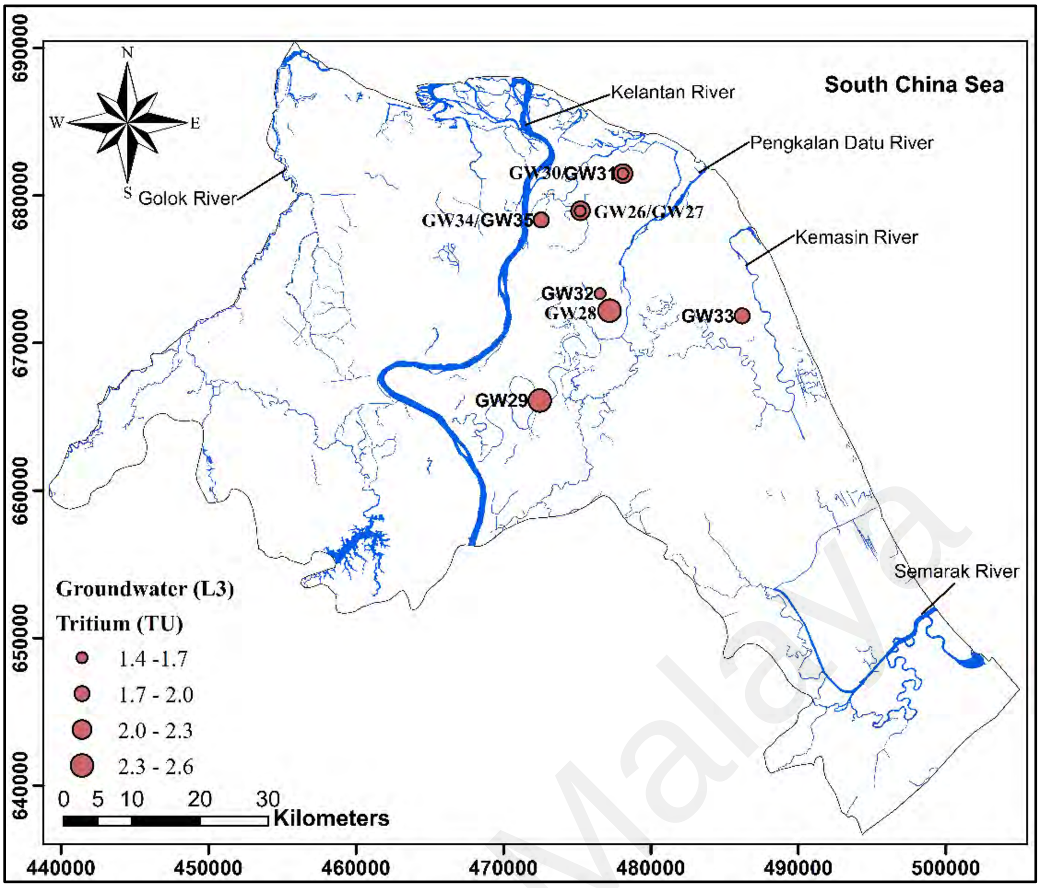

Figure 5.12, continued.

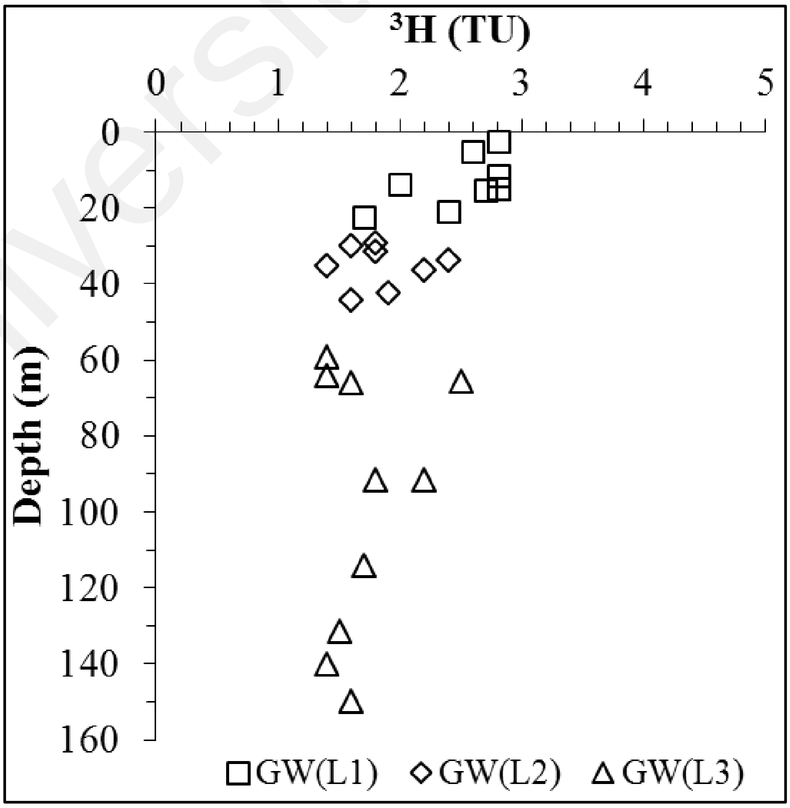

Figure 5.13: Distribution groundwater tritium with depth

5.2.2.3 Qualitative 'age' of Groundwater

The occurrence of tritium in groundwater directly depends on recharge regime, infiltration of runoff through unsaturated zone and the transition from one aquifer to the another aquifer as well as hydraulic connection between surface water and groundwater (Ferronsky & Polyyakov, 2012). The indication of 'age' based on qualitative assessment was mentioned previously in Chapter 2 which can provide the relative age on a time scale of about the past 50 years (Ako *et al.*, 2013) whether the groundwater is modern (less than about 50 years in age) or pre-modern (older than about 50 years in age) (Clark & Fritz, 1997a). Clark and Fritz (1997a) has proposed a qualitative interpretation of groundwater residence time based on the tritium content for coastal/low-latitude regions by assuming that piston flow conditions (no dispersion or mixing). The tritium content of less than 0.8 TU is considered to indicate that groundwater is recharged by sub-modern water prior to 1952, 0.8 to 2.0 TU indicate that groundwater is recharged with mixture of sub-modern and recent water, 2 to 8 TU is indicate that groundwater is recharged by modern water which is less than 5 year to 10 years, 10 to 20 TU indicated that groundwater is recharged by the residual bomb tritium present in water for more than 20 years and tritium content more than 20 indicate groundwater has a considerable component of recharge water from 1962 or 1970s. This qualitative guideline is summarized in Table 5.5.

Table 5.5: Qualitative interpretation of groundwater residence time (Clark and Fritz, 1997)

Tritium (TU)	Qualitative Age
<0.8	Submordern – recharged prior to 1952
0.8 - 2	Mixture between submodern and recent
2- 8	Modern < 5 to 10 years
10- 20	Residual bomb tritium present >20 years
>20	Considerable component of recharge from 1960s or 1970s

By applying the classification of Clark and Fritz (1997a) in Table 5.5, the variation of groundwater (see Figure 5.9 and Table 5.4) in general is a mixture between sub-modern and modern water to modern water that recharges to the aquifer. Specifically, the mean of groundwater (see Table 5.4) indicates that Layer 1 is modern water aquifer, Layer 2 and Layer 3 are mixture of sub-modern to modern water aquifer. The details of qualitative interpretation of 'age' for each samples are is listed in Appendix B.

The relationship between tritium and oxygen-18 is shown in Figure 5.13. The use of tritium along with stable isotopes (^{2}H and ^{18}O) as stated by Morgenstern *et al.* (2010) was the most direct dating tools for groundwater because both isotopes are part of water molecules and ages are included during the travel time. The relationship in Figure 5.13 has confirmed that the sources of groundwater at LKRB have experienced modern recharge with ages less than 5 year to 10 year except in the deep aquifer which feature a mixed recharge water. Surface water and shallow groundwater (Layer 1) have high tritium content but lower than rainfall indicate that sources of modern rainfall rapidly runoff or percolate into surface water bodies or rapidly infiltrates through the unsaturated zone before reaching the shallow aquifer. Fast transmit time will reduce the tritium decay process during the water travel that contain high tritium (> 2 TU) as in Figure 5.10 and Figure 5.11 (L1).

Section 5.2.1 (stable isotopes) indicated that shallow aquifer and surface water are hydraulically connected in both wet dan dry seasons and in certain areas the connection are up to aquifer Layer 2. The presence of clay sediment with low transmissivity (Ayadi *et al.*, 2016) as continuous or uncontinuous layer or lenses has influenced the mixing process by extending the contact time, leading to longer groundwater residence time from shallow to deep aquifer. The residence time of water from shallow aquifer to deep aquifer

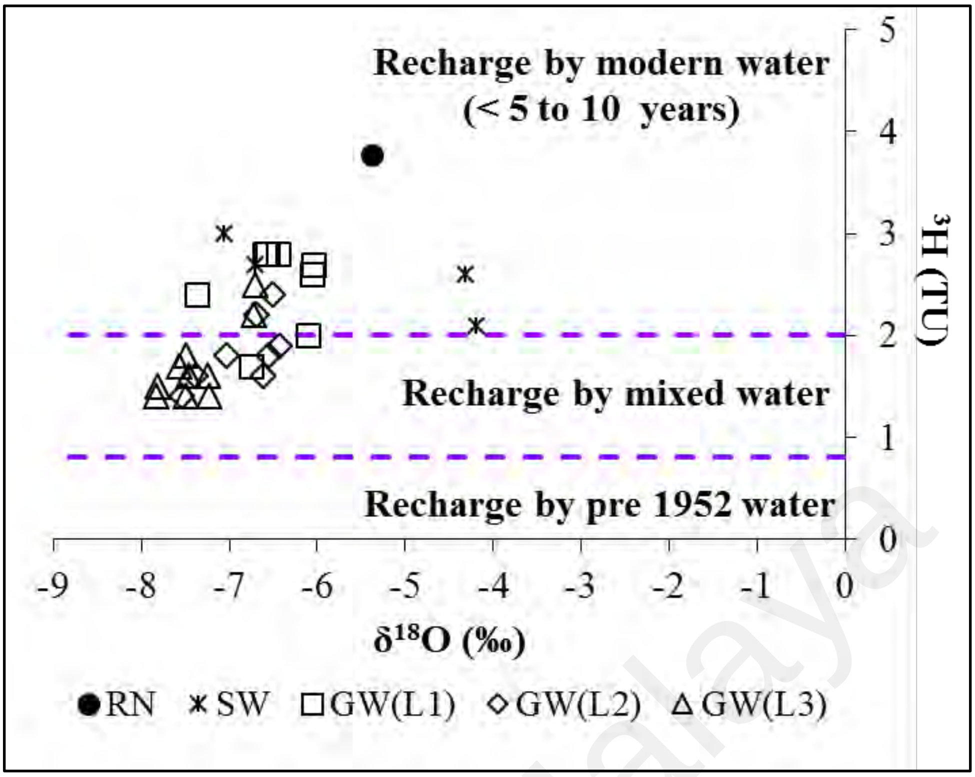

Figure 5.14: Relationship between tritium and oxygen-18

is proven (see Figure 5.13) as the tritium content decreased (< 2 TU) with depth which leads to the radioactivity decay and mixing of 'young water' (modern) with 'old water' (sub-modern). The decaying process during the water residence time does not interact with the aquifer materials (Ingraham, 1998). Rapidly mixed and greatly diluted water in Layer 2 and Layer 3 resulted in mixed water of submodern and modern water. The inter-aquifer relationship between Layer 1, Layer 2 and Layer 3 are confirmed by the mixing/leaking processes (see Figure 5.11 and Figure 5.12) especially in the area of active groundwater abstraction by AKSB at Pasir Hor (GW11), Penyadap (GW12), Kenali (GW20), Kubang Kerian (GW32), Chicha (GW28), Seribong (GW21), Tanjung Mas (GW27), Kg. Puteh (GW1) and Perol (GW29). This abstraction activity has developed piezometric depression during pumping through vertical leakage or inferred lateral flow from the potential recharge zone (Kelly, 1997; Madioune *et al.*, 2014).LKRB as an active groundwater utilization, contain recharged water of modern and mixed water.

5.2.3 Radon (^{222}Rn)

Radon as a radiogenic isotope has been appraised in detail in Chapter 2 as a tracer with short half-life for determining the surface water – groundwater interaction. Therefore, this chapter will present the results of radon at LKRB. The sampling location and analysis of radon are described in Chapter 3. The radon activity concentration of river water and groundwater is listed in Appendix C.

5.2.3.1 Radon (^{222}Rn) in River Water and Groundwater

The radon activity concentration in river water and groundwater of LKRB as tabulated in Appendix C is summarized in Table 5.6 for wet and dry seasons. During the wet season, the range of radon activity in river water is 0.19 to 0.63 Bq/L with a mean of 0.38±0.18 Bq/L while the range of radon in groundwater is 1.83 to 11.75 Bq/L with a mean of 5.75±3.13 Bq/L, 3.00 to 10.58 Bq/L with a mean of 7.74±2.88 Bq/L and 10.23 to 18.58 Bq/L with a mean of 13.96±3.86 Bq/L in Laye1 1, Layer 2 and Layer 3 respectively. In dry season, the range of radon activity in river water is 0.10 to 0.51 Bq/L with a mean of 0.29±0.13 Bq/L while the range of radon in groundwater is 2.77 to 12.50 Bq/L with a mean of 6.47±3.68 Bq/L, 4.03 to 14.29 Bq/L with a mean of 7.63±3.98 Bq/L and 6.52 to 16.44 Bq/L with a mean of 11.08±4.42 Bq/L in Layer 1, Layer 2 and Layer 3 respectively. In general, the radon activity in river water is relatively lower in several orders of magnitude than groundwater as listed in Table 5.6. The highest radon concentrations are measured at SW7 with 0.60 Bq/L and SW2, 0.51 Bq/L during wet and dry season (Appendix C). It is noticed that radon activity in groundwater varies considerably between aquifer layers.

The distribution of radon concentration in groundwater depends on the emanation potential of the soils, transport processes in groundwater and outgassing to the atmosphere (Grolander & Kärnbränslehantering, 2009). Beside that, fracture density and the presence of the radioactive minerals in the host rock play significant roles in the dissolution of radon in groundwater (Choubey *et al.*, 2003; Grolander & Kärnbränslehantering, 2009; Najeeb *et al.*, 2014). During wet season, high radon concentrations are measured at GW1 with 11.75 Bq/L, GW42 with 10.58 Bq/L and GW29 with 18.42 Bq/L for Layer 1, Layer 2 and Layer 3 aquifers, respectively. The highest concentration of radon during dry season is measured at GW2 with 12.50 Bq/L, GW20 with 14.29 Bq/L and GW33 with 16.44 Bq/L for Layer 1, Layer 2 and Layer 3 aquifers, respectively. The mean concentration of radon as in Table 5.6 indicates groundwater in Layer 3 shows high concentration of radon compared to Layer 1 and Layer 2 aquifers.

The distribution trend of radon activity with depth as shown in Figure 5.15 indicates no specific trend between wells depth and radon concentration. High concentration of radon at deeper depth is related with the position of the aquifer which is underlying by the metamorphic or granite bedrock (Chapter 4). U-Pb zircon analysis of Eastern province granitoid at Boundary Range and Noring has indicated that uranium concentration ranges from 660 ppm to 3200 ppm and 620 ppm to 2300 ppm (Ng *et al.*, 2015) respectively. Saat *et al.* (2014) and Abdul Malik *et al.* (2015) studies water quality at selected area in West Malaysia have identified a few groundwater wells that contains high radon concentration above the maximum contamination limit of 11.1 Bq/L by USEPA are located in granitic rock. Thus, emanation of radon from the radium decay of host rock rich uranium minerals enriched the dissolvability of radon in the aquifer (Najeeb *et al.*, 2014).

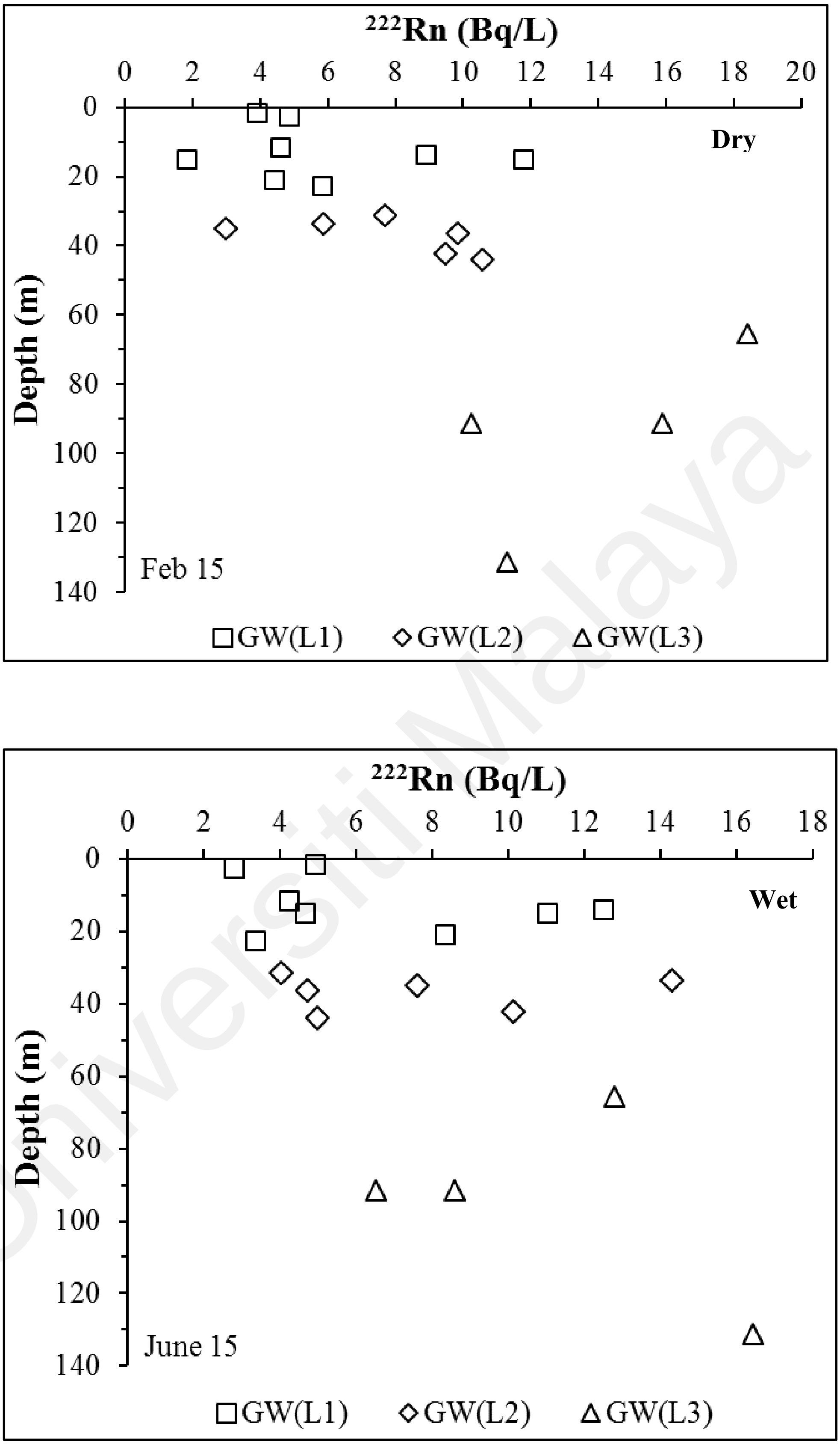

Figure 5.15: Distribution of radon activities in groundwater with depth (dry and wet season)

Table 5.6: Statistical summary of radon activities on February 2014 and June 2015

Radon Activity (Bq/L)	February 2015				June 2015			
	SW	GW(L1)	GW(L2)	GW(L3)	SW	GW(L1)	GW(L2)	GW(L3)
n	***9***	***8***	***6***	***4***	***9***	***8***	***6***	***4***
Minimum	0.19	1.83	3.00	10.23	0.10	2.77	4.03	6.52
Mean	0.38	5.75	7.74	13.96	0.29	6.47	7.63	11.08
Maximum	0.63	11.75	10.58	18.42	0.51	12.50	14.29	16.44
Standard deviation	0.18	3.13	2.88	3.86	0.13	3.68	3.98	4.42

n: number of samples

5.2.3.2 Connectivity between River Water and Groundwater

The indication to evaluate the interaction between river water and groundwater at LKRB is qualitatively according to the radon activity concentration measured in the river and groundwater samples. The spatial distribution of radon activity is shown in Figure 5.16 and Figure 5.17 for both season. There is no general trend in spatial distribution between both season of river water and groundwater concentration even though the samples during wet season are collected after the flood event occurred at LKRB. Different locations will have different radon concentrations.

Figure 5.18 shows that all river water samples have radon activity concentration below 1 Bq/L during wet and dry seasons. It can obviously be seen that groundwater has high concentration in contrast to river water. The availability of radon activity in river water indicates groundwater inflow (discharge) into the river in both seasons because river water is not directly in contact with the solid materials to the extent of the groundwater (Grolander & Kärnbränslehantering, 2009), or it may also come from the emanation of radon from the sediment in the hyporheic zone (Cook *et al.*, 2006). The low input of shallow groundwater (see Figure 5.16 and Figure 5.17) that discharged into the river water

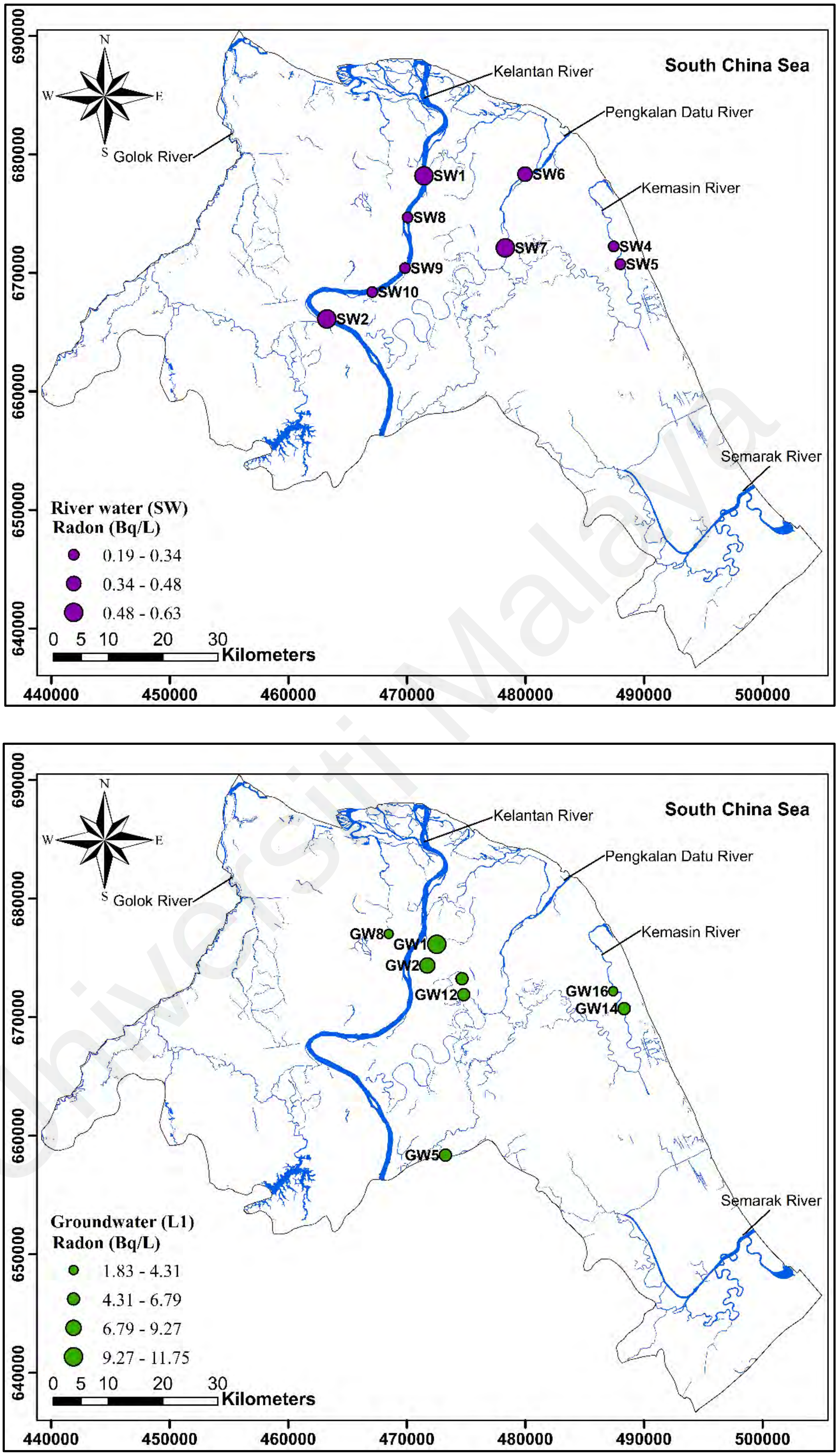

Figure 5.16: Spatial distribution of radon activity concentration in river water (SW) and groundwater (L1, L2 and L3) (wet season)

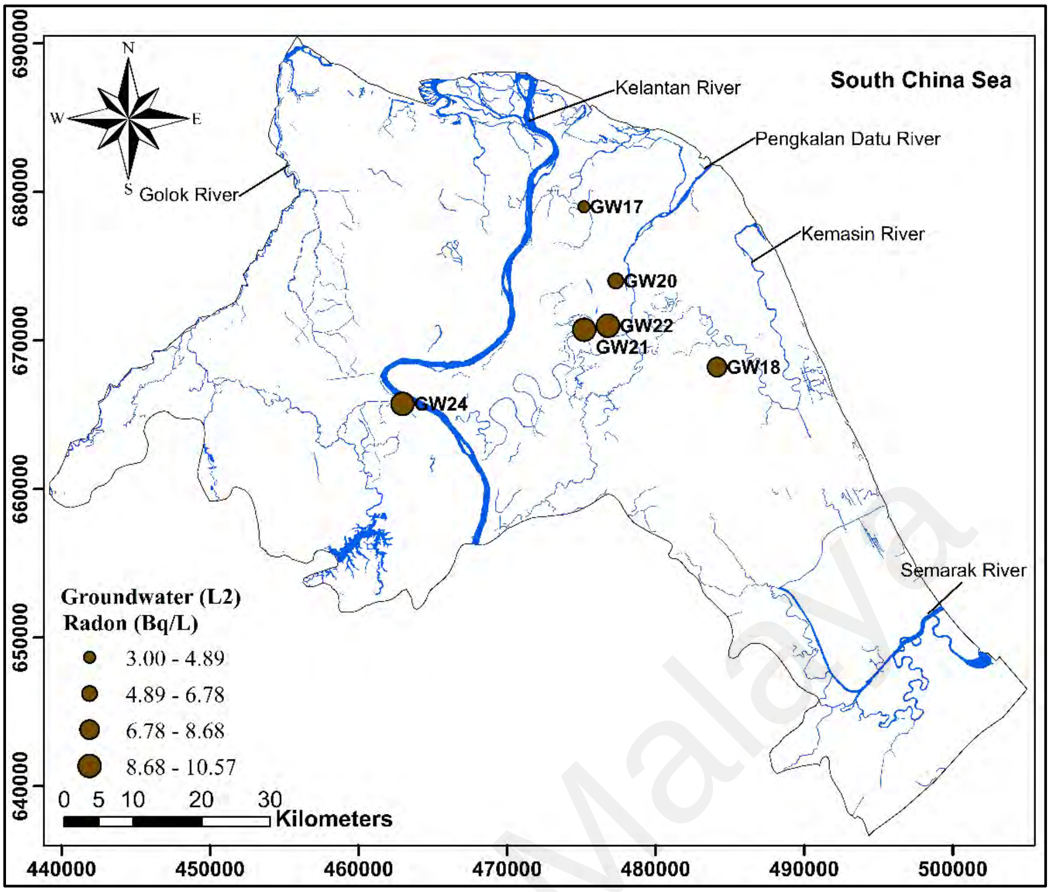

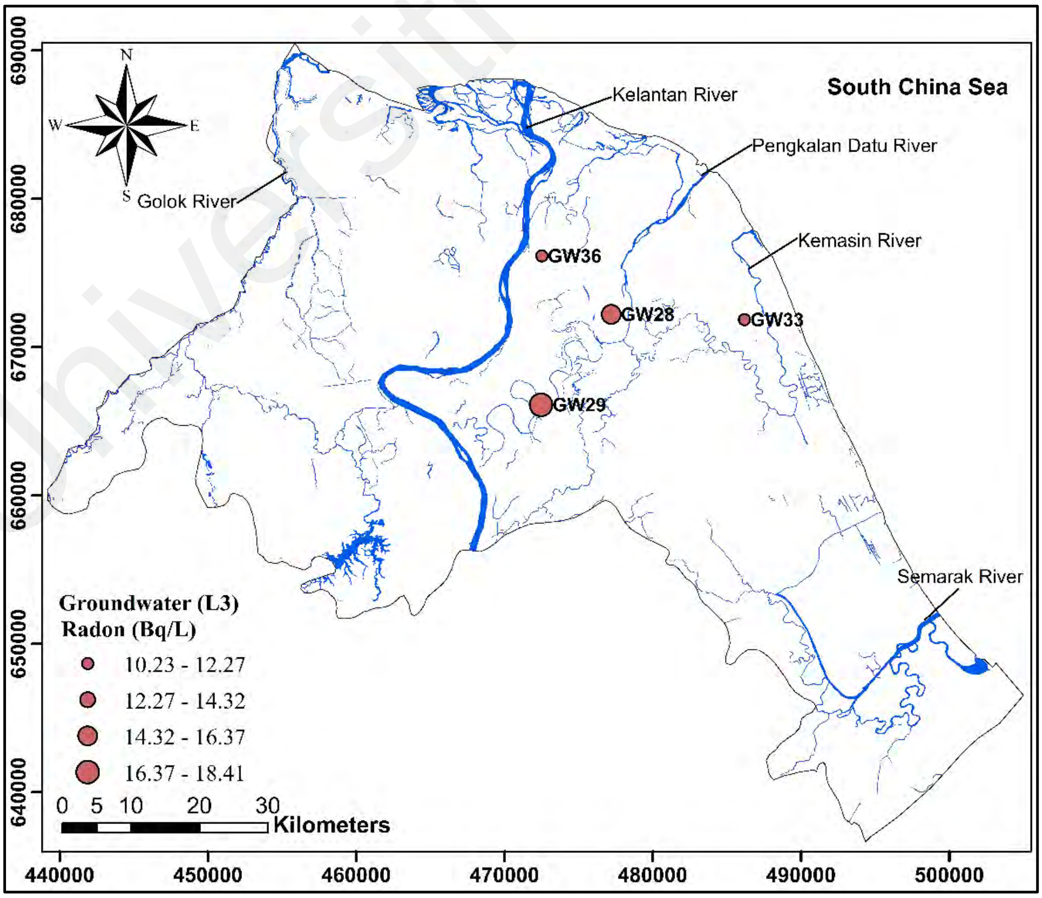

Figure 5.16, continued.

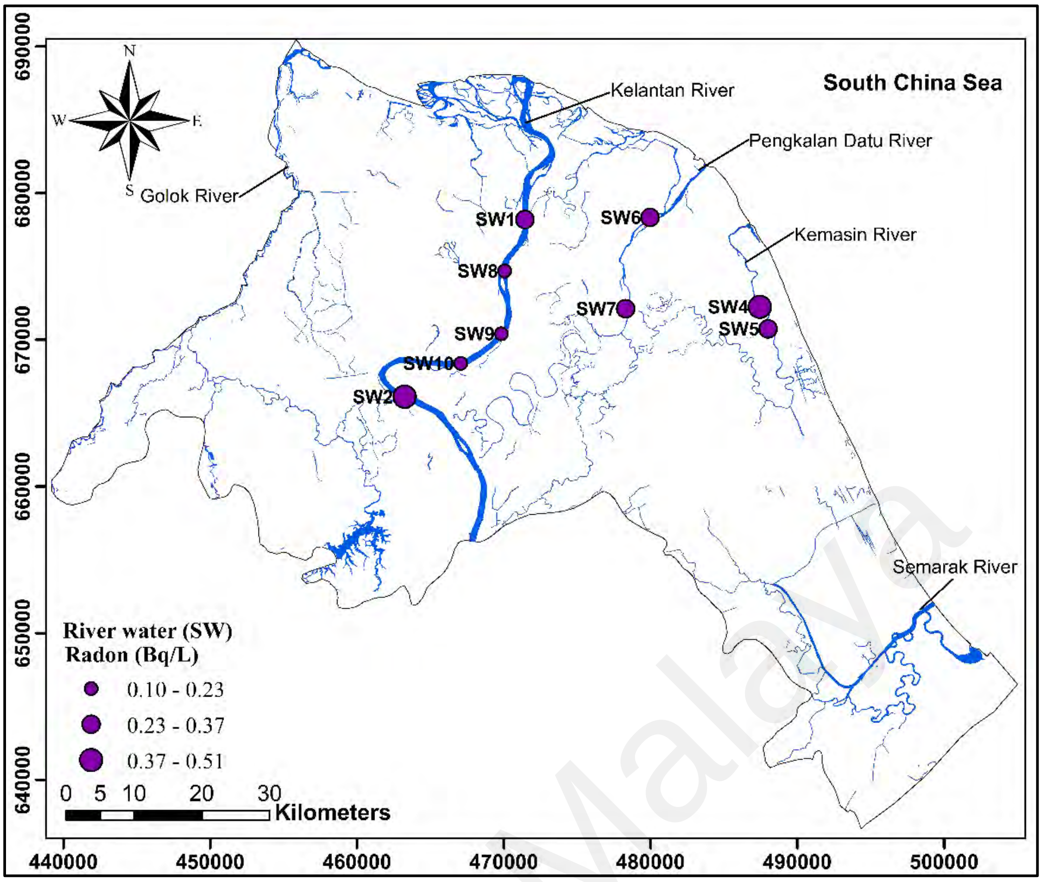

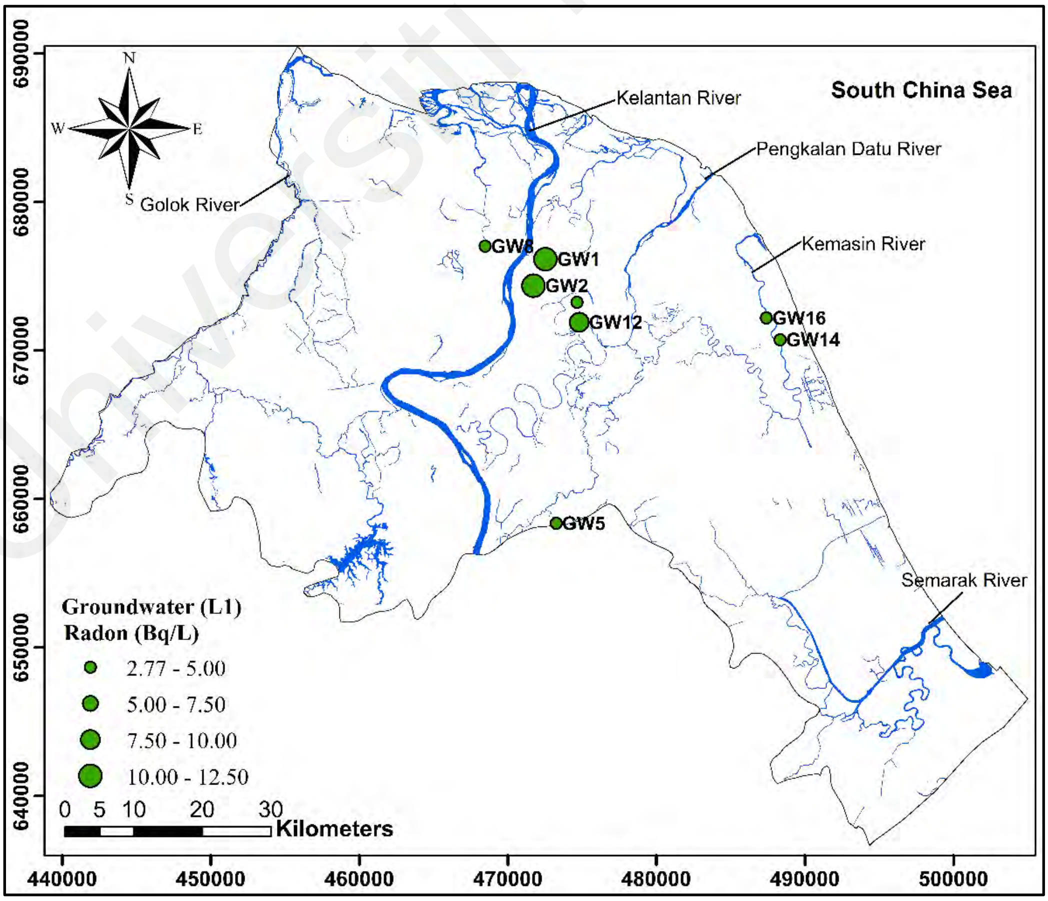

Figure 5.17: Spatial distribution of radon activity concentration in river water (SW) and groundwater (L1, L2 and L3) (dry season)

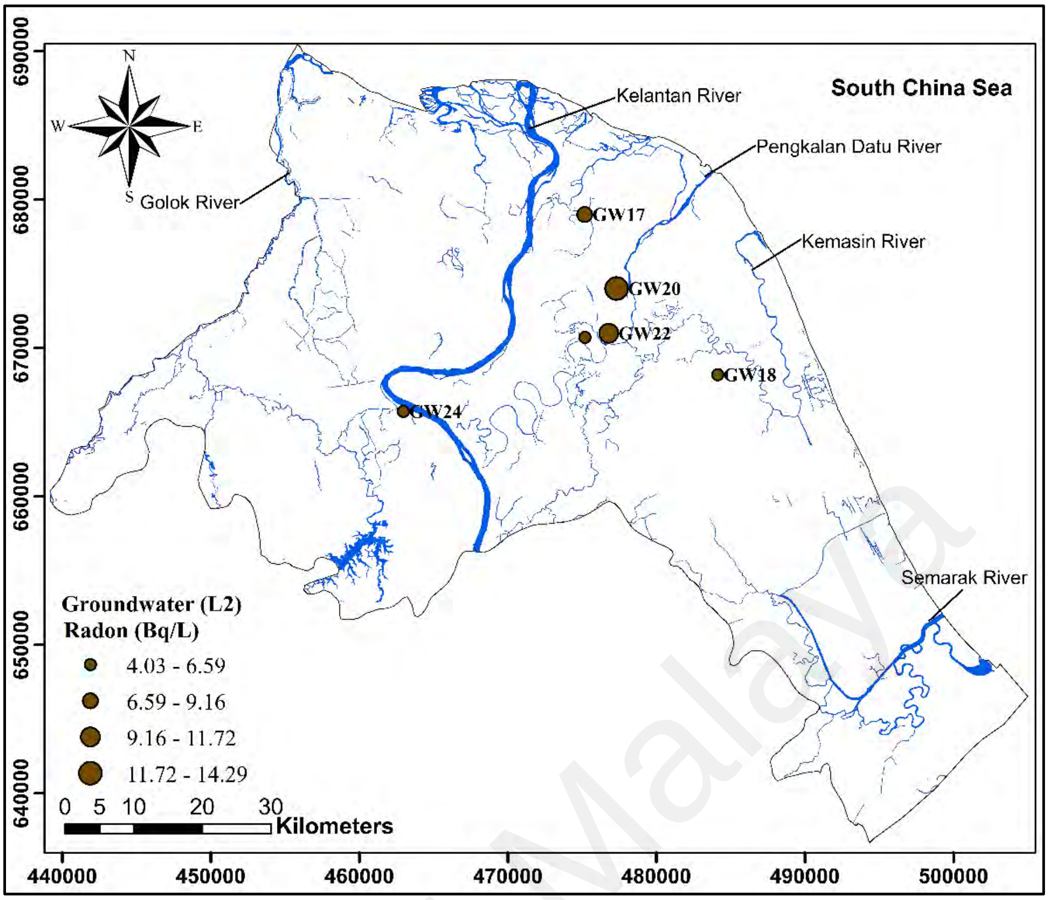

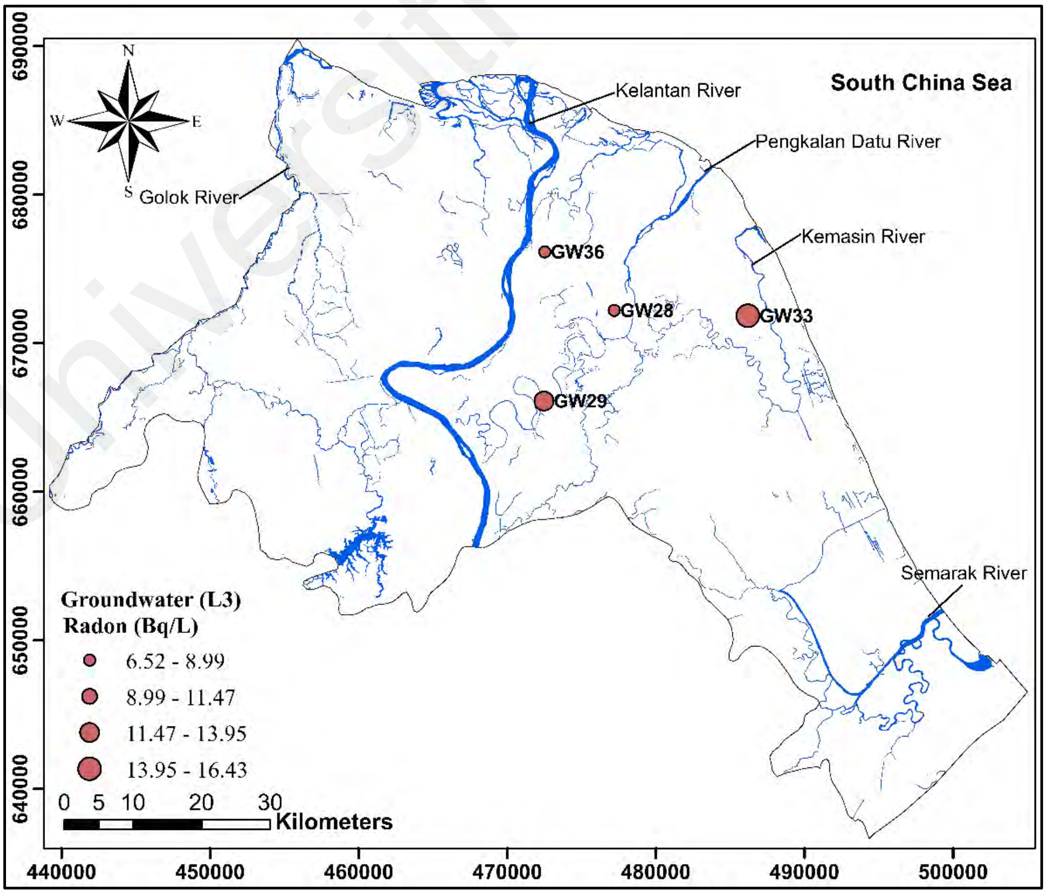

Figure 5.17, continued.

has led to the low radon activity in the river caused by the radioactive decays and was quickly lost through outgassing processes to the atmosphere which was favoured by the turbulent current in river (Bertin & Bourg, 1994; Stellato *et al.*, 2008).

The infiltrated water (recharge) from rainfall and surface water to the shallow aquifer will dilute the radon and lower its concentration in aquifer especially during heavy rainfall, since rainwater is low in radon concentration (Bertin & Bourg, 1994). However, considering the similarity trends during wet and dry seasons, it can be said that during the infiltration, radon emanates from soil in the unsaturated zone will enriched the radon concentration in water. The low radon in groundwater is possibly due to the infiltration process in which river loses water to the aquifer (Hoehn & von Gunten, 1989; Baskaran *et al.*, 2009). It takes approximately 30 days for radon in aquifer to reach equilibrium (steady state) condition in contact with the surrounding soil (Bertin & Bourg, 1994; Grolander & Kärnbränslehantering, 2009). The river recharge and groundwater discharge give an important indication of the connectivity between river water and groundwater inferred at LKRB in both seasons by using radon as a tracer.

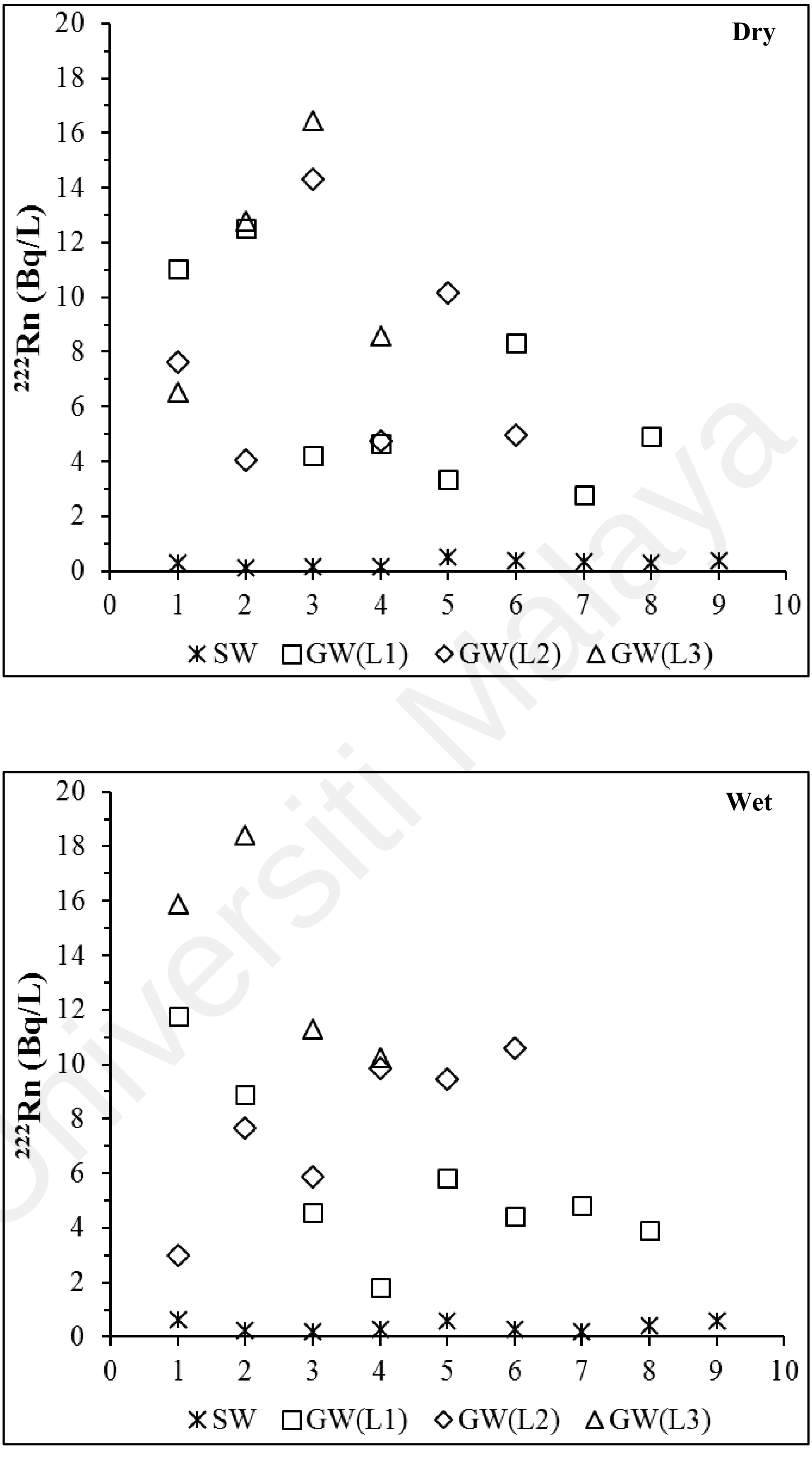

Figure 5.18: Radon activities in river water (SW) and groundwater (GW) (dry and wet season).

5.2.4 Hydrogeochemical (HC)

5.2.4.1 Hierarchical Cluster Analysis (HCA)

A long-term hydrochemistry data set from 1989 to 2012 was used to evaluate the hydrogeochemical evolution of shallow groundwater aquifer using multivariate statistical of hierarchical cluster analysis (HCA). The analysis results of 27 monitoring wells with 12 variables are presented in dendrogram as shown Figure 5.19.

The classification of the wells into clusters was based on visual observation of the dendrogram. By using the Euclidean distance as a distance measure and Ward's method as a linkage, the most distinctive groups can be produced. The phenon line was drawn across the dendrogram at a linkage distance of about 12. Thus, wells with a linkage distance lower than 12 are grouped into the same cluster. Therefore, the phenon line is the benchmark in separating the dendrogram into four (4) clusters of C1 to C4. Gu¨ler *et al.* (2002) stated that fewer or greater numbers of clusters could be defined by moving the position of the phenon line up or down on the dendrogram. This subjective evaluation made HCA a semi objective method applied for classification.

Table 5.7 shows descriptive statistics of each cluster of shallow groundwater using median values of twelve (12) variables and physical characteristics. Facies for each cluster are determined using major ions and represented using Stiff diagrams while an elevated median concentration of minor and trace constituents indicating a unique characteristic of the clusters is stated in Figure 5.19. The four clusters show two main prevalent facies of Na–HCO_3 (C1 and C3) and Ca–HCO_3 (C2 and C4) with slightly distinctive geochemical groups of shallow groundwater wells.

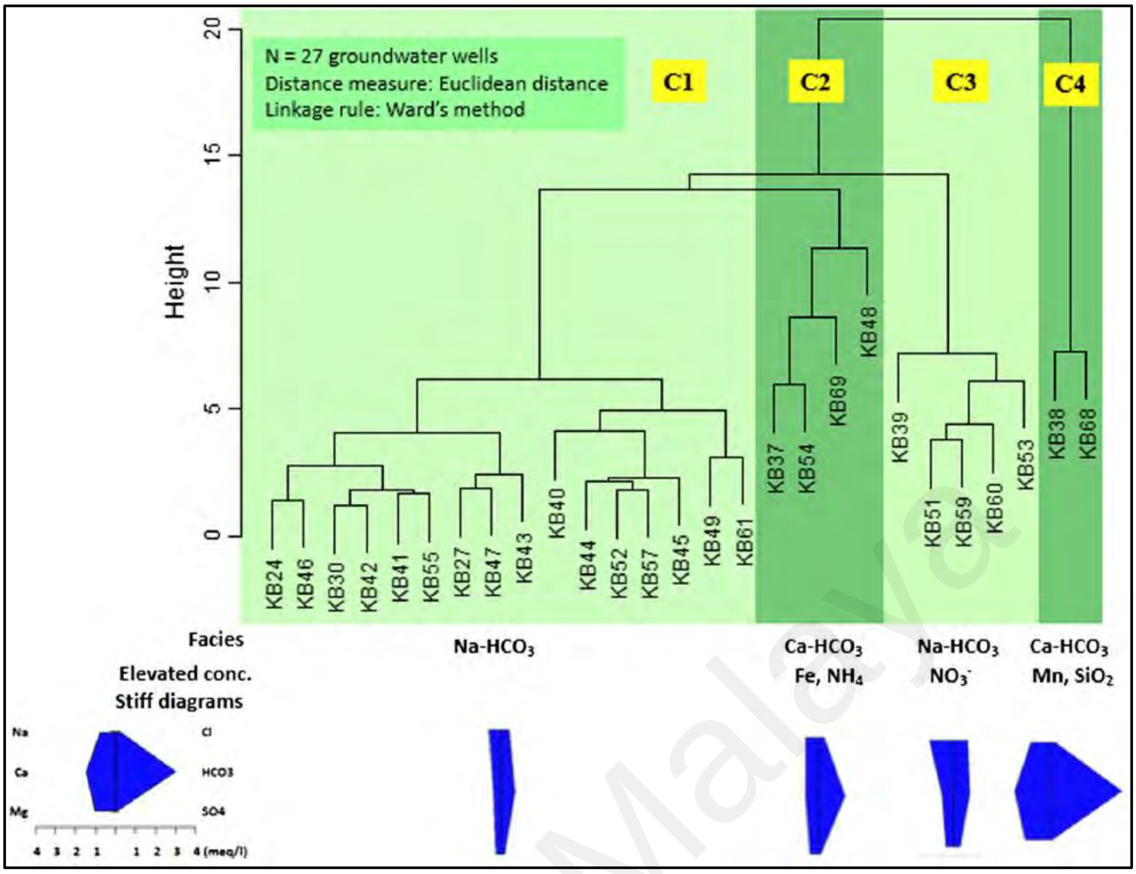

Figure 5.19: Dendrogram of the shallow groundwater wells, showing the division into four clusters and the median concentration Stiff diagram of each cluster

Cluster 1 (C1) is characterized by the lowest concentration of most major ions: Ca^{2+}, Mg^{2+}, Na^{+}, K^{+}, HCO_3^{-}, plus with Fe^{2+}, Mn^{2+}, pH, conductivity and TDS, while C3 has elevated concentrations of Na^{+}, Cl^{-}, SO_4^{2-} and NO_3^{-} with the lowest concentrations of Mn^{2+}. C2 is indicated by an elevated concentration of Fe^{2+}, and NH_4 with lowest Cl^{-}, SO_4 $^{2-}$ and NO_3^{-}, while C4 is characterized by elevated concentrations of Ca^{2+}, Mg^{2+}, K^{+}, HCO_3^{-} Mn^{2+} And SiO_2, as well as high pH, TDS and electrical conductivity (EC).

5.2.4.2 Groundwater Clusters and Facies Group

Figure 5.20 shows the spatial distribution of groundwater wells while Figure 5.21 presented the Piper diagram of groundwater wells, both are labelled according to the respective clusters. An envelope of groundwater wells group facies is drawn on the Piper

Table 5.7: Hydrochemical and physical characteristic of each cluster

Parameters	C1	C2	C3	C4
N:	16	4	5	2
Ca^{2+}	*4.70*	8.70	9.10	**29.50**
Mg^{2+}	*2.05*	3.35	3.50	**12.50**
Na^{+}	*8.70*	9.85	**21.00**	18.05
K^{+}	*1.80*	2.90	5.05	**5.58**
HCO_3^-	*26.50*	55.75	37.00	**183.50**
Cl-	9.00	*7.50*	**18.50**	7.75
SO_4^{2-}	5.00	*3.75*	**11.50**	5.13
NO_3^-	2.00	*1.88*	**7.00**	4.50
Fe	*2.00*	**15.25**	0.75	2.53
Mn	*0.10*	0.28	*0.10*	**0.30**
NH_4	0.25	**0.38**	0.25	*0.13*
SiO_2	18.29	23.60	*14.50*	**34.51**
pH	*6.50*	6.63	6.60	**7.35**
Electrical Conductivity, EC (µS/cm)	*90.00*	138.75	155.00	**326.25**
Total Dissolved Solid (TDS)	*90*	143	136	**219.5**
HCO_3^-/SiO_2	*1.37*	1.54	3.02	**5.29**
(Na+K-Cl)/(Na+K-Cl+Ca)	0.37	0.38	**0.40**	*0.30*
Mg/(Ca+Mg)	0.44	*0.38*	**0.44**	**0.44**
CAII	-0.69	-2.55	*-0.44*	**-3.53**
SI (Anhydrite)	*-4.12*	-4.01	**-3.41**	-3.50
SI (Aragonite)	*-3.05*	-2.43	-2.37	**-0.59**
SI (Calcite)	*-2.90*	-2.28	-2.23	**-0.44**
SI (Chalcedony)	0.10	0.17	*-0.01*	**0.37**
SI (Dolomite)	*-5.74*	-4.55	-4.45	**-0.94**
SI (Goethite)	6.46	7.83	*6.48*	**8.86**
SI (Gypsum)	*-3.89*	-3.77	**-3.17**	-3.26
SI (Halite)	*-8.60*	-8.55	**-7.91**	-8.46
SI (Hematite)	*14.90*	17.65	14.95	**19.70**
SI (Pyrite)	**-86.18**	-87.67	-86.94	*-100.12*
SI (Siderite)	-0.98	0.33	*-1.75*	**0.40**

Median concentrations in mg/L, N: number of samples, Bold: highest values, italics: lowest values diagram for comparison. The groundwater wells are scattered among the different facies on the Piper diamond shape and mainly given Na–HCO_3 and Ca–HCO_3 facies,wells facies are also shown as reference for a clear classification of groundwater in which Na–HCO_3 facies of water quality can be made. Table 5.8 simplifies the relationship between clusters and facies of groundwater wells. Most of the groundwater wells from C1 to C3 belong to G2 (Na–HCO_3), while C4 represents a mixture of G1 (Ca–HCO_3) and G2 (Na–HCO_3). Therefore, a connection between groundwater well clusters and group facies are apparent as in HCA. Major ions are also considered as the most important ions that controls the hydrogeological setting of the basin. The ability of HCA to show the presence of minor and trace elements could help in recognizing the distinct minor elements signature related to geological formations.

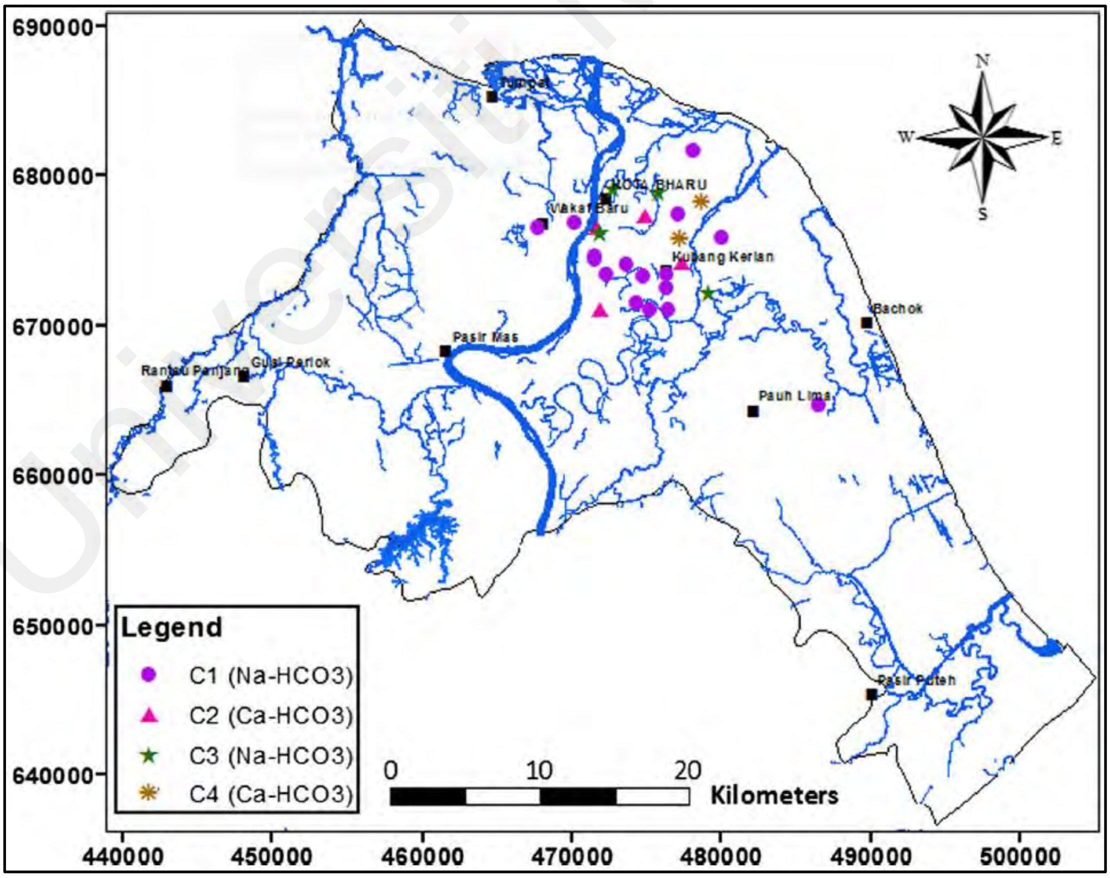

Figure 5.20: Spatial distribution of groundwater wells according to clusters

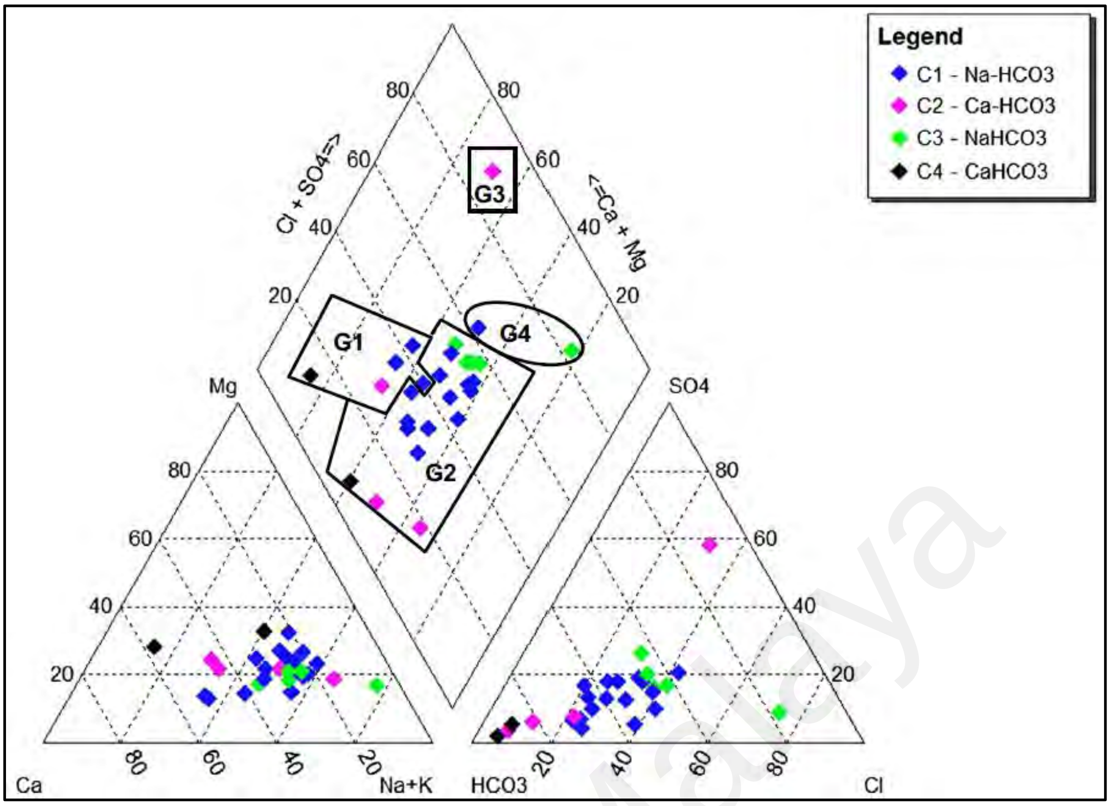

Figure 5.21: Piper diagram of wells according to respective clusters

Table 5.8: Relationship between wells cluster and facies

Clusters	Groups				N total
	G1 ($Ca\text{-}HCO_3$)	G2 ($Na\text{-}HCO_3$)	G3 ($Ca\text{-}SO_4$)	G4 (Na-Cl)	
C1	3	12	0	1	**16**
C2	1	2	1	0	**4**
C3	0	4	0	1	**5**
C4	1	1	0	0	**2**
N total	**5**	**19**	**1**	**2**	

5.2.4.3 Hydrogeochemical Evolution

The regional spatial distribution shows that shallow groundwater is evolving from Ca–HCO_3 to Na–HCO_3 facies. The Ca–HCO_3 facies is characterized as fresh groundwater at/or close to recharge areas in the general flow regime. Ca–HCO_3 facies are often associated with carbonate mineral and/or incongruent silicate mineral weathering

(Drever, 1988; Appelo & Postma, 2005). Na–HCO_3 groundwater facies result from the interaction or mixing of groundwater influenced by two processes of mineral dissolution. Incongruent weathering of albite and related plagioclase feldspars have the potential to result in Na–HCO_3 compositional groundwater facies.

A Gibbs diagram (Gibbs, 1970) in Figure 5.22 and Figure 5.23 are plotted in the TDS concentration as a function of the weight ratio of Na/(Na + Ca) and Cl/(Cl + HCO_3) to provide information of three major important natural mechanisms controlling the hydrogeochemical evolution of groundwater: (1) atmospheric precipitation dominance, (2) rock dominance and (3) evaporation and fractional crystallization dominance. The TDS spreads from low to high with a small variation of concentration. All clusters in Figure 5.22 and Figure 5.23 show that rock weathering and precipitation are the dominant mechanisms controlling the hydrogeochemical evolution of shallow groundwater in the study area. Cluster C1 and C3 samples are influenced by the precipitation and freshening, which correspond to recently infiltrated recharge or mixed to intermediate facies (Ghesquiere *et al.*, 2015). Cluster C2 and C4 samples are more influenced by water–rock interaction.

The molar ratio of HCO_3^-/SiO_2 in Table 5.7 also shows that C1 to C3 clusters have ratios <5, which indicates silicate weathering while C4 is ambiguous. If the ratio is >10 (HCO_3^- >> SiO_2), carbonate weathering is predominant in the area. The saturation indices in Table 5.7 show that calcite, aragonite and dolomite (SI<0) are undersaturated, suggesting their absence in the formation and/or not enough time to interact (Wirmvem *et al.*, 2013).

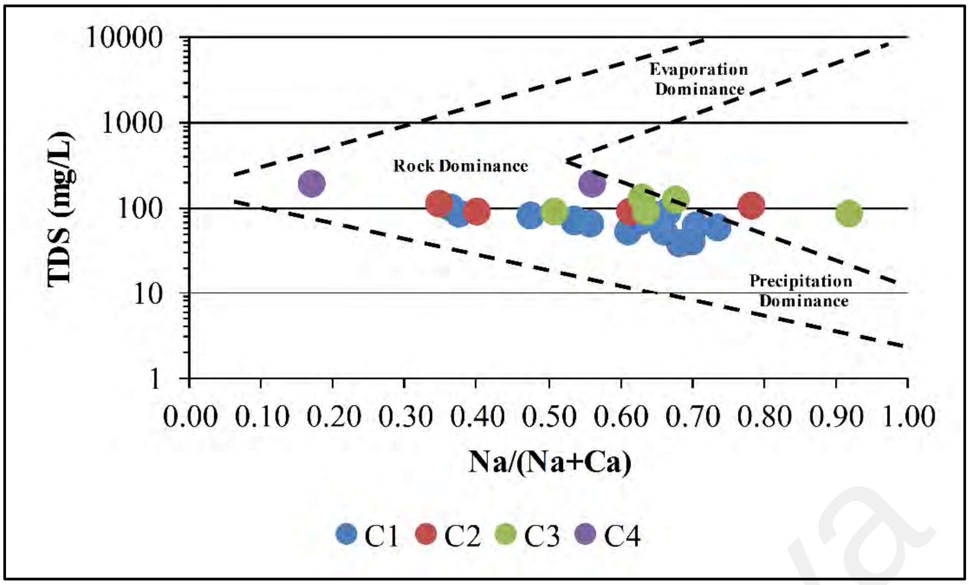

Figure 5.22: Plot TDS versus Na/(Na+Ca)

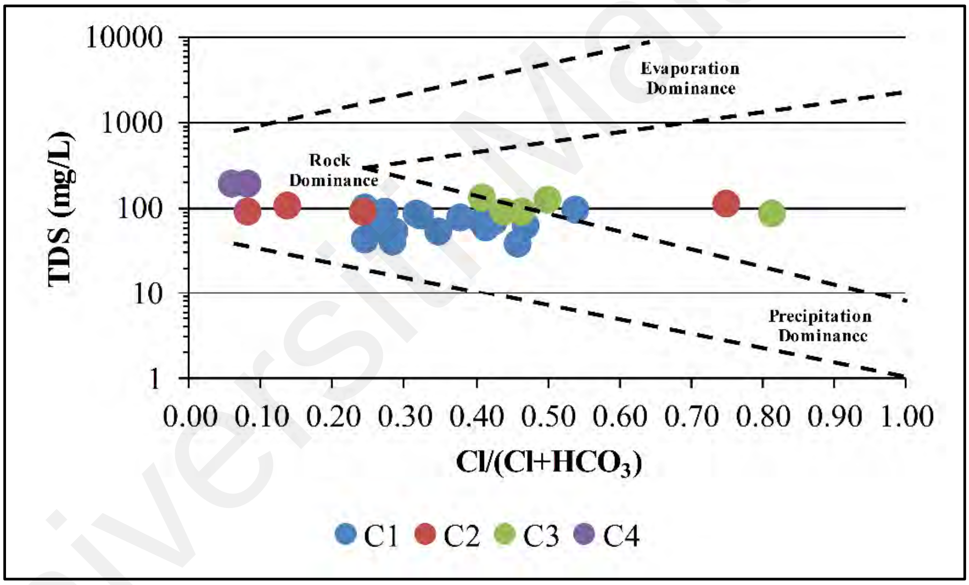

Figure 5.23: Plot of TDS versus Cl/(Cl+HCO3)

The Na/Cl ratio in Figure 5.24 is relatively higher than seawater (0.86) (Hounslow, 1995; Millero *et al.*, 2008). The Na/Cl ratio, which is approximately equal to 1, is usually attributed to halite dissolution, whereas >1 is typically interpreted as reflecting Na^+ released from silicate weathering reactions (Fisher & Mullican, 1997; Cendon *et al.*, 2010). This ratio suggests that the excess of Na^+ is likely from silicate weathering of feldspar or plagioclase and not from the dissolution of halite. Based on the (Na+

K+Cl)/(Na+K+Ca + Cl) ratios in Table 5.7, the source of Na^+, K^+ and Ca^{2+} for all clusters is likely from plagioclase weathering.

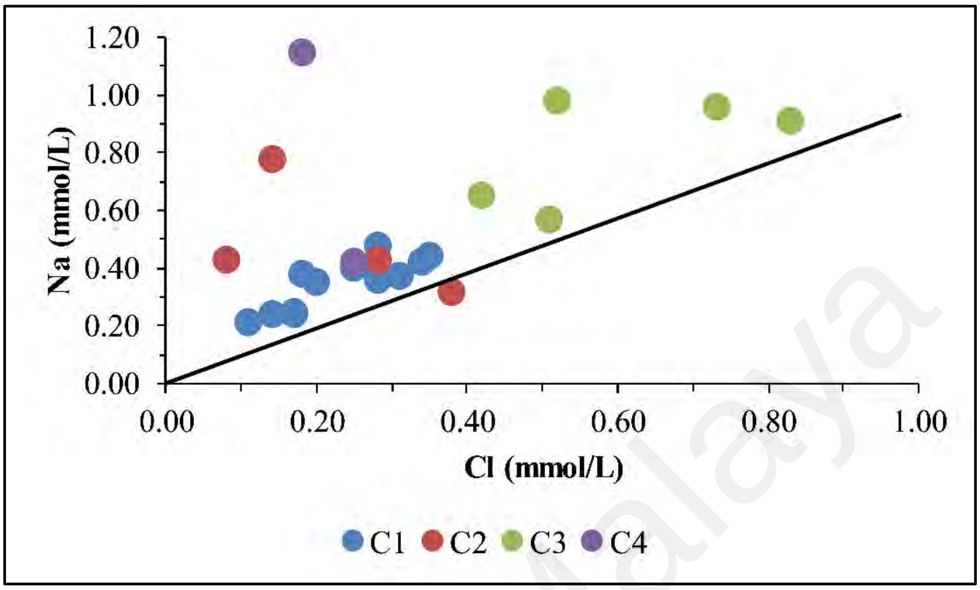

Figure 5.24: Plot of Na versus Cl

The Mg/(Ca+Mg) ratio indicates that sources of Ca^{2+} and Mg^{2+} are mostly from ferromagnesian minerals, with a few from dolomite and granitic weathering. Table 5.7 shows that all clusters are supersaturated (SI>0) with respect to hematite and goethite while undersaturated (SI<0) with respect to pyrite and siderite. Under an oxidative environment, the Fe^{2+} is released during dissolution and is precipitated as iron oxide and oxyhydroxides. This indicates that precipitation of iron phases from aquifer layers is thermodynamically favorable. Hematite precipitates more because it is more stable as compared to goethite. Groundwater is undersaturated with respect to major iron phase of pyrite and siderite. Therefore, iron remains dissolved after mobilization. Under an anoxic environment, the pyrite dissolves and is followed by partial oxidation that reflects the increase in Fe^{2+} and SO_4^{2-} in the groundwater.

The relationship between (HCO_3+SO_4) and (Ca+Mg) in Figure 5.25 shows that most of the cluster samples fall along and below the equiline, indicating the influence of silicate weathering. If samples fall above the 1:1 line, they reflect the effect of carbonate and sulfate mineral dissolution (Yidana & Yidana, 2010; Yu *et al.*, 2012). Figure 5.26 indicates that the concentrations of sulfate and bicarbonate are affected by dissolution of silicate minerals.

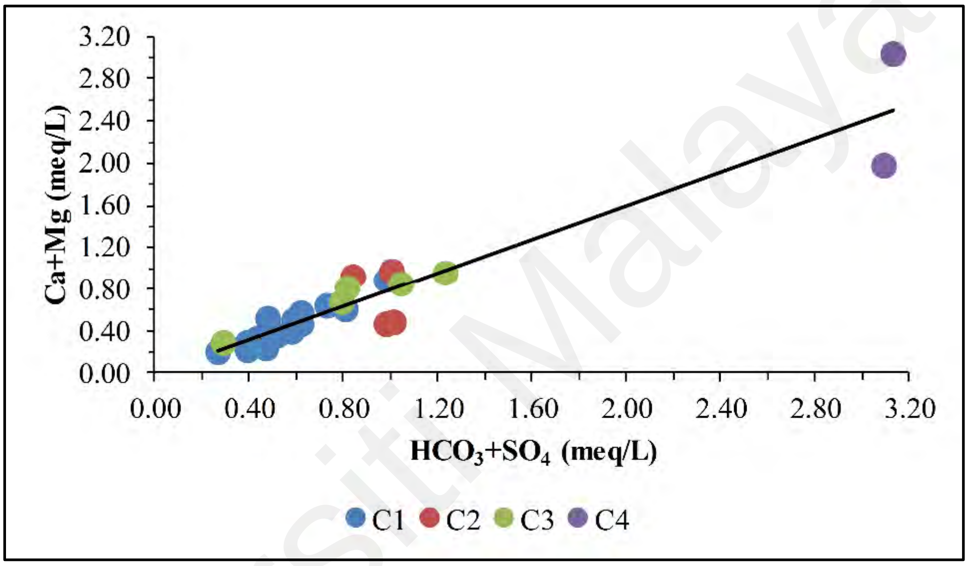

Figure 5.25: Plot of Ca+Mg versus HCO_3+SO_4

Thus, the Gibbs diagram as well as the ratios HCO_3/SiO_2, (Na + K + Cl)/(Na + K/Ca + Cl), Mg/(Ca + Mg) and (HCO_3 + SO_4) and (Ca + Mg) strongly indicates incongruent weathering of silicate minerals (water–rock interaction) as the main control on hydrogeochemical evolution, in agreement with the geology. Equations 5.1–5.5 show the silicate weathering products:

$$\underset{\text{Albite}}{2NaAlSi_3O_8}+2CO_2+11H_2O \rightarrow \underset{\text{Kaolinite}}{Al_2Si_2O_5(OH)_4}+2Na^{+}+2HCO_3^{-}+4H4SiO_4 \quad (5.1)$$

$$\underset{\text{Albite}}{2NaAlSi_3O_8}+2CO_2+6H_2O \rightarrow \underset{\text{Montmorilonite}}{Al_2Si_2O_{10}(OH)_2}+2Na^{+}+HCO_3^{-}+4H4SiO_4 \quad (5.2)$$

$$\underset{\text{Anothite}}{CaAlSi_3O_8}+2CO_2+3H_2O \rightarrow \underset{\text{Kaolinite}}{Al_2Si_2O_5(OH)_4}+Ca^{2+}+2HCO_3^{-} \quad (5.3)$$

$$\underset{\text{Biotite}}{2KMg_3AlSi_3O_{10}(OH)_2}+14CO_2+15H_2O \rightarrow \underset{\text{Kaolinite}}{Al_2Si_2O_5(OH)_4}+2K^{+}+6Mg^{2+}+14HCO_3^{-}+4H4SiO_4 \quad (5.4)$$

$$\underset{\text{Biotite}}{2KMg_3AlSi_3O_{10}(OH)_2}+14CO_2+10H_2O \rightarrow \underset{\text{Montmorilonite}}{Al_2Si_2O_{10}(OH)_2}+2K^{+}+6Mg^{2+}+14HCO_3^{-}+4H4SiO_4 \quad (5.5)$$

Ion exchange between the groundwater and its host environment during residence or travel time can be understood by studying the chloro-alkaline indices (Table 5.7), i.e., CA-I [Cl - Na + K]/Cl, where all ions are expressed in meq/L (Schoeller, 1965, 1967; Gupta *et al.*, 2008; Marghade *et al.*, 2012). Na^+ and K^+ ions in water are exchanged with Mg^{2+} and Ca^{2+} ions, in which if the indices are positive, it indicates a base exchange reaction, whereas negative values indicate chloro-alkaline disequilibrium. The reaction is known as cation exchange. During the process, the host rocks/aquifer materials are the primary sources of dissolved solids in the water. The Schoeller indices of groundwater sample clusters in Table 5.7 reveal that cation exchange (chloro-alkaline disequilibrium) exists in all clusters. Clay minerals exhibit a preference for ions occupying an exchange site. Kaolinite appears as a dominant clay mineral in the aquifer as studied by (Noor, 1980). The cation exchange process effectively increases the Na^+ concentrations at the expense of Ca^{2+} and Mg^{2+} as shown in Equations 5.6–5.8.

$$Ca^{2+} + 2Na\_X \rightarrow 2Na^{+} + Ca - X \quad (5.6)$$

$$Ca^{2+} + Mg\_X \rightarrow Mg^{2+} + Ca - X \quad (5.7)$$

Na-X is Na adsorbed onto a clay mineral

$$Mg^{2+} + 2Na - X \rightarrow 2Na^{+} + Mg - X \quad (5.8)$$

The weight ratio of Na/(Na + Ca) in Figure 5.22 varies significantly with a small variation of TDS, supporting the conclusion that cation exchange also plays a role by increasing Na and decreasing Ca under the background of rock dominance. During the cation exchange process, the TDS values do not change significantly because 2 mmol/L of Na^+ is released by 1 mmol/L Ca^{2+} exchange, and the weight of 1 mmol/L of Ca^{2+} (40 mg/L) is nearly equal to that of 2 mmol/L of Na^+ (46 mg/L) (Liu *et al.*, 2015).

In addition, a plot of (Ca + Mg)–(HCO_3+SO_4) versus Na–Cl (Figure 5.26) is used to determine the significance of base exchange in enhancing the water chemistry. If cation exchange is the most significant process in the system, the water should form a line with a slope of -1 (Rajmohan & Elango, 2004; Adomako *et al.*, 2011). The diagrams show that all the clusters of groundwater samples give a line with a slope of -1.0287. This confirms that Ca, Mg and Na concentrations are interrelated through cation ion exchange.

Precipitation and river bank infiltration bring recharge into the groundwater system from the inland part of the study area. Infiltration of recharge water into the aquifer layers is very common, especially when there are no impermeable layers of clay overlying the unconfined aquifer. In some parts, the unconfined aquifer may represent a recharge for deeper aquifer systems. As the water recharges, CO_2 rapidly dissolves (Freeze & Cherry, 1979) in aquifer layers where CO_2 provides the required acid condition for silicate mineral weathering (Yidana *et al.*, 2012). The dissolution of CO_2 also occurs in soil at partial pressures larger than the atmospheric value, which is primarily caused by root and microbial respiration (Domenico & Schwartz, 1990) as shown in Equation 5.9–5.11. This process will increase the HCO_3^- in groundwater. The main contributor of HCO_3^- is from the hydrolysis of silicate weathering (Equation 5.1–5.5) as shown in Figure 5.25 as an active process in the groundwater flow system.

$$CO_2\,(g) + H2O \rightarrow H_2CO_3 \qquad (5.9)$$

$$H_2CO_3 \rightarrow HCO3 + H^+ \qquad (5.10)$$

$$HCO_3^- \rightarrow CO_3^{2-} + H^+ \qquad (5.11)$$

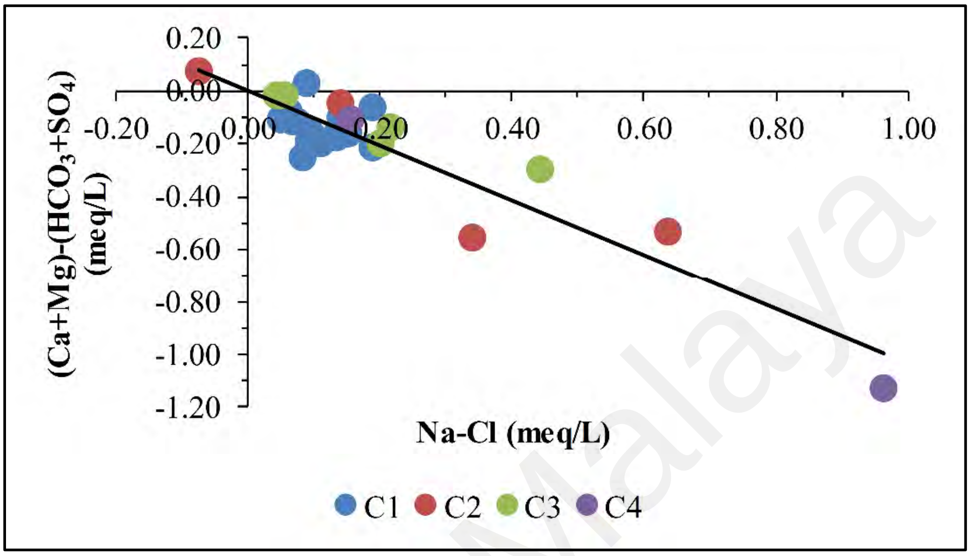

Figure 5.26: Plot of (Ca+Mg)-(HCO_3+SO_4) versus HCO_3+SO_4

5.3 LKRB Groundwater Recharge Estimation Rates

5.3.1 Chloride Mass Balance (CMB)

Reviews on CMB method have been discussed in Chapter 2 as one of the successful methods used to estimate groundwater recharge. Chapter 3 provided the details of sampling location, analysis and the methodology of the CMB method.

5.3.1.1 Chloride in Rainwater

Chloride deposition as reviewed in Chapter 2 is one of the sources of chloride in hydrological system. It can be in the form of dry and wet depositions. According to Eriksson (1959, 1960) cited in (Guan *et al.*, 2010) around 10% of chloride from the sea salt aerosols moved on the land surface and deposited within 100 km from the coastal area. The deposition decreased from coast to inland (Ten Harkel, 1997). The amount of chloride deposition on the land surface is influenced by the coastal distance, elevation and terrain aspect, slope, wind speed, rainfall (intensity and amount) and aerosol size (Guan *et al.*, 2010; Bresciani *et al.*, 2014). Dry deposition to a spruce forest canopy has velocity 1 to 2 cm/s with aerosol size of 2 to 5 um in diameter while the size can exceed 20 um with velocity over 3.5 cm/s to an open field area (Deng *et al.*, 2013).

There were no data of chloride via dry deposition has been recorded at LKRB. The only source of chloride deposition is from the rainwater. It is believed that with high amount of rainfall in the basin, dry chloride deposition (aerosol) can be rained out from the cloud or washed out by the falling rain drops (Guan *et al.*, 2010). Figure 5.27 shows the monthly distribution of chloride concentration in rainwater collected at Kg. Puteh wellfield (Chapter 3) from 2012 to 2015. The highest chloride deposition was measured in the month of April with 10.33 mg/L and the lowest was measured in November with 1.77 mg/L. Based on the Figure 5.27, it can be said that chloride deposition is high during dry season vice-versa, which indicated that circulation of south-west monsoon brings along high chloride aerosol to be deposited at LKRB. Since, LKRB has low terrain elevation (Chapter 4), most of the deposition of the chloride is likely by the rainfall intensity and amount as mentioned in section 5.1.2 (Stable Isotopes). This rainfall will naturally have rainout the dry (aerosol) onto the land surface as the rainfall event usually occurred as heavy downpours at LKRB. Therefore, majority of the wet chloride deposit is assumed to be as the total or bulk deposition even though it may fail to collect settling chloride aerosols properly during the sampling (Alcala & Custodio, 2008). Nolan *et al.* (2007) assumed that the wet deposition of chloride based on the available wet deposition data of ammonia, nitrate and sulphate was accounted on average of 92% of total depositions of these constitutes.

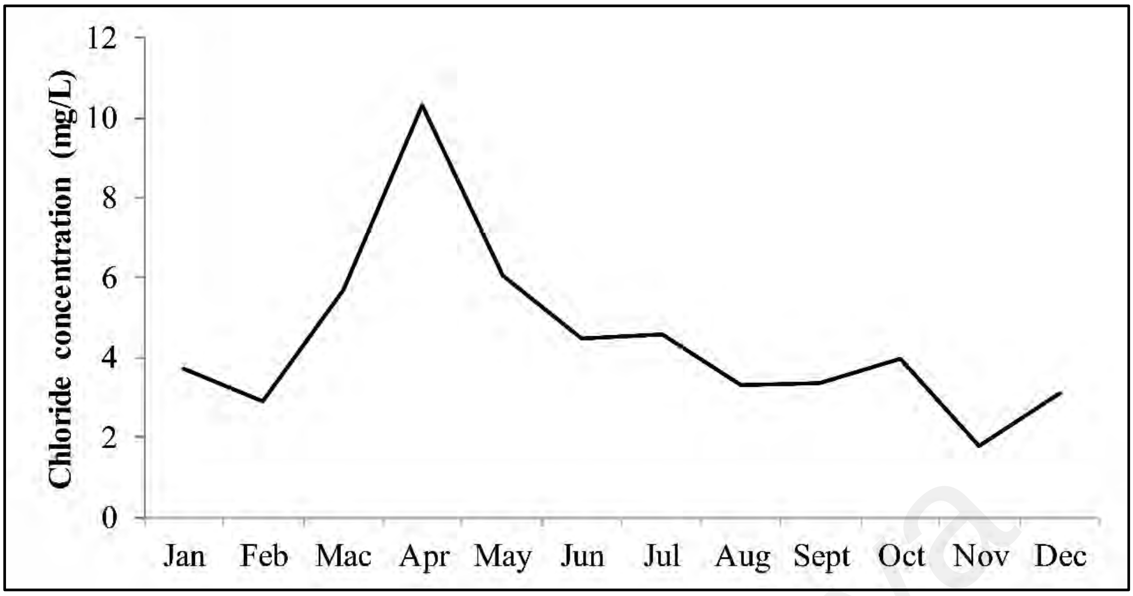

Figure 5.27: Monthly chloride concentration in rainwater (2012-2015)

The weighted average of chloride concentration in rainwater (Cl_P) was calculated using the Equation 3.2 as in Chapter 3. Monthly distribution of chloride concentration in rainwater collected at Kg Puteh wellfield is shown in Figure 5.27. The weighted mean annual chloride, Cl_P concentration in rainwater is 1.18 mg/L. This value will be utilized later as an input parameter to estimate the groundwater recharge in section 5.3.1.3 and will be considered as total deposition of chloride at LKRB.

5.3.1.2 Unsaturated Zone Soil Profiles

In total there are 10 unsaturated soil samples collected within LKRB during 2013 and 2015 sampling campaigns as shown in Figure 5.28 (detailed in Chapter 3). The soil samples were collected until it reached the water table that varies within location. The depth to water level of soil profiles ranging from 0.65 m to 1.71 m were recorded during 2013 sampling campaign while 0.51 m to 1.96 m were recorded on 2015 sampling campaign as summarized in Table 5.9. The particle size distribution (%) of sand, silt and clay of each soil profile is shown in Figure 5.30 and Figure 5.31. In 2013, the sand particle ranges were from 48% to 99%, silt from 0.3% to 17% and clay from 0.12% to 35% while in 2015, the particle size can be divided into two groups; group 1 had sand particle between 39% to 99%, silt is between 0.10% to 19% and clay is between 0.40% to 42% and group 2 has sand particle between 7% to 99%, silt is between 0.02% to 35% and clay is between 0.2% to 82% respectively as tabulated in Table 5.9. Group 1 is considered as an unsaturated soil profiles that contains more sandy texture covering the area of eastern part (S1-S4) and upper (S5) and lower (S10) of western part of the LKRB. Group 2 contains more clayey silt in texture that covers middle area of western part (S6-S9) of the basin. This texture will slow the process of infiltrating rainfall into deeper zones in soil profiles (Liu *et al.*, 2009).

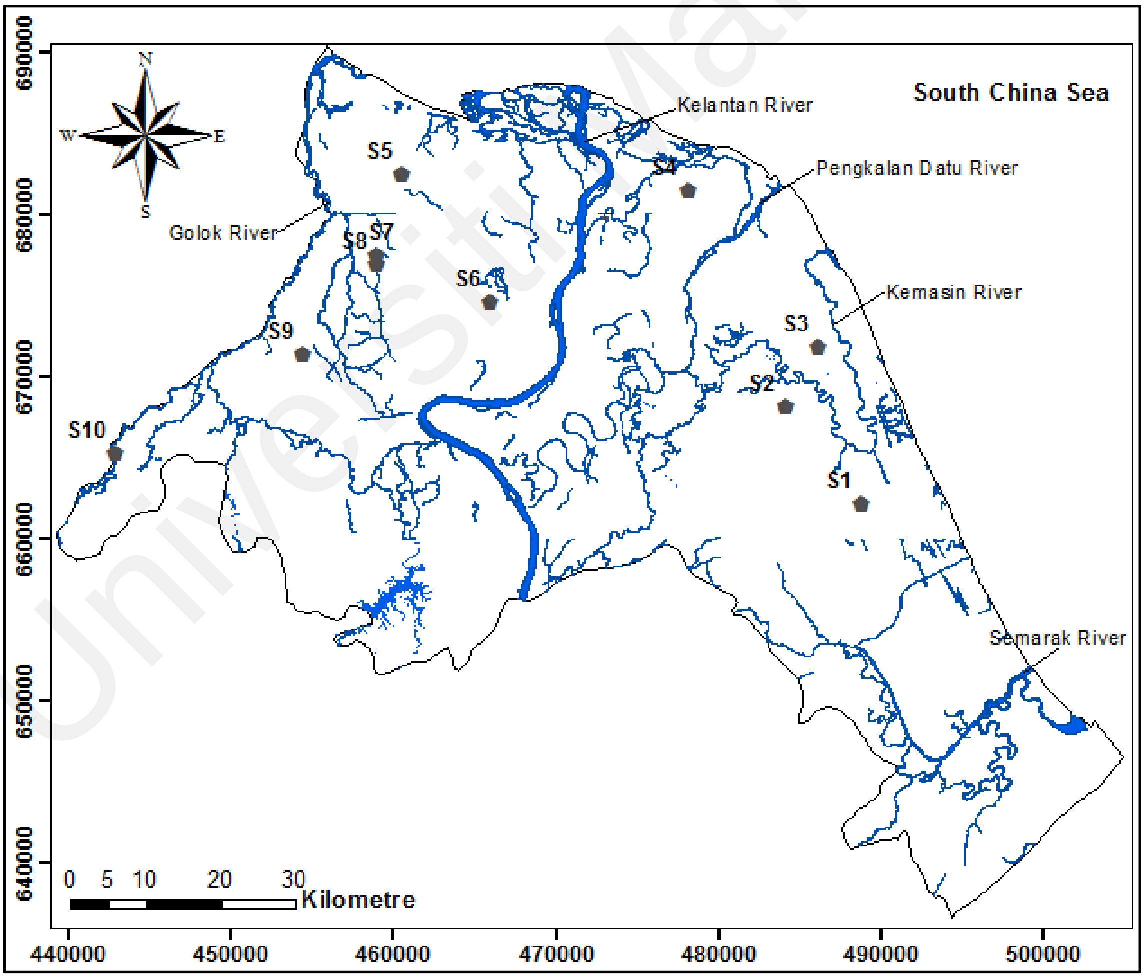

Figure 5.28: Soils sampling location

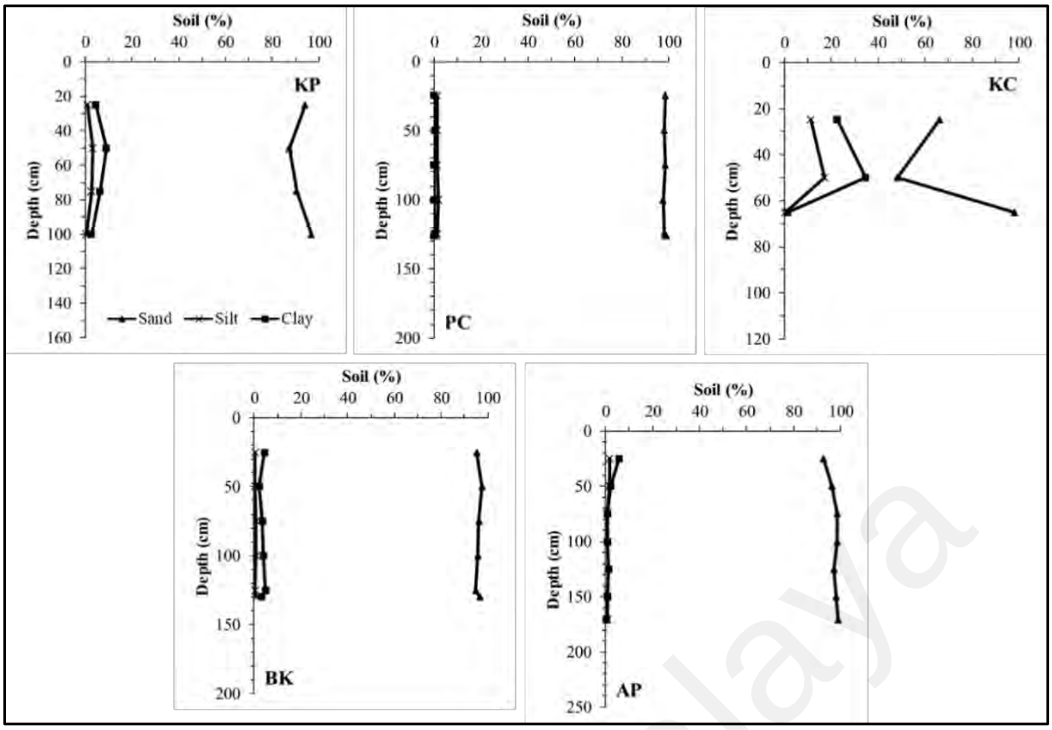

Figure 5.29: Distribution percentage of particle size in soil profiles in 2013

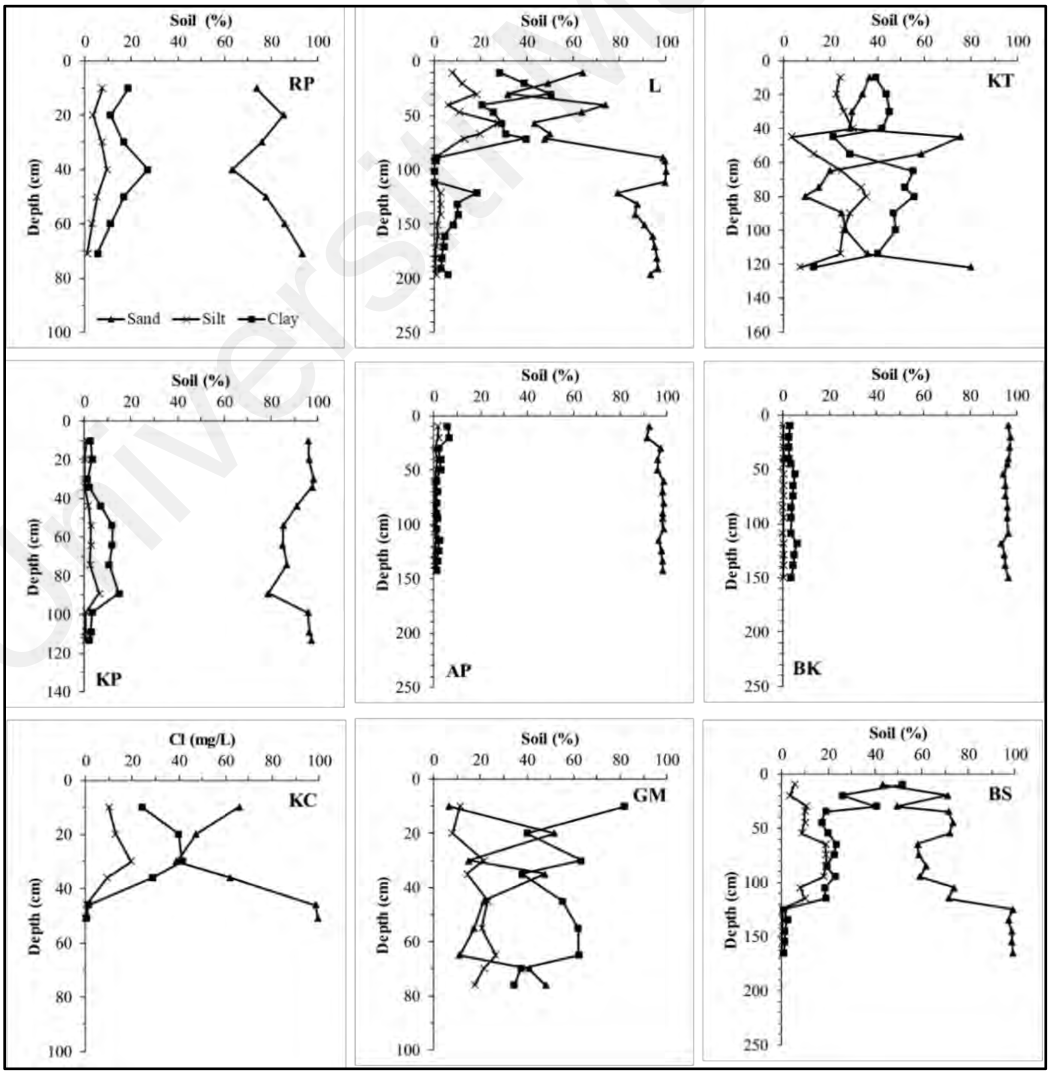

Figure 5.30: Distribution percentage of particle size in soil profiles in 2015

Table 5.9: Summary of measured water level, chloride concentration and percentage of particle size in soil profiles

Location	Code	Water Level (m)	Chloride in unsaturated zone, C_{uz} (mg/L)	Particle Size Distribution (%)		
				Sand	Silt	Clay
2013						
Alor Pulai	S1	1.71	8.38-11.60	92.47-98.85	0.68-1.83	0.47-5.70
Kg. Chap	S2	0.65	13.27-17.12	48.26-98.12	0.28-17.13	1.60-34.61
Beris Kubor	S3	1.30	2.83-10.36	94.78-97.45	0.37-0.58	2.18-4.82
Kubang Panjang	S4	0.80	5.88-10.89	87.63-96.74	0.63-3.07	2.63-9.30
Pengkalan Chepa	S5	1.26	1.66-3.34	97.83-98.86	1.02-2.03	0.12-0.31
2015						
Alor Pulai	S1	1.42	2.06-13.27	91.42-98.47	0.39-1.95	1.02-6.63
Kg. Chap	S2	0.51	1.40-7.63	39.05-99.53	0.10-19.44	0.37-41.51
Beris Kubor	S3	1.5	0.21-15.04	93.44-97.14	0.22-0.50	2.54-6.12
Kubang Panjang	S5	1.13	0.53-17.60	78.91-98.39	0.16-6.34	1.45-14.75
Bunut Susu	S6	1.65	0.05-10.16	43.25-98.99	0.19-18.97	0.82-51.38
Lati	S7	1.96	0.23-6.00	31.75-99.80	0.02-27.82	0.18-50.06
Gelang Mas	S8	0.76	0.57-4.97	6.61-51.90	8.10-26.56	34.56-81.98
Kedai Tanjung	S9	1.22	0.46-9.82	9.18-80.24	3.39-35.17	12.56-55.65
Rantau Panjang	S10	0.71	0.99-6.71	63.34-93.50	1.04-9.63	5.47-27.02

The depth distribution of chloride concentration in unsaturated soil profiles is presented in Figure 5.31 and Figure 5.32. The range of chloride concentration in 2013 is between 1.66 mg/L to 17.12 mg/L while in 2015 the range is from 0.21 mg/L to 17.60 mg/L respectively (see Table 5.9). The presence of several peaks or through within the profiles could be related to the changes of chloride input due to chloride deposition or man-made influenced (Gaye and Edmunds, 1996). The anthropogenic effects are not considered in this study. During rainfall event, chloride ion percolates with infiltrating water into unsaturated zone. The chloride ion in porewater tends to increase with depth through root zone as a result of evapotranspiration because plants will exclude the chloride during the process and water will return to the atmosphere through bare-soil evaporation that is pure (Healy, 2010). The concentrated chloride in the root zone later will be flushed downward by infiltrating rainfall which increases the chloride in the deeper profiles (Huang & Pang, 2011). The downward movement and accumulation of chloride ion is influenced by the soil textures where profiles comprised of predominantly clay and silt will have slow process (Liu *et al.*, 2009; Huang & Pang, 2011).

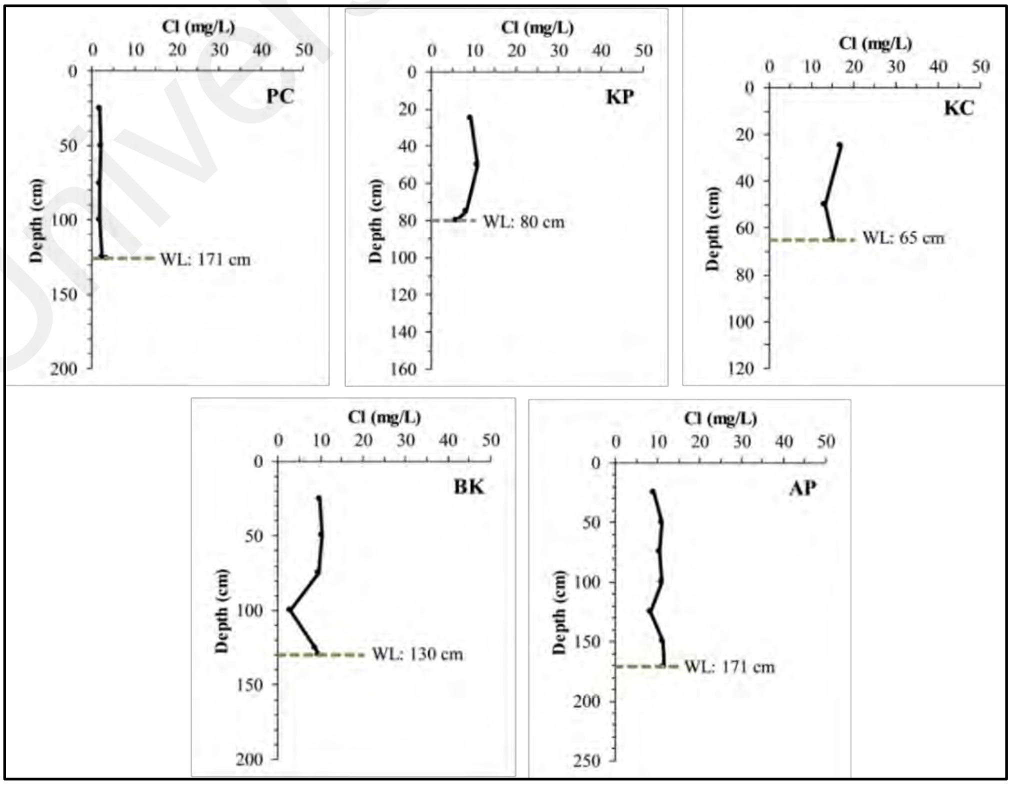

Figure 5.31: Depth distribution of chloride concentration in soil profiles 2013

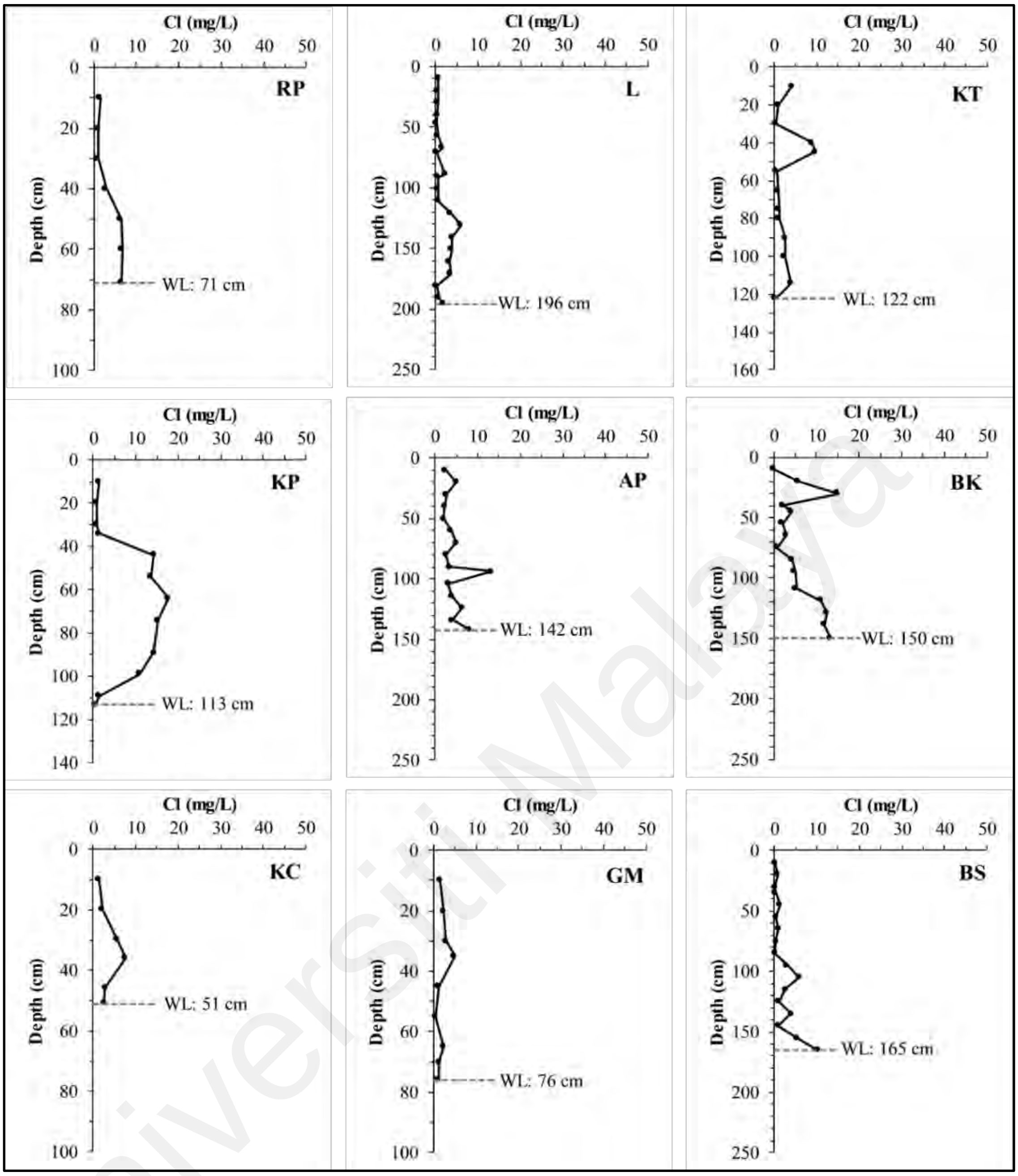

Figure 5.32: Depth distribution of chloride concentration in soil profiles 2015

5.3.1.3 Groundwater Recharge Rate

Equation 3.1 in Chapter 3 was used to estimate the groundwater recharge using chloride as a tracer by assuming that the only source of chloride is from rainfall (wet deposition) and there is no contribution of chloride from weathering or anthropogenic sources (Diouf *et al.*, 2012). The weighted mean chloride in rainwater (see section 5.3.1.1) is 1.18 mg/L. The mean of chloride concentration of unsaturated soil zone in 2013 is 2.15 mg/L to 14.91 mg/L while in 2015 the chloride concentration ranges from 1.74 mg/L to

6.48 mg/L, respectively as tabulated in Table 5.10. There is a decreasing trend in chloride concentration between 2013 and 2015 for repetition site sampling of S1 to S4. This trend is influenced by the sampling period that is drier during 2013 compared to 2015 which brings high accumulation of chloride concentration in soil profiles .

By considering the annual rainfall in 2013 of 2539 mm, the site-specific recharge ranges from 200.94 mm/yr to 1393.00 mm/yr with 8% to 55% of annual rainfall (see Table 5.10). Pengkalan Chepa (S4) gives the highest percentage of recharge with 55% of annual rainfall while Kg. Chap (S2) gives the lowest recharge with 8% of annual rainfall. In 2015, the annual rainfall received was 1933 mm. Therefore, the estimated recharge was between 297.47 mm/yr to 1046.04 mm/yr with 15% to 68% of annual rainfall as tabulated in Table 5.10. The highest percentage of recharge was S7 at Lati with 68% of annual rainfall while the lowest recharge was S5 at Kubang Panjang with 15% of annual rainfall. The results indicated that recharge were vary within locations at LKRB.

Figure 5.33 presents the spatial distribution percentage of recharge while details estimation are tabulated in Table 5.11. The percentage of annual recharge varies within the LKRB with 13% to 68% of annual rainfall with a mean of 36%. The distribution of recharge can be separated into the centre area of the western part that shows high recharge percentage ranging from 40% to 68% of rainfall while the eastern part that includes the upper and lower area of western part shows low recharge percentage with 13% to 32% of annual rainfall respectively. The mean recharge estimated in this study is within the range of humid tropical of 15% to 47% of the annual rainfall as studied by Tesfaldet *et al.* (2019) at Phuket, Thailand and Takounjou *et al.* (2011) at Yaounde, Cameroon.

Table 5.10: Summary of groundwater recharge estimation

Location	Code	"Mean chloride in unsaturated zone, C_{uz} (mg/L)"	Mean weighted chloride in rainwater C_P (mg/L)	Rainfall (mm)	Recharge (mm/yr)	Percent of Rainfall (%)
2013						
Alor Pulai	S1	10.38	1.18	2538.97	288.65	11
Kg. Chap	S2	14.91			200.94	8
Beris Kubor	S3	8.54			350.80	14
Pengkalan Chepa	S4	2.15			1393.00	55
Kubang Panjang	S5	8.56			349.84	14
2015						
Alor Pulai	S1	4.58	1.18	1932.56	498.21	26
Kg. Chap	S2	3.71			614.67	32
Beris Kubor	S3	6.48			351.92	18
Kubang Panjang	S5	7.67			297.47	15
Bunut Susu	S6	2.18			1046.06	54
Lati	S7	1.74			1310.59	68
Gelang Mas	S8	2.07			1101.30	57
Kedai Tanjung	S9	2.97			767.82	40
Rantau Panjang	S10	3.72			612.48	32

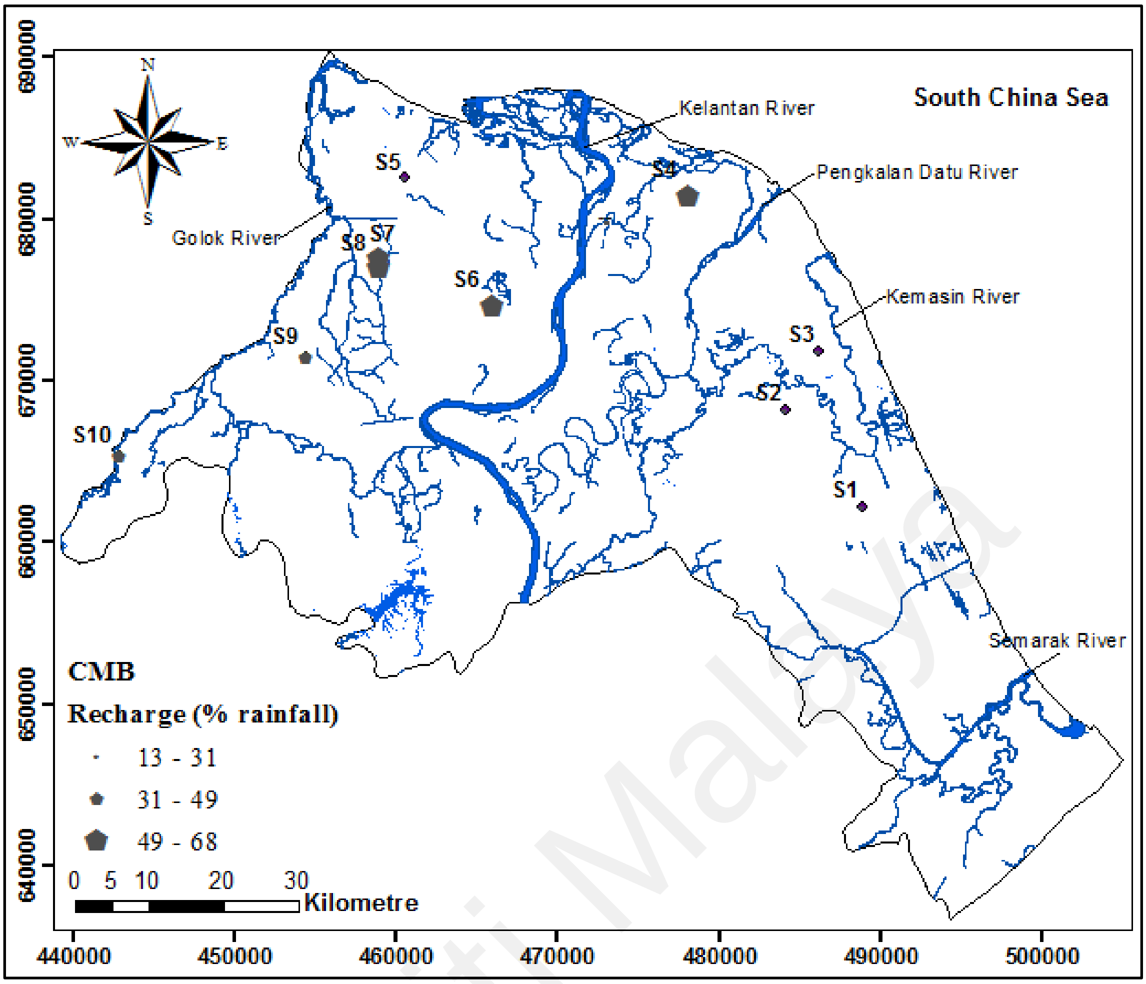

Figure 5.33: Spatial distribution of recharge (% of rainfall)

Table 5.11: Mean groundwater recharge estimated from different location

Location	Code	"Mean chloride in unsaturated zone, C_{uz} (mg/L)"	Mean weighted chloride in rainwater, C_P (mg/L)	Rainfall (mm)	Recharge (mm/yr)	Percent of rainfall (%)
Alor Pulai	S1	7.48	1.18	2235.77	352.70	16
Kg. Chap	S2	9.31		2235.77	283.37	13
Beris Kubor	S3	7.51		2235.77	351.29	16
Pengkalan Chepa	S4	2.15		2538.97	1393.00	55
Kubang Panjang	S5	8.12		2235.77	324.90	15
Bunut Susu	S6	2.18		1932.56	1046.06	54
Lati	S7	1.74		1932.56	1310.59	68
Gelang Mas	S8	2.07		1932.56	1101.30	57
Kedai Tanjung	S9	2.97		1932.56	767.82	40
Rantau Panjang	S10	3.72		1932.56	612.48	32
				Mean	**754.35**	**36**

5.3.2 Water Table Fluctuation (WTF)

Water table fluctuation is one of the method that is frequently applied in estimating groundwater recharge all over the continent. It has been briefly reviewed in Chapter 2. The methodology of the WTF has been given in detail in Chapter 3 while the data related with WTF are listed in Appendix D for comparison and interpretation of groundwater recharge rate.

In total, 14 MGD monitoring well sites as shown in Figure 5.34 are selected to be used for WTF method in estimating recharge rate. All well sites are in shallow aquifer (L1) with depth ranges from 9.4 m to 17 m as tabulated in Table 3.2. This monitoring wells have been selected based on long-term groundwater level data availability. Only monitoring wells with 96 % and 100 % of completed data are used to estimate the groundwater recharge. These data are selected according to water year which start from May to April. Seven water years were identified which are 1991-1992, 1992-1993, 1993-1994, 1994-1995, 2000-2001, 2004-2005 and 2007-2008 respectively.

Figure 5.35 shows the relationship between groundwater level of monitoring wells with rainfall event at LKRB from 1991 to 2008. The fluctuation of groundwater level responds well with the monthly amount of rainfall received in the basin where the pattern of groundwater level's rise during the high monthly rainfall can be seen through Figure 5.35. In general, the range of each groundwater level at sites is between -5.36 m to 5.53 m with a mean of –2.20 m to 3.18 m. The highest monthly rainfall is usually received in November and December where the north-east monsoon begins (Chapter 4) and caused flooding in several area of the basin. During the rainfall infiltration through the unsaturated zone, possible entrapment of air within the unsaturated zone can cause the *Lisse* effect at a depth of less than 1.3 m (Healy & Cook, 2002; Weeks, 2002; Crosbie *et al.*, 2005). However, this effect can be negligible within the basin as most of the groundwater fluctuates are above 1.3 m below the ground surface and the effect is less in the coastal sandy environment .

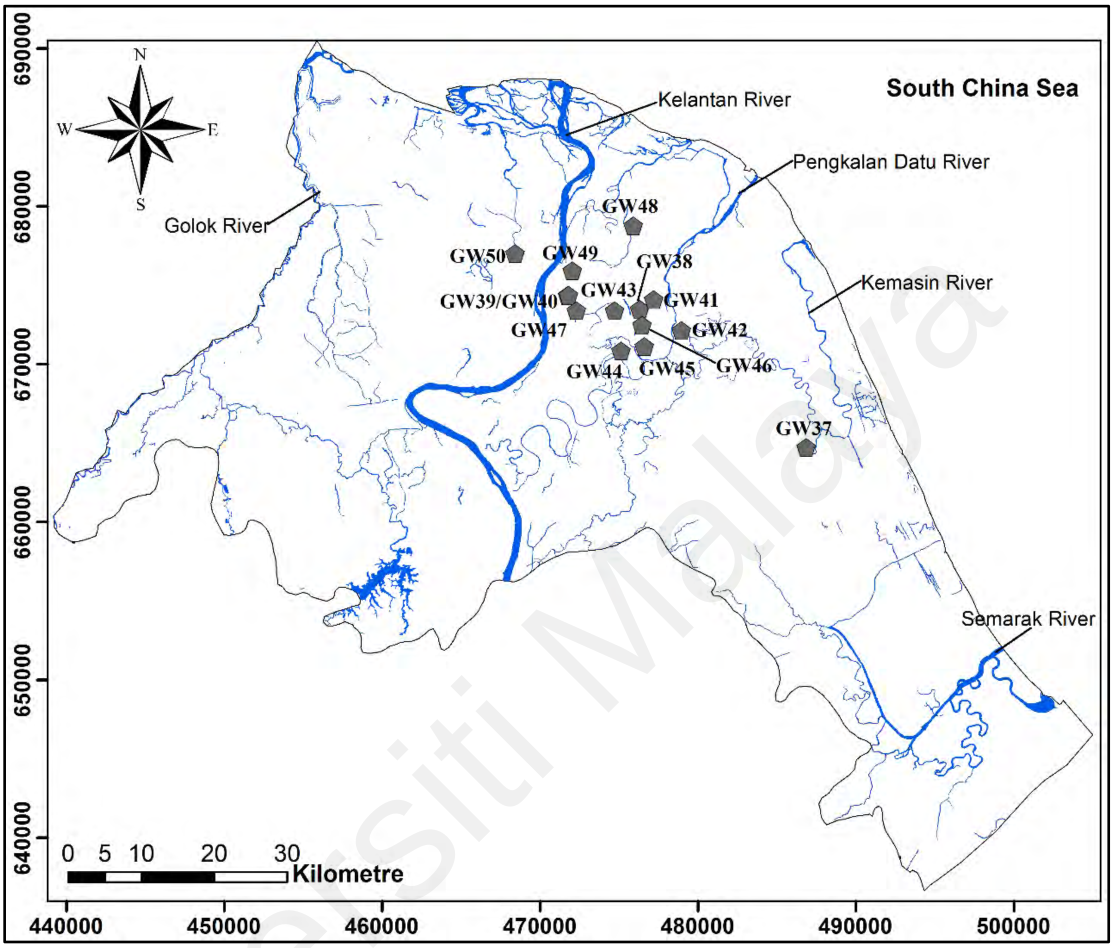

Figure 5.34: Location of MGD monitoring well sites

5.3.2.1 Groundwater Level Hydrograph

Groundwater level hydrographs were created to illustrate the recession curve using graphical approach (Delin *et al.*, 2007) as mentioned in section 3.6.2. The hydrograph is plotted according to the monthly groundwater level data. An example of well hydrograph for one of the monitoring wells at LKRB is shown in Figure 5.36. The groundwater level rise (Δh) is determined from the different peak of rise and the extrapolated low point of the antecedent recession at time of peak. The estimated values of groundwater rise (Δh) will be used later to calculate the groundwater recharge rate in section 5.3.2.3.

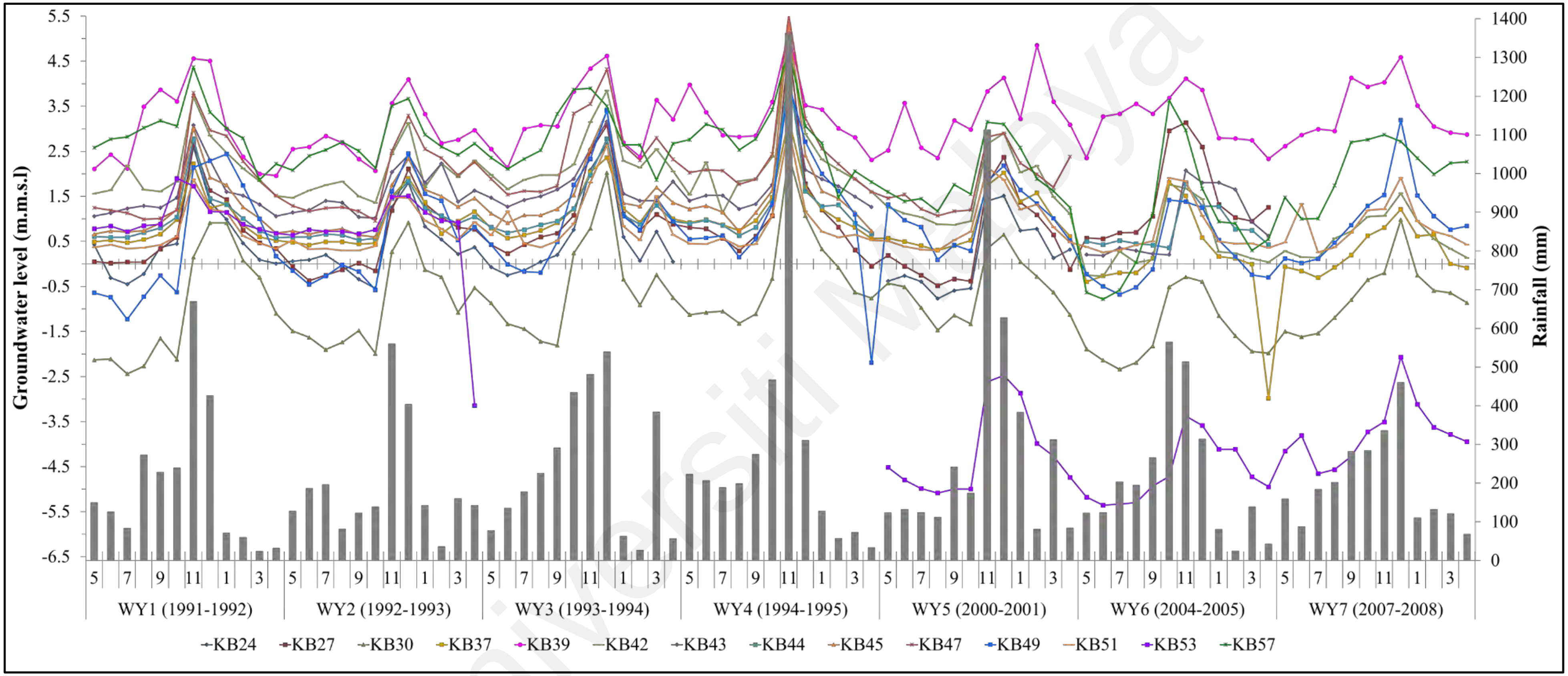

Figure 5.35: Mean monthly precipitation and groundwater level (m.m.s.l)

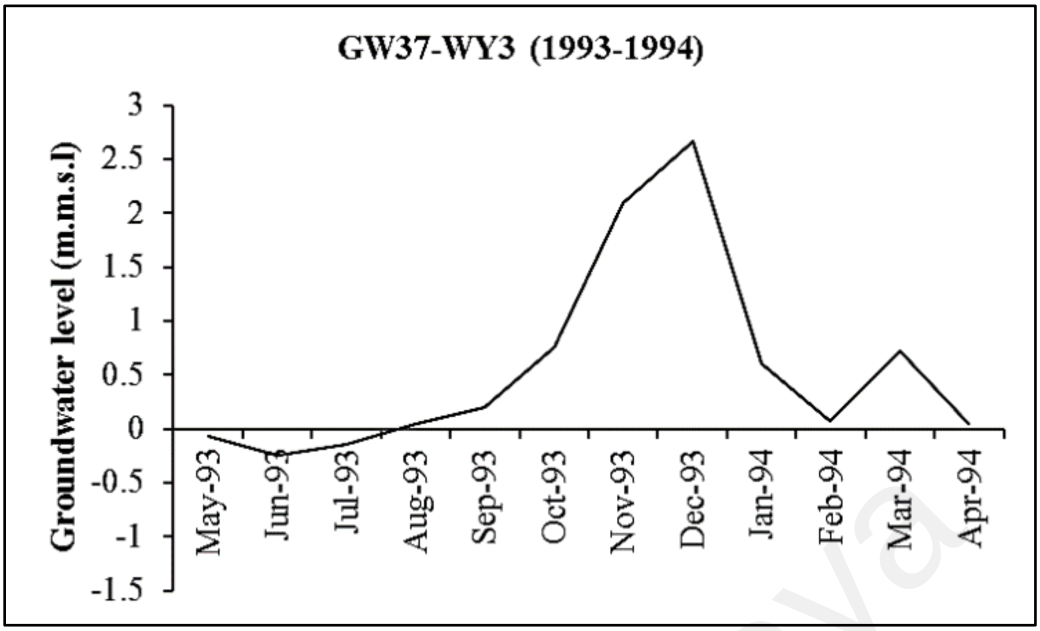

Figure 5.36: Example hydrograph of shallow well at GW37

The groundwater level rise of each monitoring well is presented in Table 5.12. Details of the high and low peak of monitoring wells hydrograph are tabulated in Appendix D. The range groundwater level rise (Δh) for water cycles WY1, WY2, WY3, WY4, WY5, WY6 and WY7 are from 1.50 m to 4.44 m with a mean of 2.80±0.80 m, 1.31 m to 3.45 m with a mean of 2.18±0.67 m, 2.26 m to 4.12 m with a mean of 3.12±0.63 m, 2.81 m to 5.24 m with a mean of 3.97±0.96 m, 2.12 m to 3.27 m with a mean of 2.52±0.37 m, 1.37 m to 4.63 m with a mean of 2.46±0.84 m and 1.91 to 3.69 m with a mean of 2.63±0.63 m respectively as shown in Figure 5.37. WY4 shows a high ranges of groundwater level rise compared to other water years since it received high annual rainfall of 3520 mm (see section 5.3.2.3).

Table 5.12: Groundwater level fluctuation of wells at different water cycles

Code	WY1	WY2	WY3	WY4	WY5	WY6	WY7
GW37	3.21	1.91	3.36		2.61		
GW38	2.78	3.11	3.28	5.09	3.27	2.89	
GW39	3.91	3.12	4.12	4.12	2.35	2.61	2.98
GW40	2.02	1.8	2.26	2.81	2.12	2.61	1.91
GW41	3.26	2.2	3.04	2.82	2.43	2.11	2.69
GW42	3.11	2.33	3.05	4.6	2.40	2.26	2.27
GW43	2.38	1.62	2.66	3.45		1.37	
GW44	2.58	1.54	2.58	3.97		1.68	
GW45	2.92	2.04	3.19	5.24			
GW46	3.1	2.59	3.92	5.23	2.40		
GW47	4.44	3.45	4.11	4.49	2.58	2.42	3.69
GW48	1.78	1.38	2.74	2.9	2.15	2.01	2.02
GW49	1.5	1.31			3.13	2.43	3.24
GW50	2.27	2.17	2.3	2.97	2.25	4.63	2.27

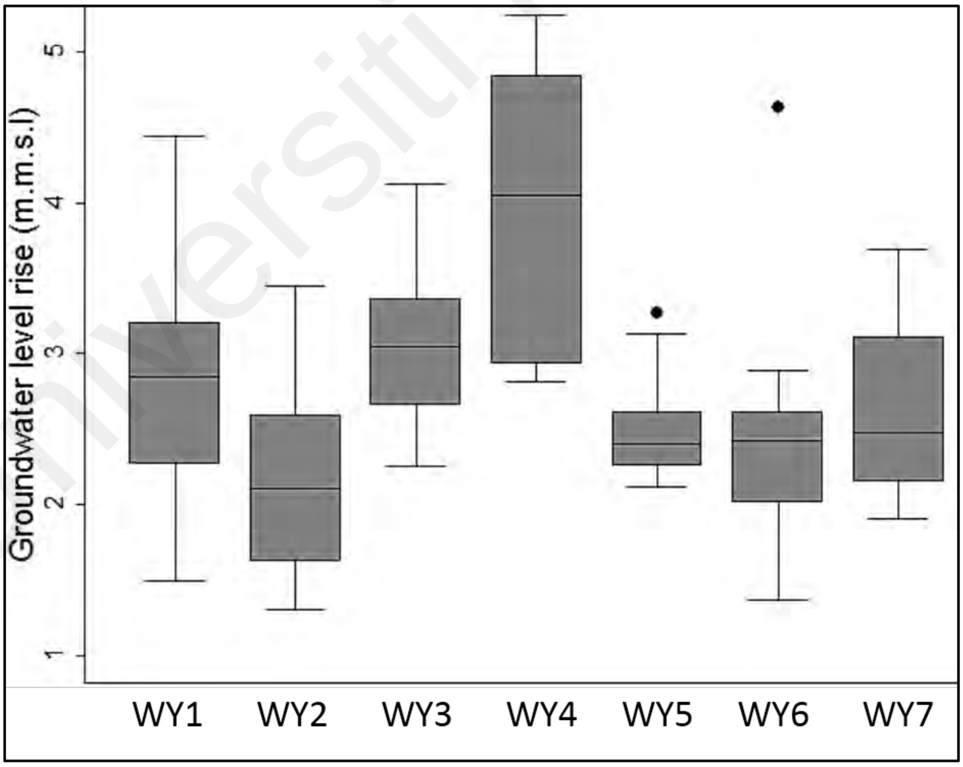

Figure 5.37: Groundwater level rise of different water year

5.3.2.2 Specific Yield (S_y)

The specific yield (S_y) values reported at LKRB ranges from 0.06 to 0.30 (Noor, 1980; Awadalla *et al.*, 1989; Sofner, 1992) as shown in Table 5.13. Based on the range values, 0.15 will be used later to estimate recharge.

Table 5.13: Estimated specific yield by previous study

Study	Specific Yield (Sy)
Noor (1980)	0.06
Awadalla *et al.* (1989)	0.1
Sofner (1992)	0.2-0.3*

* *effective porosity can be of as equivalent to specific yield*

5.3.2.3 Groundwater Recharge Rate

Recharge for each monitoring well was estimated using Equation 3.3 (see section 3.6.2). This value is calculated by multiplying the groundwater level rise (Δh) listed in Table 5.12 with the specific yield value of 0.15. Later, the recharge values will be calculated as the percentage of water year annual rainfall. The water year annual rainfall of WY1, WY2, WY3, WY4, WY5, WY6 and WY7 are 2382 mm, 2297 mm, 2895 mm, 3521 mm, 3509 mm, 2590 mm and 2426 mm, respectively as shown in Figure 5.38 with mean of 2803 mm. The highest rainfall is gained during WY4 while the lowest rainfall is during WY2.

Based on the water year cycles of WY1, WY2, WY3, WY4, WY5, WY6 and WY7 as presented in Figure 5.39, the range of groundwater recharge rate are from 225 to 666 mm/yr representing 11% to 28% of annual rainfall, 197 to 518 mm/yr representing 9% to 23% of annual rainfall, 339 to 618 mm/yr representing 12% to 21% of annual rainfall, 422 to 786 mm/yr representing 12% to 22% of annual rainfall, 319 to 490 mm/yr representing 9% to 14% of annual rainfall, 206 to 694 mm/yr representing 8% to 27% of annual rainfall

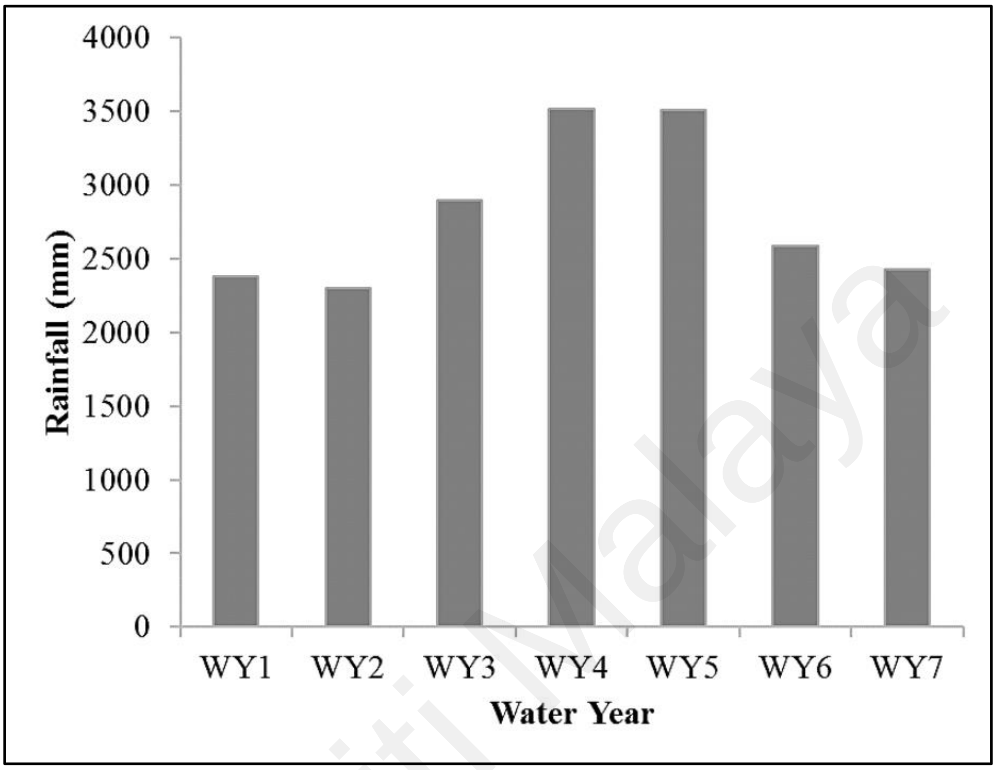

Figure 5.38: Water year annual rainfall at LKRB

and 287 to 554 mm/yr representing 12% to 23% of annual rainfall, respectively. The largest and smallest recharge values are estimated at monitoring well sites of GW47 and GW49 for WY1, GW47 and GW49 for WY2, GW39 and GW40 for WY3, GW45 and GW40 for WY4, GW38 and GW40 for WY5, GW50 and GW43 for WY6 and lastly GW47 and GW40 for WY7, respectively as shown in Figure 5.40. Details of the estimated recharge for each monitoring well at different water years are tabulated in Appendix D.

The spatial distribution mean recharge of monitoring well sites based on average of all water years is presented in Figure 5.41. The estimated groundwater recharge ranges from 321 mm/yr to 540 mm/yr with a mean annual recharge of 425±79 mm/yr representing

11% to 19% with 15% of the long term mean annual rainfall (2790 mm) in the basin as tabulated in Table 5.14.

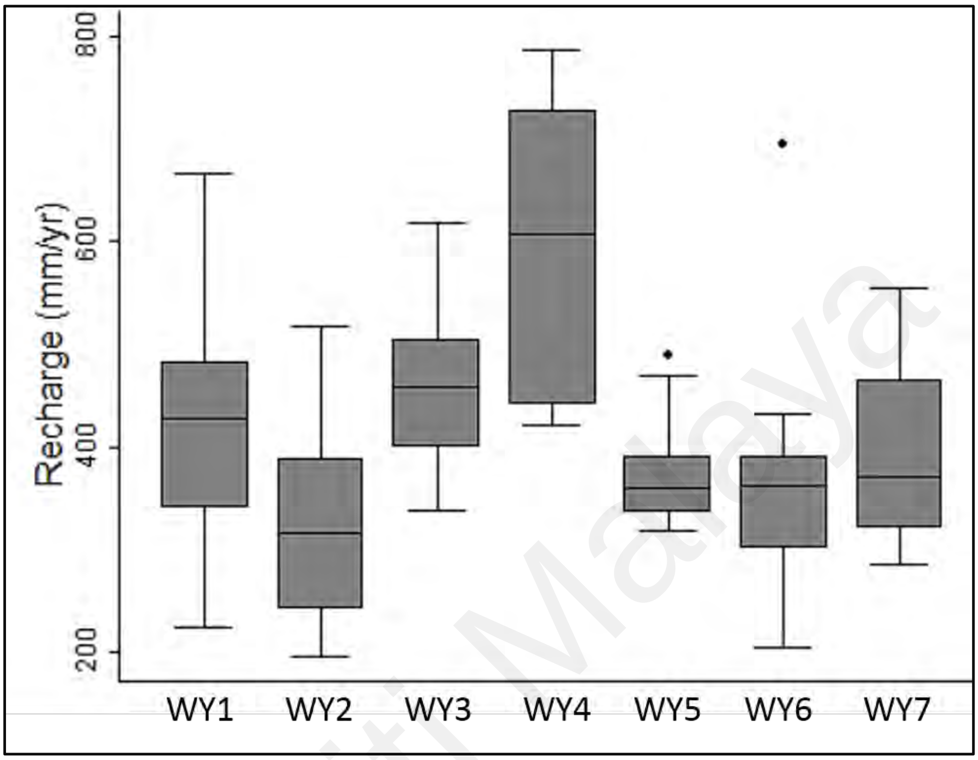

Figure 5.39: Box plot groundwater recharge (mm/yr) at different water year

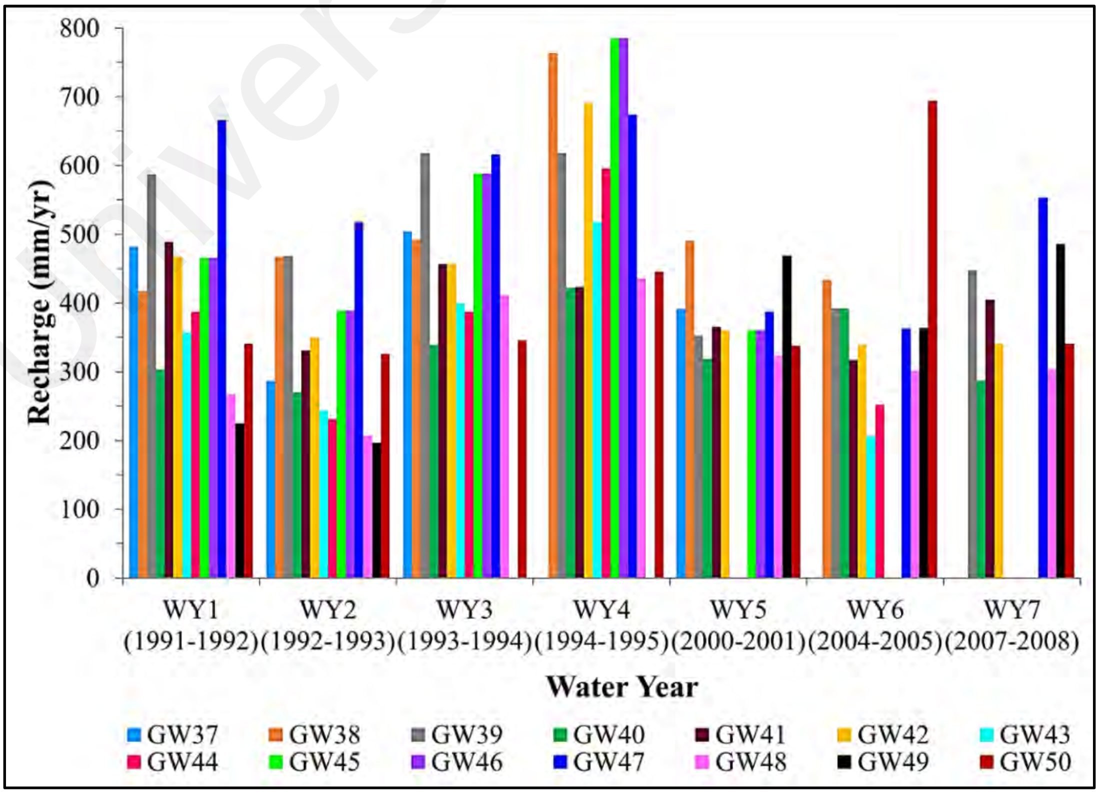

Figure 5.40: Annual groundwater recharge at different monitoring wells

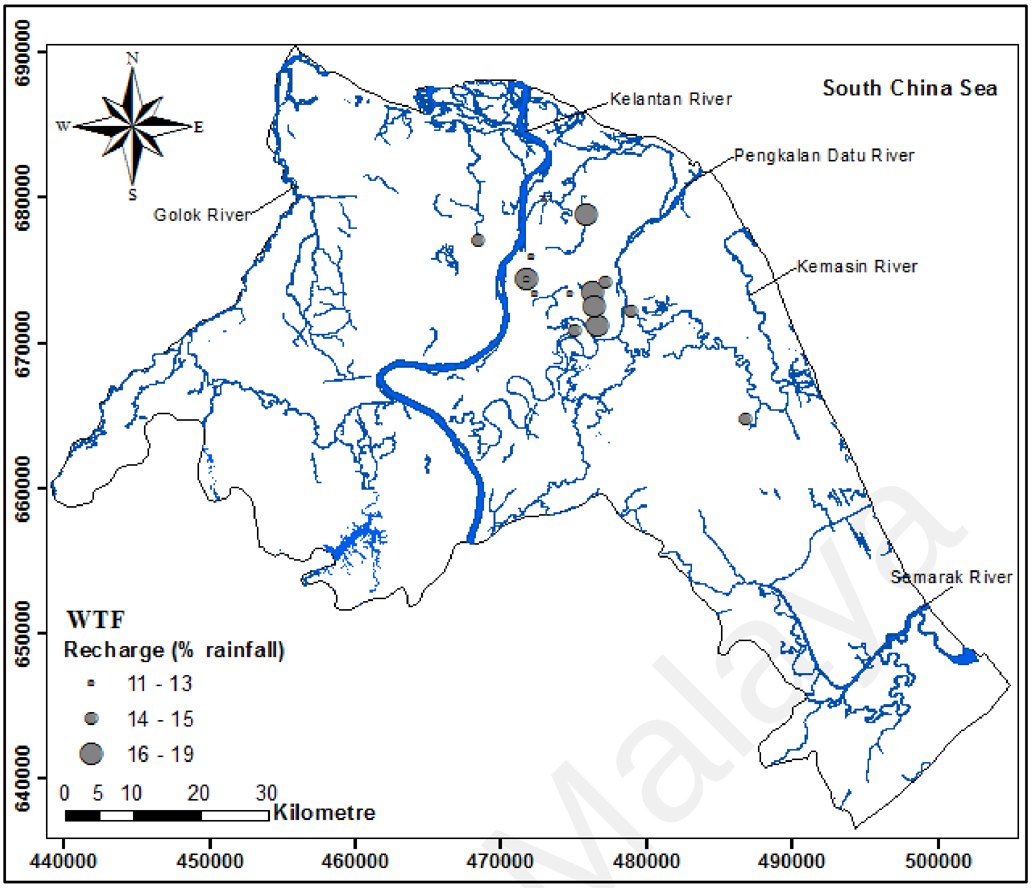

Figure 5.41: Spatial distribution of groundwater recharge (% of rainfall)

Table 5.14: Summary of estimated groundwater recharge (mm/yr and %)

Code	Rainfall (mm)	Recharge (mm/yr)	Percent of rainfall (%)
GW37	2771	416	15
GW38	2866	510	18
GW39	2803	497	18
GW40	2803	333	12
GW41	2803	398	14
GW42	2803	429	15
GW43	2737	345	13
GW44	2737	370	14
GW45	2774	502	18
GW46	2921	540	18
GW47	2803	540	19
GW48	2803	321	11
GW49	2641	348	13
GW50	2803	404	14
Mean	**2790**	**425±79**	**15**

The finding mean recharge of 15% annual rainfall is considered similar within the ranges reported for part of humid area of Pampa plain, Argentina, with a range of 4% to 33% of annual rainfall and a mean of 14% and 18% at different *Sy* of 0.07 and 0.09, respectively (Varni, 2013), Takounjou *et al.* (2011) at Younde, Cameroon, which has a recharge that ranges from 1.4% to 12.3% with a mean 5.7% of annual rainfall and mean recharge of 20% annual rainfall was estimated for both Holocene and Pleistocene aquifer at Hanoi, Vietnam .(Hung Vu & Merkel, 2019).

5.3.3 Temperature-Depth Profile (TDP)

Temperature-depth profile (TDP) as briefly reviewed in Chapter 2 has been demonstrated as an excellent heat tracer to comprehend the water movement in subsurface. The sampling locations and methodology of analysis are described in Chapter 3.

5.3.3.1 Surface Air Temperature

Over the last 20th century, the increase in surface air temperature is not only attributed by the global climate change but also the rapid development in urban area (Taniguchi & Uemura, 2005; Taniguchi, 2006; Huang *et al.*, 2009; Gunawardhana & Kazama, 2012; Colombani *et al.*, 2016; Dong *et al.*, 2018). Hansen and Lebedeff (1987) in their studied on global trends of surface air temperature have indicated that global warming magnitude is about 0.5°C/100 years. While, Huang et.al., (2000) estimated the same value of 0.5°C/100 years of increasing surface temperature using the borehole temperature data. In Bangkok, the record increased was 3.3°C/century from 1950 to 2005 while in Tokyo, the increased was 2.0°C/century from 1921 to 2010 and 2.2°C/century from 1926 to 2010 was recorded at Sendai, Japan (Taniguchi, 2006).

The annual means of air temperature and rainfall from 1968 to 2015 in the Kota Bharu Meteorological Station are 27.0°C and 2619 mm, respectively (Figure 5.42). A linear trend of increasing in air temperature can be seen from the figure with increament by 0.76 °C/47 years (R^2 of 0.431). This long-term record for the past 47 years show a warming trend that follows the general trend of global warming (Hansen *et al.*, 2010). The increase of local warming trends is influenced by the urbanization process especially in Kota Bharu area where the growth of the urban population resulted in redevelopment of agricultural land for urban used. The alternation in diurnal and seasonal surface air temperature strongly correlated with the shallow subsurface temperature variations especially in urban area and this is referred as 'urban heat island' (UHI) (Ferguson & Woodbury, 2004; Huang *et al.*, 2009; Gunawardhana & Kazama, 2012). According to Figure 5.42, there was no significant trend in the annual rainfall with increased of air temperature. However, any anomalous annual rainfall amount might disturb the subsurface temperature by changing the groundwater recharge/discharge rates (Dong *et al.*, 2018).

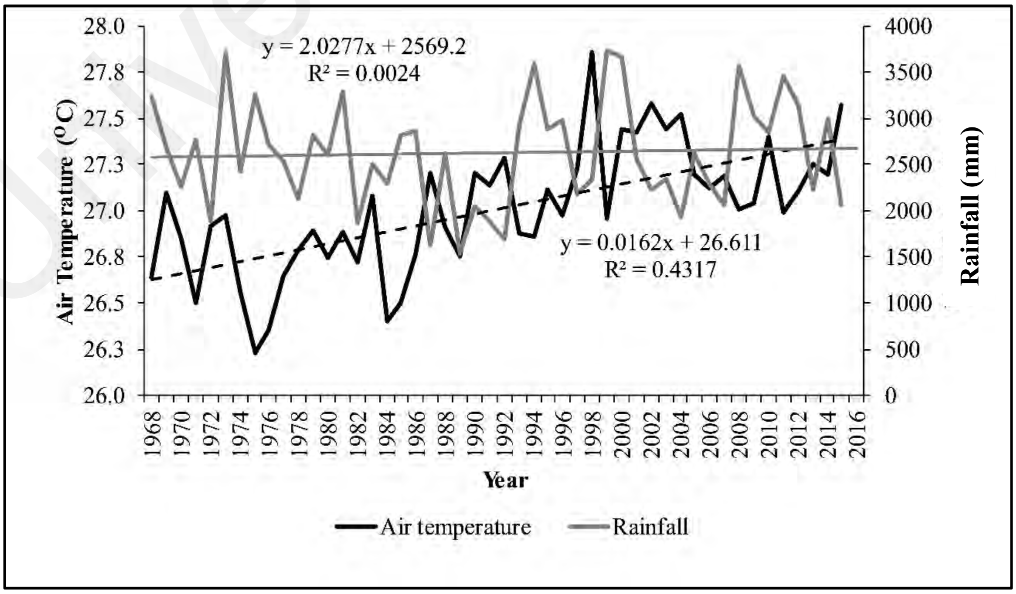

Figure 5.42: Annual air temperature and rainfall at Kota Bharu station from 1968 to 2015

5.3.3.2 Subsurface Temperature

In total 21 DMG monitoring wells are used for subsurface temperature profiles studies as shown in Figure 5.43 at depth interval of 1 m measurement. The well depth ranges from 15 m to 150 m with screen length ranging from 1 m to 9 m and well diameter of 2" to 6" as presented in Table 5.15. A small diameter of wells will ensure that there will be no significant occurance of free convective flow is expected as studied by Dapaah-Siakwan and Kayane (1995) in the Tokyo metropolitan area. Most of the monitoring wells are drilled before the 1980s and included with case. Therefore, the water temperature in the wells represent the temperature of groundwater surrounding the wells.

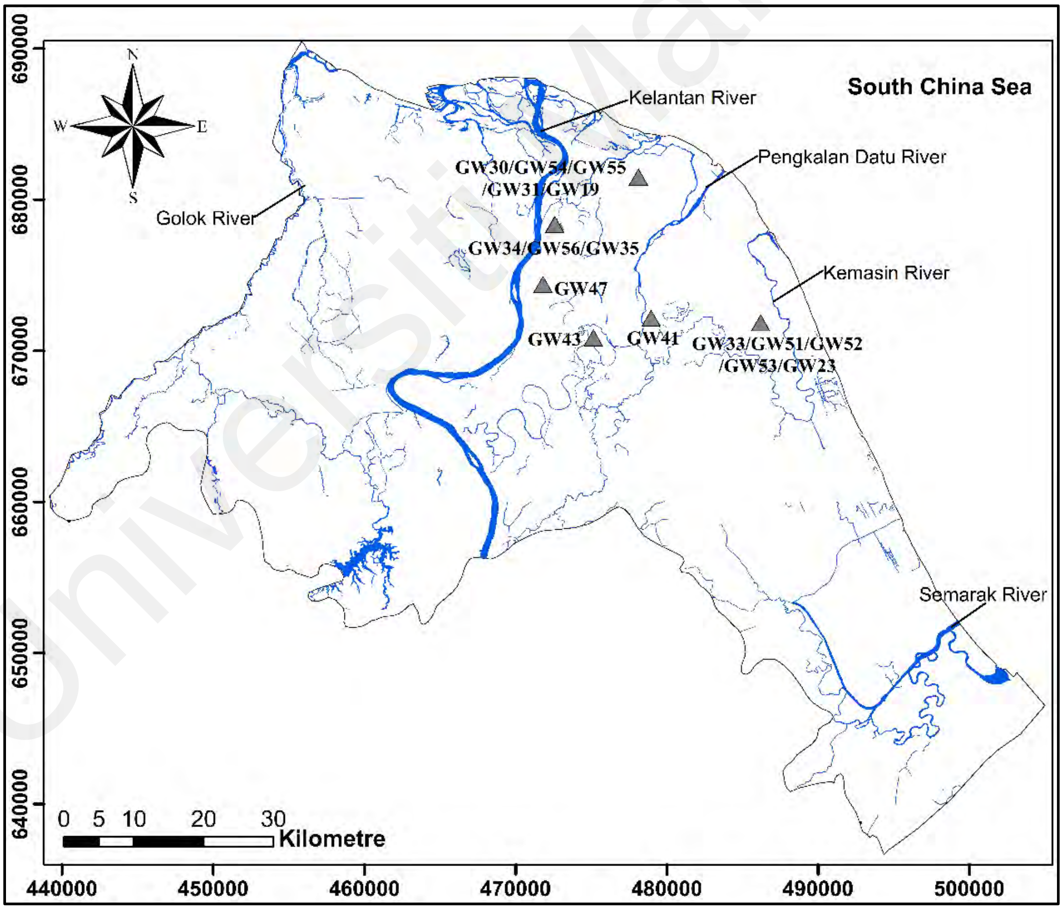

Figure 5.43: Location of wells used to measure the subsurface temperature

Table 5.15: Well depth, screen length, screen position and water level

Location	Well ID	Aquifer Layer	Depth (m)	Elevation (m)	Screen Length (m)	Screen Position (m)	Depth to Water Level (m, bgl)
2014							
Pintu Geng	GW47	L1	15.0	7.44	9.0	5.0-14.0	8.97
Kg. Binjai	GW41	L1	17.0	5.88	8.0	8.0-16.0	1.60
SK Seribong	GW43	L1	16.1	6.26	7.0	7.5-14.5	5.88
Beris Kubor	GW33	L3	113.4	3.39	1.6	106-107.6	2.99
	GW51	L3	101.2	3.60	1.5	93.5-95.0	2.96
	GW33	L3	83.4	3.33	1.5	76.0-77.5	2.95
	GW53	L2	44.4	3.34	1.5	38.3-39.8	3.25
	GW23	L2	29.2	3.39	1.5	24.0-25.5	2.97
2015							
Pengkalan Chepa	GW30	L3	114.0	5.93	1.5	98.5-100.0	5.38
	GW54	L3	91.0	5.93	1.5	85.5-87.0	5.37
	GW55	L3	73.0	5.87	1	67.0-68.0	5.26
	GW31	L3	64.0	5.85	1.5	58.0-59.5	5.30
	GW19	L2	30.0	5.79	1.5	23.0-24.5	4.70
Jalan Merbau	GW34	L3	150.0	6.57	1.5	125.0-126.5	5.50
	GW56	L3	88.0	6.60	1.5	83.5-85.0	5.36
	GW35	L3	66.0	6.55	1.5	64.0-65.5	5.45

*bgl: below ground level

The measurement of temperature and groundwater level is described in detail in section 3.2. The depth to water level (bgl) was measured at sites in 2014 and 2015 ranges from 1.60 m to 8.97 m with Layer 1 ranging from 1.60 m to 8.97 m, Layer 2 ranging from 2.86 m to 4.70 m and Layer 3 ranging from 2.95 m to 5.50 m, respectively as listed in Table 5.15. According to the literatures, most of the groundwater fluxes studies from steady state temperature-depth profiles are relatively from deep aquifer with a depth of more than 200 m (Taniguchi, 1993; Gosnold *et al.*, 1997; Taniguchi, 2002;

Gunawardhana & Kazama, 2012; Majumder *et al.*, 2013). Therefore, the same concept is applied even though the maximum depth at LKRB is only up to 150 m and wells are not spatially distributed within the basin.

The measured temperature-depth profiles are presented in Figure 5.44. Based on the temperature-depth profiles, the range of subsurface temperature are from 27.0°C to 32°C. An increase in temperature trend as the depth increases can be seen from the figure. This similar trend can be found in studies related with subsurface temperature (Taniguchi *et al.*, 2003b; Majumder *et al.*, 2013; Salem, 2016). The changes in the slope of the temperature-depth profile can possibly be attributed to the different thermal of aquifer layer (Irvine *et al.*, 2017).

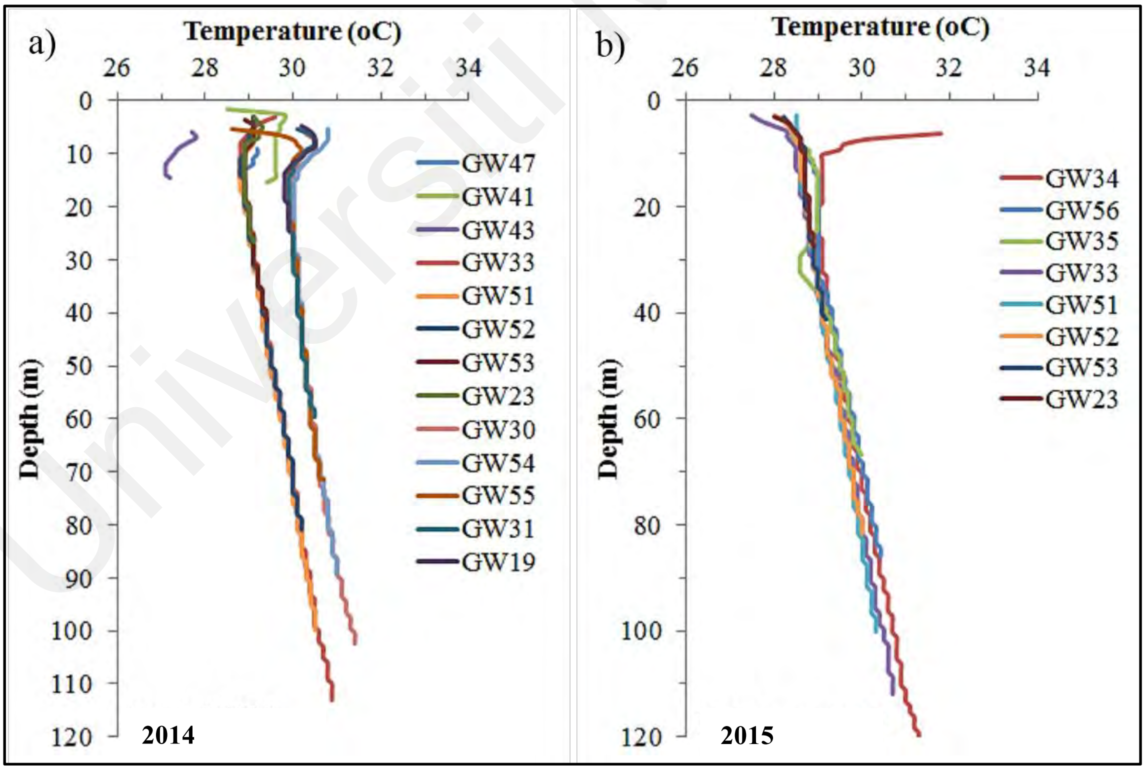

Figure 5.44: Temperature-depth profiles measured at LKRB

5.3.3.3 Groundwater Flux

The temperature–depth profiles with heat advection caused by the movement of groundwater flow in the subsurface were analysed using Equation 3.6 (section 3.6.3) to calculate the vertical groundwater fluxes at LKRB. The T_0 is set as 27 ºC and this is considered as the mean annual of surface air temperature because there is no available long-term data on ground surface temperature at LKRB. Surface temperature usually changes according to the change in air temperature (Taniguchi *et al.*, 2003a). The geothermal gradient, T_G of 0.045 ºC/m is used in the calculation based on the ranges of geothermal gradient at Penyu basin 0.036 ºC/m to 0.055 ºC/m (Madon, 1999). The thermal diffusivity, α is 6.5 E-7 m^2s^{-1} is adapted from (Taniguchi *et al.*, 1989). 100 years (t) is considered as the time after semi equilibrium and the increase in surface temperature at LKRB, b is 0.0162 ºC/year. $U=vc_o\rho_o/c\rho$ where v is the vertical groundwater flux, $c_o\rho_o$ is the heat capacity of water and $c\rho$ is the heat capacity of aquifer. Different U values were used to compute the calculated temperature-depth profiles. The positive U value will show downward movement of groundwater flow (recharge) while the negative U value will represent upward movement of groundwater flow (discharge). The calculation is limited by the semi-infinite layers in which only vertical conduction and convection, and vertical groundwater flux are assumed to be constant with depth (Taniguchi *et al.*, 2003).

The calculated temperature–depth profiles are shown in Figure 5.45 and Figure 5.46, respectively. The calculated profiles represent the best shape of the observed profiles at shallow and deep aquifer. The misfit in the profiles may result from a difference of thermal properties (thermal conductivity and thermal diffusivity) of the aquifer materials which may affect heat convection within the aquifer (Majumder *et al.*, 2013; Irvine *et al.*, 2017).

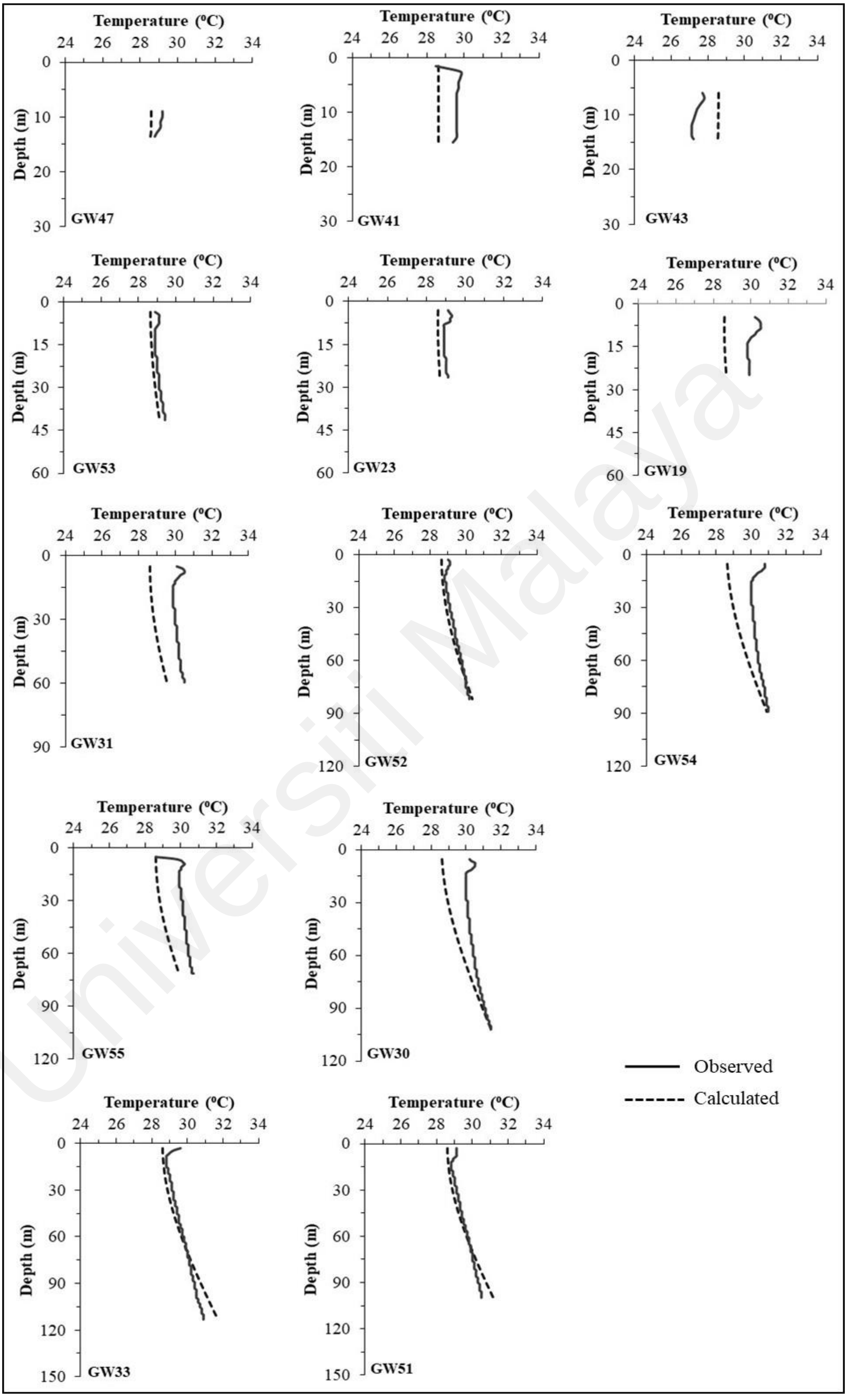

Figure 5.45: Observed and calculated subsurface temperature profiles August 2014

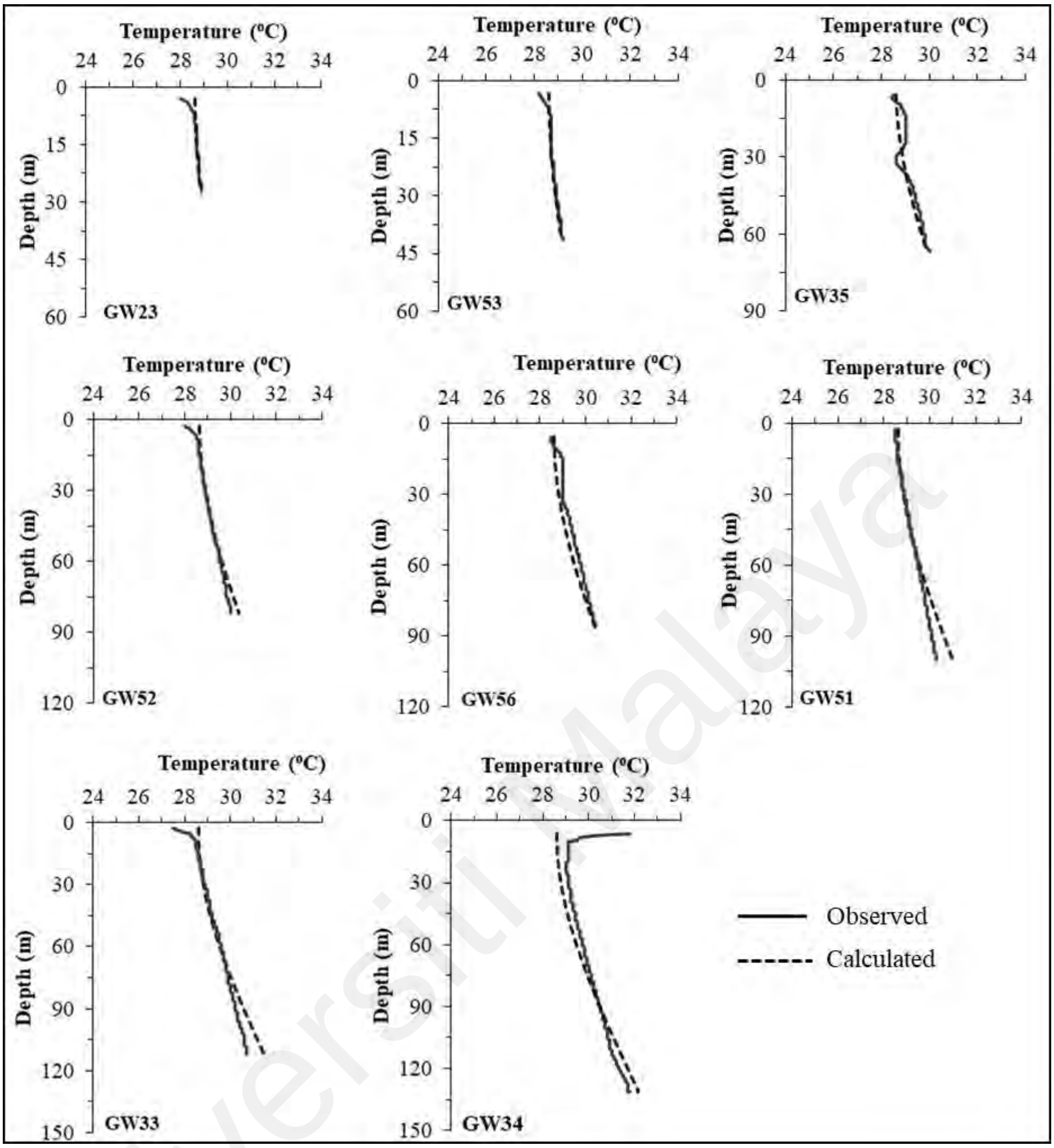

Figure 5.46: Observed and calculated subsurface temperature profiles February 2015

Table 5.16 listed the best *U* values for each profiles. In 2014, the calculated profiles give *U* values in Layer 1 ranges from 200 mm/yr to 300 mm/yr, whereas in Layer 2 the *U* values ranges from 110 mm/yr to 200 mm/yr and in Layer 3 the *U* values ranges from 50 mm/yr to 150 mm/yr, respectively. In 2015, the calculated profiles give *U* values in Layer 2 100 mm/yr and in Layer 3 the *U* values ranges from 120 mm/yr to 180 mm/yr, respectively. According to the positive *U* values in Table 5.16, all wells are recharged type with downward groundwater flow (Domenico & Palciauskus, 1973) of the groundwater flow system in the basin. The root mean square (RMSE) of the observed and calculated profiles is between 0.10 to 1.43. The uncertainties arise in this flux estimates can be induced by the parameterisation of the initial conditions (Irvine *et al.*, 2017) as in Equation 3.6.

Table 5.16: Groundwater flux, *U* values from calculated temperature-depth profiles

Well ID	Aquifer Layer	Flux Rate *U* (m/yr)	Flux Rate *U* (mm/yr)	Type	RMSE
2014					
GW47	L1	0.25	250	R	0.49
GW41	L1	0.20	200	R	0.99
GW43	L1	0.30	300	R	1.24
GW53	L2	0.11	110	R	0.29
GW23	L2	0.19	190	R	0.38
GW33	L3	0.10	100	R	0.35
GW51	L3	0.10	100	R	0.27
GW52	L3	0.11	110	R	0.21
GW19	L2	0.20	200	R	1.43
GW30	L3	0.05	50	R	0.86
GW54	L3	0.05	50	R	0.11
GW55	L3	0.15	150	R	1.11
GW31	L3	0.15	150	R	1.22
2015					
GW53	L2	0.10	100	R	0.10
GW23	L2	0.10	100	R	0.15
GW33	L3	0.15	150	R	0.29
GW51	L3	0.14	140	R	0.26
GW52	L3	0.12	120	R	0.31
GW34	L3	0.18	180	R	0.85
GW56	L3	0.15	150	R	0.22
GW35	L3	0.10	100	R	0.18

R: recharge; RMSE: root mean square error

Based on the groundwater flux listed in Table 5.16, it can be summarised that the recharge in Layer 1 which ranges from 200 mm/yr to 300 mm/yr with a mean of 250 mm/yr, whereas in Layer 2 ranges from 105 mm/yr to 200 mm/yr with a mean of 150 mm/yr, and in Layer 3 ranges from 50 mm/yr to 180 mm/yr with a mean of 119 mm/yr respectively as tabulated in Table 5.17

Table 5.17: Summary percent of rainfall (%) of groundwater recharge

Aquifer Layer	Rainfall (mm)	Recharge (mm/yr)	Percentage of Rainfall (%)
Layer 1	2619	200 to 300 (250)	8 to 11 (10)
Layer 2		105 to 200 (150)	4 to 8 (6)
Layer 3		50 to 180 (119)	2 to 7 (5)

() :mean value

By taking the long-term rainfall of 2619 mm (see section 5.3.3.1) into consideration, the groundwater recharge rate based on the percentage of rainfall is listed in Table 5.17. For Layer 1, the percentage of rainfall is between 8% to 11% with a mean of 10%, whereas Layer 2, the percentage is between 4% to 8% with a mean of 6% while for Layer 3 the percentage is between 2% to 7% with a mean of 5%. In general, the average values percentage of rainfall shows a decreasing trend from Layer 1 to Layer 3 of 10% to 6% respectively. This study has indicated that the spatial variations of subsurface temperature at LKRB by the presence of shallow and deep groundwater flow systems.

The effect of surface air temperature were not considered during groundwater recharge interpretation. According to Hiscock and Bense (2014), groundwater temperature down to the depth of ~ 25 m was strongly affected by seasonal variations in surface temperature. The fluctuation of surface temperature creates a temperature wave which propagates down into the subsurface rather than the heat convection caused by groundwater flow (Taniguchi *et al.*, 2003a; Bense & Kooi, 2004; Colombani *et al.*, 2016). Gosnold *et al.* (1997) have shown that shallow subsurface temperature (up to 75 m) is closely related with the surface air temperature during non-seasonal ground freezing and this correlation was confirmed by the modelling results using synthetic transient temperature-depth profiles at the northern Plain of USA (Harris & Gosnold, 1999). Taniguchi (1993) stated that groundwater fluxes in shallow aquifers are more complex as they are influenced by changes in surface air temperature and aquifer is actively used as a resources.

5.3.4 Groundwater Modelling

Reviews on groundwater modelling were briefly explained in Chapter 2 and the model development and input parameters were described in detail in Chapter 3. The groundwater model using Visual MODFLOW will be used as a tool to testify the recharge amount estimated through water balance approach. In most modelling works it is recommended that the value between 5 to 20% of the annual rainfall as a reasonable value for the groundwater recharge (Waterloo Hydrogeologic, 2005).

5.3.4.1 Water Balance

The water balance of the aquifer system studied by Hussin (2011) is tabulated in Table 5.18. This water balance has considered rainfall, potential evapotranspiration and river discharge of 3.09E+10 m^3/yr, 1.23E+10 m^3/yr, and 1.53E+10 m^3/yr, respectively. The estimated value of change in storage is 3.26E+09 m^3/yr (11%) which is equivalent to recharge into the basin.

Table 5.18: Estimated water balance of Kelantan River Basin from Hussin (2011)

Description	Value	Percentage (%)
Rainfall (m^3/yr)	3.09E+10	100.00
Potential evapotranspiration (m^3/yr)	1.23E+10	39.88
Discharge (m^3/yr)	1.53E+10	49.58
Δ± change in storage (m^3/yr)	3.26E+09	10.55

5.3.4.2 Model Calibration and Validation

The steady-state condition was simulated using piezometric heads of 49 monitoring wells with dataset from 1989 to 2000. The model was calibrated by trial-and-error adjustments of the hydraulic conductivity parameter to match the calculated heads with the observed heads. The hydraulic conductivity was adjusted within the range in Table 3.5 of each unit and a uniform constant recharge as in Table 3.4 through the calibration processes. The model was successfully converged after maximum outer and inner iterations of 100 and 50 with head change and residual criterion of 0.01. A scatter plot of the best fit between the observed heads and calculated heads of the calibration simulation is shown in Figure 5.47 with RM, RMSE, NRMSE and R^2 of 0.003 m, 1.460 m, 13.54% and 79.2%, respectively. Table 5.18 tabulated the accepted input parameters of simulated calibration model.

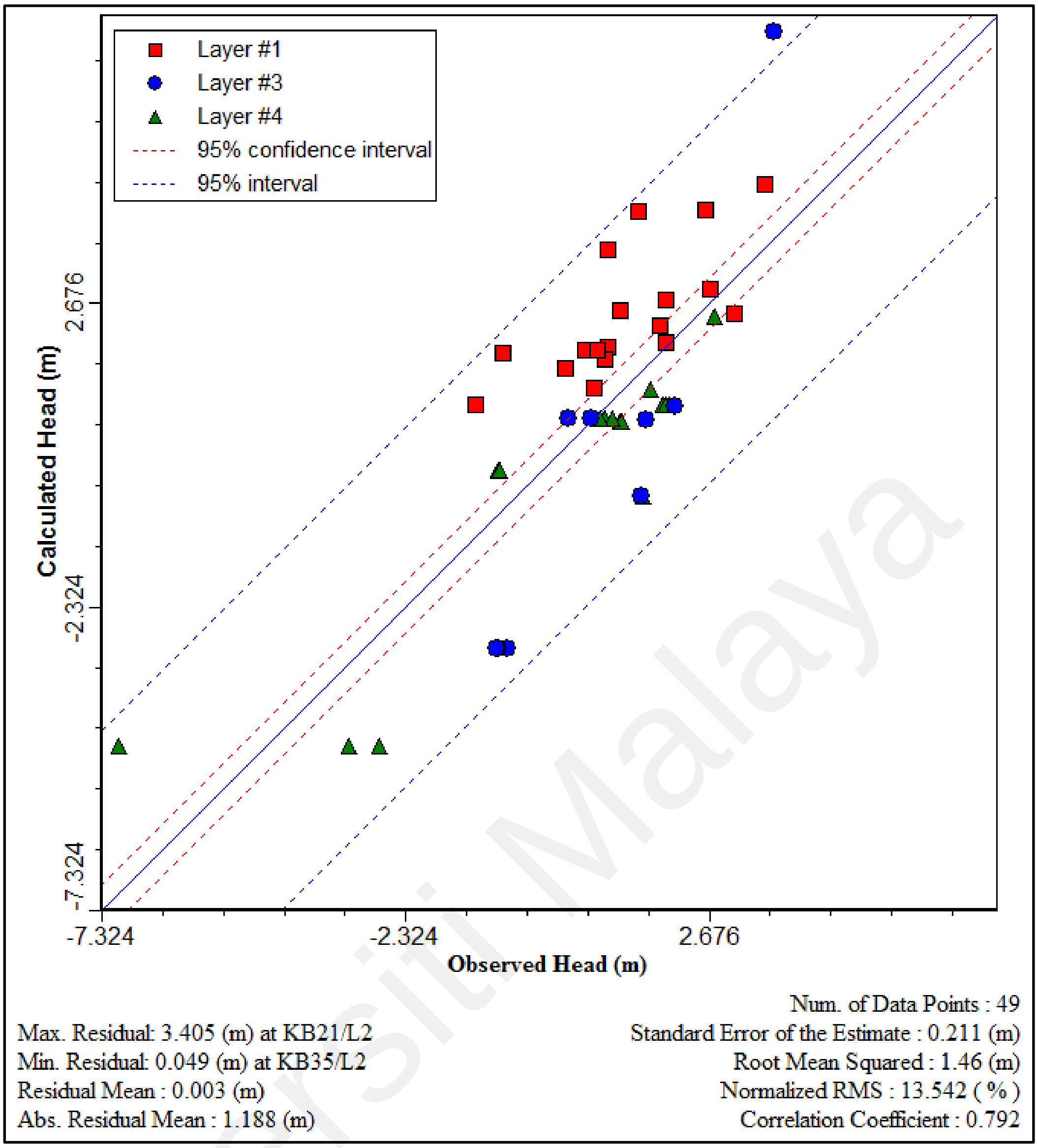

Figure 5.47: Plot of observed head and calculated head achieved after calibration

Table 5.19: Input parameters after model calibration

<table>
<tr><th rowspan="2">Parameter</th><th colspan="5">Value</th></tr>
<tr><th>Unit 1</th><th>Unit 2</th><th>Unit 3a</th><th>Unit 3b</th><th>Unit 4</th></tr>
<tr><td>K_x (m/s)</td><td>0.01</td><td>10^{-6}</td><td>8×10^{-4}</td><td>10^{-5}</td><td>10^{-4}</td></tr>
<tr><td>K_y (m/s)</td><td>0.01</td><td>10^{-6}</td><td>8×10^{-4}</td><td>10^{-5}</td><td>10^{-4}</td></tr>
<tr><td>K_z (m/s)</td><td>0.001</td><td>10^{-7}</td><td>8×10^{-5}</td><td>10^{-6}</td><td>10^{-5}</td></tr>
<tr><td colspan="6"></td></tr>
<tr><td>S_s</td><td colspan="5">1.65×10^{-3}</td></tr>
<tr><td>S_y</td><td colspan="5">0.23</td></tr>
<tr><td>Recharge</td><td>11%</td><td>5%</td><td></td><td>7%</td><td></td></tr>
<tr><td>Total Porosity</td><td colspan="5">0.20</td></tr>
<tr><td>Effective porosity</td><td colspan="5">0.11</td></tr>
<tr><td>River</td><td colspan="4">Golok,Kelantan, Pengkalan Datu, Kemasin, Mulong, Semarak, Ketereh, Lemal</td><td>Tok' Uban Lake</td></tr>
<tr><td>Riverbed Conductivity (m/s)</td><td colspan="4">10^{-4}</td><td>10^{-6}</td></tr>
<tr><td>Riverbed Thickness (m)</td><td colspan="5">0.50</td></tr>
<tr><td>River stage and bottom (m)</td><td colspan="5">Stage and river cross section data from DID</td></tr>
<tr><td>River width (m)</td><td colspan="5">Estimated based on Google Earth</td></tr>
<tr><td colspan="6"></td></tr>
<tr><td rowspan="8">Groundwater pumping (m^3/d)</td><td colspan="3">Wakaf Bharu</td><td colspan="2">23,188</td></tr>
<tr><td colspan="3">Tanjung Mas</td><td colspan="2">18,143</td></tr>
<tr><td colspan="3">Chicha</td><td colspan="2">107,362</td></tr>
<tr><td colspan="3">Kg. Puteh</td><td colspan="2">73,670</td></tr>
<tr><td colspan="3">Pintu Geng</td><td colspan="2">19,334</td></tr>
<tr><td colspan="3">Kg. Chap</td><td colspan="2">8,971</td></tr>
<tr><td colspan="3">Perol</td><td colspan="2">6,109</td></tr>
<tr><td colspan="3">Total</td><td colspan="2">256,777</td></tr>
</table>

The parameters determined during the model calibration are then validated by using piezometric heads of 28 monitoring wells with dataset from 2001 to 2012. A scatter plot of the best fit between the observed heads and calculated heads of the validation simulation is shown in Figure 5.48 with RM, RMSE, NRMSE and R^2 of 0.806 m, 2.097 m, 15.841 % and 78.8 %, respectively. The validation result of RMSE is higher 0.637 m than the calibration but still within the 2-3 m acceptable ranges of heads decreased.

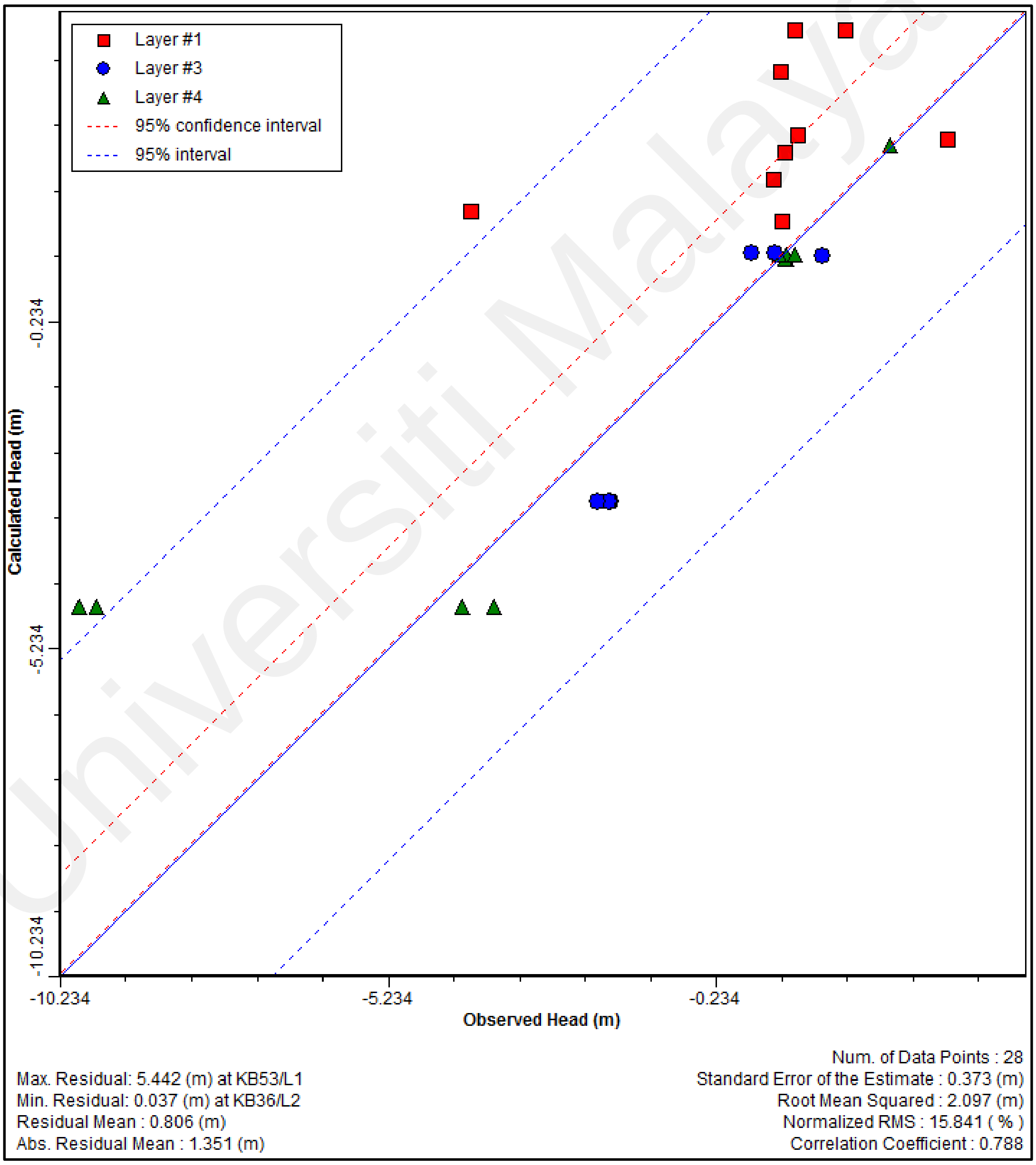

Figure 5.48: Plot of observed head and calculated head achieved after validation

5.3.4.3 Sensitivity Analysis

Sensitivity analysis is a good measure to quantify the uncertainty of the calibrated model especially when the model was developed with limited data (Lenhart *et al.*, 2002). This is caused by the uncertainties of the aquifer parameters and sometimes the model boundary conditions (e.g., hydraulic conductivity and recharge). It is carried out by varying both increasing and decreasing of one selected parameter within plausible range while holding constant all other parameters. To further determine the acceptable water balance recharge value, a sensitivity analysis was performed manually by standardising the 10% increment and decrement of each recharge zones as listed in Table 5.20. The results for the sensitivity analysis are presented in Figure 5.49 and Figure 5.50. The relationship between RMSE and change in recharge shows a slight decreased from 1.457 m to 1.465 m when the percentage of recharge decreased from 10% to 40%. while RMSE values increased from 1.465 m to 1.496 m when the percentage of recharge increased from 10% to 40% (see Figure 5.49). The relationship between residual mean and change in recharge shows a linear increasing and decreasing trend of residual mean as the recharge percentage is increased and decreased within 10% to 40%. The R^2 values tabulated in Table 5.20 indicates that the calibrated model is the most reasonable model compared to others. This indicates that recharge is a sensitive parameter and the values selection, or its representation is very crucial in the model calibration processes.

Table 5.20: Changes in recharge during sensitivity analysis

Change in recharge (%)	Zone 1 (11%)	Zone 2 (5%)	Zone 3 (7%)	R^2	Remarks
0	**297.98**	**135.45**	**189.63**	**0.792**	**Reasonable**
10	327.78	149.00	208.59	0.790	Calculated
20	357.58	162.54	227.56	0.789	Calculated
30	387.37	176.09	246.52	0.787	Calculated
40	417.17	189.63	265.48	0.786	Calculated
-10	268.18	121.91	170.67	0.793	Calculated
-20	238.38	108.36	151.70	0.794	Calculated
-30	208.59	94.82	132.74	0.795	Calculated
-40	178.79	81.27	113.78	0.797	Calculated

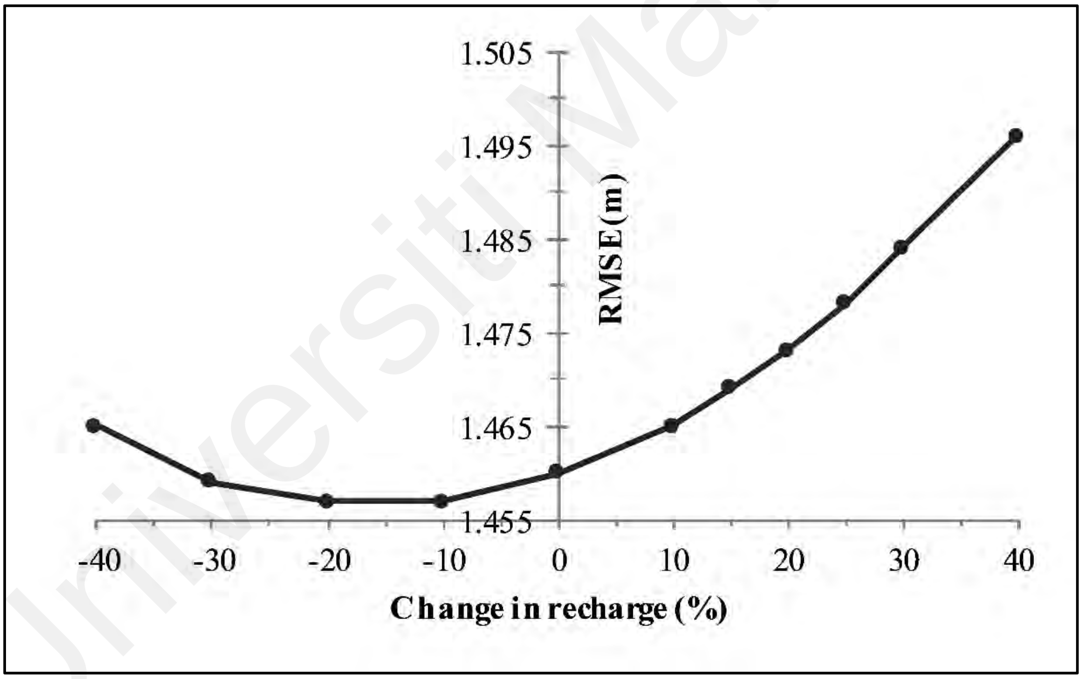

Figure 5.49: RMSE (m) at different recharge percentage

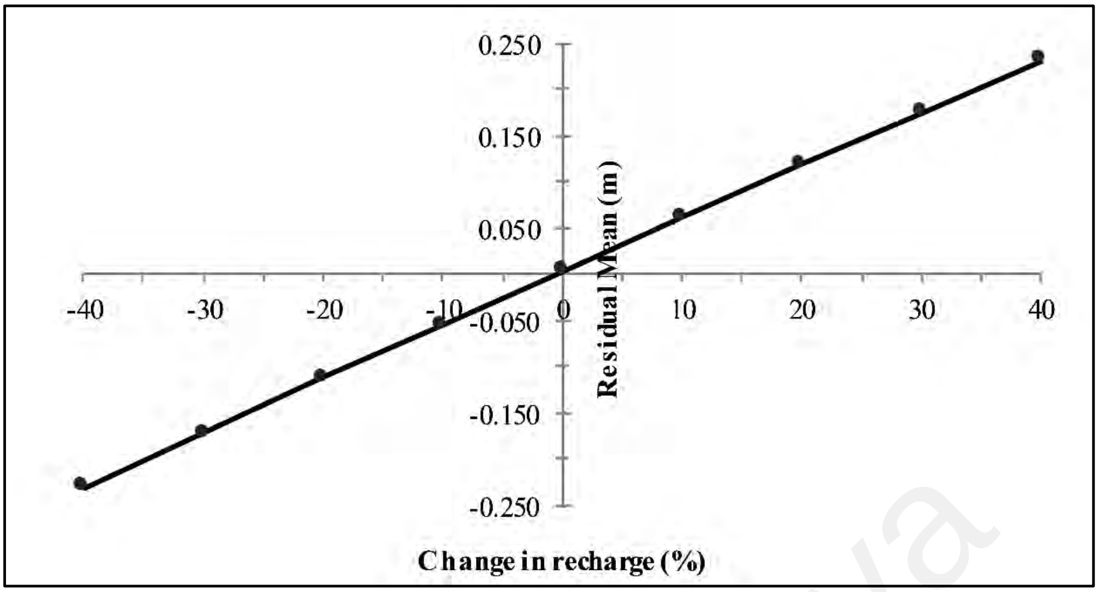

Figure 5.50: Residual mean (m) at different recharge percentage

The distribution contour between the calibrated model and the model during sensitivity analysis can be seen in Figure 5.51 and Figure 5.52. An example piezometer heads contour of 40% increase and decrease in recharge are used for comparison. It is noticed that when 40% recharge is increased, the contour heads pattern is slightly above the calibrated contour heads and while 40% recharge is decreased, the contour heads pattern is slightly below the calibrated contour heads. The cone of depression developed surrounding the wellfields is deeper when recharge is reduced by 40% as reduced in rainfall input. The model is sensitive to recharge because recharge is the primary input source (precipitation and river leakage) and the model is simulated under steady state condition where inflow balances outflow with no change in storage (Seneviratne, 2007).

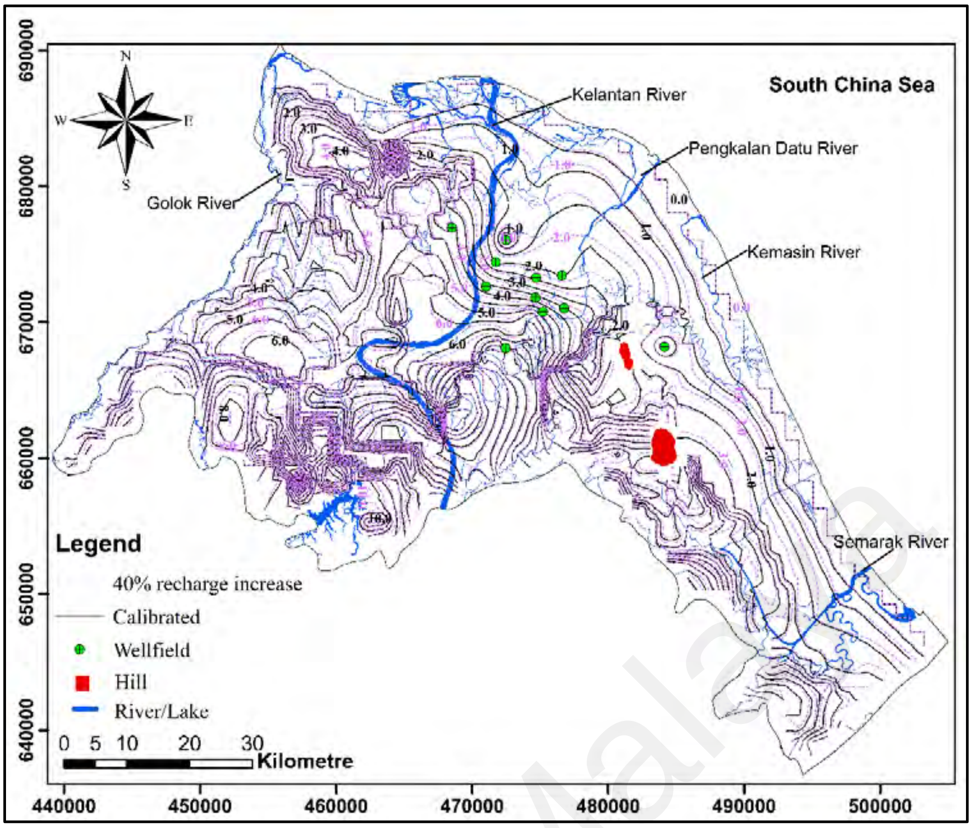

Figure 5.51: Distribution of contour heads during model calibration and sensitivity at 40% recharge increased

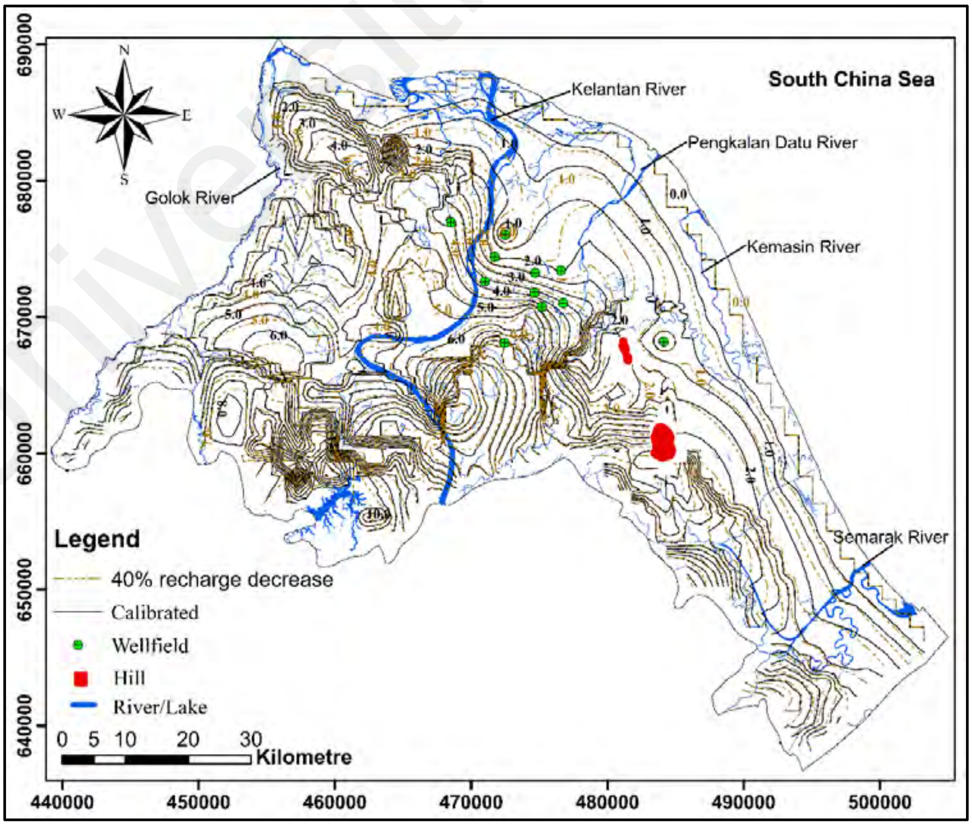

Figure 5.52: Distribution of contour heads during model calibration and sensitivity at 40% recharge decreased

CHAPTER 6: DISCUSSIONS

6.1 Introduction

The Lower Kelantan River Basin (LKRB) is a heterogenous aquifer of Quaternary deposit consisting a mixture of clay, silt, and fine to coarse sand. LKRB has been exploited for groundwater resources since 1930s and the demand is continously increasing for water supply. Therefore, a basic prerequisite for efficient and sustainable management of groundwater resources is necessary to avoid depletation and degradation of the natural resources. This research represents a baseline study to gain insight on groundwater recharge mechanism at LKRB. The first part of the chapter will discuss the source and processes that had occurred during the groundwater recharge flow processes and the second part will discuss the groundwater recharge rate quantify in the basin.

6.1.1 Evaluation of Groundwater Recharge Flow Processes

Groundwater recharge flow processes have been evaluated using four methods of stable isotopes, tritium, radon and hydrogeochemical, respectively. Stable isotope indicates that isotopic composition of local rainwater is influenced by amount effect during monsoon seasons (Rozanski *et al.*, 1993; Araguás-Araguás *et al.*, 1998; Majumder *et al.*, 2011). Rainwater is having fractionation of primary and secondary evaporation in relation to GMWL and LMWL before reaching ground surface (Dansgaard, 1964; Clark & Fritz, 1997a; Gupta & Deshpande, 2005). The tritium content in rainwater has shown a decreasing trend to natural level with mean of 3.8 TU following the global trend of Otawa at Northern Hemisphere and Kaitoke at Southern Hemisphere (Harms *et al.*, 2016; Wirmvem *et al.*, 2017). Rainwater is classified as modern water age and the content is almost the same to Melbourne with 3.5 TU which classified as modern water (IAEA, 2011a).

Rainfall of modern water age that has experienced evaporation in isotopic composition is the main source of surface water and diffuse recharge into the aquifer system. LKRB is recharged by modern water age, less than 5 years to10 years at shallow aquifer (Layer 1) while deep aquifer (Layer 2 and Layer 3) has featured of mixed recharge water (of sub-modern and modern water) according to Clark and Fritz (1997a) and supported by the relationship of tritium and oxygen-18. In general surface water and groundwater has depleted isotopic composition compared to rainwater. Surface water is enriched with heavy isotopic composition during dry season compared to wet season and having low radon concentration due to the lost of radon through outgassing of turbulent current (Bertin & Bourg, 1994; Grolander & Kärnbränslehantering, 2009). Towards the downstream, the surface water (river) is depleted in stable isotopes but experienced an increase in tritium content. Groundwater shows depletion in heavy isotope compared to surface water and has small ranges of isotopic composition within aquifer layers. In dry season, Layer 1 is slightly enriched in heavy isotope as compared to wet season while Layer 2 and Layer 3 are slightly enriched in light isotope during dry season but depleted in wet season. Groundwater shows a trend of depleting in stable isotopes, decreasing in tritium content and increasing in radon concentration with increased aquifer depth. The groundwater has evolved from $CaHCO_3$ to $NaHCO_3$ towards the coastal area and the major processes which controlled the groundwater chemistry are silicate weathering, dissolution and ion exchange.

The interconnection processes between river - groundwater and aquifer - aquifer layer is either by infiltration, leaking and/or mixing are proven by the composition of stable isotopes, tritium, radon and hydrogeochemical. During rainfall event, rainwater will dissolve CO_2 at the atmosphere and enhance the dissolving power and increased the HCO_3 ion in rainwater It will rapidly experience runoff and/or percolate into the river and infiltrate quickly into the shallow aquifer (Layer 1) through the unsaturated zone. At the same time, there are dissolution of silicate weathering and ion-exchange between aquifer materials. The river will recharge into Layer 1 during dry season while Layer 1 will discharge into the river on wet season. Therefore, river and Layer 1 have similar ranges of stable isotopes and tritium content due to the fast transmit time that classified both as modern water. The input radon in river is less than 1 Bq/L and it is possibly comes from Layer 1 as the river has no direct contact with the solid materials to the extends of groundwater. Hydrogeochemical processes in Layer 1 indicate that groundwater has evolved from $CaHCO_3$ to $NaHCO_3$ towards the coastal. $CaHCO_3$ facies is prominent in recharge area. It is also identified that the interconnection between river-groundwater is up to Layer 2.

Aquifer-aquifer interconnection was revealed through wells at Layer 1 with Layer 2 and Layer 2 with Layer 3. During water travel, long residence time from Layer 1 to Layer 3 (shallow to deep) will reduce the tritium content through decaying process. The decaying process does not involve the aquifer materials but rapid mixing and dilution with old water in aquifer resulted the in the mixing water of sub-modern and modern water in Layer 2 and Layer 3. The increase in radon concentration from Layer 1 to Layer 3 is related to the position of aquifer that is closed to the underlying bedrock containing uranium, the decay parent of radon. Simplification of groundwater recharge flow processes is illustrated in Figure 6.1. The integration of various methods has provided an understanding on recharge flow processes at LKRB.

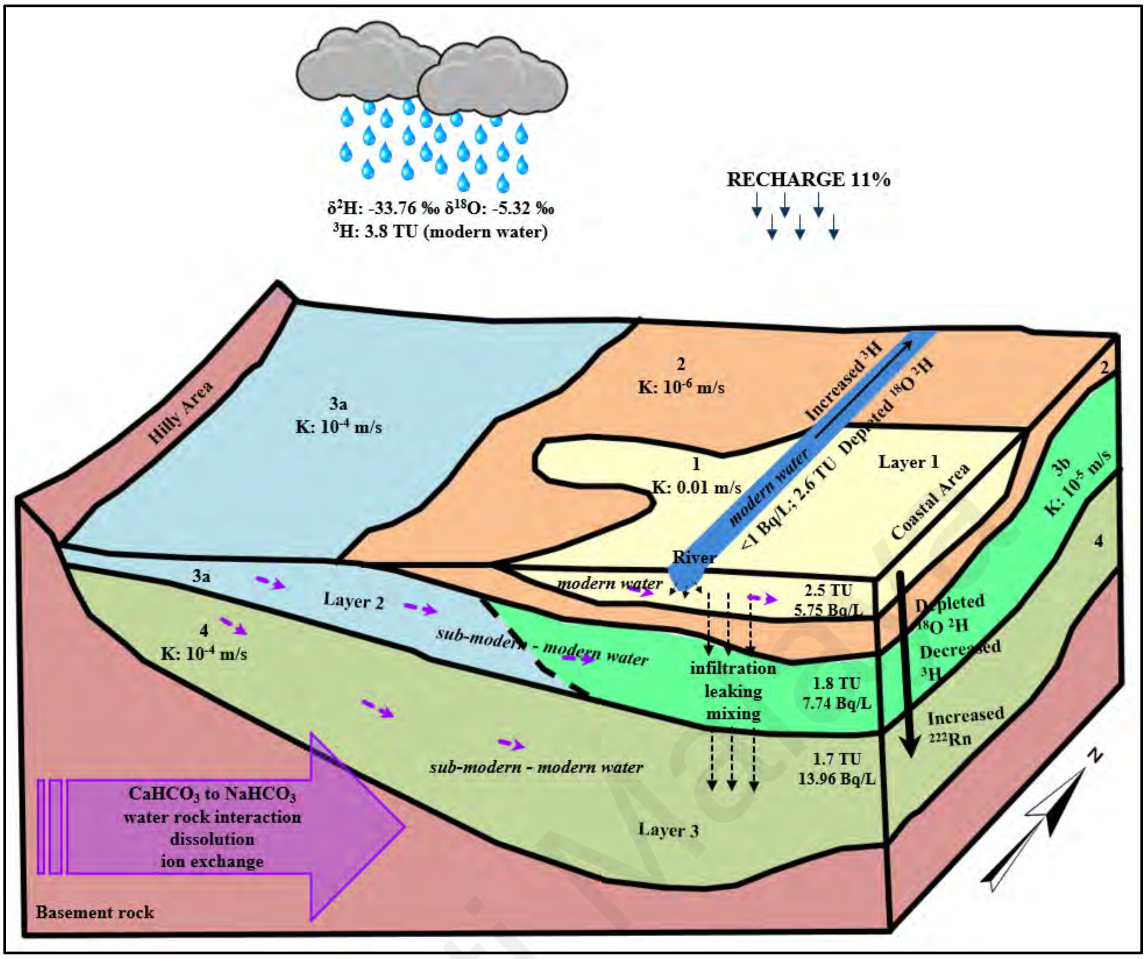

Figure 6.1: Conceptual model of groundwater recharge mechanism at LKRB

6.1.2 Evaluation of Groundwater Recharge Rate

Various methods of recharge estimation using CMB, WTF, TDP and GM(WB) have been used at LKRB. Selection of these methods was dependent on the existing and accessible data that were available within this period of study. Explanation on the comparison of methods is based on percentage of annual rainfall because each method that was applied in this study has a different range of annual rainfall. The range of recharge estimation is summarised in Table 6.1.

Table 6.1: Summary of recharge estimation using different methods.

Method	Recharge, (% of rainfall)
CMB	13-68 (36)
WTF	11-19 (15)
TDP	8-11 (10)
GM(WB)	11

*() average value

CMB method shows a large variation in recharge estimation ranges from 13% to 68% with mean of 36% of annual rainfall as tabulated in Table 6.1. In CMB method, rainfall amount and chloride concentration measured in rainfall and unsaturated zone (soils) are used to estimate the recharge. An assumption that the primary source of recharge is rainfall has met CMB's criteria at LKRB, with rainfall records at over 1000 mm annually. Uncertainty arises when determining the concentration of chloride in rainfall and soils. The available data of rainfall chloride was collected only for a short period of less than three years. The rainfall chloride data should be for a period of at least five years monitoring (Sukhija *et al.*, 2003) and should provide the most representative rainfall chloride data of the basin which is not available in the study area. Rainfall chloride of wet deposition is the only source of chloride, the atmospheric chloride of dry deposition was not accounted because no data has been recorded within the basin. Dry deposition can be neglected because heavy rainfall will wash out the dry deposition (Guan *et al.*, 2010; Gobinddass *et al.*, 2020). Even though it can be negligible, determination of dry deposition will be a good practice as the dry deposition has potential to be deposited within 100 km from the coastal area (Guan *et al.*, 2010; Gobinddass *et al.*, 2020). Consideration of both wet and dry can improve the recharge estimates.

Caution during soil sample preparation to extract the chloride and to conduct particles size analysis (Deng et al., 2011) will reduce the error level. Following the assumption in

CMB method, chloride in soils are not from weathering or anthropogenic sources. Soil texture play a significant role in holding chloride concentration (Liu *et al.*, 2009; Huang & Pang, 2011) along the soil profiles. Infiltrated rainfall will flush and take the chloride ions deeper downward. Changes of soil texture from clay silt materials to coarse materials are expected to result in high recharge value (Ting *et al.*, 1998; Ifediegwu, 2020). The variation of chloride concentration and soil texture in the soil profiles has shown the heterogeneity within the basin. Therefore, to have a good recharge estimation using CMB, rainfall and soils samples must be spatially represent the basin and repeated sampling data is a must to reduce the uncertainty of the method.

The recharge estimation using WTF method ranges from 11% to 19% with mean of 15% of annual rainfall, as tabulated in Table 6.1. In WTF method, component of specific yield, *Sy* and groundwater level rise are used to calculate recharge. The availability of long-term groundwater water level data at LKRB gives an advantage in using WTF. The groundwater level data show a quick response of recharge as the fluctuation of water level corresponds well with the rainfall event (Figure 5.36). The *Lisse* effect (Healy & Cook, 2002; Weeks, 2002; Crosbie *et al.*, 2005) at LKRB can be said to be negligible or minimal within the basin because the depth to water table in shallow aquifer is more than 1.30 m and LKRB itself is coastal sandy aquifer. Currently, LKRB is actively pumping but there is no indication of sharp difference in water level fluctuation based on the long-term data (MGD, 2014b) or ground settlement has occurred in the basin (Che Sulaiman, 2010). The uncertainty may come during the extrapolation of water cycle hydrograph via graphical approach (Delin *et al.*, 2007) to identify the groundwater level rise. An *Sy* value of 0.15 was set to be constant throughout the aquifer following a common practice of researchers (Delin *et al.*, 2007) because *Sy* value is difficult to determine even with proper planning (Healy, 2010). *Sy* values actually vary with depth and location (Song & Chen, 2010) and this applies to LKRB as well as a heterogeneous aquifer. Assumption of a constant *Sy* may lead to either overestimates and underestimates of recharge. The scarcity of monitoring wells that are not spatially distributed within the basin has influenced the *Sy* value and groundwater level data with imcomplete temporal record.

Like WTF method, TDP method also give a small range of recharge estimation from 8% to 11% with mean of 10% of annual rainfall as shown in Table 6.1. TDP results indicate that LKRB is dominated by the downward movement groundwater flux of recharge type for both shallow and deep aquifer systems. Recharge area is recognised to have low thermal gradient (Uchida & Hayashi, 2005). In the TDP method, recharge estimation was calculated using Carslaw and Jaeger (1959) equation. The uncertainty is induced by input parameters of the equation in the initial condition (Irvine *et al.*, 2017). To apply this TDP method, some of the parameter value were adopted from literature (Taniguchi *et al.*, 1989; Madon, 1999) due to unavailable data related to LKRB which might give overestimation or underestimation of recharge. The effect of surface air temperature in wells caused by seasonal changes are not accounted (Taniguchi, 1993; Taniguchi *et al.*, 2003a; Hiscock & Bense, 2014; Colombani *et al.*, 2016) especially in shallow aquifer which can reflect the recharge quantification. Lacking in number of monitoring wells that represent the basin and aquifer layer has limited the interpretation of temporal and spatial variation of recharge estimation and also an understanding the groundwater flow pattern. The need for repeated measurement of temperature-depth profiles and measurement the local thermal properties perhaps will also improve the recharge estimation and reduce the ucertainty.

GM(WB) applied 11% of recharge from water balance (WB) study (Hussin, 2011). The steady state model was constructed using available local data input for the basin. The model has successfully calibrated and validated with correlation coefficient of 79.2% and 78.8%. The calibration processes reduced the uncertainty within the model. The sensitivity analysis result has indicates that recharge WB is sensitive during parameter adjustment of 10% increment and decrement in the model. The model is sensitive to recharge because rainfall is the primary input source of the model. Uncertainty in GM(WB) usually arises during the construction of the conceptual model. The model input parameters still need to be improved or updated because a lack in data inputs will produce an unreasonable model. Modeller knowledge is also important as this helps to increase understanding of the model. The advantages of using GM(WB) are that it can be used to predict future recharge that help in groundwater resources management and that the model can be used to represent a range of scales from point to regionally (Scanlon *et al.*, 2006; Zhou & Li, 2011).

Table 6.1 summarised recharge estimations quantified using four methods. Generally, recharge ranges showed high variability within 8% to 68% of annual rainfall. CMB ranged from 16% to 68%, WTF ranged from 11% to 19%, TDP ranged from 8% to 11% and GM(WB) based on WB value of 11% of annual rainfall, respectively. The average recharge of CMB, WTF and TDP methods is 20% of annual rainfall with diversion as compared to average values rnaging from 12% to 48%. A wide range of recharge is evidenced to different factors subject to inherent principles and assumptions in the methods applied, data quality and quantity, and geological condition. All methods are sensitive to the input parameters, therefore, it is essential to reduce the uncertainty and errors inherent in quantifying recharge estimation from any single method as discussed above.

Based on results of four methods applied at LKRB indicates that 11% of recharge shows GM(WB) is the best method to estimate groundwater recharge for this humid tropical basin. This selection is because GM(WB) has constructed and calibrated using locally derived data input parameters. GM(WB) is the only method that involved calibration process by comparing the observed and calculated values. Recharge is sensitive to the adjustment parameter as rainfall is the primary source in steady-state model simulation. WTF gives reasonable recharge value to be used together with GM(WB) to ensure the reliability of recharge value approximately in the same range. WTF based on long-term hydrological data records and the method itself estimates actual recharge of local scale even less monitoring wells used to represent the basin. Even though TDP gives mean recharge 10% close to GM(WB), this method is not suitable to be paired with because selected input parameter is not locally and data not represent the whole basin. 36% of mean recharge by CMB does not mean this value is inaccurate because CMB is point scale estimation and required rainfall and chloride data to represent the basin heterogeneity.

This study has highlighted the importance of applying various methods in quantification of recharge estimation. The reliability and suitability of recharge estimation can be improved by obtaining reliable and spatiotemporal data within LKRB that are applicable to the method used. Methods can be accepted as long as land use are not changing dramatically in the basin. Spatial distribution of recharge can imply better recharge proxy that is good for future urban planning at LKRB, which was limited in this study as data were lacking in number representative points of sampling or monitoring wells to represent the aquifer layer and basin area. In addition, there is the need of repeated sampling and frequency of measurement. This study has provided insight into quantification groundwater recharge and method selection for humid tropical areas of LKRB and is useful as a baseline study for groundwater resources management at LKRB, in particular and for Malaysia as a whole. Lysimeter as a direct and best method to quantify groundwater recharge was unable to be installed during the studies due to difficulty in obtaining approval and permission from the land owner.

CHAPTER 7: CONCLUSIONS AND RECOMMENDATIONS

7.1 Conclusions

The conclusions derived from this study are listed below:

1. Stable isotopes indicate local rainfall origin is from monsoon meteoric air masses that have experienced primary and secondary evaporation. Tritium content in rainfall is almost back to natural level, classified as modern water age (< 5 year to 10 year). Rainfall is the main source of surface water (river) and diffuse recharge into groundwater system at LKRB.
2. Rapidly percolated and infiltrated rainfall runoff through unsaturated zone into aquifer has recharged Layer 1 with modern water age while Layer 2 and Layer 3 have mixed recharge water of modern water and sub-modern water age as infiltrated water took longer transmit time to arrive and has mixed with available water in aquifer.
3. Isotopic composition (stable isotopes, tritium and radon) and hydrogechemcal reveal that interactions between river-groundwater and aquifer-aquifer at LKRB through the infiltration, leaking and mixing are governed by the process of silicate weathering, dissolution and ion exchange. Shallow aquifer has evolved from $CaHCO_3$ to $NaHCO_3$ from inland towards the coastal area. Groundwater shows depletion in stable isotopes, decrease in tritum content and increase in radon concentration with increased aquifer depth.
4. The range of recharge quantified using CMB, WTF, TDP and GM(WB) methods is within 8% to 68% of annual rainfall. Recharge by CMB, WTF and TDP is 20% of annual rainfall with diversion compared to average values which ranges from 12% to 48 % of annual rainfall.

5. The variability of recharge range is evidenced to different factors subjected to inherent principles and assumptions in the methods applied, data quality and quantity, and geological condition within the basin.
6. 11% of recharge shows GM(WB) is the best method to estimate the groundwater recharge. GM(WB) model was constructed and calibrated using locally derived data input parameters, the only method that involves a calibration and recharge that is sensitive to the adjustment parameter as rainfall is the primary source in steady-state model simulation. WTF method based on the long-term hydrological records gives a reasonable recharge value to be used together with GM(WB) to ensure the reliability of recharge value approximately in the same range for humid tropical basin of LKRB.
7. The study has provided insight into integrated groundwater recharge mechanism as a baseline study for groundwater resources assessment at LKRB, in particular and for Malaysia as a whole.
8. The conceptual model of groundwater recharge mechanism is shown in Figure 7.1.

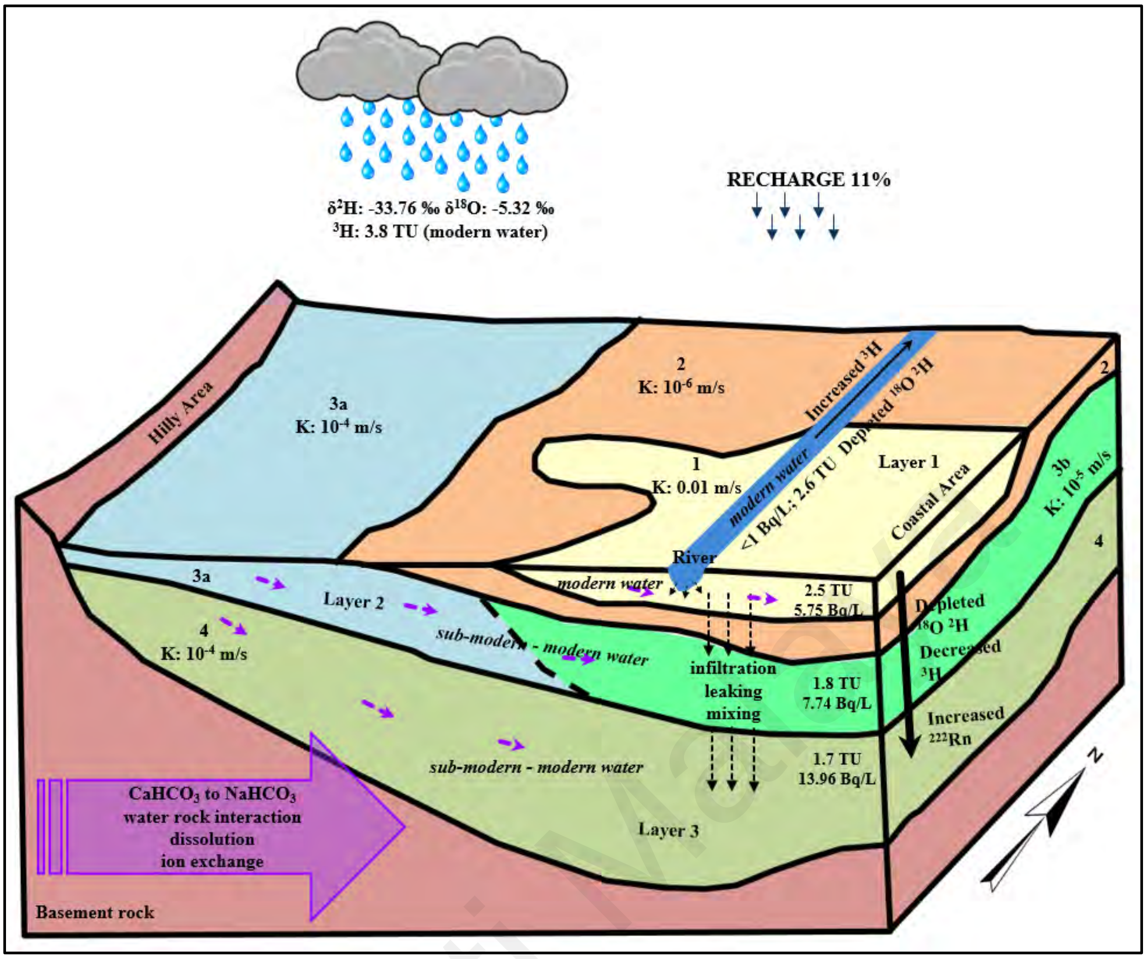

Figure 7.1: Conceptual model of groundwater recharge mechanism at LKRB

7.2 Recommendations

In future, the research topic can be enchanced by these recommendations as listed below:

1. Installation of lysimeter as a direct method to estimate recharge rate in selected and representated location in the basin.
2. Instllation of more wells at selected and represented depth as well as selected location to represent the basin includes with automatic data loggers.
3. Continous sampling and monitoring of present site and new site to provide long-term data for more comprehensive recharge flow and estimation recharge rate for all methods.
4. Improve recharge mechanism methods using different approaches by using experimental design, mass balance calculation, mixing model of isotopes, time series analysis, consider chloride from dry deposition, agricultural and

antrophogenic sources and apply in-deep statistical, geostatistical and testing analysis to accurately identify and quantify surface water groundwater interaction, groundwater recharge/discharge flow area.

5. Combine current research methods with other methods such as helium (^{3}He), carbon (^{13}C and ^{14}C), chlorofluorocarbon (CFC), sulphur hexafluoride (SF_6), krypton (^{85}Kr), chlorine-36 (^{36}Cl) and other isotopes to enhance the knowledge that infers the water flow processes (direction and velocity), resolved the extent of mixing occurred in groundwater and to be able to verify better quantification of recharge rates.

REFERENCES

Abdul Malik, M. F. I., Rabaiee, N. A., & Jaafar, M. S. (2015). *Determination of radon concentration in water using Rad7 and Rad H2O accessories* Paper presented at the National Physics Conference 2014 (PERFIK 2014).

Abdullah, K., & Mohamed, A. (1998). *Water – A situation appraisal and possible actions at the community level*. Paper presented at the Seminar on local communities and the environment II, Environmental Protection Society of Malaysia, Petaling Jaya, Malaysia.

Abreha, A. G. (2014). *Hydrochemical and water quality investigation on irrigation and drinking water supplies in the Mekelle region, Northern Ethiopia.* (Master thesis), University of Twente, Netherlands. Retrieved from https://webapps.itc.utwente.nl/librarywww/papers_2014/msc/wrem/abreha.pdf

Acheampong, S. Y., & Hess, J. W. (2000). Origin of the shallow groundwater system in the Southern Voltain Sedimentary Basin of Ghana: An isotopic approach. *Journal of Hydrology, 233*, 37-53.

Adams, S., Titus, R., & Xu, Y. (2004). *Groundwater recharge assessment of the basement aquifers of Central Namaqualand.* (Report No. 1093/1/04). Retrieved from GEZINA: Water Research Commission:

Adomako, D., Osae, S., Akiti, T. T., Faye, S., & Maloszewski, P. (2011). Geochemical and isotopic studies of groundwater conditions in the Densu River Basin of Ghana. *Environmental Earth Sciences, 62*, 1071-1084.

Afrifa, G. Y., Sakyi, P. A., & Chegbeleh, L. P. (2017). Estimation of groundwater recharge in sedimentary rock aquifer systems in the Oti basin of Gushiegu District, Northern Ghana. *Journal of African Earth Sciences, 131*, 272-283.

Aggarwal, P. K., Basu, A. R., Kulkarni, K. M., Froehlich, K., Tarafdar, S. A., Ali, M., & Hussain, A. (2000). *A report on isotope hydrology of groundwater in Bangladesh: Implications for characterization and mitigationofarsenicingroundwater*. Retrieved from http://ripcnt01.iaea.org/ih/publications/BGD_Report.pdf

Ahmed, A. M., Abdel Samie, S. G., & El-Maghrabi, H. M. (2011). Recharge and contamination sources of shallow and deep groundwater of pleistocene aquifer in El-Sadat industrial city: isotope and hydrochemical approaches. *Environmental Earth Sciences, 62*, 751–768.

Ahmed, K. M., & Burgess, W. G. (1995). Bils and the Barind aquifer, Bangladesh. In B. AG (Ed.), *Geomorphology and ground- water* (pp. 143–155). New York: John Wiley and Sons.

Aishlin, P., & McNamara, J. P. (2011). Bedrock infiltration and mountain block recharge accounting using chloride mass balance. *Hydrological Processes, 25*(12), 1934-1948.

Ako, A. A., Shimada, J., Hosono, T., Kagabu, M., Richard, A., Nkeng, G. E., . . . Mouncherou, O. F. (2013). Flow dynamics and age of groundwater within a humid equatorial active volcano (Mount Cameroon) deduced by dD, d18O, 3H and chlorofluorocarbons (CFCs). *Journal of Hydrology, 502*, 156–176.

Al-Charideh, A., & Hasan, A. (2013). Use of isotopic tracers to characterize the interaction of water components and nitrate contamination in the arid Rasafeh area (Syria). *Environmental Earth Sciences, 70*(1), 71–82.

Al-Gamal, S. A. (2011). An assessment of recharge possibility to North-Western Sahara Aquifer System (NWSAS) using environmental isotopes. *Journal of Hydrology, 398*, 184–190.

Alain, F. T., Gloria, T. E., Dorice, K., Robert, K., Wilson, F. Y., Josephine, N., & Alex, T. (2020). Hydrogeochemistry and groundwater flow mechanisms in shallow aquifer in Yaounde, Cameroon. *Water Supply*. Doi:10.2166/ws.2020.050.

Alberto, W. D., del Pilar, D. M., Valeria, A., Fabiana, P. S., Cecilia, H. A., & de los Angles, B. M. (2001). Pattern recognition techniques for the evaluation of spatial and temporal variations in water quality, a case study: Suquia river basin (Cordoba–Argentina). *Water Resources, 35*, 2881-2894.

Alcala, F. J., & Custodio, E. (2008). Atmospheric chloride deposition in continental Spain. *Hydrological Processes, 22*, 3636-3650.

Alcala, F. J., & Custodio, E. (2014). Spatial average aquifer recharge through atmospheric chloride mass balance and its uncertainty in continental Spain. *Hydrological Processes, 28*(2), 218-236.

Alcala, F. J., & Custodio, E. (2015). Natural uncertainty of spatial average aquifer recharge through atmospheric chloride mass balance in continental Spain. *Journal of Hydrology, 524*, 642-661.

Alcalá, F. J., & Custodio, E. (2008). Using the Cl/Br ratio as a tracer to identify the origin of salinity in aquifers in Spain and Portugal. *Journal of Hydrology, 359*, 189-207.

Ali, M. H., & Mubarak, S. (2017). Approaches and methods of quantifying natural groundwater recharge – A review. *Asian Journal of Environment & Ecology, 5*(1), 1-27.

Allison, G. B., Gee, G. W., & Tyler, S. W. (1994). Vadose-zone techniques for estimating groundwater recharge in arid and semiarid regions. *Soil Science Society of America Journal, 56*, 6-14.

Allison, G. B., & Hughes, A. K. (1978). The use of environmental chloride and tritium to estimate total recharge to an unconfined aquifer. *Australian Journal of Soil Research, 16*, 181-195.

Ammar, S. B., Taupin, J. D., Zouari, K., & Khouatmia, M. (2016). Identifying recharge and salinization sources of groundwater in the Oussja Ghar el Melah plain (northeast Tunisia) using geochemical tools and environmental isotopes. *Environmental Earth Sciences, 75*, Article#606.

Anderson, M. P. (2005). Heat as a ground water tracer. *Groundwater, 43*(6), 951-968.

Anderson, M. P., & Woessner, W. W. (1992). *Applied groundwater modelling: Simulation of flow and advective transport*. San Diego: Academic Press.

Andrade, E. M., Arau´jo, H., Pala´cio, Q., Souzab, I. H., Len˜o, R. A., & Guerreiro, M. J. (2008). Land use effects in groundwater composition of an alluvial aquifer (Trussu River, Brazil) by multivariate techniques. *Environmental Research, 106*, 170-177.

Andreo, B., Liffñán, C., Carrasco, F., Jimenez de Cisneros, C., Caballero, F., & Mudry, J. (2004). Influence of rainfall quantity on the isotopic composition (18O and 2H) of water in mountainous areas. Apllication for groundwater research in the Yunquera-Nieves Karst Aquifers (S Spain). *Applied Geochemistry, 19*, 561-574.

Appelo, C. A. J., & Postma, D. (2005). *Geochemistry, groundwater and pollution. 2nd edition*. Amsterdam: AA Balkema Publishers.

Araguás-Araguás, L., Froehlich, K., & Rozanski, K. (1998). Stable isotope composition of precipitation over southeast Asia. *Journal of Geophysical Research, 103*(D22), 28721-28742.

Araguás-Araguás, L., Froehlich, K., & Rozanski, K. (2000). Deuterium and oxygen-18 isotope composition of precipitation and atmospheric moisture. *Hydrological Processes, 14*, 1341-1355.

ASTM. (2006). Standard guide for application of a groundwater flow model to a site-specific problem. In S. A. Arendt, S. J. Bailey, & N. C. Baldini (Eds.), *ASTM Standards related to environment site characterization (3rd ed.)*. United States: Baltimore, MD.

Atiaa, A. M., Al-Shamma'a, A. Y., & Aljabbari, M. H. (2014). Estimation of Groundwater Recharge for the Main Aquifer in the Northeastern Missan Governorate, South of Iraq Using Chloride Mass Balance Technique. *Iraqi Journal of Science, 55*(2A), 463-470.

Awadalla, S., Noor, I. B. M., & Ibrahim, I. (1989). *Comparative Model Study for Groundwater Resources Evaluation in Kelantan Malaysia; Part 1: Model Evaluation.* Paper presented at the International Workshop on Appropriate

Methodologies for Development and Management of Groundwater Resources in Developing Countries Hyderabad, India.

Ayadi, R., Zouari, K., Saibi, H., Trabelshi, R., Khanfir, H., & Itoi, R. (2016). Determination of the origins and recharge rates of the Sfax aquifer system (southeastern Tunisia) using isotope tracers. *Environmental Earth Sciences, 75*, Article#636.

Babel, M. S., Gupta, A. D., & Domingo, N. D. S. (2006). Land Subsidence: A Consequence of Groundwater Over-Exploitation in Bangkok, Thailand. *International Review for Environmental Strategies, 6*(2), 307-328.

Bachik, A. R. (1989). *Hydrogeological investigation in the Kg. Chap-Jelawat area Bachok, Kelantan Darul Naim*. (GPH No. 3/1989). Kuala Lumpur: Department of Mineral and Geoscences.

Bajjali, W. (2006). Recharge mechanism and hydrochemistry evaluation of groundwater in the Nuaimeh area, Jordan, using environmental isotope techniques. *Hydrogeology Journal, 14*, 180-191.

Banoeng-Yakubo, B., Yidana, S. M., Ajayi, J. O., Loh, Y., & Asiedu, D. K. (2010). Hydrogeology and groundwater resources of Ghana: a review of the hydrogeological zonation of Ghana. In J. M. McMann (Ed.), *Potable water and sanitation* (pp. 115–150). New York: Nova Science Publishers.

Barron, O. V., Crosbie, R. S., Dawes, W. R., Charles, S. P., Pickett, T., & Donn, M. J. (2012). Climatic controls on diffuse groundwater recharge across Australia. *Hydrology and Earth System Sciences, 16*(12), 4557-4570.

Barzegara, R., Moghaddamc, A. A., Tziritisd, E., Adamowskia, J., Nassara, J. B., Nooric, M., . . . Kazemiane, N. (2020). Exploring the hydrogeochemical evolution of cold and thermal waters in the Sarein-Nir area, Iran using stable isotopes (δ18O and δD), geothermometry and multivariate statistical approaches. *Geothermics, 85*, Article#101815.

Baskaran, S., Ransley, T., Brodie, R. S., & Baker, P. (2009). Investigating groundwater–river interactions using environmental tracers. *Australian Journal of Earth Sciences, 56*, 13-19.

Bauer, S., Fulda, C., & Schafer, W. (2001). A multi-tracer study in a shallow aquifer using age dating tracers 3H, 85Kr, CFC-113 and SF6 - indication for retarded transport of CFC-113. *Journal of Hydrology, 248*, 14-34.

Bazuhair, A. S., & Wood, W. W. (1996). Chloride mass-balance method for estimating ground water recharge in arid areas: examples from western Saudi Arabia. *Journal of Hydrology, 186*, 153-159.

Belkhiri, L., Boudoukha, A., Mouni, L., & Baouz, T. (2010). Application of multivariate statistical methods and inverse geochemical modeling for characterization of groundwater–a case study: Ain Azel Plain (Algeria). *Geoderma, 159*, 390-398.

Bense, V. F., & Kooi, H. (2004). Temporal and spatial variations of shallow subsurface temperature as a record of lateral variations in groundwater flow. *Journal of Geophysical Research, 9*, Article#B04103.

Bertin, C., & Bourg, A. C. M. (1994). Radon-222 and chloride as natural tracers of the infiltration of river water into an alluvial aquifer in which there is significant river/groundwater mixing. *Environmental Science & Technology, 28*, 794-798.

Beyer, M., Morgenstern, U., & Jackson, B. (2014). Review of techniques for dating young groundwater (<100 Years) in New Zealand. *Journal of Hydrology, 53*(2), 93-111.

Blasch, K. W., & Bryson, J. R. (2007). Distinguishing sources of groundwater recharge by using d2H and d18O. *Ground Water, 45*, 294–308.

Bosch, J. H. A. (1986). Quaternary. In C. S. T. Hutchison, D.N.K. (Ed.), *Geology of Peninsular Malaysia*. Kuala Lumpur: University of Malaya and Geological Society of Malaysia.

Bredehoeft, J. D., Papadopoulos, S. S., & Cooper, H. H. (1982). Groundwater: The water-budget myth *Scientific Basis of Water-Resource Management* (pp. 51-57). Washington, D.C.: National Academy Press.

Bredehoeft, J. D., & Papadopulos, I. S. (1965). Rates of vertical groundwater movement estimated from Earth's thermal profile. *Water Resource Research, 1*(2), 325-328.

Bredenkamp, D. B., Botha, L. T., van Tonder, G. J., & van Rensburg, H. J. (1995). *Quantitative Estimation of Groundwater Recharge and Aquifer Storativity based on practical hydro-logical methods* (Report TT 73/95). Retrieved from Pretoria, South Africa:

Bresciani, E., Ordens, C. M., Werner, A. D., Batelaan, O., Guan, H., & Post, V. E. A. (2014). Spatial variability of chloride deposition in a vegetated coastal area: Implications for groundwater recharge estimation. *Journal of Hydrology, 519*, 1177-1191.

Briganti, A., Paola, T., Voltaggio, M., Galli, C. C., & Lucchetti, C. (2020). Assessing methyl tertiary butyl ether residual contamination in groundwater using radon *Applied Geochemistry, 116*, Article#104583.

Bromley, J., Edmunds, W. M., Fellman, E., Brouwer, J., Gaze, S. R., Sudlow, J., & Taupin, J. D. (1997). Estimation of rainfall inputs and direct recharge to the deep unsaturated zone of southern Niger using the chloride profile method *Joumal of Hydrology, 188-189*, 139-154.

BS1377. (1990). Methods of test for soils for civil engineering purposes. Part 2: Classification tests. (pp. 68p): BSI Group UK.

Burnett, W. C., Peterson, R., Moore, W. S., & de Oliveira, J. (2008). Radon and radium isotopes as tracers of submarine groundwater discharge Results from the Ubatuba, Brazil SGD assessment intercomparison. *Estuarine, Coastal and Shelf Science, 76*, 501-511.

Cai, Z., & Ofterdinger, U. (2016). Analysis of groundwater-level response to rainfall and estimation of annual recharge in fractured hard rock aquifers, NW Ireland. *Journal of Hydrology, 535*, 71-84.

Calvache, M. L., Duque, C., Gomez Fontalva, J. M., & Crespo, F. (2011). Processes affecting groundwater temperature patterns in a coastal aquifer. *International Journal Environmental Science & Technology, 8*(2), 223-236.

Cappa, C. D., Hendricks, M. B., DePaolo, D. J., & Cohen, R. C. (2003). Isotopic fractionation of water during evaporation. *Journal Geophy Research Atmospheres, 108(D16)*, 1–10.

Carrier, M. A., Lefebvre, R., & Asare, E. B. (2008). *Groundwater recharge assessment in northern Ghana using soil moisture balance and chloride mass balance.* Paper presented at the 61st Canadian Geotechnical Conference and 9th Joint CGS/IAH-CNC Groundwater Conference, Edmonton, Canada.

Carslaw, H. S., & Jaeger, J. C. (1959). *Conduction of heat in Solids, 2nd ed*. Oxford: Oxford University Press.

Cartwright, I., Cendon, D., Currell, M., & Meredith, K. (2017). A review of radioactive isotopes and other residence time tracers in understanding groundwater recharge: possibilities, challenges, and limitations. *Journal of Hydrology, 55*, 797-811.

Cartwright, I., & Gilfedder, B. (2015). Mapping and quantifying groundwater inflows to Deep Creek (Maribyrnong catchment, SE Australia) using 222Rn, implications for protecting groundwater-dependant ecosystems. *Applied Geochemistry, 52*, 118-129.

Cartwright, I., Hofmann, H., Gilfedder, B., & Smyth, B. (2014). Understanding parafluvial exchange and degassing to better quantify groundwater inflows using 222Rn: The King River, southeast Australia. *Chemical Geology, 380*, 48–60.

Cartwright, I., & Morgenstern, U. (2012). Constraining groundwater recharge and the rate of geochemical processes using tritium and major ion geochemistry: Ovens catchment, southeast Australia. *Journal of Hydrology, 475*, 137–149.

Cartwright, K. (1970). Groundwater discharge in the Illinois Basin as suggested by temperature anomalies. *Water Resources Research, 6*(3), 912-918.

Caschetto, M., Colombani, N., Mastrocicco, M., Petitta, M., & Aravena, R. (2016). Estimating groundwater residence time and recharge patterns in a saline coastal aquifer. *Hydrological Processes, 30*(22), Article#10942.

Cecil, L. D., & Gesell, T. (1992). Sampling and analysis for radon-222 dissolved in groundwater and surface water. *Environmental Monitoring and Assessment, 20*, 55-66.

Cendon, D. I., Larsen, J. R., Jones, B. G., Nanson, G. C., Rickleman, D., Hankin, S. I., . . . Maroulis, J. (2010). Freshwater recharge into a shallow saline groundwater system, Cooper Creek floodplain, Queensland, Australia. *Journal of Hydrology, 392*(3-4), 150-163.

Ceron, J. C., Jimenez-Espinosa, R., & Pulido-Bosch, A. (2000). Numerical analysis of hydrochemical data: a case study (Alto Guadalentı´n, southeast Spain). *Applied Geochemistry, 157*(7), 1053-1067.

Chae, G. T., Yun, S. T., Kim, D. S., Kim, K. H., & Joo, Y. S. (2016). Time-series analysis of three years of groundwater level data (Seoul, South Korea) to characterize urban groundwater recharge *Quarterly Journal of Engineering Geology and Hydrogeology, 43*, 117-127.

Che Sulaiman, M. Y. (2010). *Pemantauan pemendapan tanah di kawasan Lembangan Sungai Kelantan*. (JMG.KLT.SAT 1/2010). Kota Bharu, Kelantan: Jabatan Mineral dan Geosains Malaysia.

Chen, J. E., Huang, C. C., Wang, Y. S., Tsai, J. P., Chang, L. C., Chen, Y. W., . . . Wang, Y. C. (2013). *Applying model simulation to identify the importance of protecting groundwater recharge area - A case study of Choshuihsi Alluvial Fan, Taiwan*. Paper presented at the European Geosciences Union General Assembly 2013, Vienna, Austria.

Chen, Y. T., Tung, T. H., Wang, L. C., & Lu, C. J. (2014). Field study of using naturally occurring radon to assess the dense nonaqueous phase liquid distribution in saturated zone *Journal of Environmental Radioactivity, 128*, 75-83.

Chen, Z., Nie, Z., Zhang, G., Wan, L., & Shen, J. (2006). Environmental isotopic study on the recharge and residence time of groundwater in the Heihe River Basin, northwestern China. *Hydrogeology Journal, 14*, 1635–1651.

Choubey, V. M., Bartarya, S. K., & Ramola, R. C. (2003). Radon in groundwater of eastern Doon valley, Outer Himalaya. *Radiation Measurements, 36*, 401-405.

Chung, I.-M., Sophocleous, M. A., Mitiku, D. B., & Kim, N. W. (2016). Estimating groundwater recharge in the humid and semi-arid African regions: review. *Geosciences Journal, 20*(5), 731-744.

Clark, I., & Fritz, P. (1997a). *Environmental isotopes in hydrogeology* Boca Raton: Lewis Publishers.

Clark, I., & Fritz, P. (1997b). Tracing the hydrological cycle. . In I. Clark & P. Fritz (Eds.), *Environmental isotopes in hydrogeology.* (pp. pp 35–61). Boca Raton: CRC Press.

Cloutier, V., Lefebvre, R., Therrien, R., & Savard, M. M. (2008). Multivariate statistical analysis of geochemical data as indicative of the hydrogeochemical evolution of groundwater in a sedimentary rock aquifer system. *Journal of Hydrology, 353*(3-4), 294-313.

Colombani, N., Giambastiani, B. M. S., & Mastrocicco, M. (2016). Use of shallow groundwater temperature proflies to infer climate and land use change: interpretation and measurement challenges. *Hydrological Processes, 30*(14), Article#10805.

Constantz, J. (1998). Interaction between streambed temperature, streamflow, and groundwater exchanges in alpine streams. *Water Resources Research, 34*, 1609-1615.

Constantz, J. (2008). Heat as a tracer to determine streambed water exchanges. *Water Resources Research, 44*, Article#W00D10.

Constantz, J., Cox, M. H., & Su, G. W. (2003). Comparison of heat and bromide for examing stream exchanges with shallow groundwater. *Groundwater, 41*, 647-656.

Cook, P. G., & Herczeg, A. L. (2000). *Environmental tracers in subsurface hydrology.* . Boston, USA: Kluwer Academic Publishers.

Cook, P. G., Lamontagne, S., Berhane, D., & Clark, J. F. (2006). Quantifying groundwater discharge to Cockburn River, southeastern Australia, using dissolved gas tracers 222Rn and SF6. *Water Resources Research, 42*, Article#W10411.

Craig, H. (1961). Isotopic variations in meteoric water. *Science, 133*, 1702-1703.

Craig, H., & Gordon, L. I. (1965). Deuterium and oxygen 18 variations in the ocean and marine atmosphere. In E. Tongiogi (Ed.), *Stable Isotopes in Oceanographic Studies and Paleotemperatures* (pp. 9-130). Spoleto, Italy: Laboratiorio di geologica nucleare.

Crosbie, R. S., Binning, P., & Kalma, J. D. (2005). A time series approach to inferring groundwater recharge using the water table fluctuation method. *Water Resources Research, 41*(1), 1-21.

Crosbie, R. S., Davies, P., Harrington, N., & Lamontagne, S. (2015). Ground truthing groundwater-recharge estimates derived from remotely sensed evapotranspiration: a case in South Australia. *Hydrogeology Journal, 23*(2), 335-350.

Crosbie, R. S., Doble, R. C., Turnadge, C., & Taylor, A. R. (2020). Constraining the magnitude and uncertainty of specific yield for use in the water table fluctuation method of estimating recharge. *American Geophysical Union.* Doi:10.1029/2019WR025285.

Crosbie, R. S., Jolly, I. D., Leaney, F. W., & Petheram, C. (2010). Can the dataset of field based recharge estimates in Australia be used to predict recharge in data-poor areas? *Hydrology and Earth System Sciences, 14*(10), 2023-2038.

Cuthbert, M. O. (2010). An improved time series approach for estimating groundwater recharge from groundwater level fluctuations. *Water Resources Research, 46*, Article#W09515.

Dansgaard, W. (1964). Stable isotopes in precipitation. *Tellus, 16*(4), 436-468.

Dapaah-Siakwan, S., & Kayane, I. (1995). Estimation of vertical water and heat fluxes in the semi-confined aquifers in Tokyo metropolitan area, Japan. *Hydrological Proccesses, 9*, 143-160.

Das, B. K., Kakar, Y. P., Moser, H., & Stichler, W. (1988). Deuterium and oxygen-18 studies in groundwater of the Dehli area. *Journal of Hydrology, 98*, 133–146.

Dassi, L. (2010). Use of chloride mass balance and tritium data for estimation of groundwater recharge and renewal rate in an unconfined aquifer from North Africa: a case study from Tunisia. *Environmental Earth Sciences, 60*(4), 861-871.

Dassi, L. (2011). Investigation by multivariate analysis of groundwater composition in a multilayer aquifer system from North Africa: A multi-tracer approach. *Applied Geochemistry, 26*(8), 1386-1398.

Davis, B. M., Semprini, L., & Istok, J. D. (2003). *Final Report: Development of radon-222 as a natural tracer for monitoring the remediation of NAPL in the subsurface* (Project No. 60158). Retrieved from Corvallis, OR: https://www.osti.gov/servlets/purl/809809

de Vries, J. J., & Simmers, I. (2002). Groundwater recharge: an overview of processes and challenges. *Hydrogeology Journal, 10*(1), 5-17.

Delin, G. N., Healy, R. W., Lorenz, D. L., & Nimmo, J. R. (2007). Comparison of local- to regional-scale estimates of ground-water recharge in Minnesota, USA. *Journal of Hydrology, 334*(1-2), 231-249.

Delin, G. N., & Risser, D. W. (2007). *Ground-Water Recharge in Humid Areas of the United States—A Summary of Ground-Water Resources Program Studies, 2003-06*. Reston, VA: U.S. Geological Survey.

Delinom, R. M. (2008). *Groundwater management issues in the Greater Jakarta area, Indonesia.* Paper presented at the Proceedings of International Workshop on Integrated Watershed Management for Sustainable Water Use in a Humid

Tropical Region, JSPS-DGHE Joint Research Project, Tsukuba, October 2007. Bull. TERC, University of Tsukaba, No.8 Supplement, no. 2, 2008.

Deng, Z. J., Priestley, S. C., Guan, H. D., Love, A. J., & Simmons, C. T. (2013). Canopy enhanced chloride deposition in coastal South Australia and its application for the chloride mass balance method. *Journal of Hydrology, 497*, 62-70.

DID. (2000). *National water resources study 2000–2050 (Malaysian Peninsula). Groundwater Studies*. (vol. 04). Kuala Lumpur, Malaysia: Author.

Dillon, P., Stuyfzand, P., Grischek, T., Lluria, M., Pyne, R. D. G., Jain, R. C., . . . Sapiano, R. M. (2019). Sixty years of global progress in managed aquifer recharge. *Hydrogeology Journal, 27*, 1-30.

Diouf, O. C., Faye, S. C., Diedhiou, M., Kaba, M., Faye, F., Gaye, C. B., . . . Wohnlich, S. (2012). Combined uses of water-table fluctuation (WTF), chloride mass balance (CMB) and environmental isotopes methods to investigate groundwater recharge in the Thiaroye sandy aquifer (Dakar, Senegal). *African Journal of Environmental Science and Technology, 6*(11), 425-437.

Doble, R. C., & Crosbie, R. S. (2017). Review: Current and emerging methods for catchment-scale modelling of recharge and evapotranspiration from shallow groundwater. *Hydrogeology Journal, 25*(1), 3-23.

Domenico, A. P., & Palciauskus, V. V. (1973). Theoretical analysis of forced convective heat transfer in regional groundwater flow. *Geological Society of America Bulletin, 84*, 3803-3814.

Domenico, P. A., & Schwartz, F. W. (1990). *Physical and chemical hydrogeology, 2nd edition*. New York: Wiley.

Dong, L., Fu, C., Liu, J., & Wang, Y. (2018). Disturbances of temperature-depth profiles by surface warming and groundwater flow convection in Kumamoto Plain, Japan. *Geofluids, 2018*, Article#8451276.

Drever, J. I. (1988). *Geochemistry of natural waters, 2nd edn*. Englewood Cliffs, New Jersey: Prentice Hall.

Dripps, W. R., & Bradbury, K. R. (2007). A simple daily soil–water balance model for estimating the spatial and temporal distribution of groundwater recharge in temperate humid areas. *Hydrogeology Journal, 15*(3), 433-444.

Du, S., Deng, Z., Liu, Y., Zhang, L., Xu, H., & Yang, H. (2019). Evaluation of surface water–groundwater interaction using environmental isotopes (D, 18O and 222Rn) in Chongli Area, China. *Journal of Radioanalytical and Nuclear Chemistry, 321*, 303–311.

Dugan, H. A., Gleeson, T., Lamoureux, S. F., & Novakowski, K. (2012). Tracing groundwater discharge in a High Arctic lake using radon-222. *Environmental Earth Sciences, 66*(5), 1385–1392.

Durov, S. A. (1948). Classification of natural waters and graphical representation of their composition. *Doklady Akademii Nauk SSSR, 59*(1), 87-90.

Edmunds, W. M., Darling, W. G., & Kinniburgh, D. G. (1988). Solute Profile Techniques for Recharge Estimation in Semi-Arid and Arid Terrain. In I. Simmers (Ed.), *Estimation of Natural Groundwater Recharge*. Dordrecht: Springer.

Edmunds, W. M., Darling, W. G., Kinniburgh, D. G., Kotouband, S., & Mahgoub, S. (1992). Sources of recharge at Abu Delaig, Sudan. *Journal of Hydrology, 131*, 1-24.

Edmunds, W. M., Fellman, E., Goni, I. B., & Prudhomme, C. (2002). Spatial and temporal distribution of groundwater recharge in northern Nigeria. *Hydrogeology Journal, 10*(1), 205-215.

Eissa, M. A., Shawky, H., Samy, A., Khalil, M. M. H., & Malky, M. E. (2018). Geochemical and Isotopic Evidence of Groundwater Salinization Processes in El Dabaa Area, Northwestern Coast, Egypt. *Geosciences, 8*(392), 1-17.

Eissa, M. A., Thomas, J. M., Pohll, G., Shouakar-Stash, O., Hershey, R. L., & Dawoud, M. (2016). Groundwater recharge and salinization in the arid coastal plain aquifer of the Wadi Watir delta, Sinai, Egypt. *Applied Geochemistry, 71*, 48-62.

El Mekki, O. A., Laftouhi, N. E., & Hanich, L. (2017). Estimate of regional groundwater recharge rate in the Central Haouz Plain, Morocco, using the chloride mass balance method and a geographical information system. *Applied Water Science, 7*(4), 1679-1688.

El Yaouti, F., El Mandour, A., Khattach, D., Benavente, J., & Kaufmann, O. (2009). Salinization processes in the unconfined aquifer of Bou-Areg (NE Morocco): a geostatistical, geochemical, and tomographic study. *Applied Geochemistry, 24*(1), 16-31.

Ellins, K. K., A., R.-M., & R., L. (1990). Using 222Rn to examine Groundwater/surface discharge interaction in the Rio Grande de Manati, Puerto Rico. *Journal of Hydrology, 115*, 319-341.

Eriksson, E. (1959). The yearly circulation of chloride and sulphur in nature; meteorological, geochemical and pedological implications, part I. *Tellus, 11*(4), 375-403.

Eriksson, E. (1960). The yearly circulation of chloride and sulphur in nature; meteorological, geochemical and pedological implications, part II. *Tellus, 12*, 63-109.

Eriksson, E. (1976). *The distribution of salinity in groundwaters of the Delhi region and recharge rates of groundwater.* Paper presented at the Advisory group meeting on interpretation of environmental isotope and hydrochemical data in groundwater hydrology, Vienna, Austria.

Eriksson, E., & Khunakasem, V. (1969). Chloride concentration in groundwater, recharge rate and rate of deposition of chloride in Israel Coastal Plain. *Journal of Hydrology, 7*, 178-197.

Famiglietti, J. S. (2014). The global groundwater crisis. *Nature and Climate Change, 4,* 945-948.

Fan, J. L., Oestergaard, K. T., Guyot, A., & Lockington, D. A. (2014). Estimating groundwater recharge and evapotranspiration from water table fluctuations under three vegetation covers in a coastal sandy aquifer of subtropical Australia. *Journal of Hydrology, 519*, 1120-1129.

Farnham, I. M., Stetzenbach, K. J., Singh, A. K., & Johannesson, K. H. (2000). Deciphering groundwater flow systems in Oasis Valley, Nevada, using trace element chemistry, multivariate statistics, and geographical information system. *Mathematical Geology, 32*, 943-968.

Ferguson, G., & Woodbury, A. D. (2004). Subsurface heat flow in an urban environment. *Journal of Geophysical Research, 109*, Article#B02402.

Ferguson, G., & Woodbury, A. D. (2005). The Effects of Climatic Variability on Estimates of Recharge from Temperature Profiles. *Groundwater, 43*(6), 837-842.

Ferguson, G., Woodbury, A. D., & Matile, G. L. D. (2003). Estimating deep recharge rates beneath an interlobate moraine using temperature logs. *Groundwater, 41*, 640-646.

Ferronsky, V. I., & Polyyakov, V. A. (2012). *Isotopes of the Earth's Hydrosphere*. B.V: Springer Netherlands.

Feth, J. H. (1981). *Chloride in Natural Continental Water – A Review*. Retrieved from Washington, D.C.:

Fisher, R. S., & Mullican, W. F. (1997). Hydrochemical evolution of sodiumsulfate and sodium-chloride groundwater beneath the northern Chihuahuan Desert, Trans-Pecos, Texas, USA. *Hydrogeology Journal, 5*, 4-16.

Flusch, M. A., Seltzer, G., Rodbell, D., Siegel, D., & Samson, S. (2005). Constraining water sources and hydrologic processes from the isotopic analysis of water and dissolved strontium, Lake Junin, Peru. *Journal of Hydrology, 312*, 1–13.

Freeze, R. A., & Cherry, J. A. (1979). *Groundwater*. Englewood Cliffs, New Jersey: Prentice-Hall Inc.

Fu, X., Tang, Z., Lv, W., Wang, X., & Yan, B. (2018). Exploitation potential of groundwater in Yangzhuang Basin, China under recharge enhancement. *International Journal of Heat and Technology, 36*(2), 483-493.

Fynn, O. F., Yidana, S. M., Chegbeleh, L. P., & Yiran, G. B. (2016). Evaluating groundwater recharge processes using stable isotope signatures—the Nabogo catchment of the White Volta, Ghana. *Arabian Journal of Geosciences, 9*, 279.

Gat, J. R. (1971). Comments on the Stable Isotope Method in Regional Groundwater Investigations. *Water Resources Research, 7*(4), 980 - 993.

Gat, J. R., Bowser, C. J., & Kendall, C. (1994). The contribution of evaporation from the Great Lakes to the continental atmosphere: estimate based on stable isotope data. . *Geophysical Research Letters, 21*(7), 557–560.

Gat, J. R., & Carmi, I. (1970). Evolution of the isotopic composition of atmospheric waters in the Mediterranean Sea area. *Journal Geophysical Research, 75*, 3039-3048.

Gat, J. R., & Dansgaard, W. (1972). Stable isotope survey of the fresh water occurrences in Israel and the Northern Jordan Rift Valley. *Journal of Hydrology, 16*, 177-212.

Gat, J. R., Mook, W. G., & Meijer, A. J. (2001) Atmospheric water. *Environmental isotopes in the hydrological cycle: principles and applications* (pp. 39). Paris: UNESCO.

Gat, J. R., & Tzur, Y. (1967). *Modification of the isotopic composition of rainwater by processes which occur before groundwater recharge.* Paper presented at the Isotopes in Hydrology-Proceedings of a Symposium, Vienna.

Gaye, C. B., & Edmunds, W. M. (1996). Groundwater recharge estimation using chloride, stable isotopes and tritium profiles in the sands of northwestern Senegal. *Environmental Geology, 27*, 246-251.

Gebremeskel, G. (2015). *Estimation of groundwater recharge and potentials under changing climate in Werii watershed, Tekeze River Basin.* (Master's thesis), Haramaya University, Haramaya, Ethiopia. Retrieved from https://hdl.handle.net/10568/76191

Gerhart, J. M. (1986). Groundwater recharge and its effects on nitrate concentration beneath a manured field site in Pennsylvania. *Groundwater, 24*(2), 483-489.

Geyh, M. (2000) Groundwater saturated and unsaturated zone. *Vol. Volume IV. Environmental isotopes in the hydrological cycle: principles and applications. International Hydrological Programme* (pp. 196). UNESCO, Paris: UNESCO/IAEA.

Ghanbari, R. N., & Bravo, H. R. (2011). Evaluation of correlations between precipitation, groundwater fluctuations, and lake level fluctuations using spectral methods (Wisconsin, USA). *Hydrogeology Journal, 19*, 801-810.

Ghesquiere, O., Walter, J., Chesnaux, R., & Rouleau, A. (2015). Scenarios of groundwater chemical evolution in a region of the Canadian Shield based on multivariate statistical analysis. *Journal of Hydrology: Regional Studies, 4*, 246-266.

Ghouili, N., Horriche, F. J., Zammouri, M., Benabdallah, S., & Farhat, B. (2017). Coupling WetSpass and MODFLOW for groundwater recharge assessment: case study of the Takelsa multilayer aquifer, Northeastern Tunisia. *Geosciences Journal, 21*(5), 791–805.

Giap, V. T. (2003). Use of Radon-222 as a Tracer to estimate Groundwater Infiltration Velocity in a River Bank Area. *Nuclear Science and Technology, 2*(2), 12-17.

Gibbs, R. J. (1970). Mechanisms controlling world water chemistry. *Science, 170*, 1088-1090.

Gibson, J. J., Edwards, T. W. D., & Bursey, G. G. (1993). Estimating evaporation using stable isotopes: quantitative results and sensitivity analysis for two catchments in northern Canada. *Nordic Hydrology, 24*, 79–94.

Gibson, J. J., Prepas, E. E., & McEachern, P. (2002). Quantitative comparison of lake throughflow, residency and catchment runoff using stable isotopes: modelling and results from a regional survey of Boreal lakes. *Journal of Hydrology, 262*, 128-144.

Gil-Márquez, J. M., Sültenfuß, J., Andreo, B., Mudarra, M.,. (2019). Groundwater dating tools (3H, 3He, 4He, CFC-12, SF6) coupled with hydrochemistry to evaluate the hydrogeological functioning of complex evaporitekarst settings. *Journal of Hydrology*, 1-72.

Gilfedder, B. S., Cartwright, I., Hofmann, H., & Frei, S. (2019). Explicit modelling of radon-222 in HydroGeoSphere during steady state and dynamic transient storage. *Groundwater, 57*(1), 36-47.

Girard, P., Hillaire-Marcel, C., & Oga, M. S. (1997). Determining the recharge mode of Sahelian aquifers using water isotopes. *Journal of Hydrology, 197*, 189–202.

Glose, T. J., Lowry, C. S., & Hausner, M. B. (2019). Limits on Groundwater-Surface Water Fluxes Derived from Temperature Time Series: Defining Resolution-Based Thresholds. *Water Resources Research, 55*, 1-12.

Gobinddass, M. L., Molinie, J., Richard, S., Panechou, K., Jeannot, A., & Jean-Louis, S. (2020). Coastal Sea Salt Chlorine Deposition Linked to Intertropical Convergence Zone (ITCZ) Oscillation in French Guiana. *Journal of the Atmospheric Sciences, 77*(5), 1723–1731.

Gonfiantini, R., Frölich, K., Araguás-Araguás, L., & Rozanski, K. (1998). Isotopes in groundwater hydrology. In C. Kendall & J. J. McDonnell (Eds.), *Isotope tracers in catchment hydrology* (pp. 203-246). Amsterdam, The Netehrlands: Elsevier Sci.

Gooddy, D. C., Darling, W. G., Abesser, C., & Lapworth, D. J. (2006). Using chlorofluorocarbons (CFCs) and sulphur hexafluoride (SF6) to characterise roundwater movement and residence time in a lowland Chalk catchment. *Journal of Hydrology, 330*, 44-52.

Gosnold, W. D., Todhunter, P. E., & Schmidt, W. (1997). the borehoe temperature record of climate warming in the mid-continent of North America. *Global and Planetary Change, 15*, 33-45.

Green, G., & Stewart, S. (2008). *Interactions between groundwater and surface water systems in the Eastern Mount Lofty Ranges* (Report DWLBC 2008/27). Retrieved from South Australia:

Grolander, S., & Kärnbränslehantering, A. B. S. (2009). *Radon as a groundwater tracer in Forsmark and Laxemar* (SKB report R-09-47). Retrieved from Stockholm:

Gu¨ler, C., Thyne, G., McCray, J. E., & Turner, A. K. (2002). Evaluation and graphical and multivariate statistical methods for classification of water chemistry data. *Hydrogeology Journal, 10*, 455-474.

Gu¨ler, C., & Thyne, G. D. (2004). Hydrologic and geologic factors controlling surface and groundwater chemistry in Indian Wells-Owens Valley area, southeastern California, USA. *Journal of Hydrology, 285*, 177-198.

Guan, H. D., Love, A. J., Simmons, C. T., Makhnin, O., & Kayaalp, A. S. (2010). Factors influencing chloride deposition in a coastal hilly area and application to chloride deposition mapping. *Hydrology and Earth System Sciences, 14*(5), 801-813.

Guida, M., Guida, D., Guadagnuolo, D., Cuomo, C., & Siervo, V. (2013). Using Radon-222 as a Naturally Occurring Tracer to investigate the streamflow-groundwater interactions in a typical Mediterranean fluvial-karst landscape: the interdisciplinary case study of the Bussento river (Campania region, Southern Italy). *WSEAS TRANSACTIONS on SYSTEMS, 12*(2), 85-104.

Gunawardhana, L. N., & Kazama, S. (2012). Statistical and numerical analyses of the influence of climate variability on aquifer water levels and groundwater temperatures: the impacts of climate change on aquifer thermal regimes. *Global and Planetary Change, 86-87*, 66-78.

Gupta, S., Mahato, A., Roy, P., Datta, J. K., & Saha, R. N. (2008). Geochemistry of groundwater, Burdwan District, West Bengal, India. *Environmental Geology, 53*, 1271-1282.

Gupta, S. K., & Deshpande, R. D. (2005). Groundwater isotopic investigations in India: What has been learned? *Current Science, 89*(5), 825-835.

Gusyev, M. A., Morgenstern, U., Stewart, M. K., Yamazaki, Y., Kashiwaya, K., Nishihara, T., . . . Iwami, Y. (2016). Application of tritium in precipitation and baseflow in Japan: a case study of groundwater transit times and storage in Hokkaido watersheds. *Hydrology and Earth System Scienes, 20*, 3043–3058.

Ha, K. C., Ngoc, N. T. M., Lee, E. H., & Jayakumar, R. (2016). *Current Status and Issues of Groundwater in the Mekong River Basin* (TH/SC/15-02). Retrieved from

Ha, Q. K., & Koontanakulvong, S. (2015). *Impact of climate change on groundwater recharge in Ho Chi Minh City area, Vietnam*. Paper presented at the THA 2015 International Conference on "Climate Change and Water & Environmental Management in Monsoon Asia" Bangkok, Thailand.

Hall, B., Currell, M., & Webb, J. (2020). Using multiple lines of evidence to map groundwater recharge in a rapidly urbanising catchment: implications for future land and water management. *Journal of Hydrology, 580*, Article#124265.

Hamzah, Z., Saat, A., & Kassim, M. (2011). Determination Of Radon Activity Concentration In Hot Spring And Surface Water Using Gamma Spectrometry Technique. *The Malaysian Journal of Analytical Sciences, 15*(2), 288-294.

Hancox, J., Garfias, J., Aravena, R., & Rudolph, D. (2010). Assessing the vulnerability of over-exploited volcanic aquifer systems using multiparameter analysis, Toluca Basin, Mexico. *Environmental Earth Sciences, 59*(8), 1643–1660.

Hansen, J., & Lebedeff, S. (1987). Global Trends of Measured Surface Air Temperature. *Journal of Geophysical Research, 92*(D11), 13345-13372.

Hansen, J., Ruedy, R., Sato, M., & Lo, K. (2010). Global surface temperature change. *Reviews of Geophysics, 48*, 1-29.

Hao, S., Li, F., Li, Y., Gu, C., Zhang, Q., Qiao, Y., . . . Zhua, N. (2019). Stable isotope evidence for identifying the recharge mechanisms of precipitation, surface water, and groundwater in the Ebinur Lake basin. *Science of the Total Environment, 657*, 1041-1050.

Haque, M. A. M., Jahan, C. S., Mazumder, Q. H., Nawaz, S. M. S., Mirdha, G. C., Mamud, P., & Adham, M. I. (2012). Hydrogeological condition and assessment of groundwater resource using visual modflow modeling, Rajshahi city aquifer, Bangladesh. *Journal of the Geological Society of India, 79*(1), 77-84.

Hariharan, V., & Uma Shankar, M. (2017). *A review of visual MODFLOW applications in groundwater modelling*. Paper presented at the IOP Conf. Series: Materials Science and Engineering.

Harms, P. A., Visser, A., Moran, J. E., & Esser, B. K. (2016). Distribution of tritium in precipitation and surface water in California. *Journal of Hydrology, 534*, 63–72.

Harris, R. N., & Gosnold, W. D. (1999). Comparisons of borehole temperature-depth profiles and surface air temperatures in the northern plain of the USA. *Geophysical Journal International, 138*, 541-548.

Hartmann, A., Gleeson, T., Wada, Y., & Wagener, T. (2017). Enhanced groundwater recharge rates and altered recharge sensitivity to climate variability through subsurface heterogeneity. *Proceedings of the National Academy of Sciences of the United States of America, 114*(11), 2842-2847.

Hasegawa, H., Ueda, S., Akata, N., Kakiuchi, H., & Hisamatsu, S. (2015). Tritium Activity Concentrations And Residence Times Of Groundwater Collected In Rokkasho, Japan. *Radiation Protection Dosimetry, 167*(No. 1–3), 201–205.

Hashemi, H., Berndtsson, R., Kompani-Zare, M., & Persson, M. (2013). Natural vs. artificial groundwater recharge, quantification through inverse modeling. *Hydrology and Earth System Sciences, 17*, 637-650.

Hatch, C. E., Fischer, A. T., Revenaugh, J. S., Constantz, J., & Ruehl, C. (2006). Quantifying surface water/groundwater interaction using time series analysis of streambed thermal records: Method development. *Water Resources Research, 42*, Article#W10410.

Healy, R. W. (2010). *Estimating Groundwater Recharge*. UK: Cambridge University Press.

Healy, R. W., & Cook, P. G. (2002). Using groundwater levels to estimate recharge. *Hydrogeology Journal, 10*(1), 91-109.

Heilweil, V. M., Ortiz, G., & Susong, D. D. (2009a). *Assessment of managed aquifer recharge at Sand Hollow Reservoir, Washington County, Utah, updated to conditions through 2007*. (Scientific Investigations Report 2009-5050). U.S. Geological Survey.

Heilweil, V. M., Solomon, D. K., Gingerich, S. B., & Verstraeten, I. M. (2009b). Oxygen, Hydrogen, and Helium Isotopes for Investigating Groundwater Systems of the Cape Verde Islands, West Africa. *Hydrogeology Journal, 17*, 1157-1174.

Helsrup, T., Jorgensen, N. O., & Banoeng-Yakubo, B. (2007). Investigation of hydrochemical characteristics of groundwater from Cretaceous–Eocene limestone aquifers in southern Ghana and Togo using hierarchical cluster analysis. *Hydrogeology Journal, 15*, 977-989.

Hendrickx, J. M. H., & Walker, G. R. (1997). Recharge from precipitation. In I. Simmers (Ed.), *Recharge of Phreatic Aquifers in (Semi-) Arid Areas*. Rotterdam/Brookfield: A.A. Belkema.

Henry, C. M. (2011). *An integrated approach to estimating groundwater recharge and storage variability in Southern Mali, Africa.* (Master of Science), Simon Frase University.

Hepburn, E., Cendón, D. I., Bekele, D., & Currell1, M. (2019). Environmental isotopes as indicators of groundwater recharge, residence times and salinity in a coastal urban redevelopment precinct in Australia. *Hydrogeology Journal, 28*, 503-520.

Herczeg, A. L., & Edmunds, W. M. (2000). Inorganic ions as tracers. In P. G. Cook & A. L. Herczeg (Eds.), *Environmental Tracers in Subsurface Hydrology* (pp. 31-78). Boston, USA: Kluwer Academic Press.

Herczeg, A. L., & Love, a. J. (2007). *Review of recharge mechanisms for the Great Artesian Basin*. Adelaide, Australia: CSIRO

Hiscock, K. M., & Bense, V. F. (2014). *Hydrogeology: Principles and practice (2nd Ed.)*. West Sussex, UK: John Wiley & Sons, Ltd.

Hoefs, J. (2009). *Stable Isotope Geochemistry* (6th ed.). Germany: Springer-Verlag Berlin Heidelberg.

Hoehn, E., & Cirpka, O. A. (2006). Assessing residence times of hyporheic ground water in two alluvial flood plains of the Southern Alps using water temperature and tracers. *Hydrology and Earth System Sciences, 10*, 553–563.

Hoehn, E., & von Gunten, H. R. (1989). Radon in Groundwater: A Tool to Assess Infiltration From Surface Waters to Aquifers. *Water Resources Research, 25*(8), 1795-1803.

Hornero, J., Manzano, M., Ortega, L., & Custodio, E. (2016). Integrating soil water and tracer balances, numerical modelling and GIS tools to estimate regional groundwater recharge: Application to the Alcadozo Aquifer System (SE Spain). *Science of the Total Environment, 568*, 415-432.

Hounslow, A. W. (1995). *Water quality data: analysis and interpretation.* Boca Raton: CRC Press Inc.

Houston, J. (2007). Recharge to groundwater in the Turi Basin, northern Chile: An evaluation based on tritium and chloride mass balance techniques. *Journal of Hydrology, 334*(3-4), 534-544.

Huang, S., Taniguchi, M., Yamano, M., & Wang, C. (2009). Detecting urbanization effects on surface and subsurface thermal environment - A case study of Osaka. *Science of the Total Environment, 407*(9), 3142-3152.

Huang, T., Yang, S., Liu, J., & Li, Z. (2016). How much information can soil solute profiles reveal about groundwater recharge? *Geosciences Journal, 20*(4), 495–502.

Huang, T. M., & Pang, Z. H. (2011). Estimating groundwater recharge following land-use change using chloride mass balance of soil profiles: a case study at Guyuan and Xifeng in the Loess Plateau of China. *Hydrogeology Journal, 19*(1), 177-186.

Huang, T. M., Pang, Z. H., & Edmunds, W. M. (2013). Soil profile evolution following land-use change: implications for groundwater quantity and quality. *Hydrological Processes, 27*(8), 1238-1252.

Huang, T. M., Pang, Z. H., Liu, J. L., Yin, L. H., & Edmunds, W. M. (2017). Groundwater recharge in an arid grassland as indicated by soil chloride profile and multiple tracers. *Hydrological Processes, 31*(5), 1047-1057.

Hung Vu, V., & Merkel, B. J. (2019). Estimating groundwater recharge for Hanoi, Vietnam. *Science of the Total Environment, 651*, 1047–1057.

Hussin, N. H. (2011). *Hydrogeochemical study and iron removal of groundwater in North Kelantan.* (MS.c), University of Malaya, Kuala Lumpur, Malaysia.

Hussin, N. H., Yusoff, I., Alias, Y., Mohamad, S., Rahim, N. Y., & Ashraf, M. A. (2014). Ionic liquid as a medium to remove iron and other metal ions: a case study of the North Kelantan Aquifer, Malaysia. *Environmental Earth Sciences, 71*(5), 2105-2113.

Hutton, J. T. (1976). Chloride in rainwater in relation to distance from the ocean *Search, 7*(5), 207-208.

IAEA. (2011a). Global Network of Isotopes in Precipitation (GNIP) program. Retrieved from http://www-naweb.iaea.org/napc/ih/IHS_resources_gnip.html

IAEA. (2011b). *Using isotopes effectively to support comprehensive groundwater management*. Paper presented at the 55th IAEA General Conference, Vienna, Austria.

IAEA. (2014). Groundwater Sampling Procedures for Isotope Hydrology. Water Resources Program: IHS Publications.

IAEA/WMO. (2017). Global Network of Isotopes in Precipitation. The GNIP Database. Accessible at: https://nucleus.iaea.org/wiser.

Ifediegwu, I. S. (2020). Groundwater recharge estimation using chloride mass balance: a case study of Nsukka local government area of Enugu State, Southeastern, Nigeria. *Modeling Earth Systems and Environment, 6*, 799–810

Ingebritsen, S. E., Sanford, W. E., & Neuzil, C. E. (2006). *Groundwater in geological processes (2nd Ed.)*. Cambridge, UK: Cambridge University Press.

Ingraham, N. L. (1998). Isotopic Variations in Precipitation In C. Kendall & J. J. McDonnel (Eds.), *Isotope Tracers in Catchment Hydrology* (pp. 87–118). Amsterdam: Elsevier.

Irvine, D. J., Kurylyk, B. L., Cartwright, I., Bonham, M., Post, V. E. A., Banks, E. W., & Simmons, C. T. (2017). Groundwater flow estimation using temperature-depth profiles in a complex environment and a changing climate. *Science of the Total Environment, 574*, 272-281.

Islami, I., Taib, S., Yusoff, I., & Abdul Ghani, A. (2012). Integrated geoelectrical resistivity, hydrochemical and soil property analysis methods to study shallow groundwater in the agriculture area, Machang, Malaysia. *Environmental Earth Sciences, 65*, 699-712.

Izady, A., Abdalla, O., Joodavi, A., Karimi, A., Chen, M., & Tompson, A. F. B. (2017). Groundwater recharge estimation in arid hardrock-alluvium aquifers using combined water-table fluctuation and groundwater balance approaches. *Hydrological Processes, 31*(19), Article#11270.

Jacobson, G., Janowski, J., & Abell, R. S. (1991). Groundwater and Surface Water Interactions at Lake George, New South Wales. *Journal Australian Geology and Geophysics, 12*, 161-190.

Jassas, H., & Merkel, B. (2014). Estimating groundwater recharge in the semiarid Al-Khazir Gomal Basin, North Iraq. *Water, 6*, 2467-2481.

Jayakumar, R., & Lee, E. (2017). Climate change and groundwater conditions in the Mekong Region–A review. *Journal of Groundwater Science and ENgineering, 5*(1), 14-30.

Jerbi, H., Hamdi, M., Snoussi, M., Abdelmalek, M. B., Jnoub, H., & Tarhouni, J. (2019). Usefulness of historical measurements of tritium content in groundwater for recharge assessment in semi-arid regions: application to several aquifers in central Tunisia. *Hydrogeology Journal, 27*, 1645-1660.

Jie, Z., van Heydan, J., Bendel, D., & Barthel, R. (2011). Combination of soil-water balance models and water-table fluctuation methods for evaluation and improvement of groundwater recharge calculations. *Hydrogeology Journal, 19*, 1487-1502.

Jones, I. C., & Banner, J. L. (2003). Estimating recharge thresholds in tropical karst island aquifers: Barbados, Puerto Rico and Guam. *Journal of Hydrology, 278*(1-4), 131-143.

Jones, I. C., Banner, J. L., & Humphrey, J. D. (2000). Estimating recharge in a tropical karst aquifer. *Water Resources Research, 36*(5), 1289-1299.

Joshi, S. K., Rai, S. P., Sinha, R., Gupta, S., Densmore, A. L., Rawat, Y. S., & Shekhar, S. (2018). Tracing groundwater recharge sources in the northwestern Indian alluvial aquifer using water isotopes (d18O, d2H and 3H). *Journal of Hydrology, 559*, 835-847.

Jurgens, B. C., Böhlke, J. K., & Eberts, S. M. (2012). *TracerLPM (Version 1): An Excel® workbook for interpreting groundwater age distributions from environmental tracer data: Techniques and Methods* (Report 4-F3). Reston, Virginia: U.S. Geological Survey.

Kabeya, N., Shimizu, A., Chann, S., Tsuboyama, Y., Nobuhiro, T., Keth, N., & Tamai, K. (2007). Stable isotope studies of rainfall and stream water in forest watersheds in Kampong Thom, Cambodia. In H. Sawada, M. Araki, N. A. Chappell, J. V. LaFrankie, & S. A. (Eds.), *Forest Environments in the Mekong River Basin*. Tokyo: Springer.

Kambuku, D., Tsujimura, M., & Kagawa, S. (2018). Groundwater recharge and flow processes as revealed by stable isotopes and geochemistry in fractured Hornblende-biotite-gneiss, Rivirivi Catchment, Malawi. *African Journal of Environmental Science and Technology, 12*(1), 1-14.

Kattan, Z. (2001). Use of hydrochemistry and environmental isotopes for evaluation of groundwater in the Paleogene limestone aquifer of the Ras Al-Ain area (Syrian Jezireh). *Environmental Geology, 41*, 128-144.

Kelly, W. R. (1997). Heterogeneities in ground-water geochemistry in a sand aquifer beneath an irrigated field. *Journal of Hydrology, 198*, 154-176.

Kendall, C., & McDonnell, J. J. (1998). *Isotope Tracers in Catchment Hydrology*. AE Amsterdam, The Netherlands: Elservier.

KeTTHA. (2010). *Study on groundwater monitoring system in Kelantan.* Putrajaya: Ministry of Energy, Green Technology and Water (KeTTHA).

Keywood, M. D., Chivas, A. R., Fifield, L. K., Cresswell, R. G., & Ayers, G. P. (1997). The accession of chloride to the western half of the Australian continent. *Australian Journal of Soil Research, 35*, 1177-1189.

Kim, J., Choi, H., Kim, H., Ryu, J.-S., & Lee, K.-K. (2020). Using isotopes (strontium and radon) and microbial communities to quantify groundwater mixing influenced by anthropogenic factors at riverside area. *Journal of Hydrology, 581*, Article#124441.

Kim, S. H., Hejazi, M., Liu, L., Calvin, K., Clarke, L., & Edmonds, J. (2016). Balancing global water availability and use at basin scale in an integrated assessment model. *Climate Change, 136*(2), 217-231.

Kim, Y., Lee, K.-S., Koh, D.-C., Lee, D.-H., Lee, S.-G., Park, W.-B., . . . Woo, N.-C. (2003). Hydrogeochemical and isotopic evidence of groundwater salinization in a coastal aquifer: a case study in Jeju volcanic island, Korea. *Journal of Hydrology, 270*, 282–294.

Kimball, D. (2017). The Nuclear testing Tally. Retrieved from https://www.armscontrol.org/factsheets/nucleartesttally

King, A. C., Raiber, M., Cox, M. E., & Cendn, D. I. (2017). Comparison of groundwater recharge estimation techniques in an alluvial aquifer system with an intermittent/ephemeral stream (Queensland, Australia). *Hydrogeology Journal, 25*(6), 1759-1777.

Kinzelbach, W., Aeschbach, W., Alberich, C., Goni, I. B., Beyerle, U., Brunner, P., . . . Zoellmann, K. (2002). *A survey of methods for analysing groundwater recharge in arid and semi-arid regions* (UNEP/DEWA/RS.02-2). Retrieved from Nairobi, Kenya:

Kluge, T., Ilmberger, J., von Rohden, C., & Aeschbach-Hertig, W. (2007). Tracing and quantifying groundwater inflow into lakes using a simple method for radon-222 analysis. *Hydrology and Earth System Sciences, 11*, 1621-1631.

Koeniger, P., Gaj, M., Beyer, M., & Himmelsbach, T. (2016). Review on soil water isotope-based groundwater recharge estimations. *Hydrological Processes, 30*(16), 2817-2834.

Koh, D. C., Plummer, L. N., Solomon, D. K., Busenberg, E., Kim, Y. J., & Chang, H. W. (2006). Application of environmental tracers to mixing, evolution, and nitrate contamination of ground water in Jeju Island, Korea. *Journal of Hydrology, 327*, 258-275.

Koster, R. D., de Valpine, D. P., & Jouzel, J. (1993). Continental water recycling and H2 18O concentrations. *Geophysical Research Letters, 20*(20), 2215–2218.

Kralik, M., Humer, F., Fank, J., Harum, T., Klammler, G., Gooddy, D., . . . Purtschert, R. (2014). Using 18O/2H, 3H/3He, 85Kr and CFCs to determine mean residence times and water origin in the Grazer and Leibnitzer Feld groundwater bodies (Austria). *Applied Geochemistry, 50*, 150-163.

Krishnamurthy, R. V., & Bhattacharya, S. K. (1991). *Stable oxygen and hydrogen isotope ratios in shallow groundwater from India and a study of the role of evapotranspiration in the Indian monsoon.* (Vol. TX, 187–194). San Antonio: Geochemical Society.

Krul, W. F., & Liefrinck, F. A. (1946). *Recent Groundwater Investigations in the Netherlands*. New York: Elsevier.

Kumar, R. R., Ramana, D. V., & Singh, R. N. (2012). Modelling near subsurface temperature with mixed type boundary condition for transient air temperature and vertical groundwater flow. *Journal of Earth System and Science, 121*(5), 1177-1184.

Kurylyk, B. L., Irvine, D. J., & Bense, V. F. (2019). Theory, tools, and multidisciplinary applications for tracing groundwater fluxes from temperature profiles. *WIREs Water, 6*, Article#1329.

Kurylyk, B. L., Irvine, D. J., Carey, S. K., Briggs, M. A., Werkema, D. D., & Bonham, M. (2017). Heat as a groundwater tracer in shallow and deep heterogeneous media: analytical solution, spreadsheet tool, and field applications. *Hydrological Processes, 31*(14), 2648-2661.

Labrecque, G., Chesnaux, R., & Boucher, M.-A. (2020). Water-table fluctuation method for assessing aquifer recharge: application to Canadian aquifers and comparison with other methods. *Hydrogeology Journal, 28*(521), 521-533.

Laonamsai, J., & Putthividhya, A. (2016). *Preliminary Assessment of Groundwater and Surface Water Characteristics in the Upper Chao Phraya River Basin Land Using a Stable Isotope Fingerprinting Technique: .* Paper presented at the World Environmental and Water Resources Congress 2016: Professional Development, Innovative Technology, International Perspectves, History and Herritage, West Palm Beach, Florida.

Lee, J. Y., Yi, M. J., & Hwang, D. (2005). Dependency of hydrologic responses and recharge estimates on water-level monitoring locations within a small catchment. *Geosciences Journal, 9*(3), 277-286.

Lefebvre, K., Barbecot, F., Ghaleb, B., Larocque, M., & Gagné, K. (2013). Full range determination of 222Rn at the watershed scale by liquid scintillation counting. *Applied Radiation and Isotopes, 75*, 71-76.

Lenhart, T., Eckhardt, K., Fohrer, N., & Frede, H.-G. (2002). Comparison of two different approaches of sensitivity analysis. *Physics and Chemistry of the Earth Part B-Hydrology Oceans and Atmosphere, 27*, 645-654.

Leontiadias, I. L., Payne, B. R., & Christodoulou, T. (1988). Isotope hydrology of the Aghios Nikolaos area of Crete, Greece. *Journal of Hydrology, 98*, 121–132.

Lerner, D. N., Issar, A., & Simmers, I. (1990). *Groundwater recharge; a guide to understanding and estimating natural recharge* (Vol. 8). Heise, Hannover.

Li, F., Pan, G., Tang, C., Zhang, Q., & Yu, J. (2008). Recharge source and hydrogeochemical evolution of shallow groundwater in a complex alluvial fan system, southwest of North China Plain. *Environmental Geology, 55*, 1109-1122.

Li, J., Li, F., Liu, Q., & Zhang, Y. (2014). Trace metal in surface water and groundwater and its transfer in a Yellow River alluvial fan: Evidence from isotopes and hydrochemistry. *Science of the Total Environment, 472*, 979-988.

Li, S., Dong, L., Chen, J., Li, R., Yang, Z., & Liang, Z. (2019a). Vertical groundwater flux estimation from borehole temperature profiles by a numerical model, RFLUX. *Hydrological Processes, 33*, 1542–1552.

Li, S., & Zhang, Q. (2008). Geochemistry of the upper Han River basin, China, 1: spatial distribution of major ion compositions and their controlling factors. *Applied Geochemistry, 23*(12), 3535-3544.

Li, Z., Chen, X., Liu, W. Z., & Si, B. C. (2017). Determination of groundwater recharge mechanism in the deep loessial unsaturated zone by environmental tracers. *Science of the Total Environment, 586*, 827-835.

Li, Z., Jasechko, S., & Si, B. (2019b). Uncertainties in tritium mass balance models for groundwater recharge estimation. *Journal of Hydrology, 571*, 150-158.

Liu, F., Song, X., Yang, L., Zhang, Y., Han, D., Ma, Y., & Bu, H. (2015). Identifying the origin and geochemical evolution of groundwater using hydrochemistry and stable isotopes in the Subei Lake basin, Ordos energy base, Northwestern China. *Hydrology and Earth System Sciences, 19*(1), 551-565.

Liu, G. Q., Wang, Y. S., Zhang, Y. F., & Song, T. (2009). Application of chloride profile and water balance methods in estimating groundwater recharge in Luanjing Irrigation Area, Inner Mongolia. *Hydrological Sciences Journal, 54*(5), 961-973.

Liu, J., Chen, Z., Zhang, Y., Li, Z., Zhang, L., & Liu, F. (2016). Stable isotope evidences on sources and mechanisms of groundwater recahrge in Hohhot basin, China. *Environmental Earth Sciences, 75*, Article#410.

Llamas, M. R., & Martínez-Cortina, L. (2009). Chapter12: Specific aspects of groundwater use in water ethics. In M. R. Llamas, L. Martínez-Cortina, & A. Mukherji (Eds.), *Water Ethics. Marcelino Botín Water Forum 2007* (pp. 187-204). Leiden, Netherlands: CRC Press/Balkema.

Llamas, M. R., & Martínez-Santos, P. (2005). Intensive groundwater use a silent revolution that cannot be ignored. *WATER SCIENCE AND TECHNOLOGY SERIES, 51*(8), 167-174.

Lo Russo, S., Zavattaro, L., Acutis, M., & Zuppi, G. M. (2003). Chloride profile technique to estimate water movement through unsatured zone in a cropped area in subhumid climate (Po Valley-NW Italy). *Journal of Hydrology, 270*(1-2), 65-74.

Locsey, K. L., & Cox, M. E. (2003). Statistical and hydrochemical methods to compare basalt- and basement rock-hosted groundwaters: Atherton Tablelands, northeastern Australia. *Environmental Geology, 43*(6), 698-713.

Loh, C. H. (1992). Quaternary. In S. MacDonald (Ed.), *The geology and mineral resources of North Kelantan and North Terengganu. West Malaysia*. Kuala Lumpur: Geological Survey.

Lopez-Chicano, M., Bouamama, M., Vallejos, A., & Pulido, B. A. (2001). Factors which determine the hydrogeochemical behavior of karstic springs: a case study from the Betic Cordilleras, Spain. *Applied Geochemistry, 16*(9-10), 1179-1192.

Loveland, W. D., Morrissey, D. J., & Seaborg, G. T. (2017). *Modern Nuclear Chemistry*. Hoboken, New Jersey: John Wiley & Sons.

Lovett, G. M., Nolan, S. S., Driscoll, C. T., & Fahey, T. J. (1996). Factors regulating throughfall flux in a new New-Hampshire forested landscape. *Can. J. Forest Res., 26*(12), 2134-2144.

Lu, N., & Ge, S. (1996). Effect of horizontal heat and fluid flow on the vertical temperature distribution in a semiconfining layer. *Water Resources Research, 32*(5), 1449-1453.

Lu, Y., Li, H., Si, B., & Li, M. (2020). Chloride tracer of the loess unsaturated zone under sub-humid region: A potential proxy recording high-resolution hydroclimate. *Science of the Total Environment, 700*, Article#134465.

Lucas, L. L., & Unterweger, M. P. (2000). Comprehensive Review and Critical Evaluation of the Half-Life of Tritium. *Journal of Research of the National Institute of Standards and Technology, 105*(4), 541-549.

Luce, C. H., Tonina, D., Gariglio, F., & Applebee, R. (2013). Solutions for the diurnally forced advection-diffusion equation to estimate bulk fluid velocity and diffusivity in streambeds from temperature time series. *Water Resources Research, 49*, 488-506.

Lwimbo, Z. D., Komakech, H. C., & Muzuka, A. N. N. (2019). Estimating groundwater recharge on the southern slope of Mount Kilimanjaro, Tanzania *Environmental Earth Sciences, 78*, Article#687.

Machavaram, M. V., & Krishnamurthy, R. V. (1995). Earth surface evaporative process: a case study from the Great Lakes region of the United States based on deuterium excess in precipitation. *Geochimica Et Cosmochimica Acta, 59*(20), 4279–4283.

Madioune, D. H., Faye, F., Orban, P., Brouyère, S., Dassargues, A., Mudry, J., . . . Maloszewski, P. (2014). Application of isotopic tracers as a tool for understanding hydrodynamic behavior of the highly exploited Diass aquifer system (Senegal). *Journal of Hydrology, 511*, 443–459.

Madon, M. (1999). Regional tectonics and sedimentary basins of Malaysia: Basin types, tectono-stratigraphy provinces, structural styles. In PETRONAS (Ed.), *The Petroleum Geology and Resorces of Malaysia* (pp. 79-111). Kuala Lumpur: PETRONAS.

Majumder, R. K., Halim, M. A., Saha, B. B., Ikawa, R., Nakamura, T., Kagabu, M., & Shimada, J. (2011). Groundwater flow system in Bengal Delta, Bangladesh revealed by environmental isotopes. *Environmental Earth Sciences, 64*, 1343–1352.

Majumder, R. K., Shimada, J., & Taniguchi, M. (2013). Groundwater flow systems in the Bengal Delta, Bangladesh, inferred from subsurface temperature readings. *Songklanakarin Journal Sciences Technology, 35*(1), 99-106.

Manna, F., Cherry, J. A., McWhorter, D. B., & Parker, B. L. (2016). Groundwater recharge assessment in an upland sandstone aquifer of southern California. *Journal of Hydrology, 541*, 787-799.

Marei, A., Khayat, S., Weise, S., Ghannam, S., Sbaih, M., & Geyer, S. (2010). Estimating groundwater recharge using the chloride mass-balance method in the West Bank, Palestine. *Hydrological Sciences Journal, 55*(5), 780-791.

Marghade, D., Malpe, D. B., & Zade, A. B. (2012). Major ion chemistry of shallow groundwater of a fast growing city of Central India. *Environmental Monitoring Assessment, 184*, 2045-2418.

Marrero-Diaz, R., Alcala, F. J., Perez, N. M., Lopez, D. L., Melian, G. V., Padron, E., & Padilla, G. D. (2015). Aquifer Recharge Estimation through Atmospheric Chloride Mass Balance at Las Canadas Caldera, Tenerife, Canary Islands, Spain. *Water, 7*(5), 2451-2471.

Martindale, H. (2015). *The use of radon and complementary hydrochemistry tracers for the identification of groundwater – surface water interaction in New Zealand.* (Master of Environmental Management), University of New Zealand, Palmerston North, New Zealand.

McDonald, M. G., & Harbaugh, A. W. (1988). *A modular three-dimensional finite-difference ground-water flow model*. (Techniques of Water-Resources Investigations 06-A1). Washington, US: United States Government Printing Office.

Md Hashim, M. A. (2002). *Geologi dan geomorfologi kawasan Kuala Besar hingga Kuala Pengkalan Besar dengan penekanan permatang-permatang Holosen dan perubahan pantai.* (B.Sc.), University of Malaya, Kuala Lumpur.

Meinzer, O. E. (1923). *The occurence of groundwater in the united states with a discussion of principles*. (Water Supply Paper 489). Washington, US: United States Government Printing Office.

Meinzer, O. E., & Stearns, N. D. (1929). *A study of groundwater in the Pomperaug basin, Connecticut with special reference to intake and discharge*. (Water Supply Paper 597-B). Washington, US: United States Government Printing Office.

Mensah, F. O., Alo, C., & Yidana, S. M. (2014). Evaluation of groundwater recharge estimates in a partially metamorphosed sedimentary basin in a tropical environment: application of natural tracers. *Scientific World Journal*, Article#419508.

Meredith, K., Hollins, S., Hughes, C., Cendón, D., Hankin, S., & Stone, D. (2009). Temporal variation in stable isotopes (18O and 2H) and major ion concentrations within the Darling River between Bourke and Wilcannia due to variable flows, saline groundwater influx and evaporation. *Journal of Hydrology, 378*, 313-324.

MGD (Cartographer). (2008). Hydrogeological map

MGD. (2012). *Groundwater modelling for Lower Kelantan River Basin (Shallow aquifer).* (Report No. JMG.KLT. (SAT) 04/2012). Retrieved from Kelantan, Malaysia:

MGD (Cartographer). (2014a). Geological Map of Peninsular Malaysia (9th Ed.)

MGD. (2014b). *Groundwater modelling for Lower Kelantan River Basin* (Report No. JMG.KLT. (SAT) 04/2014.). Retrieved from Kelantan, Malaysia:

Millero, F. J., Feistel, R., Wright, D. G., & McDougall, T. J. (2008). The standard composition of seawater: the definition of a reference salinity scale. *Deep Sea Research Part I: Oceanographic Research Papers, 55*(1), 50-72.

Minnig, M., Moeck, C., Radny, D., & Schirmer, M. (2018). Impact of urbanization on groundwater recharge rates in Dübendorf, Switzerland. *Journal of Hydrology, 563*, 1135-1146.

Miyakoshi, A., Taniguchi, M., Okubo, Y., & Uemura, T. (2005). Evautions of subsurface flow for reconstructions of climate change using borehole temperature and isotope data in Kamchatka. *Physics of Earth and Planetary Interiors, 152*, 335-342.

Mizota, C., & Kusakabe, K. (1994). Spatial distribution of dD and d18O values of surface and shallow groundwaters from Japan, south Korea and east China. *Geochemical Journal, 28*, 387–410.

Moeck, C., Grech-Cumbo, N., Podgorski, J., Bretzler, A., Gurdak, J. J., Berg, M., & Schirmer, M. (2020). A global-scale dataset of direct natural groundwater recharge rates: A review of variables, processes and relationships. *Science of the Total Environment, 717*, Article#137042.

Mohamad, D., & Mohd Ali, R. (1981). *IAEA Regional Co-operative Agreement Project 13-Isotope hydrology and sedimentology a preliminary study of the environmental isotope in hydrology in the Lower Kelantan River Basin Kelantan, Malaysia*. (PPA/PR/1). Kuala Lumpur: Tun Ismail Atomic Research Center.

Monjerezi, M., Vogt, R. D., Aagaard, P., & Saka, J. D. K. (2011). Hydrochemical processes in an area with saline groundwater in lower Shire River Valley, Malawi: an integrated application of hierarchical cluster and principal component analyses. *Applied Geochemistry, 26*(8), 1399-1413.

Mook, W. G. (2000). *Environmental isotopes in the hydrological cycle: principles and applications*. Paris: UNESCO/IAEA.

Moon, S. K., Woo, N. C., & Lee, K. S. (2004). Statistical analysis of hydrographs and water-table fluctuation to estimate groundwater recharge. *Journal of Hydrology, 292*, 198-209.

Moreno, G., Gallardo, J. F., & Bussotti, F. (2001). Canopy modification of atmospheric deposition in oligotrophic Quercus pyrenaica forests of an unpolluted regions (central-western Spain). *Forest Ecology and Management, 149*, 47-60.

Morgenstern, U., Stewart, M. K., & Stenger, R. (2010). Dating of streamwater using tritium in a post nuclear bomb pulse world: continuous variation of mean transit time with streamflo. *Hydrology and Earth System Sciences, 14*, 2289–2301.

Mukherjee, A., Fryar, A. E., & Rowe, H. D. (2007). Regional-scale stable isotopic signatures of recharge and deep groundwater in the arsenic affected areas ofWest Bengal, India. *Journal of Hydrology, 334*, 151–161.

Murphy, E. M., Ginn, T. R., & Phillips, J. L. (1996). Geochemical estimates of paleorecharge in the Pasco Basin: Evaluation of the chloride mass balance technique. *Water Resources Research, 32*(9), 2853-2868.

Mutoti, M. I. (2015). *Estimating groundwater recharge using chloride mass balance in the upper Berg River catchment, South Africa.* (Masters of Science), University of the Western Cape, Western Cape, South Africa.

Nachabe, M., Masek, C., & Obeysekera, J. (2004). Observations and modeling of profile soil water storage above a shallow water table. *Soil Science Society of America Journal, 68*, 719–724.

Najeeb, K. M., Vinayachandran, N., Jose, B., & Vashistha, R. (2014). Radon in groundwater in Tumkur District of Karnataka with special reference to sampling sensitivity. *JOURNAL GEOLOGICAL SOCIETY OF INDIA, 83*, 665-668.

Ng, S. W. P., Whitehouse, M. J., Searle, M. P., Robb, L. J., Ghani, A. A., Chung, S. L., . . . Roselee, M. H. (2015). Petrogenesis of Malaysian granitoids in the Southeast Asian tin belt: Part 2. U-Pb zircon geochronology and tectonic model. *Geological Society of America Bulletin, 127*(9-10), 1238-1258.

NGWA. (2016). Facts about global groundwater usage. National Groundwater Association, 1-2. Retrieved from http://www.ngwa.org/Fundamentals/Documents/global-groundwater-use-fact-sheet.pdf

Niazi, A., Bentley, L. R., & Hayashi, M. (2017). Estimation of spatial distribution of groundwater recharge from stream baseflow and groundwater chloride. *Journal of Hydrology, 546*, 380-392.

Nimmo, J. R., Healy, R. W., & Stonestrom, D. A. (2005). Aquifer Recharge. In M. G. a. B. Anderson, J. (Ed.), *Encyclopedia of Hydrological Science: Part 13. Groundwater* (Vol. 4, pp. 2229-2246). Chichester, UK: Wiley,.

Nolan, B. T., Healy, R. W., Taber, P. E., Perkins, K., Hitt, K. J., & Wolock, D. M. (2007). Factors influencing ground-water recharge in the eastern United States. *Journal of Hydrology, 332*(1-2), 187-205.

Noor, I. M. (1980). *Prefeasibility study of potential groundwater development in Kelantan, Malaysia.* (Ph.D.), University of Birmingham, Birmingham.

Obuobie, E. (2008). *Estimation of groundwater recharge in the context of future climate change in the White Volta River Basin, West Africa.* (Doctoral dissertation, Rheinischen Friedrich-Wilhelms-Universität, Bonn, Ghana).

Obuobie, E., Diekkrueger, B., Agyekum, W., & Agodzo, S. (2012). Groundwater level monitoring and recharge estimation in the White Volta River basin of Ghana. *Journal of African Earth Sciences, 71-72*, 80-86.

Ordens, C. M., Werner, A. D., Post, V. E. A., Hutson, J. L., Simmons, C. T., & Irvine, B. M. (2012). Groundwater recharge to a sedimentary aquifer in the topographically closed Uley South Basin, South Australia. *Hydrogeology Journal, 20*(1), 61-72.

Oyarzún, R., Jofre, E., Maturana, H., Oyarzún, J., & Aguirre, E. (2014). Use of 222radon as a simple tool for surface water–groundwater connectivity assessment: a case study in the arid Limarí basin, north-central Chile. *Water and Environment Journal, 28*(3), 418-422.

Panda, P., & Narasimham, M. L. (2020). A Review on Modelling and Simulation of Ground Water Resources in Urban Regions. *INFOKARA RESEARCH, 9*(1), 235-244.

Papatheodorou, G., Lambrakis, N., & Panagopoulos, G. (2007). Application of multivariate statistical procedures to the hydrochemical study of coastal aquifer: an example from Crete, Greece. *Hydrological Processes, 21*(11), 1482-1495.

Park, E. (2012). Delineation of recharge rate from a hybrid water table fluctuation method. *Water Resources Research, 48*, Article#W07503.

Park, E., & Parker, J. C. (2008). A simple model for water table fluctuations in response to precipitation. *Journal of Hydrology, 356*, 344-349.

Pathak, R., Awasthi, M. K., Sharma, S. K., Hardaha, M. K., & Nema, R. K. (2018). Ground Water Flow Modelling Using MODFLOW –A Review. *International Journal of Current Microbiology and Applied Sciences, 7*(2), 83-88.

Pavlovskii, I., Hayashi, M., & Cey, E. E. (2019). Estimation of depression-focussed groundwater recharge using chloride mass balance: problems and solutions across scales. *Hydrogeology Journal, 27*, 2263–2278.

Peling-Ba, K. B. (2009). Analysis of Stable Isotope Contents of Surface and Underground Water in Two Main Geological Formations in the Northern Region of Ghana. *West African Journal of Applied Ecology, 15*(1), Article#49430.

Peng, T. R., Huang, C. C., Wang, C. H., Liu, T. K., Lu, W. C., & Chen, K. Y. (2012). Using oxygen, hydrogen, and tritium isotopes to assess pondwater's contribution to groundwater and local precipitation in the pediment tableland areas of northwestern Taiwan. *Journal of Hydrology, 450–451*, 105–116.

Pereira, H. G., Renca, S., & Sataiva, J. (2003). A case study on geochemical anomaly identification through principal component analysis supplementary projection. *Applied Geochemistry, 18*, 37-44.

Piper, A. M. (1944). A graphic procedure in the geochemical interpretation of water analyses. *American Geophysical Union Transactions, 25*, 914–928.

Ponsin, V., Chablais, A., Dumont, J., Radakovitch, O., & Höhener, P. (2015). 222Rn as Natural Tracer for LNAPL Recovery in a Crude Oil-Contaminated Aquifer. *Groundwater Monitoring & Remediation, 35*(2), 30-38.

Qian, H., Li, P., Wu, J., & Z, Y. (2013). Isotopic characteristics of precipitation, surface and ground waters in the Yinchuan plain, Northwest China. *70*(1), 57-70.

Quinodoz, F., Blarasin, M., Panarello, H., & Ducos, E. (2017). Assessing interactions between groundwater and surface water in a Pampean stream. *Hydrology Research, 48*(4), 1045-1057.

Rai, S. N., Manglik, A., & Singh, R. N. (1994). Water table fluctuation in response to transient recharge from a Rectangular Basin. *Water Resources Management, 8*, 1-10.

Rajashekaraa, K. M., Narayanaa, Y., & Siddappab, K. (2007). 222Rn concentration in groundwater and riverwater of coastal Karnataka. *Radiation Measurements, 42*, 472 – 478.

Rajmohan, N., & Elango, L. (2004). Identification and evolution of hydrogeochemical processes in the groundwater environment in an area of the Palar and Cheyyar River Basins, Southern India. *Environmental Geology, 46*, 47-61.

Rapti-Caputo, D., & Martinelli, G. (2009). The geochemical and isotopic composition of aquifer systems in the deltaic region of the Po River plain (northern Italy). . *Hydrogeology, 17*, 467–480.

Rasmussen, W. C., & Andreasen, G. E. (1959). *Hydrologic budget of the Beaverdam Creek Basin, Maryland*. Washington, US: Geological Survey US.

Rau, G. C., Andersen, M. S., McMCallum, A. M., Roshan, H., & Acworth, R. I. (2014). Heat as a tracer to quantify water flow in near-surface sediments. *Earth-Science Reviews, 129*, 40-58.

Ravikumar, P., Davis, D., Mathew, S., Somashekar, R. K., & Prakash, K. L. (2014). Spatio-temporal Variation in Radon Concentration in Groundwater with Respect to Rock Types: A Case Study from Chitradurga District, Karnataka. *Journal of Geological Society of India, 83*, 156-164.

Ravikumar, P., & Somashekar, R. K. (2011a). Environmental Tritium (3H) and hydrochemical investigations to evaluate groundwater in Varahi and Markandeya river basins, Karnataka, India. *Journal of Environmental Radioactivity, 102*, 153-162.

Ravikumar, P., & Somashekar, R. K. (2011b). Natural 3H radioactivity analysis in groundwater and estimation of committed effective dose due to groundwater ingestion in Varahi and Markandeya river basins, Karnataka State, India. *Journal of Radioanalytical and Nuclear Chemistry, 288* 271–278.

Ren, J., Cheng, J., Yang, J., & Zhou, Y. (2018). A review on using heat as a tool for studying groundwater–surface water interactions. *Environmental Earth Sciences, 77*.

Richts, A., Struckmeier, W. F., & Zaepke, M. (2011). WHYMAP and the groundwater resources map of the world 1:25,000,000. In J. Jones (Ed.), *Sustaining Groundwater Resources, International Year of Planet Earth*. Dordrecht: Springer.

Robertson, J. A., & Gazis, C. A. (2006). An oxygen isotope study of seasonal trends in soil water fluxes at two sites along a climate gradient in Washington state (USA). *Journal of Hydrology, 328*, 375-387.

Rozanski, K., Araguas-Araguas, L., & Gonfiantini, R. (1993). Isotopic Patterns in Modern Global Precipitation In P. K. Swart, K. C. Lohman, J. McKenzie, & S. Savin (Eds.), *Climate change in congenital isotopic records.* (pp. 1–36). Washington: American Geophysical Union.

Saar, M. O. (2011). Review: Geothermal heat as a tracer of large-scale groundwater flow and as a means to determine permeabiltiy fields. *Hydrogeology Journal, 19*, 31-52.

Saat, A., Zainal, N. S., Hamzah, Z., & Wood, A. K. (2014). Determination of supported 222rn activity concentration in ground water from Cameron Highlands area using gamma spectrometry. *The Malaysian Journal of Analytical Sciences, 18*(1), 185-194.

Sakura, Y. (1993). *Groundwater flow estimated from temperatures in the Yonezawa Basin, Northeast Japan* (Vol. IAHS Publication 215). Oxfordshire, UK: IAHS.

Salem, Z. E.-S. (2016). Subsurface thermal regime to delineate the paleo-groundwater flow system in an arid area, Al Kufra, Libya. *Journal of Astronomy and Geophysics, 5*, 451-462.

Salem, Z. E., Sakura, Y., & Aslam, M. A. M. (2004). The use of temperature, stable isotopes and water quality to determine the pattern and spatial extent of groundwater flow: Nagaoka area, Japan. *Hydrogeology Journal, 12*(5).

Sallwey, J., Valverde, J. P. B., López, F. V., Junghanns, R., & Stefan, C. (2019). Suitability maps for managed aquifer recharge: a review of multi-criteria decision analysis studies. *Environmental Reviews, 27*, 138-150.

Samborska, K., Różkowski, A., & Małoszewski, P. (2013). Estimation of groundwater residencetime using environmental radioisotopes (14C,T) in carbonate aquifers, southern Poland. *Isotopes in Environmental and Health Studies, 49*(1), 73-97.

Sami, K., & Hughes, D. A. (1996). A comparison of recharge estimates to a fractured sedimentary aquifer in South Africa from a chloride mass balance and an integrated surface-subsurface model. *Journal of Hydrology, 179*(1-4), 111-136.

Sanford, W. (2002). Recharge and groundwater models: an overview. *Hydrogeology Journal, 10*(1), 110-120.

Santos, I. R., Niencheski, F., Burnett, W., Peterson, R., Chanton, J., Andrade, C. F. F., . . . Knoeller, K. (2008). Tracing anthropogenically driven groundwater discharge into a coastal lagoon from southern Brazil. *Journal of Hydrology, 353*, 275-293.

Santos, I. R., Zhang, C., Maher, D. T., Atkins, M. L., Holland, R., Morgenstern, U., & Li, L. (2017). Assessing the recharge of a coastal aquifer using physical observations, tritium, groundwater chemistry andmodelling. *Science of the Total Environment, 580*, 367-379.

Scanlon, B. (1991). Evaluation of moisture flux from chloride data in desert soils. *Journal of Hydrology, 128*, 137-156.

Scanlon, B., Healy, R. W., & Cook, P. G. (2002). Choosing appropriate techniques for quantifying groundwater recharge. *Hydrogeology Journal, 10*, 18-39.

Scanlon, B. R., Keese, K. E., Flint, A. L., Flint, L. E., Gaye, C. B., Edmunds, W. M., & Simmers, I. (2006). Global synthesis of groundwater recharge in semiarid and arid regions. *Hydrological Processes, 20*(15), 3335-3370.

Scanlon, B. R., Stonestrom, D. A., Reedy, R. C., Leaney, F. W., Gates, J., & Cresswell, R. G. (2009). Inventories and mobilization of unsaturated zone sulfate, fluoride, and chloride related to land use change in semiarid regions, southwestern United States and Australia. *Water Resources Research, 45*, Article#W00A18.

Scanlon, B. R., Tyler, S. W., & Wierenga, P. J. (1997). Hydrologic issues in arid, unsaturated systems and implications for contaminant transport. *Reviews of Geophysics, 35*(4), 461-490.

Schmidt, A., Stringer, C. E., Haferkorn, U., & Schubert, M. (2009). Quantification of groundwater discharge into lakes using radon-222 as naturally occurring tracer. *Environmental Geology, 56*, 855–863.

Schoeller, H. (1955). Géochemie des eaux souterraines. *Revue de L'Institute Francais du Pétrole, 10*, 230-244.

Schoeller, H. (1965). Qualitative evaluation of groundwater resources. In H. Schoeller (Ed.), *Methods and techniques of groundwater investigations and development. Water resource series no. 33* (pp. 54-83). Paris: UNESCO.

Schoeller, H. (1967). Chapter 15: Geochemistry of groundwater—an international guide for research and practice. Paris: UNESCO.

Schubert, M., Balcazar, M., Lopez, A., Pena, P., Flores, J. H., & Knoller, K. (2007). Combination of radon and stable isotope analysis as a tool for decision support concerning the remediation of NAPL-contaminated sites. *Isotopes in Environmental and Health Studies, 43*(3), 215-226.

Seiler, K. P., & Gat, J. R. (2007). *Groundwater recharge from Run-off, infiltration and percolation.* (Vol. 55). AA Dordrecht, The Netherlands.: Springer.

Semprini, L., Hopkins, O. S., & Tasker, B. R. (2000). Laboratory, Field and Modeling Studies of Radon-222 as a Natural Tracer for Monitoring NAPL Contamination. *Transport in Porous Media, 38*, 223-240.

Semprini, L., & Istok, J. D. (2008). *Radon-222 as Natural Tracer for Monitoring the Remediation of NAPL Contamination in the Subsurface. ESTCP Coast and Performance Report* (ER-9916). Retrieved from Arlington, VA:

Seneviratne, A. A. A. K. (2007). *Development of steady state groundwater flow model in Lower Walawa Basin -Sri Lanka (Integrating GIS, remote sensing and numeric groundwater modelling).* (Master's thesis, International Institute for Geo-information Science and Earth Observation, Enschede, Netherlands). Retrieved from https://www.itc.nl/library/papers_2007/msc/wrem/amarasinghe.pdf

Shah, N., & Ross, M. (2009). Variability in specific yield under shallow water table conditions. *Journal of Hydrologic Engineering, 14*, 1290-1298.

Shah, T., Burke, J., Villholth, K., Angelica, M., Custodio, E., Daibes, F., . . . Wang, J. (2007). Groundwater: a global assessment of scale and significance. In D. Molden (Ed.), *Water for food, water for life: a Comprehensive Assessment of Water Management in Agriculture.* (pp. 395-423.). London, UK: Earthscan; Colombo, Sri Lanka: International Water Management Institute (IWMI).

Shah, Z. A. (2013). *Qualitative and quantitative qtudy of chemical and isotopic parameters of the groundwater system in parts of Unnao District, Uttar Pradesh, India.* (Doctor of Philosophy), Aligarh Muslim University, Aligarh, India.

Shamuyarira, K. K. (2017). *Deternmination of recharge and groundwater potentials zone in Mhinga area, South Africa.* (Master's thesis, University of Venda, Thohoyandou, South Africa). Retrieved from http://ir.nrf.ac.za/handle/10907/1366

Shan, C., & Bodvarsson, G. (2004). An analytical solution for estimating percolation rate by fitting temperature profiles in the vadose zone. *Journal of Contaminant Hydrology, 68*, 83-95.

Shao, Y. S. (1989). Environmental isotope geochemistry of groundwater in Hohhot Basin, inner Mongolia. (in Chinese). *Geotech Investig Surv, 43*, 41–43

Simmers, I. (1988). *Estimation of Natural Groundwater Recharge* (Vol. 222). Dordrecht, Holland: Springer-Science+Business Media Dordrecht.

Simmers, I. (1997). Groundwater recharge principles, problems and developments. In I. Simmers (Ed.), *Recharge of Phreatic Aquifers in (Semi-)Arid Areas* (pp. 1-18). Rotterdam: A.A. Balkema.

Simone, G. D., Lucchetti, C., Pompilj, F., Gianfranco Galli, Tuccimei, P., Curatolo, P., & Giorgi, R. (2017). Soil radon survey to assess NAPL contamination from an ancient spill. Do kerosene vapors affect radon partition ? *Journal of Environmental Radioactivity, 171*, 138-147.

Şimşek, C., Demirkesen, A. C., Baba, A., Kumanlıoğlu, A., Durukan, S., Aksoy, N., . . . Tayfur, A. M. (2020). Estimation groundwater total recharge and discharge using GIS-integrated water level fluctuation method: a case study from the Alaşehir alluvial aquifer Western Anatolia, Turkey. *Arabian Journal of Geosciences, 13*(143), 1-14.

Singaraja, C., Chidambaram, S., Prasanna, M. V., Thivya, c., & Thilagavathi, T. (2014). Statistical analysis of the hydrogeochemical evolution of groundwater in hard rock coastal aquifers of Thoothukudi district in Tamil Nadu, India. *Environmental Earth Sciences, 71*, 451–464.

Singh, M., Kumar, S., Kumar, B., Singh, S., & Singh, I. B. (2013). Investigation on the hydrodynamics of Ganga Alluvial Plain using environmental isotopes: A case study of the Gomati River Basin, Northern India. *Hydrogeology Journal, 21*, 687-700.

Smerdon, B. D., Gardner, W. P., Harrington, G. A., & Tickell, S. J. (2012). Identifying the contribution of regional groundwater to the baseflow of a tropical river (Daly River, Australia). *Journal of Hydrology, 464-465*, 107-115.

Sofner, B. (1992). *Groundwater monitoring and groundwater protection at the Geological Survey Department (GSD) of Malaysia* (Project No. 88.2225.6). Retrieved from Kuala Lumpur:

Soh, Z. A. (1972). *The geomorphology of Kelantan Delta, Malaysia.* (P.hD.), University of Malaya, Kuala Lumpur.

Somaratne, N., & Smettem, R. J. (2014). Theory of the generalized chloride mass balance method for recharge estimation in groundwater basins characterised by point and diffuse recharge. *Hydrology and Earth System Sciences Discussion, 11*, 307-332.

Song, J., & Chen, X. (2010). Variation of specific yield with depth in an alluvial aquifer of the Platte River valley, USA. *International Journal of Sediment Research, 25*, 185-193.

Sophocleous, M. (1997). Managing water resources systems why 'safe yield' is not sustainable. *Groundwater, 35*(4), Article#561.

Sophocleous, M. (1998). Perspectives on sustainable development of water resources in Kansas. *Bulletin 239*.

Sophocleous, M. (2000). From safe yield to sustainable development of water resources- the Kansas experience. *Journal of Hydrology, 235*, 27-43.

Sophocleous, M. A., & Schloss, J. A. (2000). Estimated annual groundwater recharge. Retrieved from http://www.kgs.ku.edu/HighPlains/atlas/atrch.htm

Staelens, J. (2006). *Spatio-Temporal Patterns of Throughfall Water and Ion Deposition under a Dominant Beech Tree (Fagus sylvatica L.) in Relationship to Canopy Structure.* Ghent University, Ghent, Belgium.

Stallman, R. W. (1965). Steady one dimensional fluid flow in the semi-infinate porous medium with sinusoidal surface temperature. *Journal of Geophysical Research, 70*(12), 2821-2827.

Steinhorst, R. K., & Williams, R. E. (1985). Discrimination of groundwater sources using cluster analysis, MANOVA, canonical analysis and discriminant analysis. *Water Resources Research, 21*, 1149-1156.

Stellato, L., Petrella, E., Terrasi, F., Belloni, P., Belli, M., Sansone, U., & Celico, F. (2008). Some limitations in using 222Rn to assess river–groundwater interactions: the case of Castel di Sangro alluvial plain (central Italy). *Hydrogeology Journal, 16*, 701–712.

Stellato, L., Terrasi, F., Marzaioli, F., Belli, M., Sansone, U., & Celico, F. (2013). Is 222Rn a suitable tracer of stream–groundwater interactions? A case study in central Italy. *Applied Geochemistry, 32*, 108-117.

Stetzenbach, K. J., Hodge, V. F., Guo, C., Farnham, I. M., & Johannesson, K. H. (2001). Geochemical and statistical evidence of deep carbonate groundwater within overlying volcanic rock aquifer/aquitards of southern Nevada, USA. *Journal of Hydrology, 243*, 254–271.

Stewart, M. K., Morgenstern, U., McDonnell, J. J., & Pfister, L. (2012). The 'hidden streamflow' challenge in catchment hydrology: a call to action for stream water transit time analysis. *Hydrological Processes, 26*, 2061–2066.

Stewart, S., & Morgenstren, U. (2001). Age and Source of Groundwater from Isotope Tracers. In M. R. Rosen & P. A. White (Eds.), *Groundwaters of New Zealand* (pp. 161-183). Wellington: New Zealand Hydrological Society Inc.

Stiff, H. A. J. (1951). The interpretation of chemical water analysis by means of patterns. *Journal of Petroleium Technology, 3*(10), 15-17.

Stone, A. E. C., & Edmunds, W. M. (2012). Sand, salt and water in the Stampriet Basin, Namibia: Calculating unsaturated zone (Kalahari dunefield) recharge using the chloride mass balance approach. *Water Sa, 38*(3), 367-378.

Su, N., Burnett, W. C., Eller, K. T., Macintyre, H. L., Mortazavi, B., Liefer, J. D., & Novoveská, L. (2012). Radon and Radium Isotopes, Groundwater Discharge and Harmful Algal Blooms in Little Lagoon, Alabama. In K. M. M. Kawaguchi, H. Sato, T. Yokokawa, T. Itai, T. M. Nguyen, J. Ono and S. Tanabe (Ed.), *Interdisciplinary Studies on Environmental Chemistry—Environmental Pollution and Ecotoxicology* (pp. 329-337): TERRAPUB.

Subyani, A., & Sen, Z. (2006). Refined chloride mass-balance method and its application in Saudi Arabia. *Hydrological Processes, 20*, 4373-4380.

Subyani, A. M. (2004). Use of chloride-mass balance and environmental isotopes for evaluation of groundwater recharge in the alluvial aquifer, Wadi Tharad, western Saudi Arabia. *Environmental Geology, 46*(6-7), 741-749.

Suckow, A., Deslandes, A., Raiber, M., Taylor, A. R., Davies, P., Gerber, C., & Leaney, F. (2020). Reconciling contradictory environmental tracer ages in multi-tracer studies to characterize the aquifer and quantify deep groundwater flow: an example from the Hutton Sandstone, Great Artesian Basin, Australia. *Hydrogeology Journal, 28*, 75-87.

Sudhakar, S., K., V. M., & Soumya, S. (2016). Application of GIS and MODFLOW to Ground Water Hydrology- A Review. *Int. Journal of Engineering Research and Applications, 6*(1), 36-42.

Sukhija, B. S., Reddy, D. V., Nagabhushanam, P., & Hussain, S. (2003). Recharge processes: piston flow vs preferential flow in semi-arid aquifers of India. *Hydrogeology Journal, 11*, 387-395.

Sulaiman, I., Konto, K. M., & Razalim, F. A. A. (2019). Assessment of groundwater radon concentrations in Kelantan, Malaysia. *Jurnal Sains Nuklear Malaysia, 3*(21), 14-22.

Suntharalingam, T., & Teoh, L. H. (1985). Quaternary. In C. S. Hutchison & D. N. K. Tan (Eds.), *Geology of Peninsular Malaysia*. Kuala Lumpur: University of Malaya and Geological Society of Malaysia.

Suratman, S. (1997). *Groundwater Protection in north Kelantan, Malaysia: an integrated mapping approach using modeling and gis.* (Ph.D.), University of Upon Tyne, United Kingdom.

Suratman, S. (2010). *Current and future R&D on groundwater resources*. Paper presented at the IWRM: research and development (R&D) and capacity building needs in groundwater resource management, NAHRIM, Selangor, Malaysia.

Suzuki, K. (1960). Percolation measurements based on heat flow through soil with special reference to paddy fields. *Journal of Geophysical Research, 65*(9), 2883-2885.

Takounjou, A. F., Ndam Ngoupayou, J. R., Riotte, J., Takem, G. E., Mafany, G., Maréchal, J. C., & Ekodeck, G. E. (2011). Estimation of groundwater recharge of shallow aquifer on humid environment in Yaounde, Cameroon using hybrid water-fluctuation and hydrochemistry methods. *Environmental Earth Sciences, 64*(1), 107-118.

Taniguchi, M. (1993). Evaluation of vertical groundwater fluxes and thermal properties of aquifer based on transient temperature-depth profiles. *Water Resource Research, 29*(7), 2021-2026.

Taniguchi, M. (2002). Estimations of the past groundwater recharge rate from deep borehole temperature data. *Catena, 48*, 39-51.

Taniguchi, M. (2006). Anthropogenic effects on subsurface temperature in Bangkok. *Climate of the Past Discussions, 2*, 831-846.

Taniguchi, M., Shimada, J., Tanaka, T., Kayane, I., Sakura, Y., Shimano, Y., . . . Kawashima, S. (1999a). Disturbances of temperature-depth profilesdue to surface climate change and subsurface water flow: (1) An effect of linear increase in surface temperature caused by global worming and urbanization in the Tokyo metropolitan area, Japan. *Water Resource Research, 35*, 1507-1517.

Taniguchi, M., Shimada, J., & Uemura, T. (2003a). Transient effects of surface temperature anf groundwater flow on subsurface temperature in Kumamoto plain, Japan. *Physics and Chemistry of the Earth, 28*, 477-486.

Taniguchi, M., Shimano, Y., & Kayane, I. (1989). Groundwater flow analysis using the temperature in the upland areas at the western foot of Aso Volcanoes. Journal of Japan *Association of Hydrological Sciences, 19*, 171-179.

Taniguchi, M., Turner, J. V., & Smith, A. J. (2003b). Evaluation of groundwater discharge rates from subsurface temperature in Cockburn Sound, Western Australia. *Biogeochemistry, 66*(1-2), 111-124.

Taniguchi, M., & Uemura, T. (2005). Effects of urbanization and groundwater flow on the subsurface temperature in Osaka, Japan. *Physics of Earth and Planetary Interiors, 152*, 305-313.

Taniguchi, M., Williamson, D. R., & Peck, A. J. (1999b). Disturbances of temperature–depth profiles due to surface climate-change and subsurface water flow: (2) An effect of step increase in surface temperature caused by forest clearing in Southwest of Western Australia. *Water Resource Research, 35*, 1519-1529.

Taylor, R. G., Burgess, W. G., Shamsudduha, M., Zahid, A., Lapworth, D. J., Ahmed, K., . . . Nowreen, S. (2014). *Deep groundwater in the Bengal Mega Delta: new evidence of aquifer hydraulics and the influence of intensive abstraction*. (OR/14/070). UK: British Geological Survey Retrieved from http://nora.nerc.ac.uk/id/eprint/511339.

Taylor, R. G., & Howard, K. W. F. (1996). Groundwater recharge in the Victoria Nile basin of east Africa: support for the soil moisture balance approach using stable isotope tracers and flow modelling. *Journal of Hydrology, 180*, 31-53.

Ten Harkel, M. J. (1997). The effects of particle-size distribution and chloride depletion of sea-salt aerosols on estimating atmospheric deposition at a coastal site. *Atmospheric Environment, 31*(3), 417–427.

Tesfaldet, Y. T., Puttiwongrak, A., & Arpornthip, T. (2019). Spatial and temporal variation of groundwater recharge in shallow aquifer in the Thepkasattri of Phuket, Thailand. *Journal of Groundwater Science and ENgineering, 8*(1), 10-19.

Thomson, C. J. (2016). *Determining groundwater sources and ages via isotope geochemistry in big sky, Montana.* (Master of Science), University of Montana, Missoula, Montana.

Ting, C. S., Kerh, T., & Liao, C. J. (1998). Estimation of groundwater recharge using the chloride mass-balance method, Pingtung Plain, Taiwan. *Hydrogeology Journal, 6*(2), 282-292.

Tjia, H. D. (1973). Quaternary. In C. S. Hutchison & D. N. K. Tan (Eds.), *Geology of Peninsular Malaysia*. Kuala Lumpur: University of Malaya and Geological Society of Malaysia.

Tsujimura, M., Abe, Y., Tanaka, T., Shimada, J., Higuchi, J., Yamanaka, T., . . . Oyunbaatar, D. (2007). Stable isotopic and geochemical characteristics of groundwater in Kherlen River basin, asemi-arid region in eastern Mongolia. *Journal of Hydrology, 333*, 47-57.

Turner, S. W. D., Hejazi, M., Yonkofski, C., Kim, S. H., & Kyle, P. (2019). Influence of groundwater extraction costs and resource depletion limits on simulated global nonrenewable water withdrawals over the twenty-first century. *Earth's Future, 7*, 123-135.

Uchida, Y., & Hayashi, T. (2005). Effects of hydrogeological and climate change on the subsurface thermal regime in the Sendai Plain. *Physics of the Earth and Planetary Interiors, 152*, 292-304.

Uchida, Y., Sakura, Y., & Taniguchi, M. (2003). Shallow subsurface thermal regimes in major plains in Japan with references to recent surface warming. *Physic and Chemistry of the Earth, 28*(9-11), 457-466.

Udie Lmasudin, M. I. (2000). *Kajian taburan enapan resen dan perubahan pesisir pantai, Kota Bharu – Kuala Telong, Kelantan Darul Naim.* (B.Sc.), University of Malaya, Kuala Lumpur.

UNESCO. (2015). *Water for a sustainable world: Facts and figures*. Retrieved from Perugia, Italy:

Unland, N. P., Cartwright, I., Anderson, M. S., Rau, G. C., Reed, J., Gilfedder, B. S., . . . Hofmann, H. (2013). Investigating the spatio-temporal variability in groundwater and surface water interactions: a multi-technique approach. *Hydrology and Earth System Sciences, 17*, 3437-3453.

Unland, N. P., Cartwright, I., Daly, E., Gilfedder, B. S., & Atkinson, A. P. (2015). Dynamic river-groundwater exchange in the presence of a saline, semi-confined aquifer. *Hydrological Processes, 29*(23), 4817-4829.

UNSCEAR. (2000). *Report of the United Nations Scientific Committee on the Effects of Atomic Radiation to the General Assemby, Annex B: Exposures from Natural Radiation Sources*. Retrieved from New York, USA:

van der Gun, J. (2012). *Groundwater and global change: trends, opportunities and challenges.* (WWDR4, Open access:01). Retrieved from France: http://unesdoc.unesco.org/images/0021/002154/215496e.pdf

Varni, M. R. (2013). Application of several methodologies to estimate groundwater recharge in the Pampeano Aquifer, Argentina. *Tecnologia Y Ciencias Del Agua, 4*(3), 67-85.

Vazquez-Sune, E., Carrera, J., Tubau, I., Sanchez-Vila, X., & Soler, A. (2010). An approach to identify urban groundwater recharge. *Hydrology and Earth System Sciences, 14*(10), 2085-2097.

Verbovsek, T., & Kanduc, T. (2016). Isotope Geochemistry of Groundwater from Fractured Dolomite Aquifers in Central Slovenia. *Aquatic Geochemistry, 22*(2), 131–151.

Victoria EPA, E. (2009). Sampling and Analysis of Waters, Wastewaters, Soils and Wastes. Industrial Waste Resources Guidelines. In E. P. Authority (Ed.), (pp. 36). Victoria St, Carlton: Environment Protection Authority Victoria

Vishal, V., Kumar, S., & Singhal, D. C. (2014). Estimation of groundwater recharge in national capital territory, Delhi using groundwater modeling. *Journal of Indian Water Resources Society, 34*(1), 15-23.

Visser, A., Schaap, J. D., Broers, H. P., & Bierkens, M. F. P. (2009). Degassing of 3H/3He, CFCs and SF6 by denitrification: measurements and two-phase transport simulations. *J Contam Hydro, 103*(3-4), 2006-2018.

W Ismail, W. M. Z. (2011). *Groundwater management system using hydrogeological model in Sg. Kelantan River basin.* (MS.c.), University of Malaya, Kuala Lumpur.

Wada, Y., & Bierkens, M. F. (2014). Sustainability of global water use: Past reconstruction and future projections. *Environmental Research Letters, 9*(10), Article#104003.

Walker, D. (1956). Quaternary. In C. S. Hutchison & D. N. K. Tan (Eds.), *Geology of Peninsular Malaysia,* . Kuala Lumpur: University of Malaya and Geological Society of Malaysia.

Wan Ismail, W. M. Z. (2012). *Optimization of water suplly system: Kelantan case study on riverbank filtration system (RBF)*. Paper presented at the Borneo Water & Wastewater exhibition, Kuching, Sarawak.

Wan Ismail, W. M. Z. (2019). *Groundwater for public water supply*. Paper presented at the National Groundwater Conference 2019, Concarde Hotel, Shah Alam, Selangor.

Wan Muhd Tahir, W. Z., Hussin, N. H., Yusoff, I., Mamat, K., Abdul Latif, J., & Demanah, R. (2014). *Integrated assessment of groundwater recharge in the North Kelantan River Basin using environmental water stable isotopes, tritium and chloride data* (INIS-MY--2015-005). Retrieved from Malaysia: https://inis.iaea.org/collection/NCLCollectionStore/_Public/46/091/46091331.pdf?r=1

Wang, J., Liang, X., Liu, Y., Jin, M., Knappett, P., & Liu, Y. (2018). Hydrogeochemical evolution along groundwater flow paths in the Manas River Basin, Northwest China. *Groundwater*.

Wang, P., Zhang, F. e., & Chen, Z. (2020). Characterization of recharge processes and groundwater flow paths using isotopes in the arid Santanghu basin, Northwest China. *Hydrogeology Journal, 28*, 1037–1051

Wang, Y., Chen, Y., & Li, W. (2014). Temporal and spatial variation of water stable isotopes (18O and 2H) in the Kaidu River basin, Northwestern China. . *Hydrological Processes, 28*, 653-661.

Waterloo Hydrogeologic, I. (2005). *Visual MODFLOW v. 4.1 User's Manual*. Waterloo, Ontario, Canada: Author.

Weeks, E. P. (2002). The Lisse effect revisited. *Groundwater, 40*(6), 652-656.

WHO. (2011). *Guidelines for drinking-water quality. Fourth edition.* . Retrieved from Geneva:

Winstanley, D. (2007). *The water cycle: A framework for drought and water supply planning*. Paper presented at the ISAWWA Conference, Springfield.

Wirmvem, M. J., Kamtchueng, B. T., Wotany, E. R., Mimba, M. E., Fantong, W. Y., Ako, A. A., & Ohba, T. (2020). Multi-tracer (δ18O, δD, 3H, CFCs and SF6) investigation of groundwater recharge and apparent age at the Bamenda Highlands along the Cameroon volcanic line. *Sustainable Water Resources Management, 6*(2), 1-16.

Wirmvem, M. J., Mimba, M. E., Kamtchueng, B. T., Wotany, E. G., Bafon, T. G., Asaah, A. N. E., . . . Ohba, T. (2017). Shallow groundwater recharge mechanism and apparent age in the Ndop plain, northwest Cameroon. *Applied Water Science, 7*, 489–502.

Wirmvem, M. J., Ohba, T., Fantong, W. Y., Ayonghe, S. N., Suila, J. Y., Asaah, A. N. E., . . . Hell, J. V. (2013). Hydrochemistry of shallow groundwater and surface water in the Ndop plain, North West Cameroon. *Journal of Environmental Science and Technology, 7*(7), 518-530.

Wood, W. W., & Sanford, W. E. (1995). Chemical and Isotopic Methods for Quantifying Groundwater Recharge in a Regional, Semiarid Environment. *Ground Water, 33*(3), 458-468.

Wu, Y., Wen, X., & Zhang, Y. (2004). Analysis of the exchange of groundwater and river water by using Radon-222 in the middle Heihe Basin of north-western China. *Environmental Geology, 45*, 647-653.

Xiong, G.-Y., Chen, G.-Q., Xu, X.-Y., Liu, W.-Q., Fu, T.-F., Khokiattiwong, S., . . . Ali, A. (2020). A comparative study on hydrochemical evolution and quality of groundwater in coastal areas of Thailand and Bangladesh. *Journal of Asian Earth Sciences, 195*, Article#104336.

Xu, Y., & Beekman, H. E. (2019). Review: Groundwater recharge estimation in arid and semi-arid southern Africa. *Hydrogeology Journal, 27*, 929-943.

Yang, J., Yu, Z., Yi, P., Frape, S. K., Gong, M., & Zhang, Y. (2020). Evaluation of surface water and groundwater interactions in the upstream of Kui river and Yunlong lake, Xuzhou, China. *Journal of Hydrology, 583*, Article#124549.

Yang, J. H., Jun, S. C., Kwon, H. P., & Lee, K. K. (2014). Tracing of residual multiple DNAPL sources in the subsurface using 222Rn as a natural tracer at an industrial complex in Wonju, Korea. *Environmental Earth Sciences, 71*, 407–417.

Yang, L. H., Qi, Y. Q., Zheng, C. M., Andrews, C. B., Yue, S. H., Lin, S. J., . . . Li, H. T. (2018). A modified water-table fluctuation method to characterize regional groundwater discharge. *Water, 10*(503), 1-16.

Yang, Q., Li, Z., Ma, H. Y., Wang, L. C., & Martin, J. D. (2016). Identification of the hydrogeochemical processes and assessment of groundwater quality using classic integrated geochemical methods in the Southeastern part of Ordos basin, China. *Environmental Pollution, 218*, 879-888.

Yao, Z., Liu, J., Huang, H.-Q., Song, X., Dong, X., & Liu, X. (2009). Characteristics of isotope in precipitation, river water and lake water in the Manasarovar basin of Qinghai–Tibet Plateau. *Environmental Geology, 57*, 551–556.

Yidana, S. M. (2011). Groundwater flow modelling and particle tracking for chemical transport in the Voltaian aquifers. *Environmental Earth Sciences, 63*, 709-721.

Yidana, S. M., Banoeng-Yakubo, B., & Asamoah Sakyi, P. (2012). Identifying key processes in the hydrochemistry of a basin through the combined use of factor and regression models. *Journal of Earth System Science, 121*(2), 491-507.

Yidana, S. M., & Yidana, A. (2010). Assessing water quality using water quality index and multivariate analysis. *Environmental Earth Sciences, 59*(7), 1461-1473.

Yin, L., Hou, G., Su, X., Wang, D., Dong, J., Hao, Y., & Wang, X. (2011a). Isotopes (D and δ18O) in Precipitation, Groudwater, abd Surface Water in the Ordos Plateau, China: Implications with Respect to Groundwater Recharge and Circulation. *Hydrogeology Journal, 19*, 429-443.

Yin, L. H., Hu, G. C., Huang, J. T., Wen, D. G., Dong, J. Q., Wang, X. Y., & Li, H. B. (2011b). Groundwater-recharge estimation in the Ordos Plateau, China: comparison of methods. *Hydrogeology Journal, 19*(8), 1563-1575.

Yoneda, M., Inoue, Y., & Takine, N. (1991). Location of groundwater seepage points into a river by measurement of 222Rn concentration in water using activated charcoal passive collectors. *Journal of Hydrology, 124*, 307-316.

Yoon, Y. Y., Koh, D. C., Lee, K. Y., Cho, S. Y., Yang, J. H., & Lee, K. K. (2013). Using 222Rn as a naturally occurring tracer to estimate NAPL contamination in an aquifer. *Applied Radiation and Isotopes, 81*, 233-237.

Yu, J. C., Mo, X. X., Yu, X. H., Dong, G. C., Fu, Q., & Xing, F. C. (2012). Geochemical characteristics and petrogenesis of Permian basaltic rocks in Keping area, Western Tarim Basin: a record of plume –lithosphere interaction. *Journal of Earth Science, 23*(4), 442-454.

Yu, M. C. L., Cartwright, I., Braden, J. L., & de Bree, S. T. (2013). Examining the spatial and temporal variation of groundwater inflows to a valley-to-floodplain river using 222Rn, geochemistry and river discharge: the Ovens River, southeast Australia. *Hydrology and Earth System Sciences, 17*, 4907-4924.

Yuan, R. Q., Song, X. F., Han, D. M., Zhang, Y. H., Zhang, L., Zhang, B., . . . Yu, Y. L. (2011a). Rate and historical change of direct recharge from precipitation constrained by unsaturated zone profiles of chloride and oxygen-18 in dry river bed of North China Plain. *Hydrological Processes, 26*(9), 1291-1301.

Yuan, R. Q., Song, X. F., Zhang, Y. H., Han, D. M., Wang, S. Q., & Tang, C. Y. (2011b). Using major ions and stable isotopes to characterize recharge regime of a faultinfluenced aquifer in Beiyishui River Watershed, North China Plain. *405*, 512-521.

Yuge, K., Anan, M., & Nakano, Y. (2005). Evaluation of effect of the upland field on the groundwater recharge. *Journal Faculty of Agriculture Kyushu University, 50*(2), 799-807.

Yurtesever, Y., & Gat, J. R. (1981) Atmospheric waters. In. *Stable isotope hydrolgy: deutrium and oxygen-18 in the water cycle.* (pp. 103-142). Vienna, Austria: International Atomic Energy Agency.

Zhou, Y., & Herath, H. M. P. S. D. (2017). Evaluation of alternative conceptual models for groundwater modelling. *GEOSCIENCE FRONTIERS, 8*, 437-443.

Zhou, Y., & Li, W. (2011). A review of regional groundwater flow modeling. *GEOSCIENCE FRONTIERS, 2*(2), 205-214.

Zhu, B. Q., Wang, X. M., & Rioual, P. (2017). Multivariate Indications between environment and ground water recharge in a sedimentary drainage basin in northwestern China. *Journal of Hydrology and Hydromechanics, 549*, 92-113.

Zuber, A., Różański, K., Kania, J., & R., P. (2011). On some methodological problems in the use of environmental tracers to estimate hydrogeologic parameters and to calibrate flow and transport models. *Hydrogeology Journal, 19*, 53–69.

LIST OF PUBLICATIONS AND PAPERS PRESENTED

PUBLICATIONS

1. **Hussin, N. H.**, Yusoff, I., Wan Muhd Tahir, W. Z., Mohamed, I., Ibrahim, A. I. N. & Rambli, A. (2016). Multivariate statistical analysis for identifying water quality and hydrogeochemical evolution of shallow groundwater in Quaternary deposits in the Lower Kelantan River Basin, Malaysian Peninsula. *Environmental Earth Sciences, 75*, Article#1081.

2. **Hussin, N. H.**, Yusoff, I. & May, R. (2020). Comparison of applications to evaluate groundwater recharge at Lower Kelantan River Basin, Malaysia. *Geosciences,* 10, Article#289.

PAPERS PRESENTED

1. Yusoff, I., **Hussin, N. H.**, Wan Muhamad Tahir, W. Z., & Raksmey, M. (2017, Nov) *Assessment of multiple groundwater recharge estimation techniques for a quaternary aquifer in the Lower Kelantan River Basin, Malaysia.* Paper presented at 1st International Congress on Earth Science in SE Asia, Universiti Brunei Darussalam, Bandar Seri Begawan, Brunei.

2. **Hussin, N. H.**, Yusoff, I., Wan Muhamad Tahir, W. Z., & Raksmey, M. (2017, Jul) *Assessment of various groundwater recharge methods in the Lower Kelantan River Basin (LKRB).* Paper presented at Candidature Defence Seminar, University of Malaya, Kuala Lumpur, Malaysia.

3. **Hussin, N. H.**, & Yusoff, I. (2015, Aug). *Groundwater chemistry data clustering: advantages and problems.* One-day Workshop on Environmental Statistics and Statistical consulting. Paper presented at Institute of Mathematical Sciences, University of Malaya, Kuala Lumpur, Malaysia.

4. Wan Muhamad Tahir, W. Z., **Hussin, N. H.**, & Yusoff, I. (2015, May). *Qualitative assessment of groundwater recharge-rate and origin in North Kelantan River Basin using environmental water stable isotopes, tritium and chloride data.* Paper presented at International Symposium on Isotope Hydrology: Revisiting Foundations and Exploring Frontiers - CN-225, IAEA, Vienna, Austria.

5. **Hussin, N. H.**, Yusoff, I., Raksmey, M., & Wan Muhamad Tahir, W. Z. (2015, Mar). *Assessment of groundwater recharge using combined techniques at Lower Kelantan River Basin.* Paper presented at Geohydrology Group Progress Seminar, University of Malaya, Kuala Lumpur, Malaysia.

6. Wan Muhamad Tahir, W. Z., **Hussin, N. H.**, Yusoff , I., Mamat, K., Abdul Latif, J., & Demanah, R. (2014, Oct) *Integrated Assessment of Groundwater Recharge in Tte North Kelantan River Basin Using Environmental Water Stable Isotopes, Tritium and Chloride Data.* Paper presented at Research and Development Seminar, Nuclear Malaysia, Bangi, Selangor, Malaysia